AN ANALYTICAL AND EXPERIMENTAL INVESTIGATION OF STRESSES IN PLATES AND SHELLS OF HOLLOW CROSS SECTION

BY

KISHALOY NAG

Thesis submitted to the University of Edinburgh for the degree of Doctor of Philosophy

May 1969

SYNOPSIS

This thesis deals with the development of theories for plates and shells of hollow cross section for an elastic material.

Though hollow clay blocks have been used in Europe, mainly in Italy, for structural purposes such as construction of floors, cylindrical and doubly curved shells for over forty years. No reasonable design methods for such structures are available. In this thesis therefore attempts are made to develop theories applicable to plates and shells of hollow cross sections with special reference to hollow clay block structures taking both membrane and bending effects into account.

Theories are developed from first principles using the usual assumptions of elasticity. The experimental results are compared with the theoretical results to examine the validity of the theories. Three types of problem viz. 1) Plates, 2) Cylindrical shells and 3) Doubly-curved shells, under various boundary conditions and subject to different load conditions are considered.

All the problems of this thesis are solved by linearising the partial differential equations in terms of displacements applying finite difference approximations and solving the equations using a Computer. A plate under simply supported conditions is also solved using trigonometric series and the results compared with those obtained by finite difference. The effects of Poisson's ratio on the values of displacements for a cylindrical shell fixed at edges and end-arches is described. The effect of the variation of thickness of shell on the values of displacements and moments is also included. In addition a single eighth order differential equation in terms of radial displacement 'W' for a cylindrical shell of hollow cross section is derived.

As perspex is considered to be an ideal isotropic material the initial tests were made on models of plate and cylindrical shell of hollow section built of perspex. These tests were followed by tests on plate and cylindrical shell built of hollow clay blocks under various boundary conditions subject to uniformly distributed load. Sensitive dial gauges and electric resistance strain gauges were used to measure deflections and strains respectively.

The experimental results are compared with the theoretical results and are shown to be in close agreement.

ACKNOWLEDGEMENTS

The author wishes to thank Professor A. W. Hendry, B.Sc., Ph.D., D.Sc., F.I.Struct.E., F.I.C.E., F.R.S.E., for introducing him to the problem described in this thesis and for his guidance, and is grateful to Dr. S. R. Davies, B.Sc., Ph.D., M.I.C.E., for his constant encouragement, assistance and guidance throughout this work.

The author is thankful to his friends and the technical staff of the Civil Engineering Department for helping him in various ways. The valuable service rendered by the Edinburgh Regional Computer Centre is also acknowledged.

The author wishes to thank the British Structural Ceramics Research Association for sponsoring the work and is grateful to Professor Hendry for granting him a studentship.

Finally the author expresses his gratitude to Mrs. Sally Tulley for typing the thesis and to Miss Elizabeth Turner for the photographic work.

CONTENTS

		Page No:
	Synopsis	(i)
	Acknowledgements	(iii)
	Contents	(iv)
	Notation	(viii)
	CHAPTER 1	
	INTRODUCTION	1
	CHAPTER 2	
	PLATES OF HOLLOW CROSS SECTION	
	PART 1	
2.1.1	Introduction	7
2	Development of theory of plates of hollow cross section	7
3.	Solution of simply supported plate by Navier's method	11
4	Solution of plates by finite difference and computer	14
a.	Simply supported plate	15
b.	Plate: fixed on all four edges	17
c.	Plate: free at four edges, supported on four corners	18
Appendix 2-1	Finite difference approximations	21
	PART 2	
2.2.1	Introduction	22
2	Perspex model	22
a.	Construction of model	22
b.	Strain measurement	24

		Page No:
2.2.2c.	Testing procedure	24
d.	Simply supported at all four edges	24
e.	Free at edges, supported at four corners	25
3	Plate built of hollow clay blocks: fixed on all four sides	27
a.	Construction of model	27
b.	Strain and deflection measurements	28
c.	Testing procedure	29
4	Determination of Young's Modulus for Perspex beam of hollow section	30
5	Determination of the EI value for clay block structure	30
6	Conclusions	31
Appendix 2-2	Computer program for simply supported plate by Navier's method	34
Appendix 2-3	Computer program for stresses and strains for simply supported plate by finite difference	36
Appendix 2-4	Strength of hollow clay blocks and mortar cubes	40

CHAPTER 3

THEORY FOR CYLINDRICAL SHELLS OF HOLLOW CROSS SECTION

3.1	Introduction	42
2	Development of theory of thin cylindrical shells of hollow cross section	43
Appendix 3-1	Derivation of eighth order differential equations for cylindrical shell of hollow cross section	52

Page No:

CHAPTER 4

ANALYTICAL SOLUTIONS OF CYLINDRICAL SHELL OF HOLLOW CROSS SECTION

4.1	Introduction	57
2	Finite difference approximations	58
3	Method of solution	60
4	Boundary conditions	63
5	Cylindrical shells having a length/width ratio of two	63
a.	Fixed at the edges and at the end-arches	64
b.	Fixed at the edges and free at the end-arches	65
6	Cylindrical shell of any length/width ratio	69
a.	Fixed at edges and free at the end-arches	69
7	Determination of stresses and strains	72
Appendix 4-1	Comparison of theoretical results with published results	74
Appendix 4-2	Influence of Poisson's ratio on shell displacements	75
Appendix 4-3	Effect of variation of thickness of shells on the values of displacements and moments	76
Appendix 4-4	Computer program for perspex shell	78

CHAPTER 5

CYLINDRICAL SHELLS: MODEL EXPERIMENTS

5.1	Introduction	86
2	Perspex model	86
a.	Construction of model	86
b.	Strain and deflection measurements	88

		Page No:
c.	Testing procedure	89
d.	Fixed at the edges and free at the end-arches	90
e.	Fixed at the edges and at end-arches	92
3	Shell built of hollow clay blocks	95
a.	Construction of model	95
b.	Strain and deflection measurements	98
c.	Testing procedure	99
4	EI value of curved beam of perspex	101
5	EI value of curved beam of hollow blocks	101
6	Conclusions	102

CHAPTER 6

THEORY FOR DOUBLY CURVED SHELLS OF HOLLOW CROSS SECTION

6.1	Introduction	105
2	Development of theory of doubly curved shells of hollow cross section	106
3.	Some particular cases	110
4	Flat plate under pure bending	110
5	Cylindrical shell	111
6	Hyperbolic paraboloid shell	111

CHAPTER 7

CONCLUSIONS

7.1	Conclusions	113
2	Future research	115
	REFERENCES	117

PRINCIPAL NOTATION

x, y, z	Co-ordinate system
U, V, W	Displacement components in the x, y and z directions respectively
P_x, P_y, P_z	External loads in the x, y and z directions respectively
N_x, N_y	Normal Forces
N_{xy}, N_{yx}, Q_x, Q_y	Shear Forces
M_x, M_y	Bending Moments
M_{xy}, M_{yx}	Twisting Moments
$\sigma_x, \sigma_y, \sigma_z$	Direct Stresses
T_{xy}, T_{yx}	Shear Stresses
ϵ_x, ϵ_y	Direct Strains
γ_{xy}	Shear Strain
μ	Poisson's Ratio
E	Young's Modulus
G	Modulus of Rigidity
R, R_x, R_y	Radii of Curvature
D, D_x, D_y	Extensional Rigidities
S, S_x, S_y	Rigidity Moments
K, K_x, K_y	Bending Rigidities
A, A_x, A_y	Areas of Cross-Section
I, I_x, I_y	Moments of Inertia of cross-section
L, B	Length and Breadth respectively
a, b, a', b'	Mesh Lengths
$\bar{U}, \bar{V}, \bar{W}$	Non-dimensional displacement expressions.

CHAPTER 1

INTRODUCTION

Hollow clay blocks have been used in Europe for structural purposes for over forty years. The main development appears to have been in Italy where they have been used for the construction of walls, beams, floors, cylindrical and doubly curved shells. Other European countries have also used hollow clay blocks for such structures but as yet this formof construction has not been developed in Great Britain.

The use of hollow clay blocks have the following advantages:

1. Simplified shuttering compared to reinforced concrete structures.
2. Use of mobile shuttering reduces the shuttering cost to a minimum and expedites the progress of construction.
3. Saving in dead weight due to hollow blocks without much loss in strength.
4. Cheapness of the materials compared to reinforced concrete.
5. Less reinforcement required compared to reinforced concrete structures.
6. Better thermal insulation than a concrete roof due to cavities.

Therefore, this type of construction is very suitable for countries having limited resources in cement and steel and also where thermal insulation is one of the major problems.

Though the hollow clay blocks have been used for structural purposes for over forty years no reasonable design methods for such structures are available. In Italy, the cylindrical shells are designed as an arch assuming either hinged or fixed at supports depending on the support conditions. Tie bars are provided along the transverse section to take the horizontal thrust. On the

Plate: 1-1

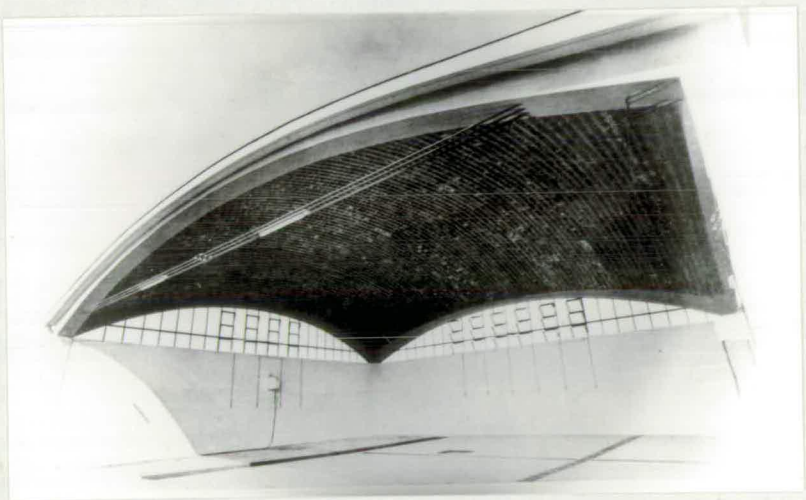

Plate: 1-2

Shells built of hollow

clay blocks (In Italy)

Various types of
hollow clay blocks

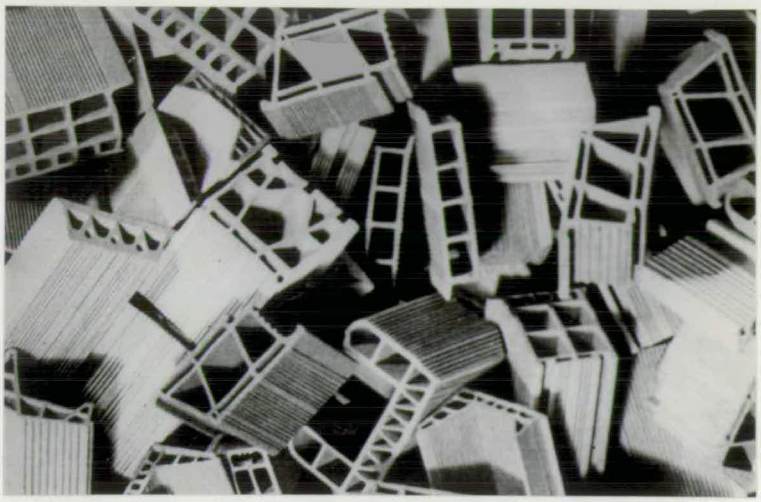

Plate: 1-3

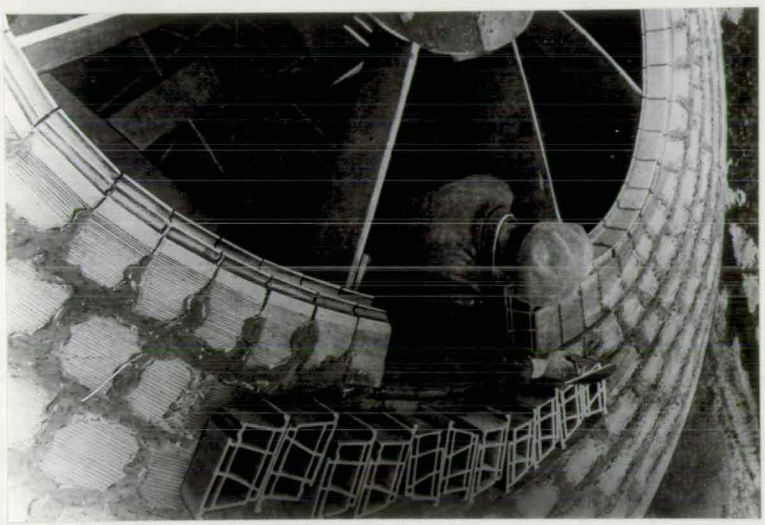

Plate: 1-4

Construction of shells of
hollow clay blocks (In Italy)

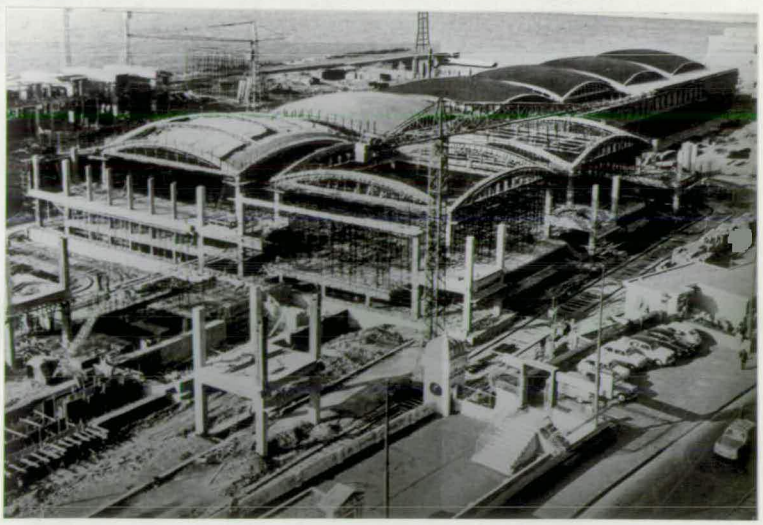

Plate: 1-5

other hand the hyperbolic paraboloid shells or doubly curved shells are designed on simplified methods based on the membrane theory. A number of full size and model shells built of hollow clay blocks were tested in Italy to study the structural behaviour and to arrive at some reasonable design methods, but all these attempts were confined to the membrane theory. In most cases, from the mode of failure of the structure, the conclusion that these structures behave according to the membrane theory have been drawn. However indications have been made regarding the 'boundary disturbances' near the edges where large deviations from membrane theory results is observed.

Salvadori (43) analyses translational shells of circular type based on the general thin shell theory of Pucher. Membrane stresses are obtained using finite difference approximations. He compares his analysis with the results for a rectangular shell of hollow clay blocks tested to destruction by Farnaci, RDB of Piacenza, Italy. Finally he concludes that this method of analysis can very well be used for determining the stresses in translational shells though the 'boundary disturbances' do exist but only limited to a small shell area.

Recently Prof. G. Ramaswamy (39) has developed a shape of doubly curved shell which he calls a funicular shell in which only compressive stresses develop due to the shape of the shell. He also tested a shell of funicular shape built of hollow blocks and examined the validity of the theory with the experimental results.

Dr. Fulton (20) has developed a theory for doubly curved shallow shell of sandwich construction where he allows shear displacements between the joints of the sandwich, but this does not truly simulate hollow shell construction. Flügge (19) gives theoretical expressions for double walled cylindrical shell, but no information regarding experimental verification of the above is available.

In this thesis therefore attempts are made to develop theories applicable to plates and shells of hollow cross section with special reference to hollow clay block structures taking both membrane and bending effects into account.

Theories are developed from first principles using the usual assumptions of elasticity and making simplifying assumptions during the process of development of the theories due to the complex sectional properties of the structure. The experimental results are compared with the theoretical results to examine the validity of the theories. Three types of problems viz. (1) Plates, (2) Cylindrical shells, and (3) Doubly curved shells under different boundary conditions are considered.

The theory for plates of hollow cross sections are developed and verified experimentally as a preliminary step to the development of the shell theories. As perspex is considered to be an ideal isotropic material so it was decided to test models of plates and shells built of perspex and to examine the validity of the theories. Finally plates and shells built of hollow clay blocks were tested to examine how far the behaviour of these structures deviate from the theoretical results. Though a clay block structure is not isotropic and homogeneous but tests on different types of structures built of clay blocks showed very good elastic behaviour. Different authors have used different approaches for analysing plate and shell structures and solved these by different techniques. The most popular method for solving such problems is the application of trigonometrical series to the partial differential equations in terms of displacements or stress-resultants, but the use of trigonometrical series cannot simulate with the possible boundary conditions. Next popular method is the use of finite difference approximations to the partial differential equations expressed in terms of displacements or stress-resultants, thus reducing the partial differential equations to a number of simultaneous linear equations which are solved either by the relaxation method or by a computer. This method can be applied to a problem subject to any boundary condition, but the accuracy of this method depends on

the size of the grid used, and by decreasing the size of the grid the accuracy of the results can be increased. This is a simple and straightforward method but a difficulty arises at the boundary where due to the application of finite difference approximations there appear fictitious points whose values are to be evaluated considering the boundary conditions. At present a new technique known as finite element method is being developed which can be used for the solution of plates and shells under various loading and boundary conditions. Due to the rapid development of computer science it appears that in future this method will be the most convenient method for solving plate and shell problems.

In this thesis all the problems of plate and shell are solved by linearising the partial differential equations in terms of displacements applying finite difference approximations and solving the equations using a computer. In addition a plate under simply supported conditions is solved using trigonometrical series and the results compared with those obtained by finite difference/computer method.

In shell tests application of appropriate loads is one of the main problems. Different arrangements of loading are being used in different laboratories depending upon the type of shell to be tested and facilities available.

In the early period loading by screeding sands was used for testing model shells. In full size shell tests loading by sand bags is the simplest, convenient and perhaps the most popular method. In some full size shell tests bricks are even used for loading.

In model shell tests, particularly doubly curved shells, loading by tripods is in extensive use but this method is cumbersome and expensive. In the case of cylindrical model shell tests loading through multibeams is very often used.

For simplicity and easy availability steel chains are sometimes used. In some laboratories loading by airbags are used for simulating uniformly distributed load but this method is expensive. Jacks are used for both simulating concentrated and uniformly distributed load. However, every method has its advantages and its disadvantages over the other methods. Depending on the facilities available in the structural laboratories the tests described in this thesis loading was done either using model bricks, a chain of lead-weights or a chain of lead-weights and bags filled with aggregate used simultaneously.

Chapter 2 is divided into two parts. In the first part the theory for plates of hollow cross section is developed and plates under three boundary conditions viz. (1) Simply supported at the edges, (2) Fixed at the edges, and (3) Simply Supported at Corners are solved using finite difference/computer. A plate under boundary condition (1) is also solved using trigonometrical series and compared with the results obtained by the former method. In part two experimental procedure for plates under above boundary conditions are described and the experimental results are compared with the theoretical results.

In Chapter 3 the theory for a cylindrical shell of hollow cross section is developed. Initially three partial differential equations of equilibrium in terms of displacements U, V and W are developed and then a single eighth order differential equation in terms of displacement W is derived.

Solution of three types of cylindrical shell of hollow cross section under two boundary conditions, viz. (1) Fixed at the edges and at the end-arches; Length = 2 x Breadth; (2) Fixed at the edges and free at the end-arches; (a) Length = 2 x Breadth; (b) Length : breadth any ratio, are obtained in Chapter 4.

In Chapter 5 the experimental details of the shell tests under the above boundary conditions are described and the experimental results are compared with the theoretical results.

Three partial differential equations in terms of displacements U, V and W for a doubly curved shell of hollow cross section are developed in Chapter 6.

CHAPTER 2

PLATES OF HOLLOW CROSS SECTION

PART I

2.1.1 INTRODUCTION

In this chapter the equation of equilibrium, in terms of displacement 'W', for plates of hollow cross section under pure bending is derived. Three boundary conditions

(1) Simply supported on all four edges

(2) Fixed at all four edges

and (3) Simply supported at four corners, are considered.

The theoretical solution of the simply supported problem case (1) is obtained by both Navier's method and also Finite Difference/Computer method. For cases (2) and (3) only the Finite Difference/ Computer method is used.

The theoretical results are compared with those obtained experimentally using models constructed of perspex and hollow clay blocks. A full description of the experimental procedure and model construction are described.

2.1.2 DEVELOPMENT OF THEORY OF PLATES OF HOLLOW CROSS SECTION UNDER PURE BENDING AS USED BY THE AUTHOR

Assumptions

In developing the theory the following assumptions are made:-

1. The over-all thickness of the plate is small compared to other dimensions.

2. Plane sections normal to the middle surface remains plane during the process of deformation and remain normal to it.
3. For all kinematic relations the distance of z of a point from the middle surface may be considered as unaffected by the deformation of the plate.
4. Normal stresses on planes parallel to the middle surface are neglected in comparison with other stresses.
5. The deflections of the plate are very small compared to radii of the curvature of the middle surface.

Strain Displacement Equations

Figure (2.1) shows a longitudinal section of a plate element after deflection when a normal fibre 'aa' rotated to 'bb' due to bending, similarly for the lateral direction.

Referring to Figure (2.1) displacements of a parallel surface can be expressed as:-

$$U_p = - z(\partial w/\partial x) \qquad (2.1.1)$$

$$V_p = - z(\partial w/\partial y) \qquad (2.1.2)$$

$$W_p = W \qquad (2.1.3)$$

where U_p, V_p and W_p are the displacements of a surface parallel to the middle surface.

The strain-parallel displacement relationships are:-

$$\epsilon_x = (\partial U_p/\partial x) \qquad (2.2.1)$$

$$\epsilon_y = (\partial V_p/\partial y) \qquad (2.2.2)$$

$$\gamma_{xy} = (\partial V_p/\partial x) + (\partial U_p/\partial y) \qquad (2.2.3)$$

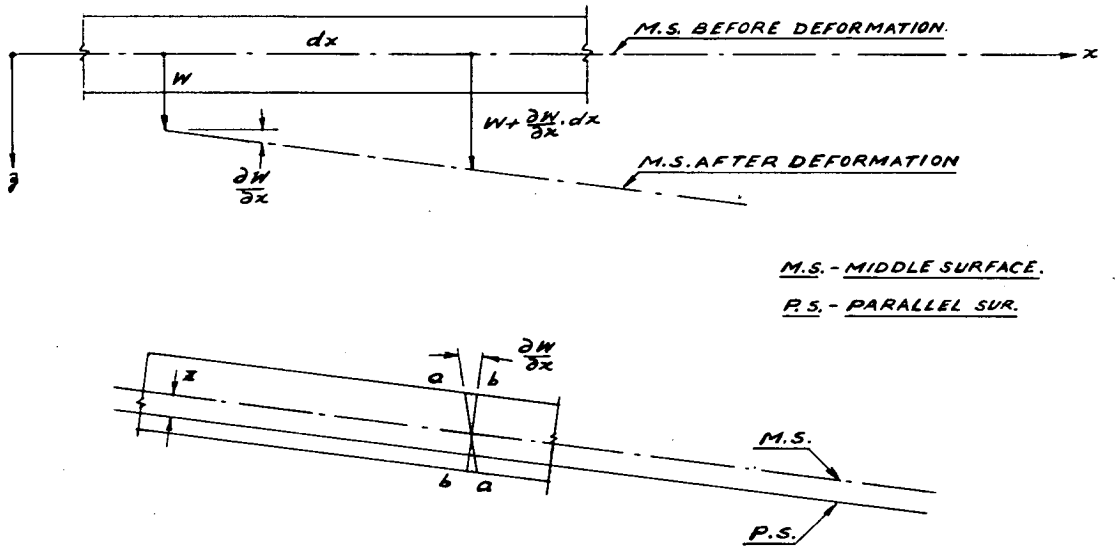

FIGURE : 2-1.

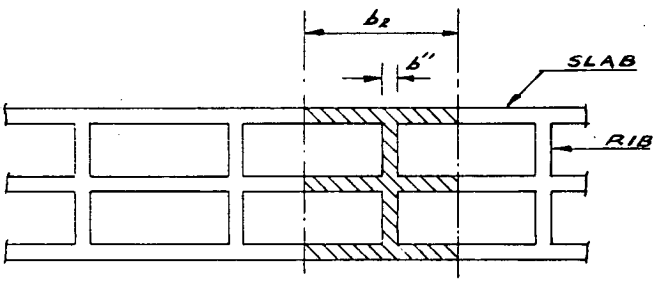

FIGURE : 2-2.

And therefore substituting for U_p, V_p and W_p in the equations (2.2.1 to 2.2.3):

$$\epsilon_x = -z(\partial^2 W/\partial x^2) \qquad (2.3.1)$$

$$\epsilon_y = -z(\partial^2 W/\partial y^2) \qquad (2.3.2)$$

$$\gamma_{xy} = -2z(\partial^2 W/\partial x \partial y) \qquad (2.3.3)$$

Now using Hooke's Law and by assumption (4) the stress strain relationships are:

For slabs:-

$$\sigma_x = (E/(1-\mu^2))(\epsilon_x + \mu\epsilon_y) \qquad (2.4.1)$$

$$\sigma_y = (E/(1-\mu^2))(\epsilon_y + \mu\epsilon_x) \qquad (2.4.2)$$

$$T_{xy} = T_{yx} = G\gamma_{xy} \qquad (2.4.3)$$

where $G = E/(2(1+\mu))$

For ribs:

$$\sigma_x = E.\epsilon_x \qquad (2.4.4)$$

$$\sigma_y = E.\epsilon_y \qquad (2.4.5)$$

For the case of a plate of hollow cross section there are no shearing stresses on the lateral surfaces of the ribs, there will be no shearing stress T_{xy} or T_{yx} in the cross section of the ribs and all the tangential shear will be carried by the slabs only.

Consider a section, x = constant, of the plate (Figure 2.2). Let b_2 be the length of the periodic repetition of the shaded part and b" be the width of the rib. Similarly in the case of a section y = constant of a plate, let b_1 be the length of the shaded part and b' be the width of the rib. As the normal stresses exist in both the slabs and the ribs M_x and M_y are integrals of the

normal stresses over the entire cross section of the slabs and the rib. In order to distinguish them notations 's' for the slab and 'r' for the rib will be used to the lower end of the integral sign. Therefore:-

$$M_x = \int_s \sigma_x \, z \, d\, z + \int_r \sigma_x (b''/b_2) \, z \, dz \qquad (2.5.1)$$

$$M_y = \int_s \sigma_y \, z \, dz + \int_r \sigma_y (b'/b_1) \, z \, dz \qquad (2.5.2)$$

$$M_{xy} = M_{yx} = \int_s T_{xy} \, z \, dz \qquad (2.5.3)$$

Using the equations (2.3.1 to 2.3.3), (2.4.1 to 2.4.5) and (2.5.1 and 2.5.2) the moments can be expressed in terms of the middle surface:-

$$M_x = -(K_x(\partial^2 W/\partial x^2) + \mu K(\partial^2 W/\partial y^2)) \qquad (2.6.1)$$

$$M_y = -(K_y(\partial^2 W/\partial y^2) + \mu K(\partial^2 W/\partial x^2)) \qquad (2.6.2)$$

$$M_{xy} = -(K(1-\mu))(\partial^2 W/\partial x \, \partial y) \qquad (2.6.3)$$

where K, K_x and K_y are the bending rigidities and defined by,

$$K = (E/(1-\mu^2)) \int_s z^2 \, dz \qquad (2.7.1)$$

$$K_x = (E/(1-\mu^2)) \int_s z^2 \, dz + E \int_r (b''/b_2) \, z^2 \, dz \qquad (2.7.2)$$

$$K_y = (E/(1-\mu^2)) \int_s z^2 \, dz + E \int_r (b'/b_1) \, z^2 \, dz \qquad (2.7.3)$$

The equations of Equilibrium (Figure 2.3 and 2.4) are :-

Equilibrium of Forces

In the z-direction, $\partial/\partial x \, (Q_x) + \partial/\partial y \, (Q_y) + P_z = 0$ (2.8.1)

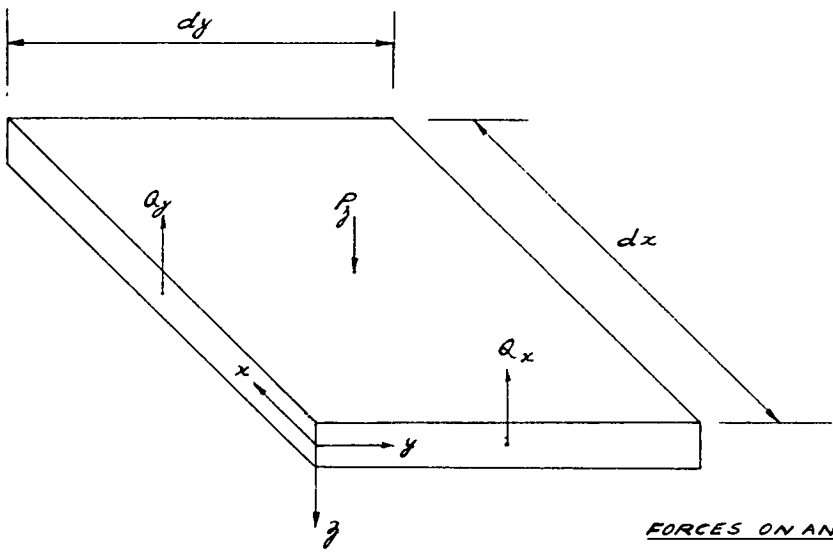

FORCES ON AN ELEMENT

FIGURE: 2-3.

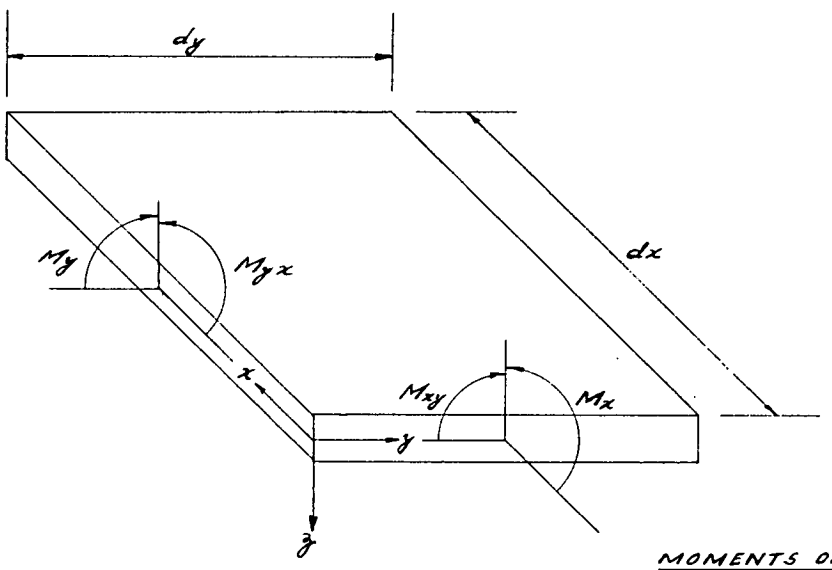

MOMENTS ON AN ELEMENT

FIGURE: 2-4

Equilibrium of Moments

About x-axis, $\partial/\partial y\ (M_y) + \partial/\partial x\ (M_{xy}) - Q_y = 0$ (2.9.1)

About y-axis, $\partial/\partial x\ (M_x) + \partial/\partial y\ (M_{yx}) - Q_x = 0$ (2.9.2)

Substituting for Q_x and Q_y from the equations (2.9.1) and (2.9.2) to the equation (2.8.1) the equation of equilibrium in terms of displacement 'W' is obtained as follows:-

$$-(K_x(\partial^4 W/\partial x^4) + 2K(\partial^4 W/\partial x^2 \partial y^2) + K_y(\partial^4 W/\partial y^4)) + P_z = 0 \quad (2.10.1)$$

In the case of a solid section $K_x = K_y = K$, and the equation (2.10.1) reduces to:

$$-K((\partial^4 W/\partial x^4) + 2(\partial^4 W/\partial x^2 \partial y^2) + (\partial^4 W/\partial y^4)) + P_z = 0 \quad (2.11.1)$$

In compact form:

$$K \nabla^4 W = P_z \quad (2.11.2)$$

where $\nabla^4 = (\partial^4/\partial x^4) + 2(\partial^4/\partial x^2 \partial y^2) + (\partial^4/\partial y^4)$

2.1.3 SOLUTION OF SIMPLY SUPPORTED PLATE BY NAVIER'S METHOD

The displacement equation of plate of hollow cross section is:

$$-(K_x(\partial^4 W/\partial x^4) + 2K(\partial^4 W/\partial x^2 \partial y^2) + K_y(\partial^4 W/\partial y^4)) + P_z = 0 \quad (2.11.1)$$

For convenience of computation dividing by K and letting $K_x/K = k'$, $K_y/K = k''$ the equation (2.11.1) changes to:

$$k'(\partial^4 W/\partial x^4) + 2(\partial^4 W/\partial x^2 \partial y^2) + k''(\partial^4 W/\partial y^4) = P_z/K \quad (2.12.1)$$

Applying Navier's method and assuming that the plate is uniformly loaded.

Load P_z can be represented in the form of a double trigonometric series:

$$P_z = (16Po/\pi^2) \sum_{m=1}^{\infty}\sum_{n=1}^{\infty} (1/mn)\sin(m\pi X/a)\sin(n\pi Y/b) \quad (2.13.1)$$

where m,n = 1,3,5,...

a,b = length and breadth of the plate

Po = intensity of the uniformly distributed load.

Therefore the displacement equation:

$$k'(\partial^4 W/\partial x^4) + 2(\partial^4 W/\partial x^2 \partial y^2) + k''(\partial^4 W/\partial y^2) = (16Po/\pi^2 K) \sum_{m=1}^{\infty}\sum_{n=1}^{\infty}(1/mn)\sin(m\pi X/a)\sin(n\pi Y/b) \quad (2.14.1)$$

One of the solutions of this equation to satisfy the boundary conditions is of the form:

$$W = \sum_{m=1}^{\infty}\sum_{n=1}^{\infty} a_{mn} \sin(m\pi X/a) \sin(n\pi Y/b) \quad (2.15.1)$$

Substituting for 'W' in the equation (2.14.1) from (2.15.1) the coefficient a_{mn} follows:-

$$a_{mn} = (16Po/\pi^6 mnK)/(k'(m/a)^4 + 2(mn/ab)^2 + k''(n/b)^4) \quad (2.16.1)$$

Therefore the solution of the equation (2.14.1) is:

$$W = (16Po/\pi^6 K) \sum_{m=1}^{\infty}\sum_{n=1}^{\infty} (\sin(m\pi X/a)\sin(n\pi Y/b))/(mn(k'(m/a)^4 + 2(mn/ab)^2 + k''(n/b)^4)) \quad (2.17.1)$$

For a plate of solid cross section $k' = k'' = 1$. This reduces to:

$$W = (16Po/\pi^6 K) \sum_{m=1}^{\infty}\sum_{n=1}^{\infty} (\sin(m\pi X/a)\sin(n\pi Y/b))/(mn((m/a)^4 + 2(mn/ab)^2 + (n/b)^4)) \quad (2.17.2)$$

Using this expression for 'W' in the expression for moments M_x and M_y:

$$M_x = -(K_x(\partial^2 W/\partial x^2) + \mu K(\partial^2 W/\partial y^2))$$

$$= (16Po/\pi^4 K) \sum_{m=1}^{\infty}\sum_{n=1}^{\infty} (k'(m/a)^2 + \mu(n/b)^2)(\sin(m\pi X/a)\sin(n\pi Y/b))/(mn(k'(m/a)^4 + 2(mn/ab)^2 + k''(n/b)^4)) \quad (2.18.1)$$

Similarly,

$$M_y = (16Po/\pi^4 K) \sum_{m=1}^{\infty} \sum_{n=1}^{\infty} (\mu(m/a)^2 + k''(n/b)^2)(\sin(m\pi X/a)\sin(n\pi Y/b)) / (mn(k'(m/a)^4 + 2(mn/ab)^2 + k''(n/b)^4)) \quad (2.18.2)$$

And stresses are given by Figure (2-5)

$$\sigma_x = M_x d/I_x \quad (2.19.1)$$

$$\sigma_y = M_y d/I_y \quad (2.19.2)$$

Therefore strains are given by:

$$\epsilon_x = (1/E)(\sigma_x - \mu\sigma_y) \quad (2.20.1)$$

$$\epsilon_y = (1/E)(\sigma_y - \mu\sigma_x) \quad (2.20.2)$$

In the present case, a plate having the following dimensions and taking the first 3 terms of the trigonometrical series i.e. m = 1,3,5 and n =1,3,5; and X = a/12, y = b/12 and P = 1 are solved (Figure (2-5)).

1) a = b = 12 inches

2) $b_1 = b_2 = 1$ inch

3) b' = 0·125 inch

4) b" = 0

5) $t_1 = 0.0625$ inch

6) $t_2 = 0.125$ inch

7) $E = 4{\cdot}2 \times 10^5$ lb/in^2

8) $\mu = 0{\cdot}35$

The values of W, M_x, M_y, σ_x and σ_y at different positions in the plate have been computed using the KDF9 computer and are shown in Figures (2-6 to 8.)

It is to be noted that the above program is a general one and can be used for a plate of any size, cross section and material only by changing

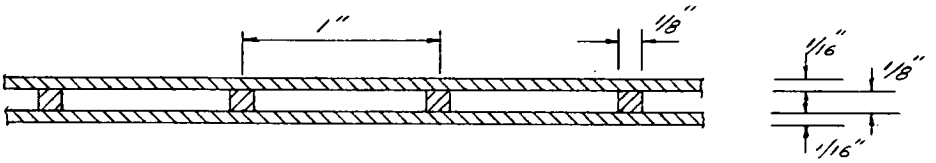

SEC-A-A

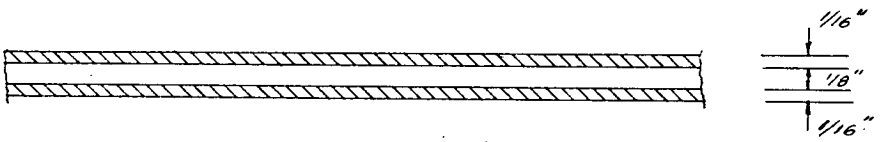

SEC-B-B

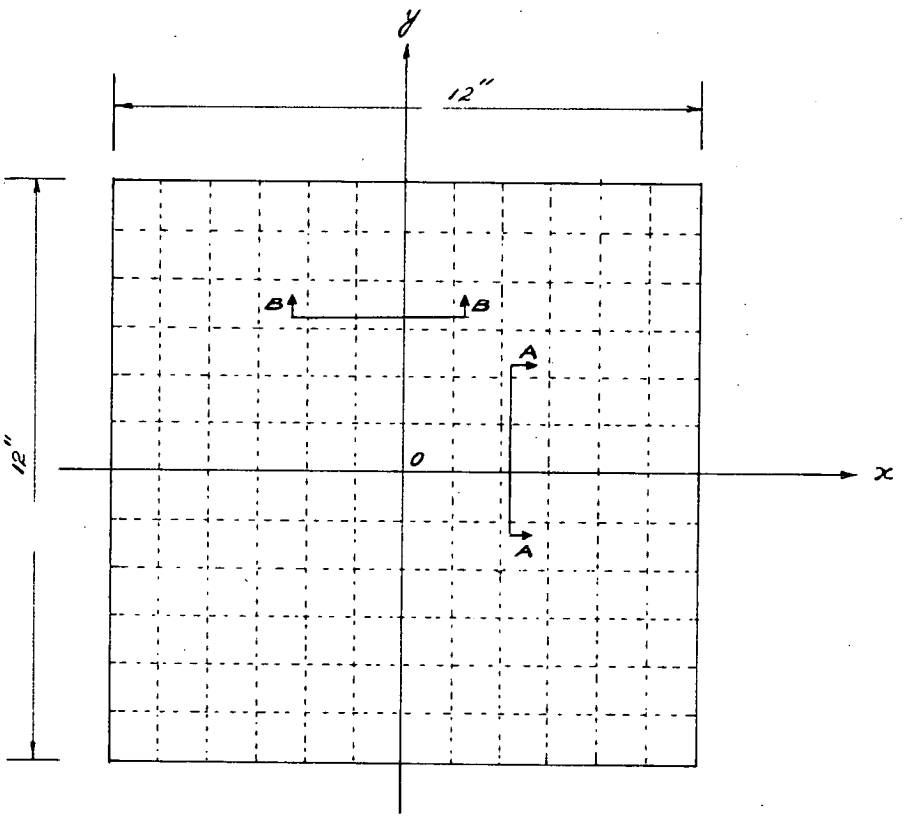

DETAILS OF PERSPEX PLATE

(INCLUDING GRIDS)

FIGURE : 2-5

$W \times 10^2$

NAVIER'S METHOD.

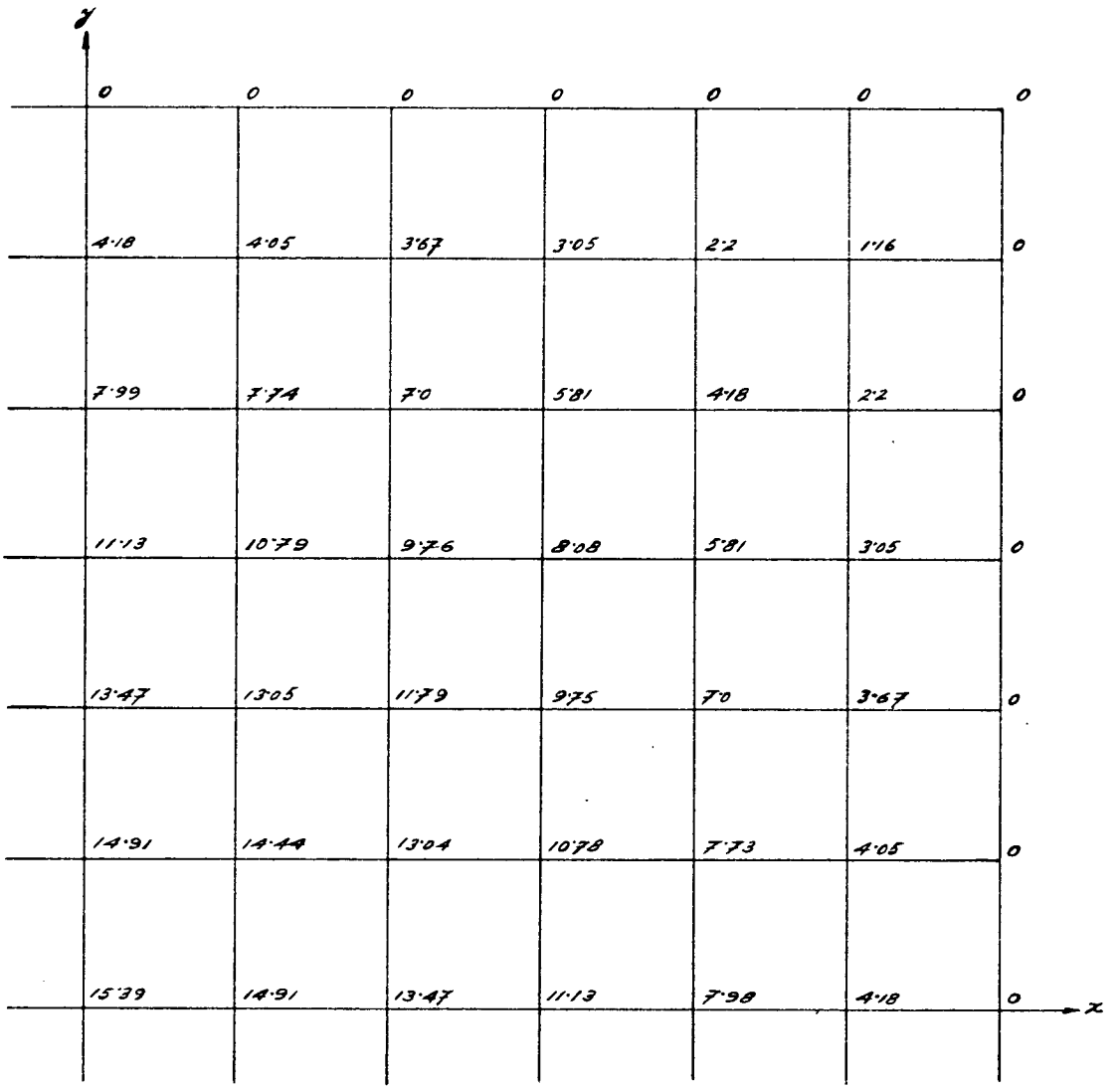

LOAD = 1 lb/in.^{2}

$E = 4{\cdot}2 \times 10^5$ lb/in.^{2}

$\mu = 0{\cdot}35$.

VERTICAL DEFLECTION IN INCHES.

PLATE: SIMPLY SUPPORTED.

FIGURE: 2-6.

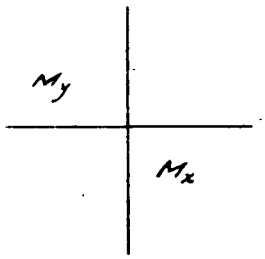

NAVIER'S METHOD.

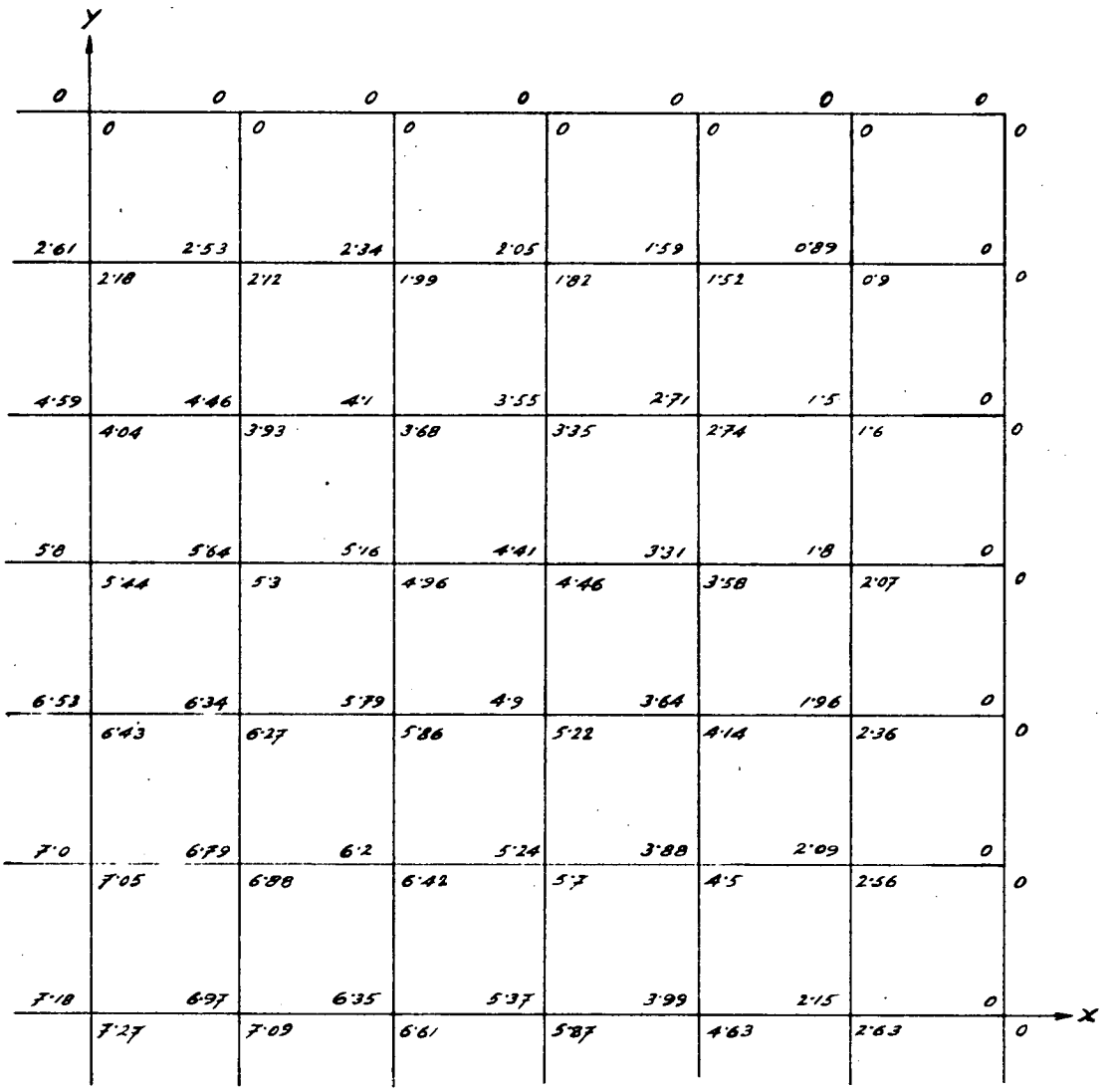

LOAD = 1 lb/in.^{2}

E = $4·2 \times 10^6$ lb/in.^{2}

μ = 0·35.

MOMENTS IN LB.IN.

FIGURE : 2-7.

$\sigma_y \times 10^{-2}$

$\sigma_x \times 10^{-2}$

NAVIER'S METHOD

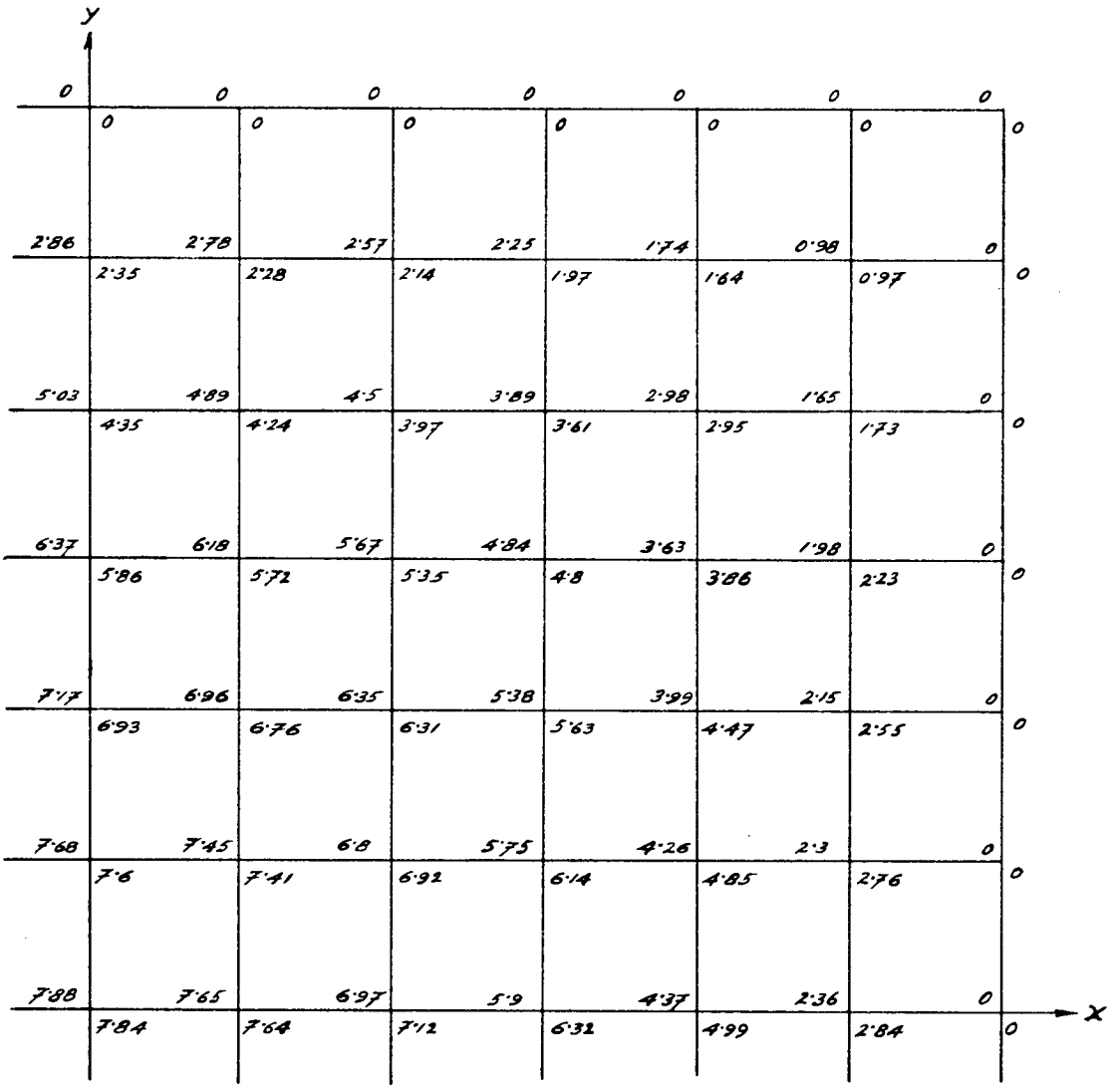

LOAD = 1 lb/in.^{2}

$E = 4{\cdot}2 \times 10^5$ lb/in.^{2}

$\mu = 0{\cdot}35$.

STRESSES IN lb/in.^{2}

FIGURE: 2-8.

the data.

The computer program is included in the Appendix (2-2)

2.1.4 SOLUTION OF PLATES BY FINITE DIFFERENCE AND COMPUTER

By using the finite difference approximations the higher order differential equations are reduced to a finite number of simultaneous equations. The solution of the simultaneous equations being obtained by use of a computer.

The displacement equation for a plate of hollow cross section is:

$$k'(\partial^4 W/\partial x^4) + 2(\partial^4 W/\partial x^2 \partial y^2) + k''(\partial^4 W/\partial y^4) = P_z/K \quad (2.12.1)$$

Referring to Figure (2.5) and APPENDIX (2-I) and taking a = b the displacement equation can be expressed in finite difference approximations for any mesh point (say) 0, as follows:

$$(k'/a^4)(6W_o - 4W_1 - 4W_3 + W_9 + W_{11}) + (2/a^4)(4W_o - 2\Sigma W_1 + \Sigma W_5) + (k''/a^4)(6W_o - 4W_2 - 4W_4 + W_{10} + W_{12}) = P_z/K \quad (2.21.1)$$

Rearranging:

$$(6k' + 6k'' + 8)W_o - 4(k' + 1)(W_1 + W_3) - 4(k'' + 1)(W_2 + W_4) + 2(W_5 + W_6 + W_7 + W_8) + k'(W_9 + W_{11}) + k''(W_{10} + W_{12}) = (P_z/K) \cdot a^4 \quad (2.21.2)$$

(Note: It is usual practice to reduce the displacement equation to a non-dimensional form before using finite difference approximations. The above displacement equations were solved in two different ways, firstly, retaining its usual form and using finite difference approximation, and secondly, non-dimensionalising the equation and then using the finite difference approximations.)

Therefore for n-number of mesh points there will be n-number of equations. Assuming loading to be uniformly distributed, the equations thus obtained can be written in the form:

$$\begin{bmatrix} A_{11} & A_{12} & \cdots & A_{1n} \\ A_{21} & A_{22} & \cdots & A_{2n} \\ \vdots & & & \\ A_{n1} & & \cdots & A_{nn} \end{bmatrix} \begin{bmatrix} W_1 \\ W_2 \\ \vdots \\ W_n \end{bmatrix} = \begin{bmatrix} 1 \\ 1 \\ \vdots \\ 1 \end{bmatrix} \quad x\,(P_z/K)\,a^4 \qquad (2.22.1)$$

The equations for interior points of the plate can be written down by inspection. But the difficulty arises at points near the boundaries which are to be obtained by considering the boundary conditions of the individual problem.

2.1.4(a) Simply Supported Plate

For a simply supported plate W = 0 on the edge. Therefore the equations for unknown values of W are only required for mesh points next to the edge. For a point (Figure 2.9) centred one mesh length inside the edge, there will be only one fictitious point one mesh length outside the edge. In order to evaluate such a fictitious value the expressions for moments M_x and M_y will be used. For a simply supported plate at the edge $M_x = M_y = 0$. Therefore

$$M_x = -(K_x(\partial^2 W/\partial x^2) + \mu K(\partial^2 W/\partial y^2)) = 0 \qquad (2.6.1)$$

or $$M_x = -K_x(W_1 + W_3 - 2W_o) - \mu K(W_2 + W_4 - 2W_o) = 0 \qquad (2.23.1)$$

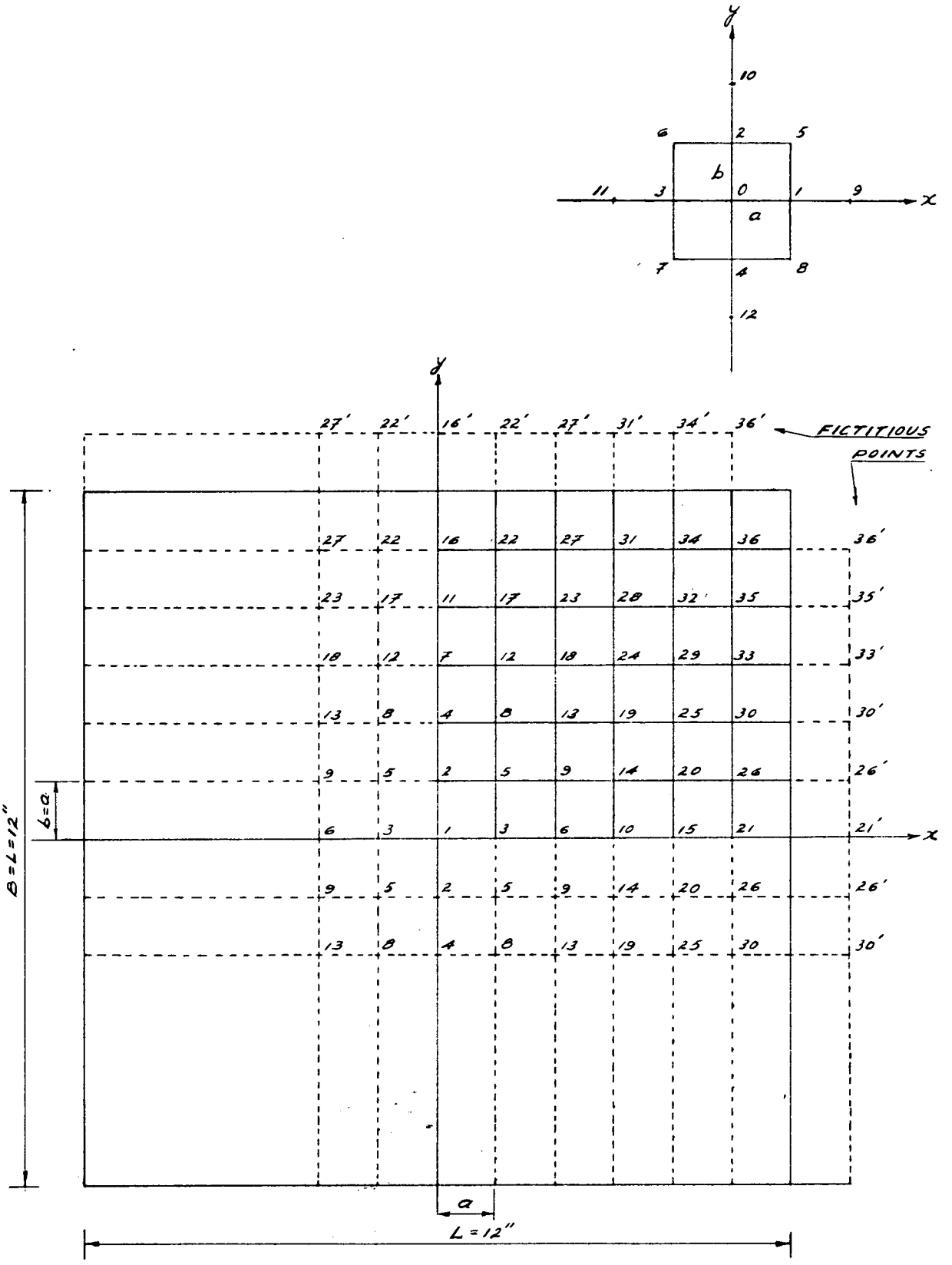

SIMPLY SUPPORTED PLATE : GRIDS.

FIGURE : 2-9.

at edge $x = 0$, $W_o = W_2 = W_4 = 0$

$$\therefore \quad W_1 = -W_3$$

Similarly for $M_y = 0$

$$W_2 = -W_4$$

Having found the values for the fictitious points the set of linear equations are written down for all the mesh points in the form of equations (2.22.1) The solutions of which are obtained by the KDF9 computer by using a standard routine "solve (K)" of the form $Ax = B$. Since the right hand side of the matrix is constant quantity the value for B in the program is used as unity. To obtain the true values of W_1, W_2 etc., each of these is multiplied by the quantity $P_z(a^4/K)$. By knowing the deflections W_1, W_2 ... etc., the moments, stresses and strains at any point can be determined.

Moments:

$$M_x = -K_x(\partial^2 W/\partial x^2) - \mu K(\partial^2 W/\partial y^2)$$

$$= -K_x(W_1 + W_3) + 2(K_x + \mu K)W_o - \mu K(W_2 + W_4) \qquad (2.24.1)$$

Similarly,

$$M_y = -K_y(W_2 + W_4) + 2(K_y + \mu K)W_o - \mu K(W_1 + W_3) \qquad (2.24.2)$$

$$M_{xy} = -K(1 - \mu)(\partial^2 W/\partial x\, \partial y)$$

$$= -(K(1 - \mu)/4a^2)(W_5 - W_6 + W_7 - W_8) \qquad (2.24.3)$$

Stresses

$$\sigma_x = M_x d/I_x \qquad (2.19.1)$$

$$\sigma_y = M_y d/I_y \qquad (2.19.2)$$

$$T_{xy} = M_{xy} D/I \qquad (2.19.3)$$

Strains

$$\epsilon_x = (1/E)(\sigma_x - \mu\,\sigma_y) \qquad (2.20.1)$$

$$\epsilon_y = (1/E)(\sigma_y - \mu\,\sigma_x) \qquad (2.20.2)$$

$$\gamma_{xy} = T_{xy}/G \qquad (2.20.3)$$

The above values for the plate solved by Navier's method are computed using a computer and the computer programs are included in Appendix(2.3). It is to be noted that while writing down the program, some of the notation is changed for convenience. The values of W, M_x, M_y, M_{xy}, σ_x, σ_y and T_{xy}. are shown in Figures (2-10 to 13).

The values of W, M_x, M_y σ_x, σ_y obtained both by Navier's method and Finite Difference/Computer method are compared in Figures (2-14 to 16).

2.1.4 (b) Plate: Fixed on all Four Edges

The solution of a plate fixed on all four edges is similar to that of the simply supported case except that due to the difference in boundary conditions the values of the fictitious points one mesh length outside the edge are changed. For a fixed plate the slope at the boundary is zero.

Therefore at the edge,

$$(\partial W/\partial x) = (\partial W/\partial y) = 0$$

or $$(1/2a)(W_1 - W_3) = 0$$

i.e. $$W_1 = W_3$$

and $$(1/2a)(W_2 - W_4) = 0$$

i.e. $$W_2 = W_4$$

In the case of a fixed edge condition the fictitious points W_1 and W_2 take the values of $+W_3$ and $+W_4$ respectively whereas in the simply supported case

$W \times 10^2$

FINITE DIFFERENCE METHOD

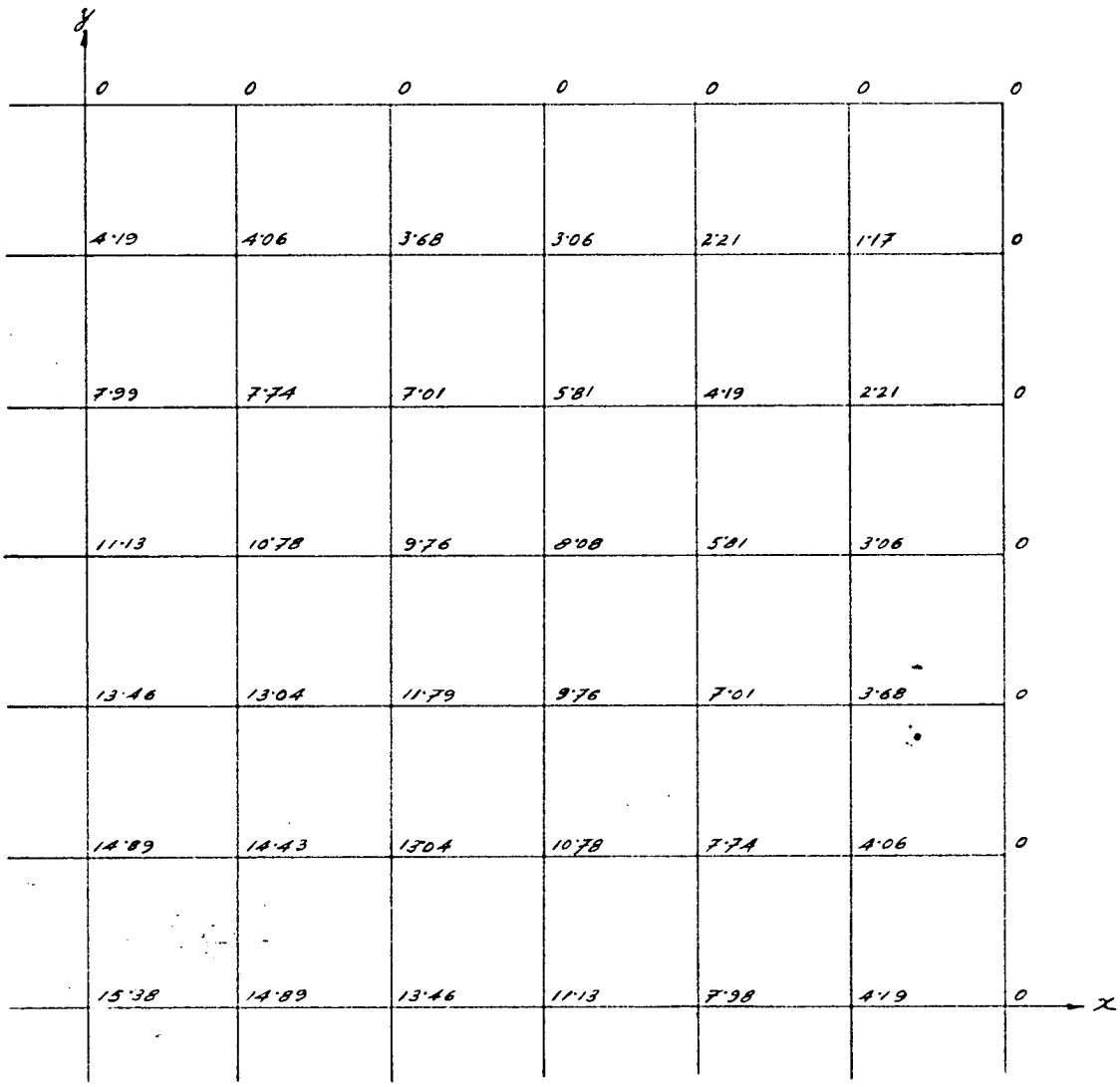

LOAD = 1 lb/in.^{2}

$E = 4{\cdot}2 \times 10^5$ lb/in.^{2}

$\mu = 0{\cdot}35$

VERTICAL DEFLECTIONS IN INCHES.

PLATE : SIMPLY SUPPORTED.

FIGURE : 2-10.

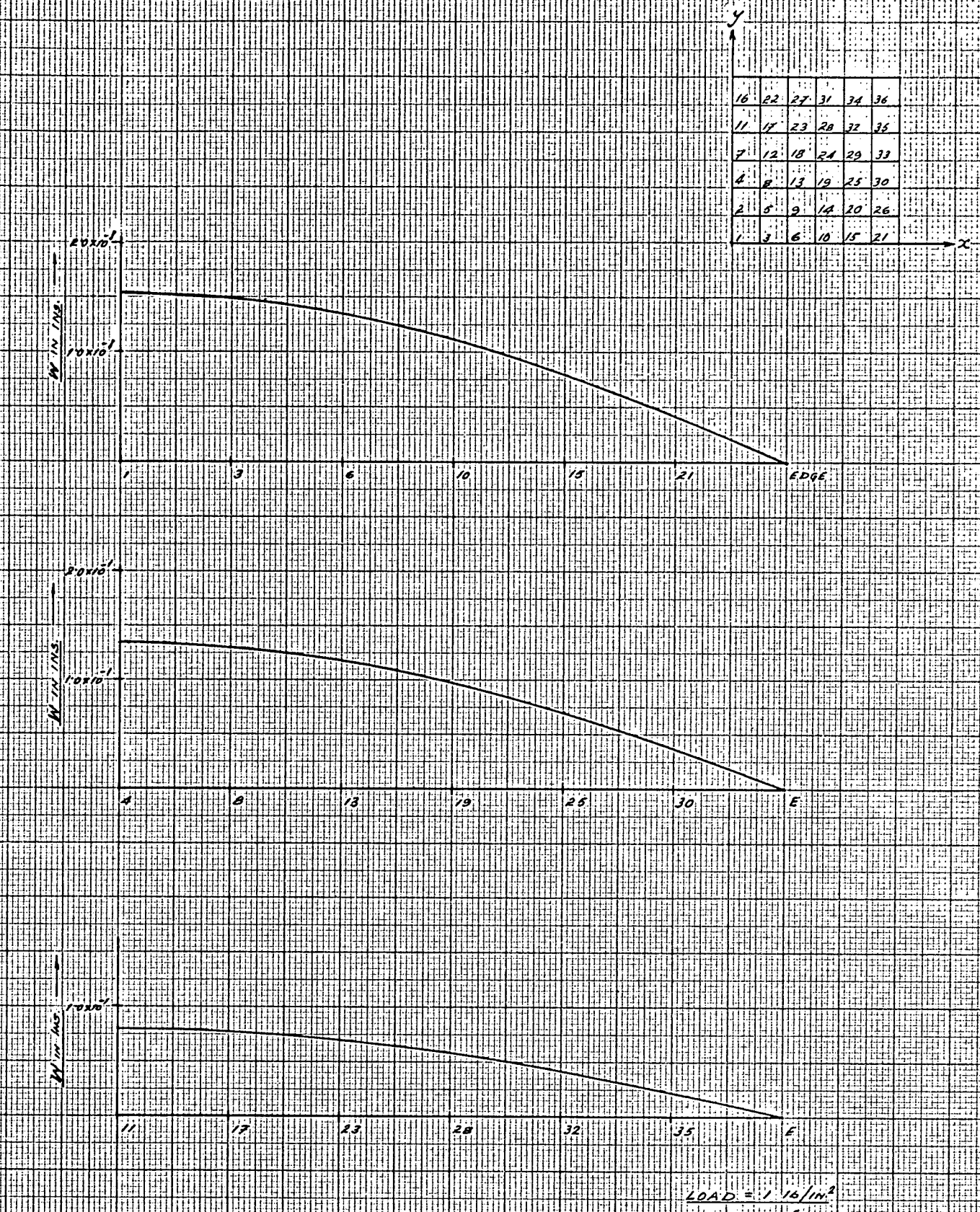

LOAD = 1 lb/in²

E = 4·2 × 10⁶ lb/in²

μ = 0·35

DEFLECTION IN INCHES

PLATE: SIMPLY SUPP.

FIGURE: 2-11

M_y	M_{xy}
	M_x

FINITE DIFFERENCE METHOD

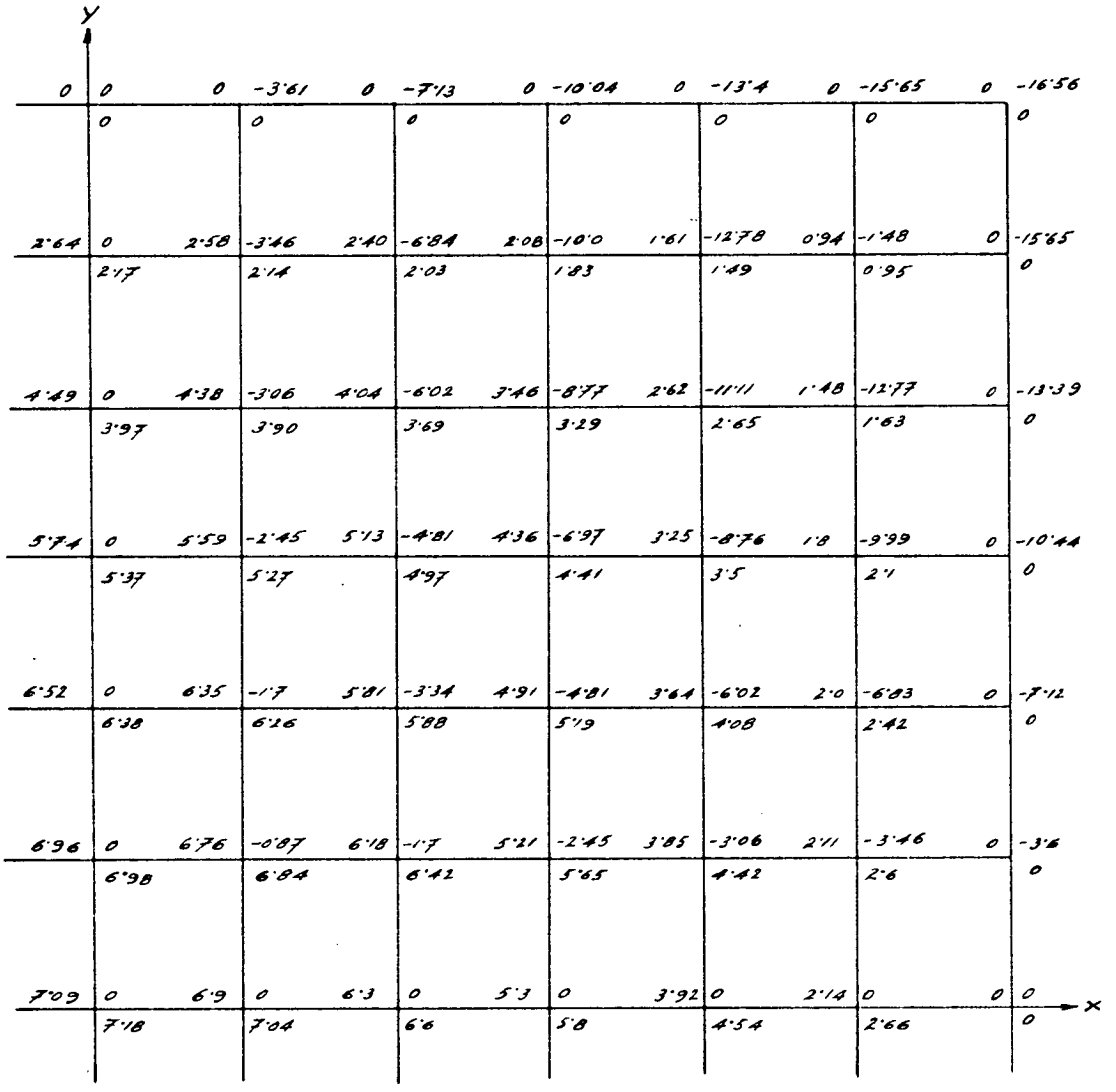

LOAD = 1 lb/in.^{2}

$E = 4{\cdot}2 \times 10^5$ lb/in.^{2}

$\mu = 0{\cdot}35$.

MOMENTS IN LB.IN.

PLATE: S.S.

FIGURE: 2-12.

$\sigma_y \times 10^{-2}$	$\tau_{xy} \times 10^{-2}$
	$\sigma_x \times 10^{-2}$

FINITE DIFFERENCE METHOD.

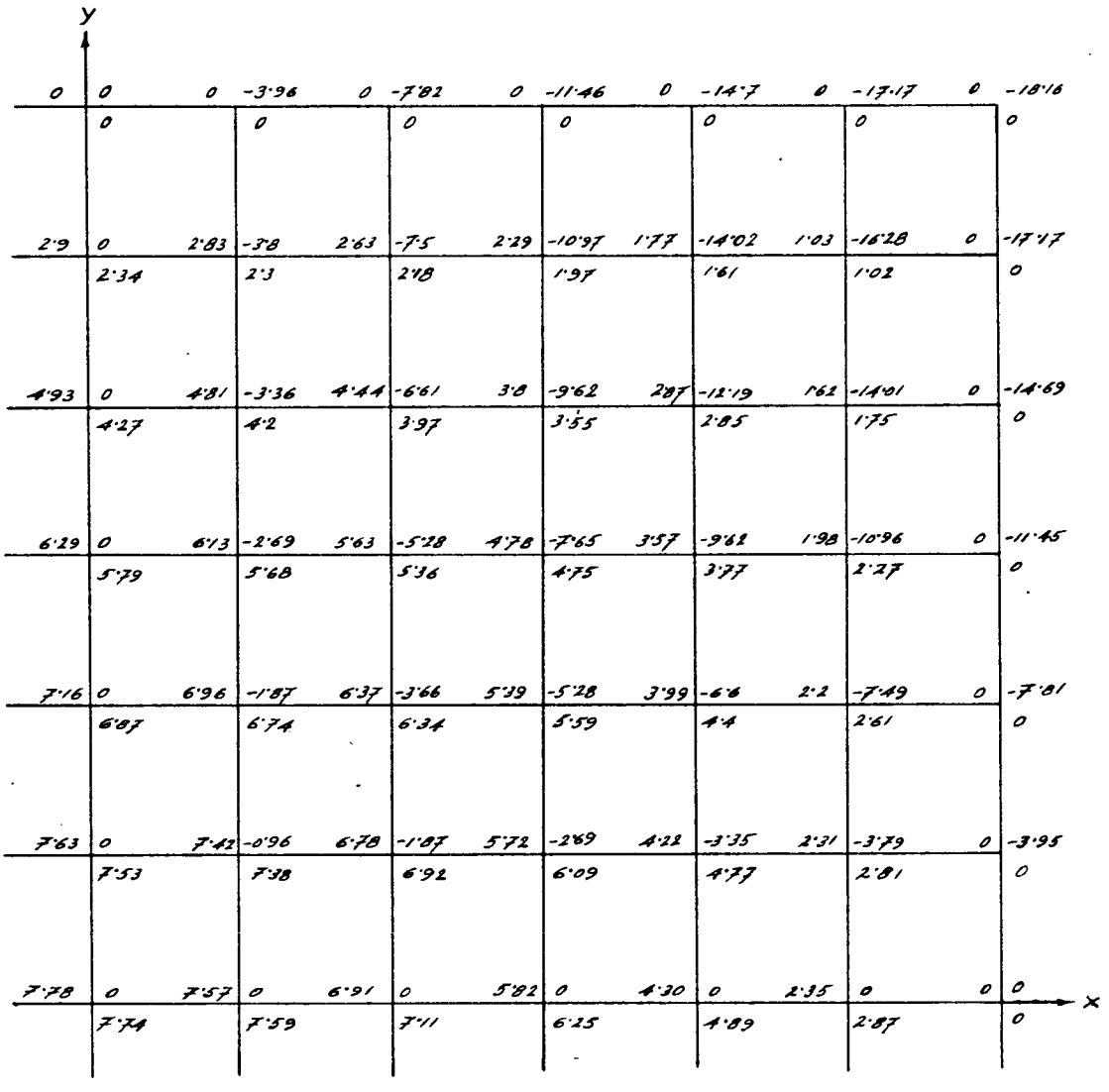

LOAD = 1 lb/in.^{2}

$E = 4{\cdot}2 \times 10^5$ lb/in.^{2}

$\mu = 0{\cdot}35$

STRESSES IN LB/INCH.^{2}

PLATE : S.S.

FIGURE:2-13.

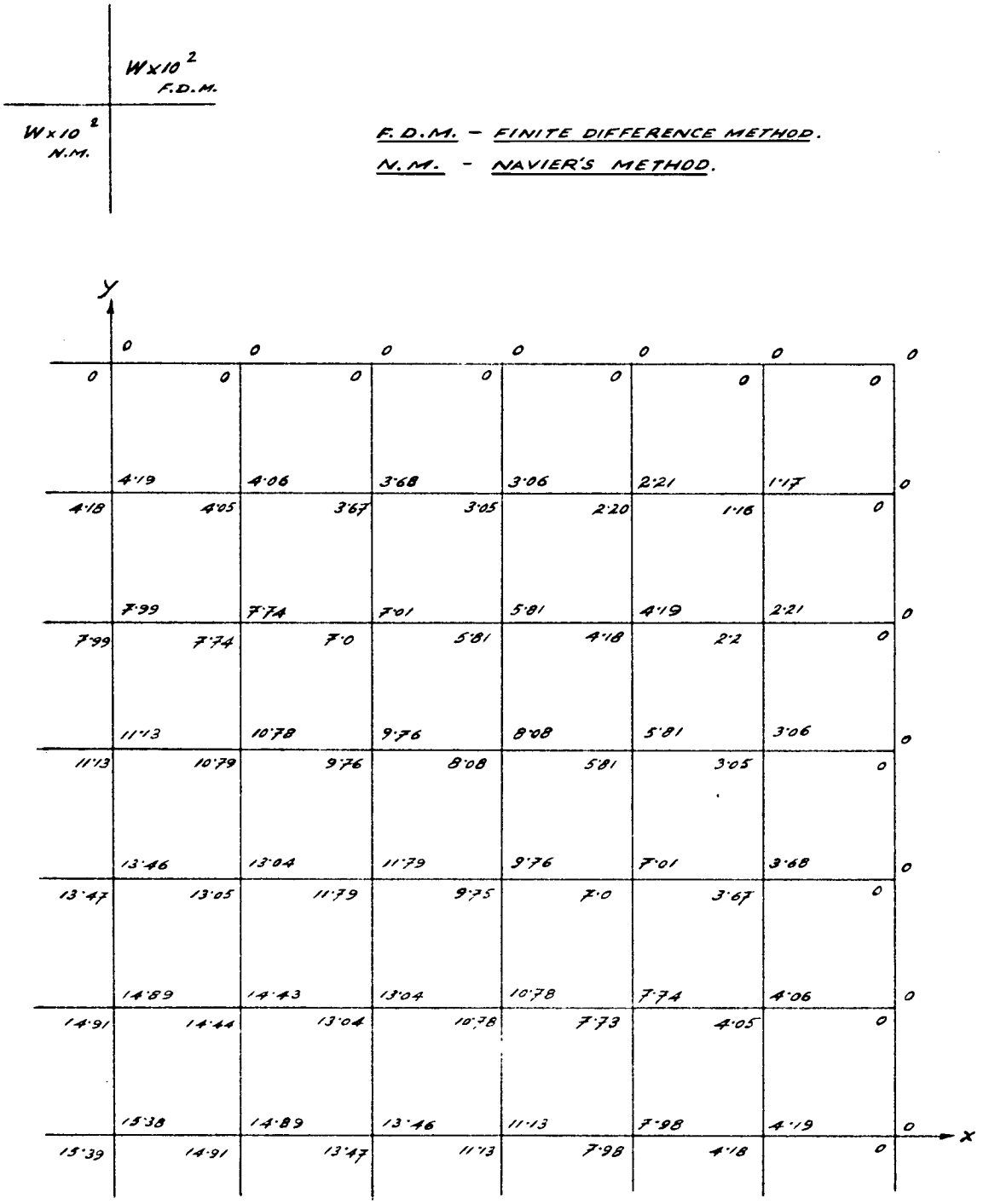

LOAD = 1 lb/INCH.^{2}

$E = 4{\cdot}2 \times 10^5$ lbs/IN.^{2} ; $\mu = 0{\cdot}35$.

VERTICAL DEFLECTIONS IN INCHES.

PLATE: SIMPLY SUPPORTED.

FIGURE: 2-14.

M_y N.M.	M_x N.M.
M_y F.D.M.	M_x F.D.M.

N.M. - NAVIER'S METHOD.

F.D.M. - FINITE DIFF. METHOD.

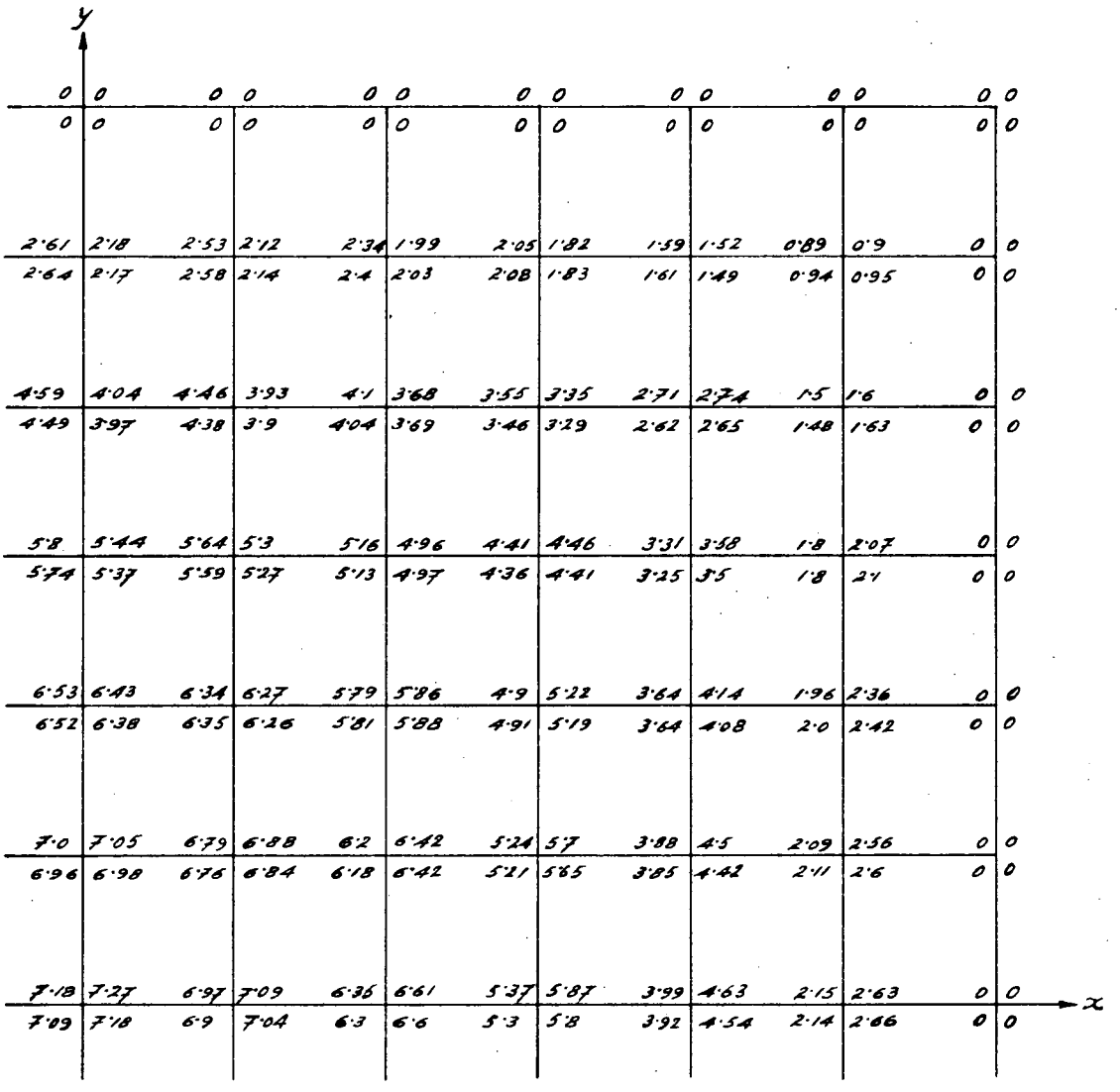

LOAD = 1 lb/in.^{2}

E = $4·2 \times 10^5$ lb/in.^{2}

μ = 0·35.

MOMENTS IN LB.IN.

PLATE : S.S.

FIGURE : 2-15.

$\sigma_y \times 10^{-2}$ N.M.	$\sigma_x \times 10^{-2}$ N.M.
$\sigma_y \times 10^{-2}$ F.D.M.	$\sigma_x \times 10^{-2}$ F.D.M.

N.M. = NAVIER'S METHOD.

F.D.M. = FINITE DIFF. METHOD.

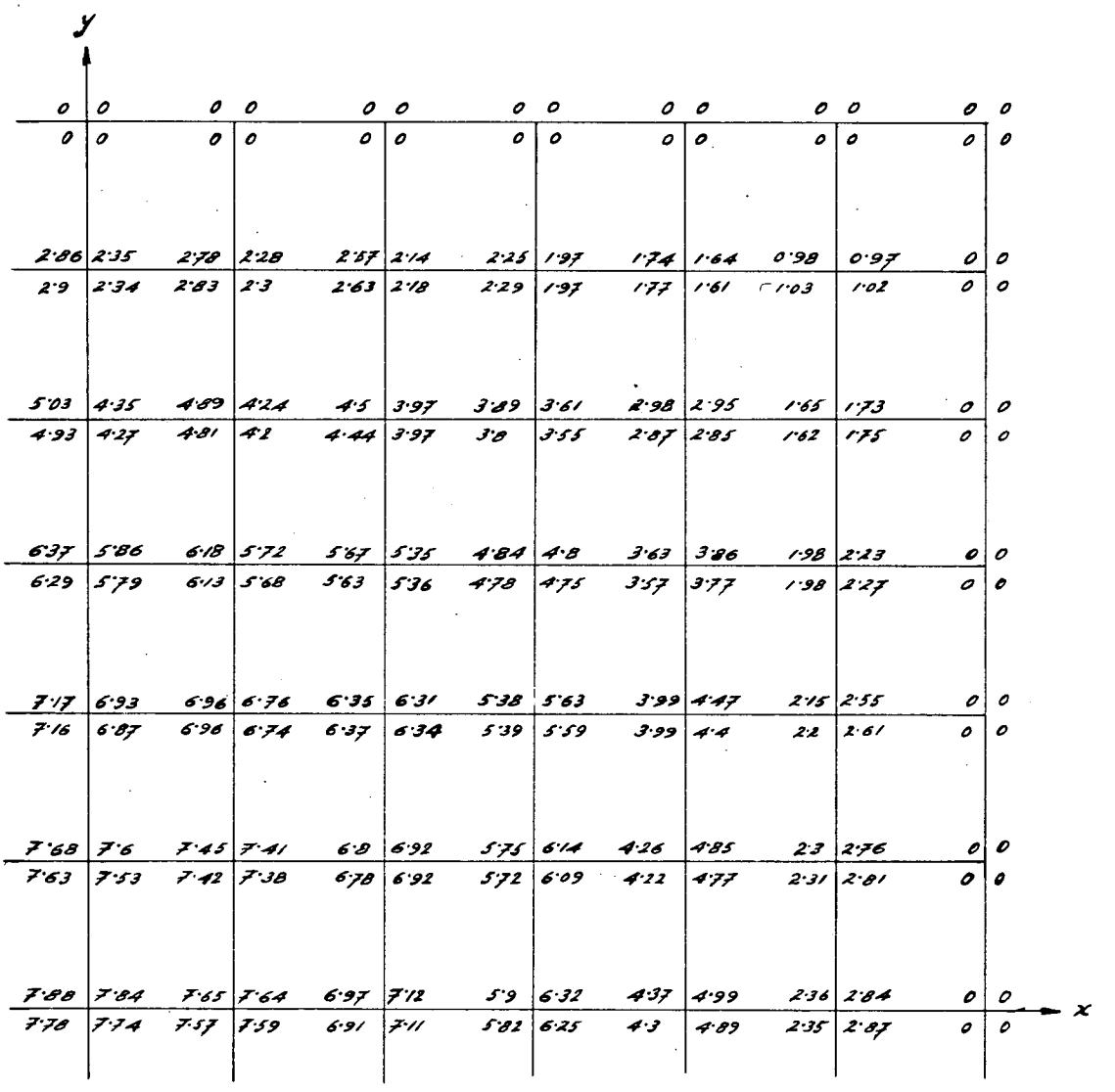

LOAD = 1 lb./in.^{2}

$E = 4{\cdot}2 \times 10^5$ lb/in.^{2}

$\mu = 0{\cdot}35$.

STRESSES IN LB./IN.^{2}

PLATE: S.S.

FIGURE: 2-16.

the values are $-W_3$ and $-W_4$ respectively.

Having obtained the values of the fictitious points the set of linear equations are written down as before in the form of equations (2.22.1). Solutions of which are obtained by using the computer as explained previously.

2.1.4(c) Plate: Free at Four Edges, Supported on Four Corners

Again a similar procedure is used as in the previous cases but this problem is more complicated due to the fact that there are too many fictitious points. Both in the x and y directions, for each displacement equation there will be 3 fictitious points one mesh length outside the free edge and 1 fictitious point two mesh lengths outside the free edge. The fictitious values are obtained as follows: (Figure (2-17)).

On the free edge, conditions are:

1(a) $$M_y = -K_y(\partial^2 W/\partial y^2) - \mu K(\partial^2 W/\partial x^2) = 0$$

$$= K_y(W_2 + W_4 - 2W_o) + K(W_1 + W_3 - 2W_o) = 0$$

$$\therefore \quad W_4 = 2(1 + K_1)W_o - K_1 W_1 - W_2 - K_1 W_3 \qquad (2.25.1)$$

where $K_1 = \mu K/K_y$

Taking the origin at (1) and (3) values for fictitious points (7) and (8) are obtained as:

$$W_8 = -K_1 W_o + 2(1 + K_1)W_1 - W_5 - K_1 W_9 \qquad (2.25.2)$$

$$W_7 = -K_1 W_o + 2(1 + K_1)W_3 - W_6 - K_1 W_{11} \qquad (2.25.3)$$

1(b) Using $M_x = 0$ at the edge, values of the fictitious points (1), (5) and (8) follow:

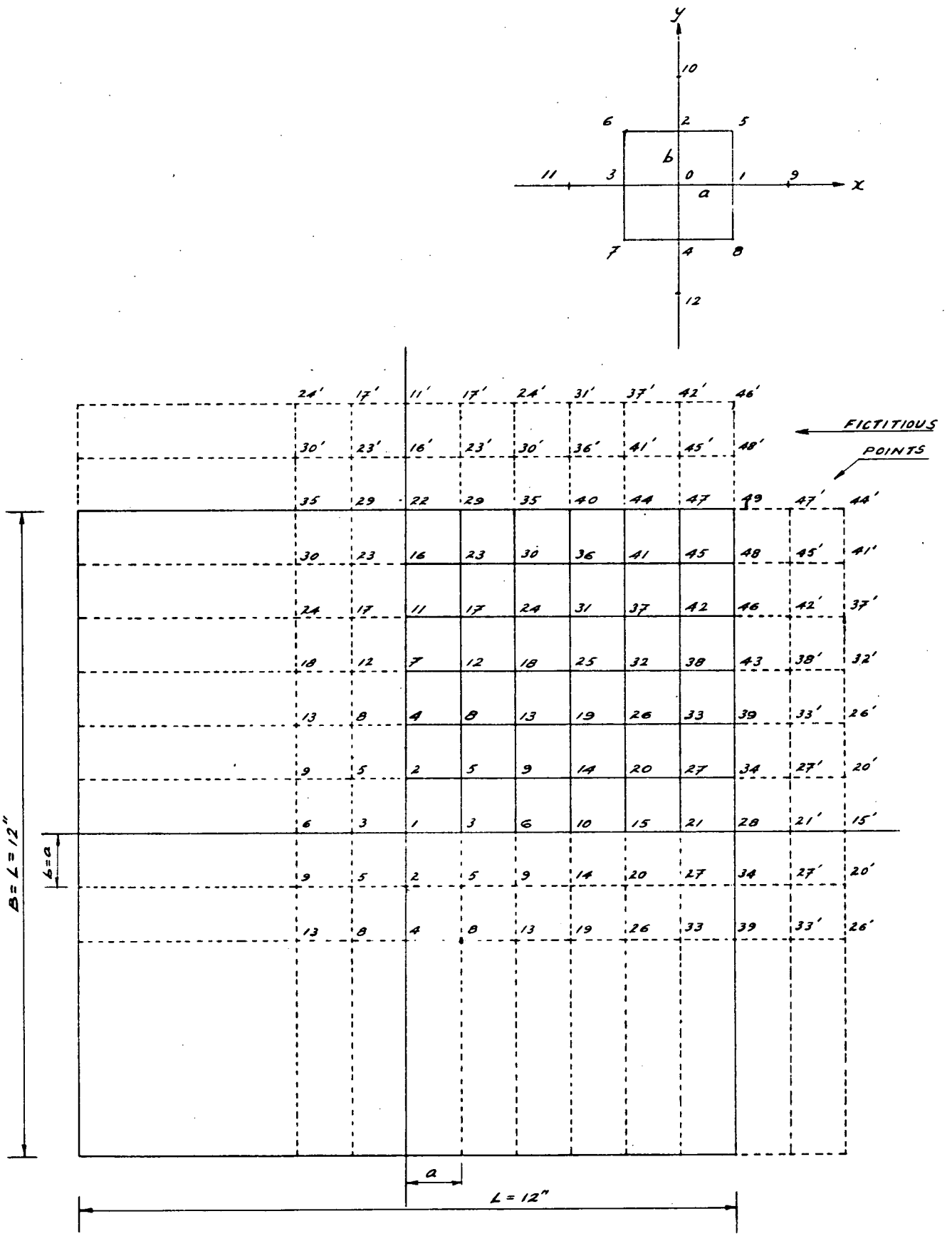

PLATE: SIMPLY SUPPORTED AT FOUR CORNERS.

FIGURE: 2-17.

$$W_1 = 2(1 + K_2)W_o - W_3 - K_2W_2 - K_2W_4 \qquad (2.25.4)$$

$$W_5 = - K_2W_o + 2(1 + K_2)W_2 - W_6 - K_2W_{10} \qquad (2.25.5)$$

$$W_8 = - K_2W_o + 2(1 + K_2)W_4 - W_7 - K_2W_{12} \qquad (2.25.6)$$

where $K_2 = \not{\kappa} K/K_x$

2(a) $$Q_y + \partial M_{xy}/\partial x = 0 \qquad (2.26.1)$$

or $$K_y(\partial^3 W/\partial y^3) + K(2 - \mu)(\partial^3 W/\partial x^2 \partial y) = 0 \qquad (2.26.2)$$

or $$K_y(W_{10} - 2W_2 + 2W_4 - W_{12}) + K_3(W_5 - W_8 - 2W_2 + 2W_4 + W_6 - W_7) = 0 \qquad (2.26.3)$$

where $K_3 = K(2 - \mu)$

from which

$$W_{12} = 2(1 + K_4)W_4 - 2(1 + K_4)W_2 - K_4(W_7 + W_8 - W_5 - W_6) + W_{10}$$

where $K_4 = K_{3/K_y}$ (2.26.4)

In this expression for W_{12}, a fictitious value two mesh lengths outside the free edge, values of W_4, W_7 and W_8 are the fictitious values. Substituting for W_4, W_7 and W_8 as already obtained, the fictitious value of W_{12} becomes:

$$W_{12} = (4(1 + K_4)(1 + K_1) + 2K_4K_1)W_o - (2(1 + K_4)K_1 + 2K_4(1 + K_1))W_1 - 4(1 + K_4)W_2 - (2K_1(1 + K_4) + 2K_4(1 + K_1))W_3 + 2K_4W_5 + 2K_4W_6 + K_4K_1W_9 + W_{10} + K_4K_1W_{11} \qquad (2.26.5)$$

Similarly the fictitious value W_9, two mesh lengths outside the free edge can be obtained by using the condition:

$$Q_x + (\partial M_{xy}/\partial y) = 0 \qquad (2.27.1)$$

And the fictitious value is:

$$W_9 = (4(1 + K_2)(1 + K_5) + 2K_2K_5)W_o - (2(1 + K_5)K_2 + 2(1 + K_2)K_5)W_2 - 4(1 + K_5)W_3 - (2K_2(1 + K_5) + 2(1 + K_2)K_5)W_4 + 2K_5W_6 + 2K_5W_7 + K_2K_5W_{10} + W_{11} + K_2K_5W_{12} \qquad (2.27.2)$$

Having found the values of the fictitious points the displacement equation for each mesh point in finite difference approximations are written down in the form of the equations (2.22.1) and the solutions of these equations are obtained using a computer. Using the same procedure as before values of M_x, M_y, M_{xy}, σ_x, σ_y, and T_{xy} for the plate used in case (1) are computed and are shown in Figures (2-18 to 21).

Here also convenient notation are used while writing down the Computer Program.

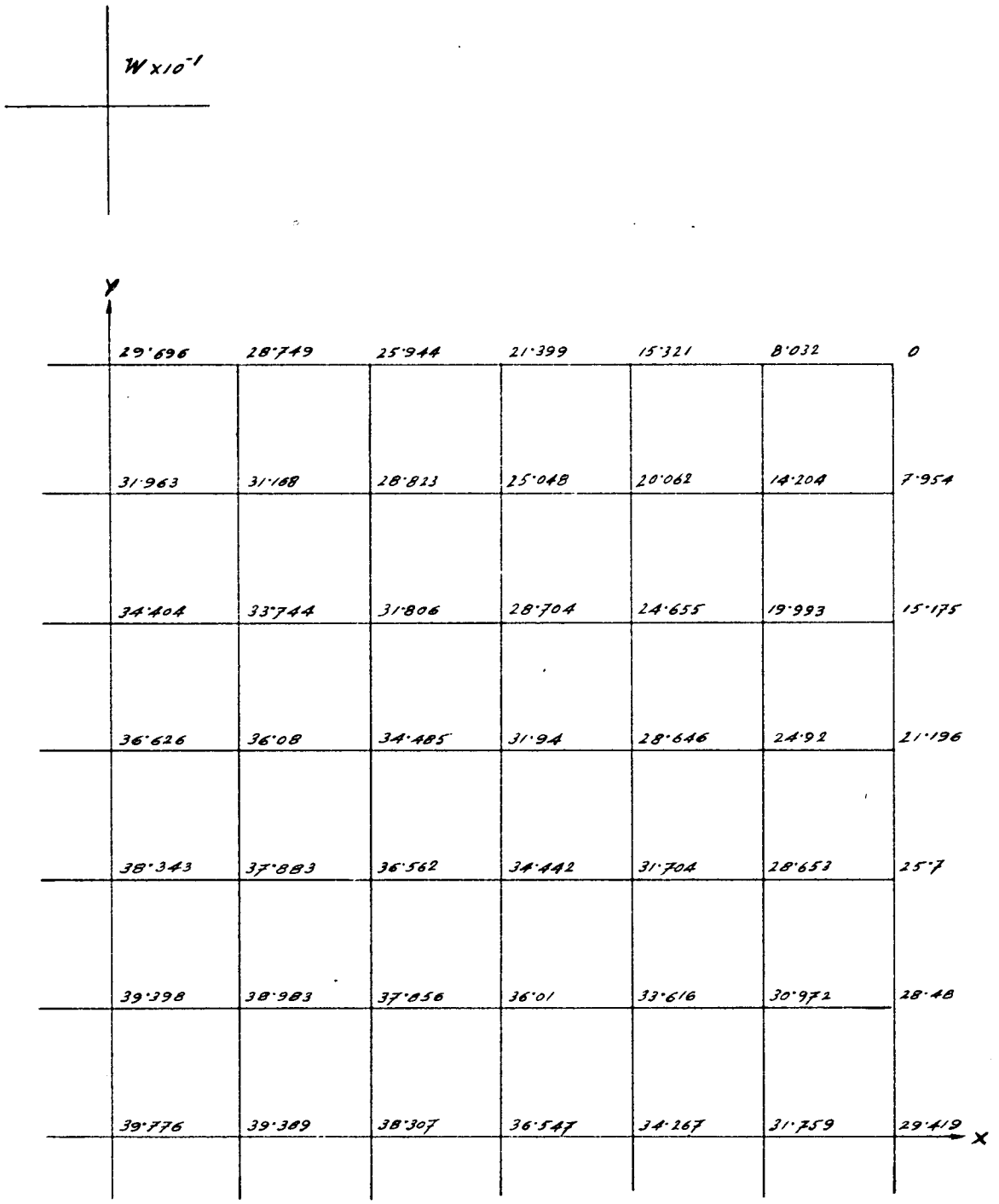

DEFLECTION CO-EFF. FOR UNIT LOAD PER SQ. INCH.

FOR TRUE DEFLECTION MULTIPLY BY $(P_z \cdot a^4/K)$.

PLATE : SIMPLY SUPPORTED AT FOUR CORNERS.

FIGURE: 2-18.

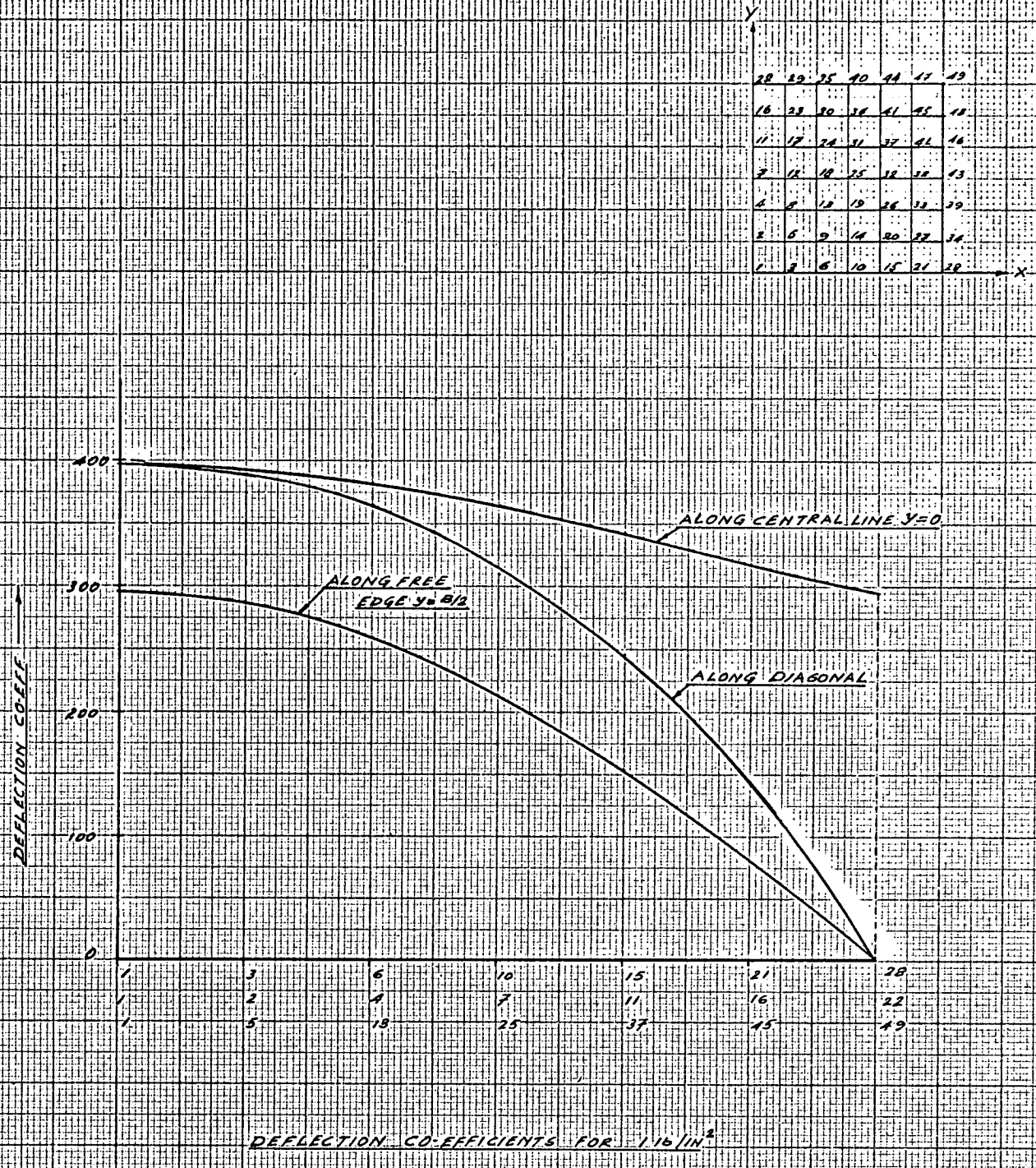

DEFLECTION CO-EFFICIENTS FOR 1/16 IN.

PLATE: SIMPLY SUPPORTED AT FOUR CORNERS.

FIGURE: 2-19

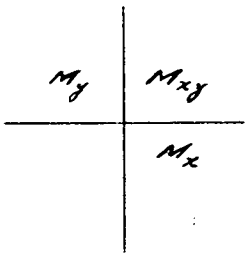

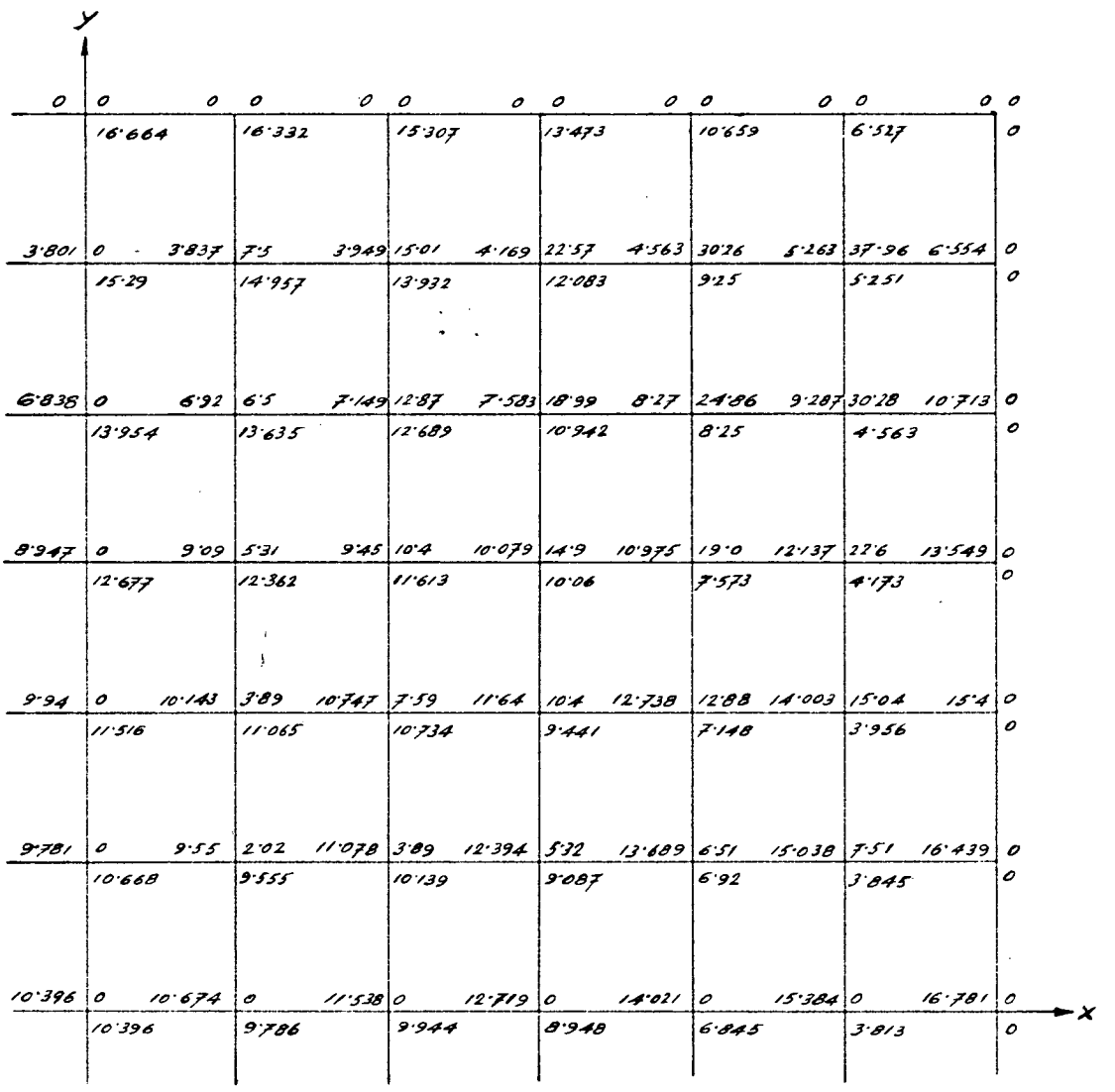

LOAD = 1·0 lb/in^2.

E = 4·2 × 10^5 lb/in.^{2}

μ = 0·35.

MOMENTS IN LB.IN.

PLATE: S.S. AT CORNERS.

FIGURE: 2-20.

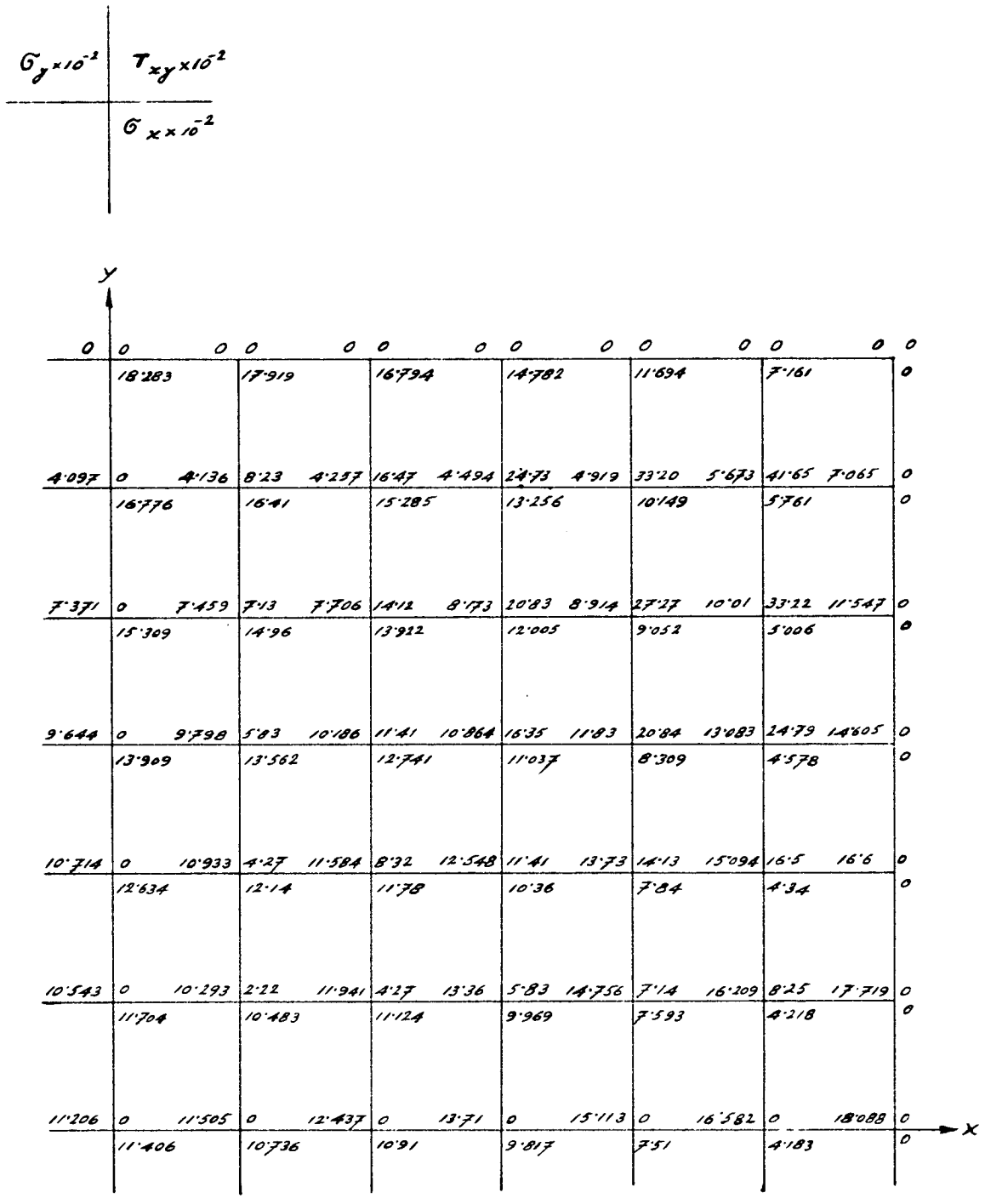

LOAD = 1·0 lb/in.^{2}

E = 4·2 × 10^5 lb/in.^{2}

K = 0·35.

STRESSES IN LB/IN.^{2}

PLATE : S.S. AT CORNERS.

FIGURE : 2-21.

A P P E N D I X (2-1)

FINITE DIFFERENCE APPROXIMATIONS

The finite difference equivalent can be derived using a Taylor's Series.

The following are the finite difference approximations for any quantity 'W' for the point '0' in terms of the values of 'W' at the surrounding nodes:

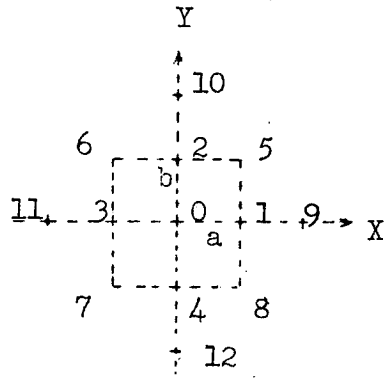

$$\left(\partial W/\partial x\right)_o = 1/2a(W_1 - W_3)$$

$$\left(\partial W/\partial y\right)_o = 1/2b(W_2 - W_4)$$

$$\left(\partial^2 W/\partial x^2\right)_o = 1/a^2(W_1 - 2W_o + W_3)$$

$$\left(\partial^2 W/\partial y^2\right)_o = 1/b^2(W_2 - 2W_o + W_4)$$

$$\left(\partial^2 W/\partial x \partial y\right)_o = 1/4ab(W_5 - W_6 + W_7 - W_8)$$

$$\left(\partial^3 W/\partial x^3\right)_o = 1/2a^3(W_9 - 2W_1 + 2W_3 - W_{11})$$

$$\left(\partial^3 W/\partial y^3\right)_o = 1/2b^3(W_{10} - 2W_2 + 2W_4 - W_{12})$$

$$\left(\partial^3 W/\partial x^2 \partial y\right)_o = 1/2a^2b(W_5 + W_6 - 2W_2 - W_8 - W_7 + 2W_4)$$

$$\left(\partial^3 W/\partial x \partial y^2\right)_o = 1/2ab^2(W_5 - W_6 - 2W_1 + W_8 - W_7 + 2W_3)$$

$$\left(\partial^4 W/\partial x^4\right)_o = 1/a^4(6W_o - 4W_1 - 4W_3 + W_9 + W_{11})$$

$$\left(\partial^4 W/\partial y^4\right)_o = 1/b^4(6W_o - 4W_2 - 4W_4 + W_{10} + W_{12})$$

$$\left(\partial^4 W/\partial x^2 \partial y^2\right) = 1/a^2b^2(2W_o - 2(W_1 + W_2 + W_3 + W_4) + (W_5 + W_6 + W_7 + W_8))$$

CHAPTER 2

PART II

2.2.1 INTRODUCTION

Before applying the theory to a plate built of hollow clay blocks it was decided to apply the theory to plates of hollow cross section built of strips of perspex cemented together. As perspex is considered to be an ideal isotropic material it was decided to test the perspex model and examine the validity of the theory. After this a plate built of hollow clay blocks was tested. From these test results it could be visualized how far the behaviour of plate of hollow clay blocks deviates from the theory which is true for an ideal isotropic material.

2.2.2 PERSPEX MODEL

2.2.2a Construction of Model

Strips of one inch width were cut from 1/16th inch thick perspex sheet. To facilitate the running of cement along the joints, the strips were champhered at both edges as shown in Figure (2.22). A drawing board was used as the mould for building the plate. Strips of double faced cellotape were stretched on the board and the strips of perspex were placed on them. Cellotape was used for two purposes viz. (1) to prevent the flowing down of cement through the joints and (2) to keep the perspex strips in position. The depressions developed along the joints due to shrinkage of cement after

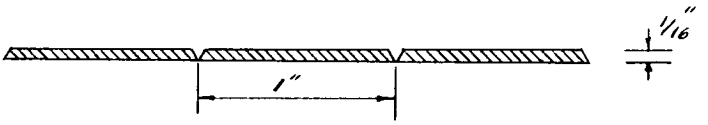

FIGURE: 2-22

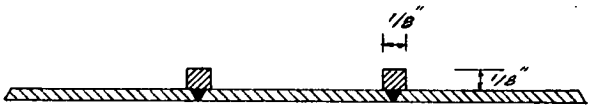

FIGURE: 2-23

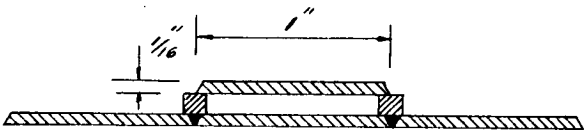

FIGURE: 2-24

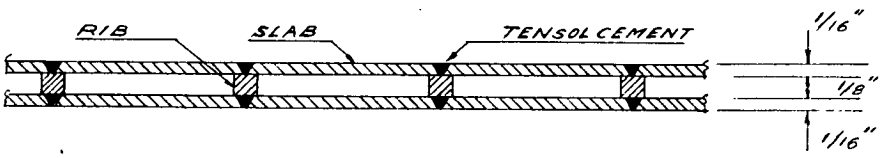

FIGURE: 2-25

the first run were roughened by using a triangular file and sand paper. The cement was run for the second time along the joints. After the cement dried the joints were brought down to level by using sand paper. To fix the ribs, cement was spread on the joints and on one face of the $\frac{1}{8}$in x $\frac{1}{8}$in perspex strip. The later strip was placed on the joint facing the cemented face and a steady pressure was applied, till the cement dried (Figure 2.23). Similar procedure was adopted for the remaining strips. For building the top slab of the plate a sufficient amount of cement was run on the $\frac{1}{8}$in x $\frac{1}{8}$in ribs and also on the edges of 1 in wide strip (after rubbing with sand paper) after which the 1 in strip was placed in position, bridging the two subsequent $\frac{1}{8}$in ribs and kept under constant pressure till the cement dried. Excess cement at the joints were chipped out and cleaned (Figure 2.24). Similar procedure was followed for the rest of the strips. The V-notches formed at the joints due to champhering of 1 in strips were made rough and cleaned and cement was run along the joints. The following day after rubbing and cleaning the depressions cement was run again to fill up the joints and the joints were rubbed down to level by using sand paper (Figure 2.25) Plate (2.1) shows the finished hollow plate before testing.

It is to be noted that before applying cement at any place, it was roughened by sand paper and thoroughly cleaned with Acetone. I.C.I.'s 'Tensol' Cement no.7 was used throughout.

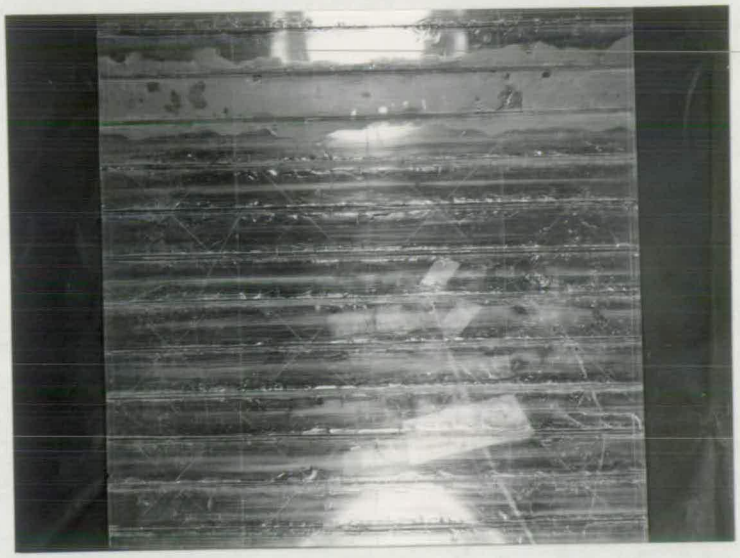

PLATE : 2-1

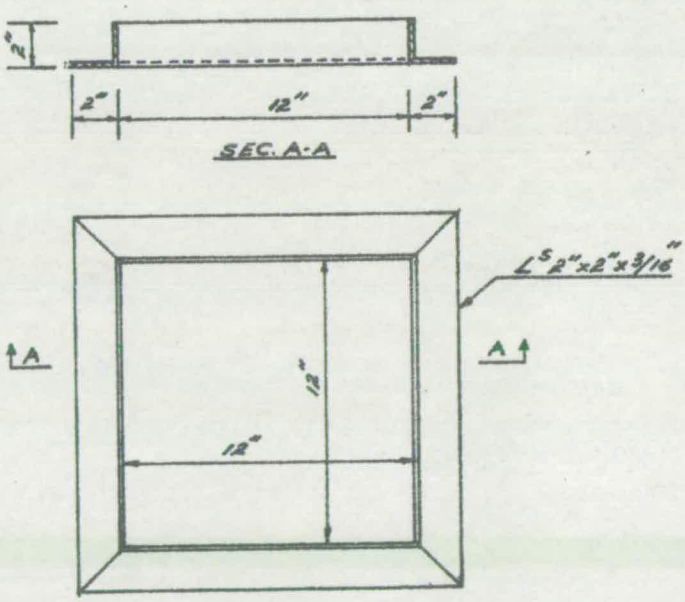

FIBURE : 2-26.

2.2.2b Strain Measurement

Electric resistance strain gauges of foil type, 85Ω, made by Saunders Roe were used for measuring strains. The size of the gauges used were $\frac{1}{4}$in x $\frac{1}{4}$in with a gauge length of $\frac{1}{4}$in. The surface of the plate where strain gauges were to be fixed was rubbed with sand paper and cleaned with Acetone. The gauges were fixed to the plate with Phillips quick hardening strain gauge cement PR 9244/04. Four strain gauges were fixed on the underside of the plate, locations of which are shown in Figure (2.27). Four strain gauges were also fixed on a strip of perspex to act as compensating gauges. Savage and Parsons strain recorder was used for measuring the strains with a voltage of 5 volts the sensitivity being 2.5 $\mu\epsilon$.

2.2.2c Testing Procedure

2.2.2d Simply Supported at all Four Edges

Four pieces of 2in x 2in x 3/16in size angles were cut at 45° angle at both ends and welded together to form a square frame (Figure 2.26) to give a span of 12 inches between the upstand legs. The upstand legs were made levelled by filing and rubbing with emery paper. The frame was clamped finally to steel trestles. For loading model bricks were used. Before placing the loads a sheet of foam rubber was spread on the top of the plate so that the load was evenly distributed.

The strain recorder was balanced and zero adjustment made. To allow for creep, readings were taken 20 minutes after the loads were applied. The strain at any point at any load stage was read directly from the strain recorder using the relation:

$$e = (1/\lambda)(1/100n)(n(100\Delta R/R))$$

$$= (1/\lambda)(1/100n)K$$

where e = strain

λ = Gauge factor

n = sensitivity factor chosen as 1, 2 and 10

$K = n(100\Delta R/R)$

= reading on strain recorder.

The strains at different load intervals are plotted in Figure (2.27), Table (2-1) & Fig. (2.28) shows the comparison between the theoretical and experimental results.

2.2.2e Free at Edges Supported at Four Corners

In this case the plate was placed on four $\frac{3}{8}$in diameter stainless steel balls placed at the four corners. Loading was applied by using cast iron weights. Here also foam rubber was used between the plate and the weights. Rest of the procedure was similar to that of simply supported case.

The strains at different load intervals are plotted in Figure (2.29) Table (2.2) and Figure (2.30) show the comparison between the theoretical and experimental results.

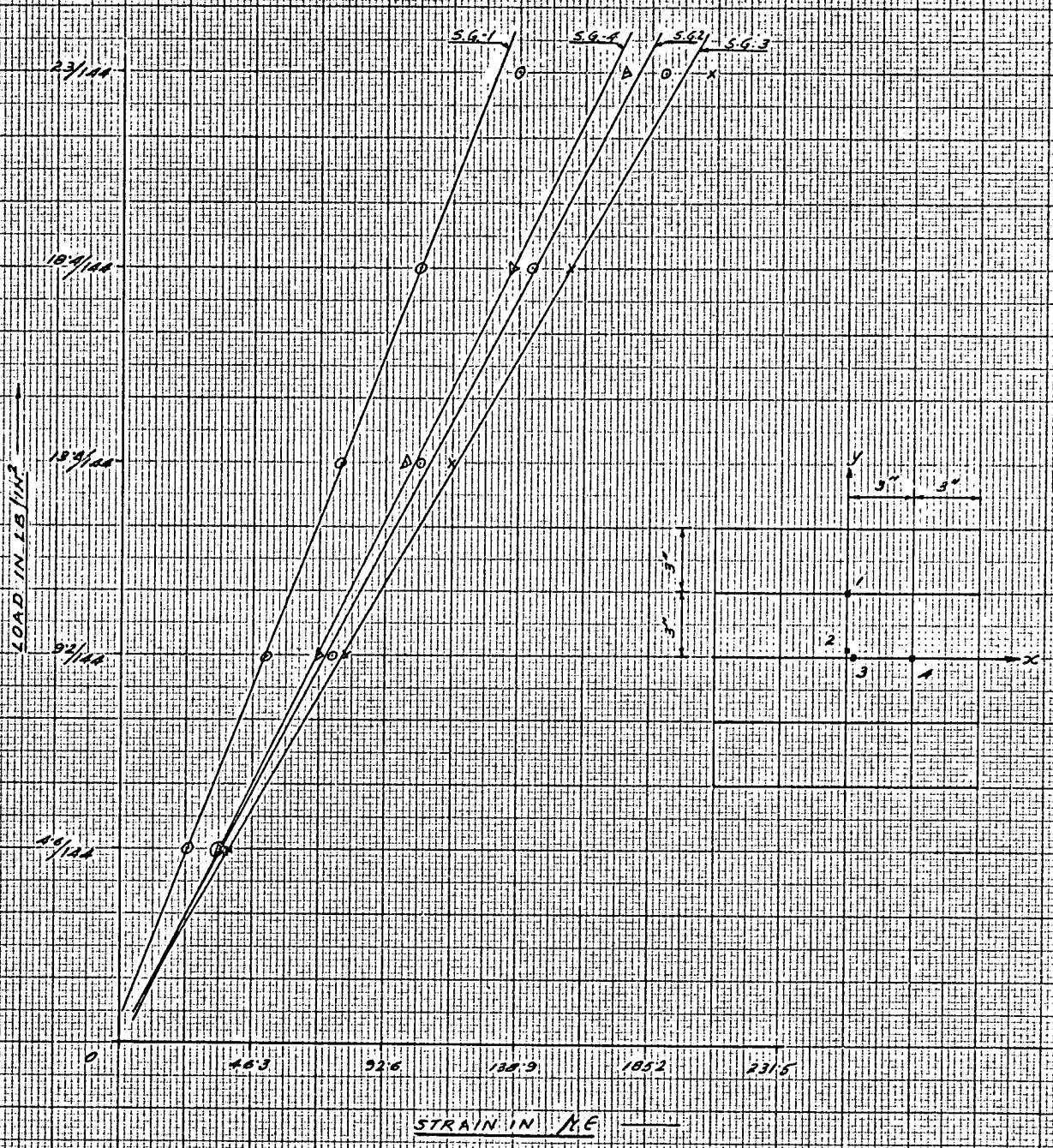

PLATE : SIMPLY SUPPORTED AT EDGES

FIGURE : 2-27

TABLE: 2-1 PERSPEX PLATE - SIMPLY SUPPORTED AT EDGES

EXPERIMENTAL AND THEORETICAL STRAINS

Strain Gauge No.	Location of Strain Gauge (Mesh Point)	Strain ($\mu\epsilon$)		Remarks
		Experimental (From Graph)*	Theoretical	Deviation from Theor. results
1	7	798	920	-13.25%
2	1	1160	1280	- 9.4 %
3	1	1245	1300	- 4.25%
4	10	1050	930	+12.9 %

* Load Intensity = (4.6/144 lb/in^2 from Graph)x(144/4.6) = 1 lb/in^2

TABLE: 2-2 PERSPEX PLATE - SUPPORTED AT FOUR CORNERS

EXPERIMENTAL AND THEORETICAL STRAINS

Strain Gauge No.	Location of Strain Gauge (Mesh Point)	Strain ($\mu\epsilon$)		Remarks
		Experimental (From Graph)*	Theoretical	Deviation from Theor. results
1	7	Not Recorded		
2	1	2040	1850	+10.03%
3	1	2000	1920	+ 4.15%
4	10	920	1230	-25.2 %

* Load Intensity = (1/36 lb/in^2 from Graph) x 36 = 1 lb/in^2

TABLE: 2-3 CLAY BLOCK PLATE - FIXED AT EDGES

EXPERIMENTAL AND THEORETICAL DEFLECTIONS

Dial Gauge No.	Location of Dial Gauge (Mesh Point)	Deflection (10^{-4}inch)		Remarks
		Experimental (From Graph)*	Theoretical	Deviation from Theor. results
1	1	9.38	10.35	- 9.37%
2	10	6.75	6.36	+ 6.13%
3	7	6.7	6.31	+ 6.18%
4	24	3.5	3.93	-10.94%

* Load Intensity = 0.25 lb/in^2

COMPARISON OF STRAINS

PLATE: SIMPLY SUPPORTED AT EDGES.

FIGURE: 2-28

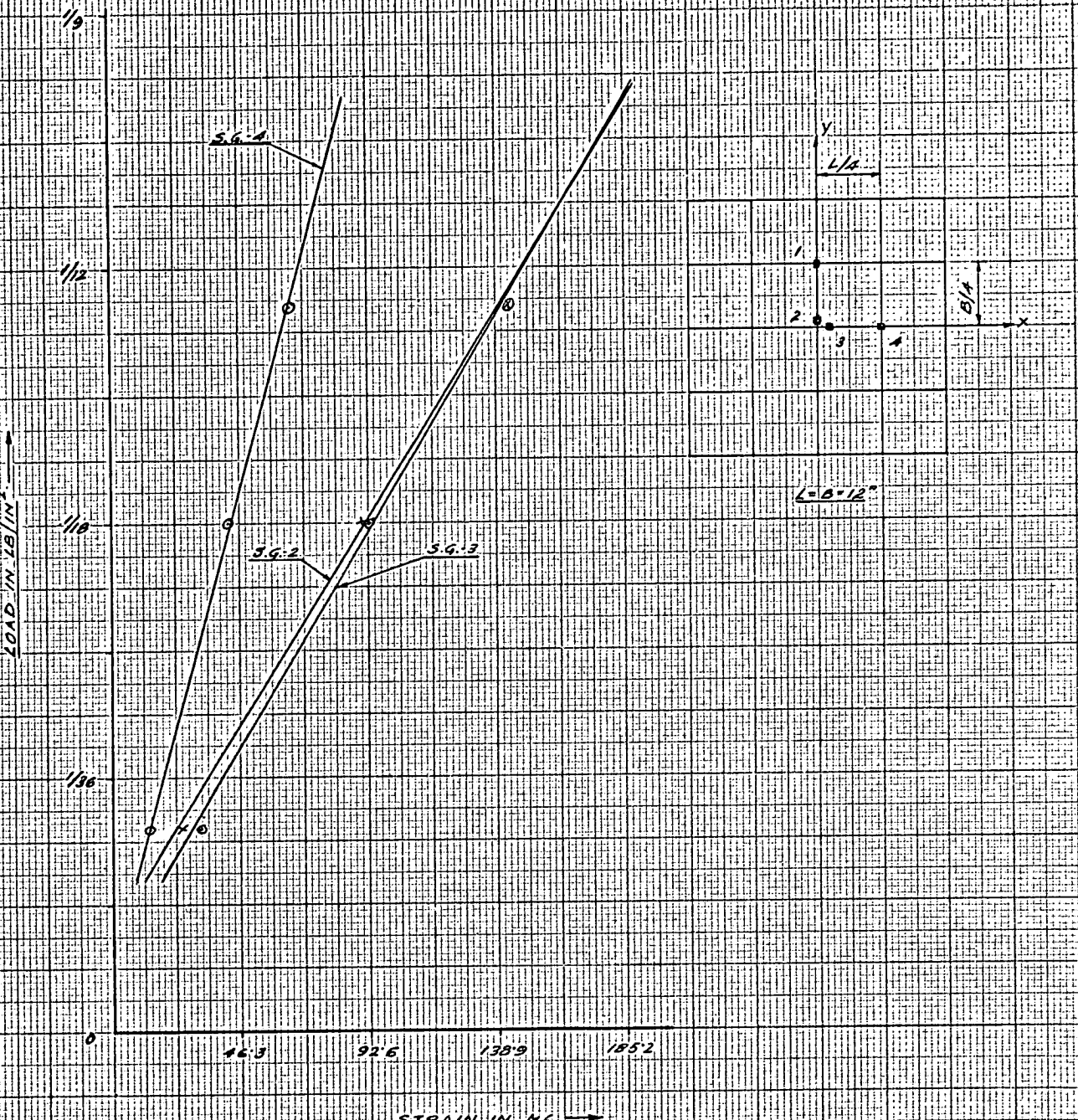

PLATE: SIMPLY SUPPORTED AT CORNERS

FIGURE: 2-29

COMPARISON OF STRAINS

PLATE: SUPPORTED AT FOUR CORNERS

FIGURE: 2-30

2.2.3 PLATE BUILT OF HOLLOW CLAY BLOCKS: FIXED AT ALL SIDES

2.2.3a Construction of Model

A plate fixed at all four edges was built by using 1/6th model hollow clay blocks of $1\frac{3}{8}$in x $1\frac{3}{8}$in x 1in thick (approx.) size. (Plates 2.2 & 3)

As it is very difficult to obtain a perfect fixed condition, it was decided to build the plate on a shuttering and then to cast the edge beams on walls. Four interconnected $4\frac{1}{2}$in thick brick walls with corner pillars were built to a height of 4 feet spanning 2 ft 6 inches inside to inside in each direction. Perforated bricks were used as the top course of the walls for fixing the shear connectors between the walls and the edge beams (Plate 2.4). Openings of 1 ft 9 inches x 2 feet high with steel channels as lintels (Plate 2.5) were kept on two sides of the walls for observation. Plywood of $\frac{7}{8}$in thickness was used as shuttering and in order to facilitate its removal the shuttering was divided into two parts and screwed on the underside to two 4in wide wooden battens. The shuttering was supported by wedges and props fixed from the bottom so that the shuttering could be removed without disturbing the plate after it was built. Square grids were marked on the shuttering for alignment and also to guide the location of the plain hollow clay blocks to which the strain gauges were to be attached. Before starting the construction mould oil was applied to the shuttering and its level checked.

Bottom reinforcement was placed during the construction of the slab. The method of cementing the clay blocks together, is shown in Plates (2.6 & 7), where the bottom reinforcement along the longitudinal joints can

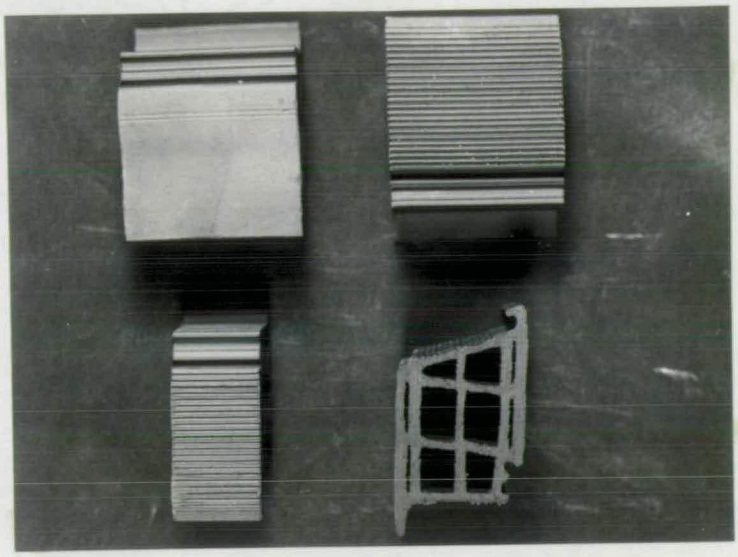

Plate: 2-2

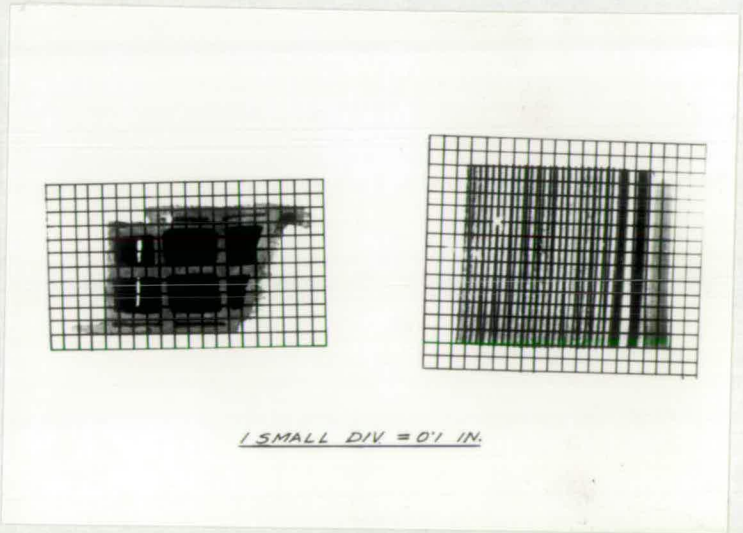

Plate: 2-3

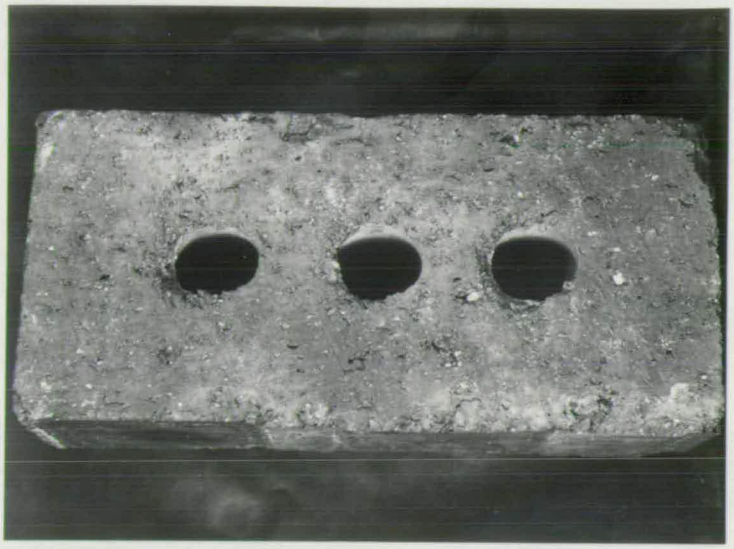

Plate: 2-4

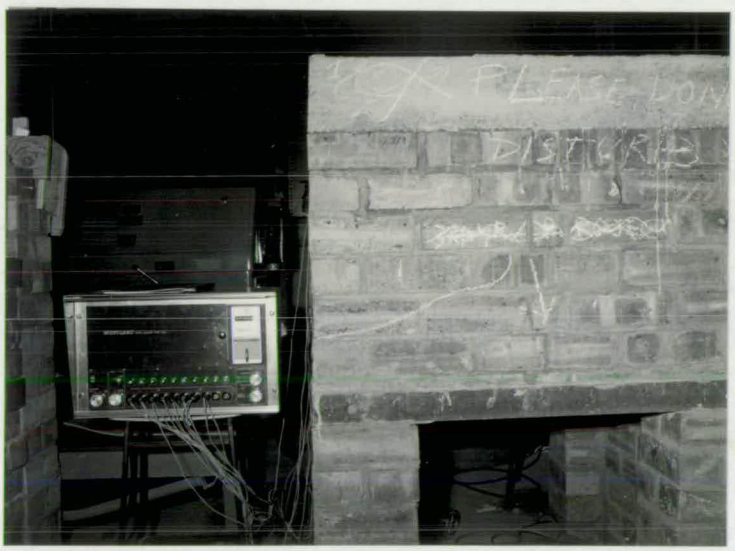

Plate: 2-5

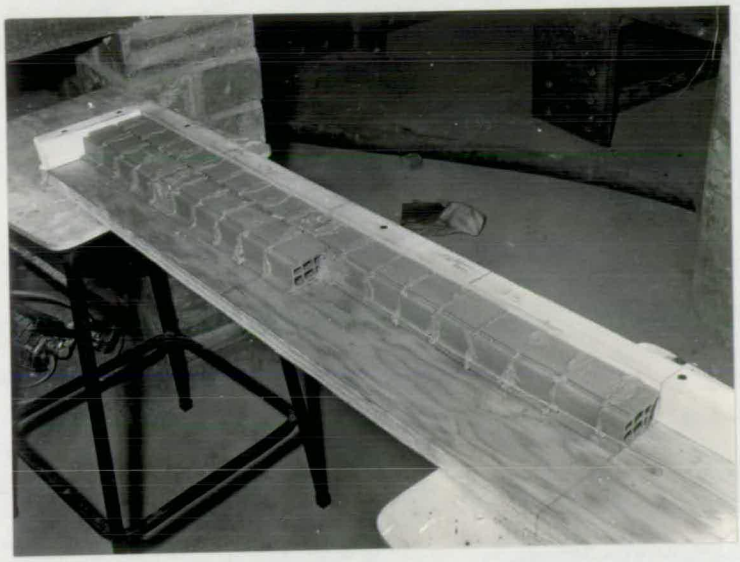

Plate: 2-6

Plate: 2-7

also be seen. Half-size blocks were used for staggering the transverse joints. After two days the top of the slab was brushed with a wire brush and the joints were cleaned to prepare for top reinforcement. The top reinforcement was placed and the joints were filled with mortar (Plate 2.8). Plates(2.9 & 10)show the details of the slab including transverse section at edge and also the reinforcement of the slab.

Reinforced concrete edge beams of 4½in x 6in deep were cast embedding 2in of slab inside them. Vertical reinforcement bars were used as shear connectors between the edge beams and the walls. Plate(2.11)shows the finished slab with edge beams. Proper care was taken for curing of slab and beams.

The mortar used was in the following proportion:

Cement	300 gms.
Sand	900 gms.
Water	175 c.c.

Cement used was ferro cement and sand was Leighton Buzzard No:21.

2.2.3b Strain and Deflection Measurements

Electric resistance strain gauges, of 4 nos. TML PL 10 and 2 nos. PC 10 type, of 120 Ω resistance having 10 mm gauge length were used for measuring strains. The surface of the plain blocks in the plate were rubbed with sand paper and cleaned with Acetone. The strain gauges were fixed with PS cement as recommended by the manufacturer. The location of the gauges is shown in Figure (2.31). 8 nos. PL 10 strain gauges were fixed on plain clay blocks with PS cement to act as compensating gauges.

Plate: 2-8

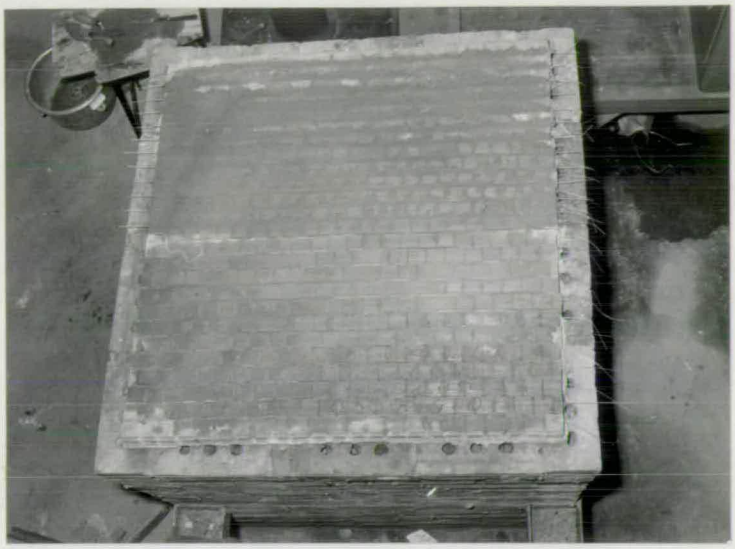

Plate: 2-9

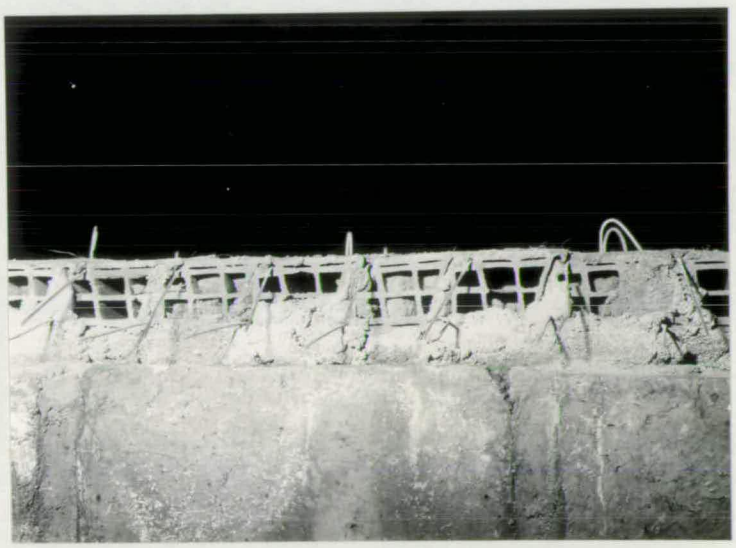

Plate: 2-10

Plate: 2-11

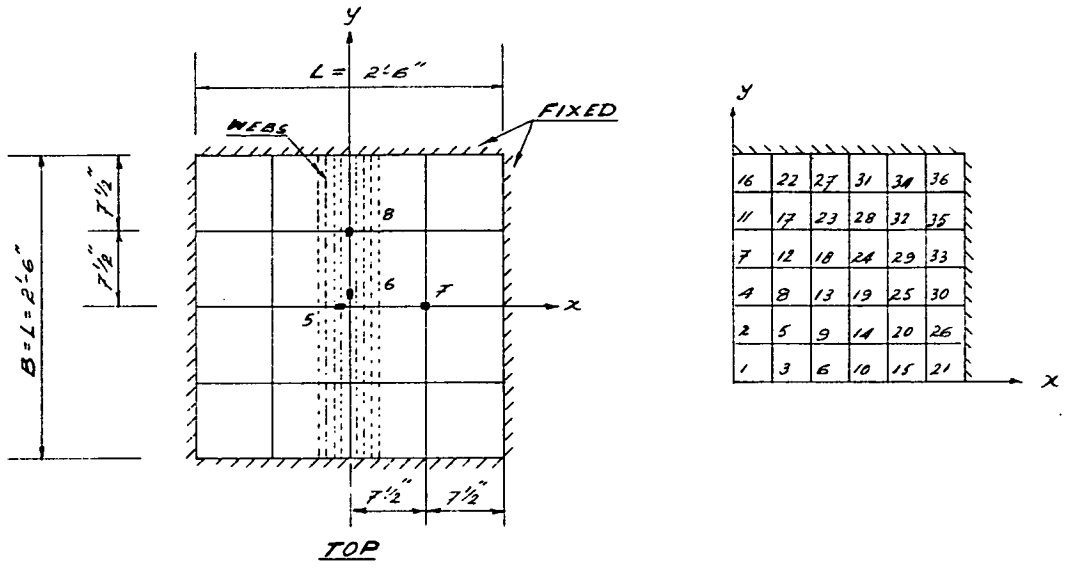

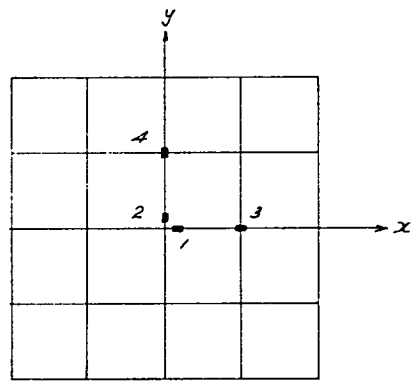

BOTTOM

FIGURE:2-31. LOCATION OF STRAIN GAUGES.

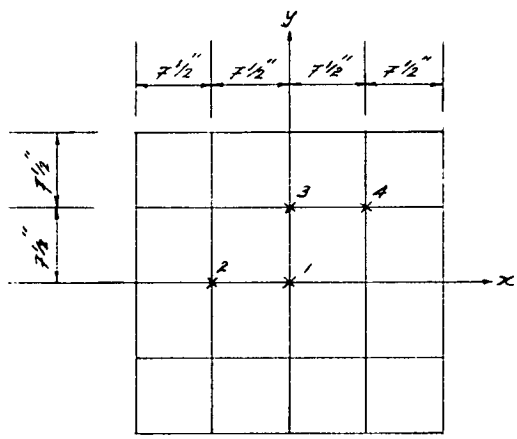

FIGURE:2-32. LOCATION OF DIAL GAUGES

The strain gauges were covered with polythene sheets to prevent the gauges from drift. For recording the strains a 10 channel data logger was used. (Plate 2.5). A voltage of 5 volts was applied across the bridge.

The plate was built of clay blocks cemented together with mortar and thus due to the high strength of the blocks the strain on a block might not be the strain of the structure as a whole at that location. Strains recorded would be the local strains on the clay blocks. Therefore, it was decided to measure the deflection as well at four points (Figure 2.32). The deflection at any point would be the deflection of the structure as a whole at that point. Plate (2.12) shows the arrangement of the dial gauges placed below the slab for measuring the vertical deflections.

2.2.3c Testing Procedure

Loads of 60 lbs distributed over the surface of the plate was applied at each stage. For the first two load stages i.e. up to 120 lbs. lead weights (each of 0.2 lbs) were used. Up to 480 lbs. loading was applied by bags filled with stone chips each weighing 4 lbs. (Plate 2.13). Then cast iron weights were used up to a total load of 660 lbs.

Before starting the experiment all the strain gauges were balanced i.e. readings of the strain recorder were brought to zero. The initial readings of the dial gauges were noted. Readings were taken twice at every load stage, once just after applying the loads and next one 20 minutes after applying the loads, to allow for creep. However there was no large difference between the two sets of readings. The test was repeated after an interval of one day.

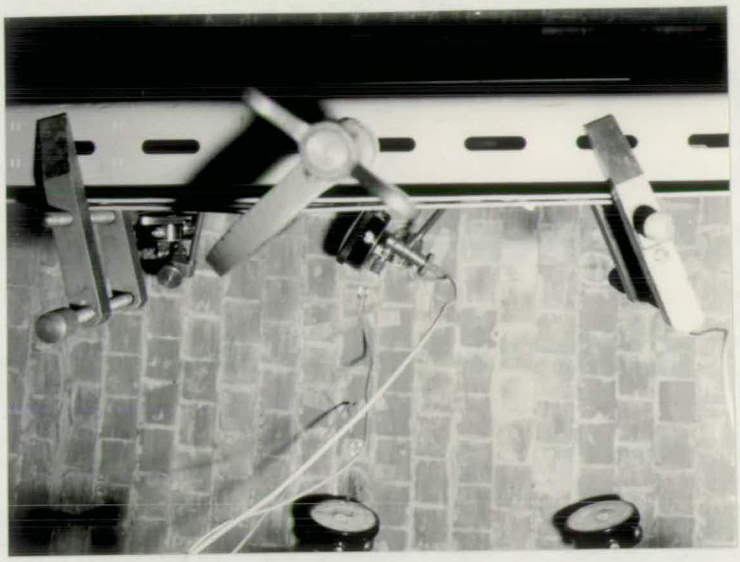

Plate: 2-12

Plate: 2-13

Unfortunately no reliable strain readings were obtained during the tests.

The deflections at different load intervals are plotted in Figure (2.34).

Table(2.3)and Figure (2.35) show the comparison between the theoretical and experimental results.

2.2.4 DETERMINATION OF YOUNG'S MODULUS FOR PERSPEX BEAM OF HOLLOW SECTION

In order to determine EI value and hence Young's Modulus a beam of hollow cross section 3 in wide was built cementing 1 in. wide strips of 1/16 thick perspex as slab and $\frac{1}{8}$in x $\frac{1}{8}$in strips as ribs spaced at 1 in. centre to centre. The beam was tested as simply supported and two concentrated loads were symmetrically placed Figure (2.36). The value of Young's Modulus thus found was 3.9×10^5 lbs/in^2 against the theoretical value of 4.2×10^5 lbs/in^2, specified by the manufacturer.

2.2.5 DETERMINATION OF THE EI VALUE FOR CLAY BLOCK STRUCTURES

In order to determine the EI value six beams were built. Four of these were built by cementing the blocks longitudinally using top and bottom reinforcement. Three courses of blocks were used to give a width of approximately 4 in and length of 26 in. (Plate 2.6 & 14). The remaining two beams were built by cementing the blocks transversely, without any reinforcement, to simulate the construction of the plate. Here also three courses of blocks were used giving a width of 4 in. and length of

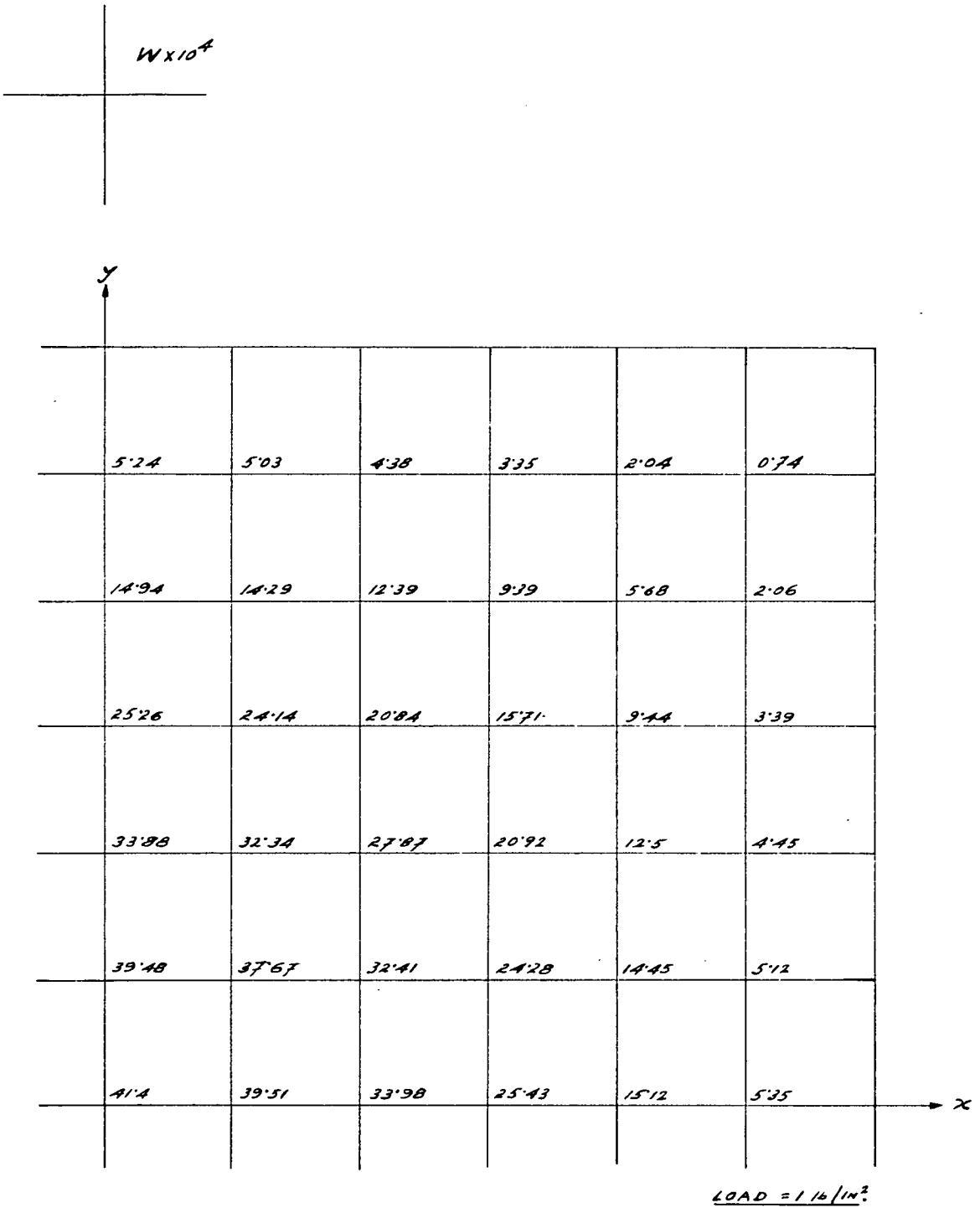

VERTICAL DEFLECTION IN INCH.

HOLLOW CLAY PLATE.

FIGURE : 2-33.

PLATE: BUILT OF CLAY-BLOCKS.

FIGURE: 2-34

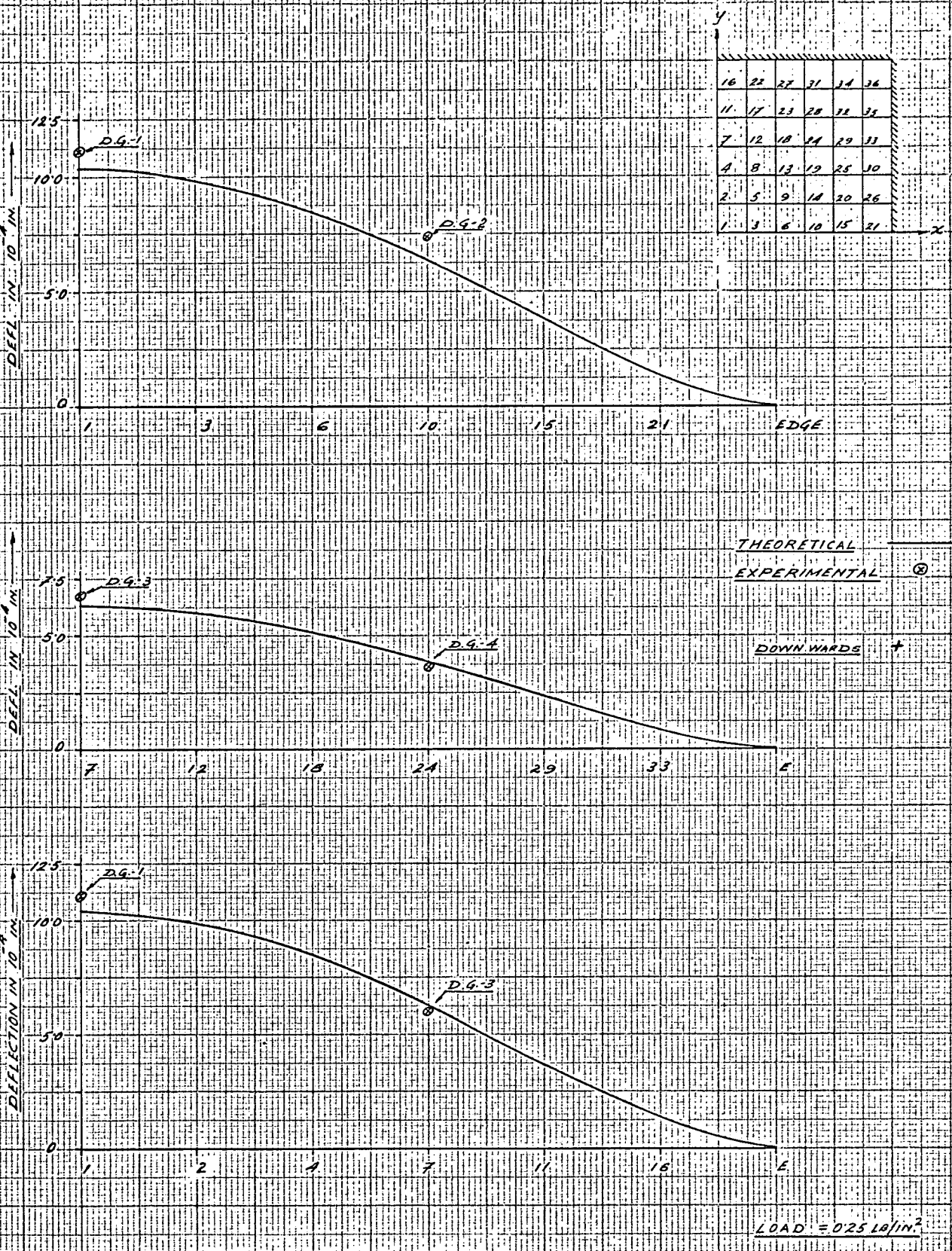

COMPARISON OF DEFLECTIONS

PLATE BUILT OF HOLLOW CLAY BLOCKS

FIGURE: 2-35

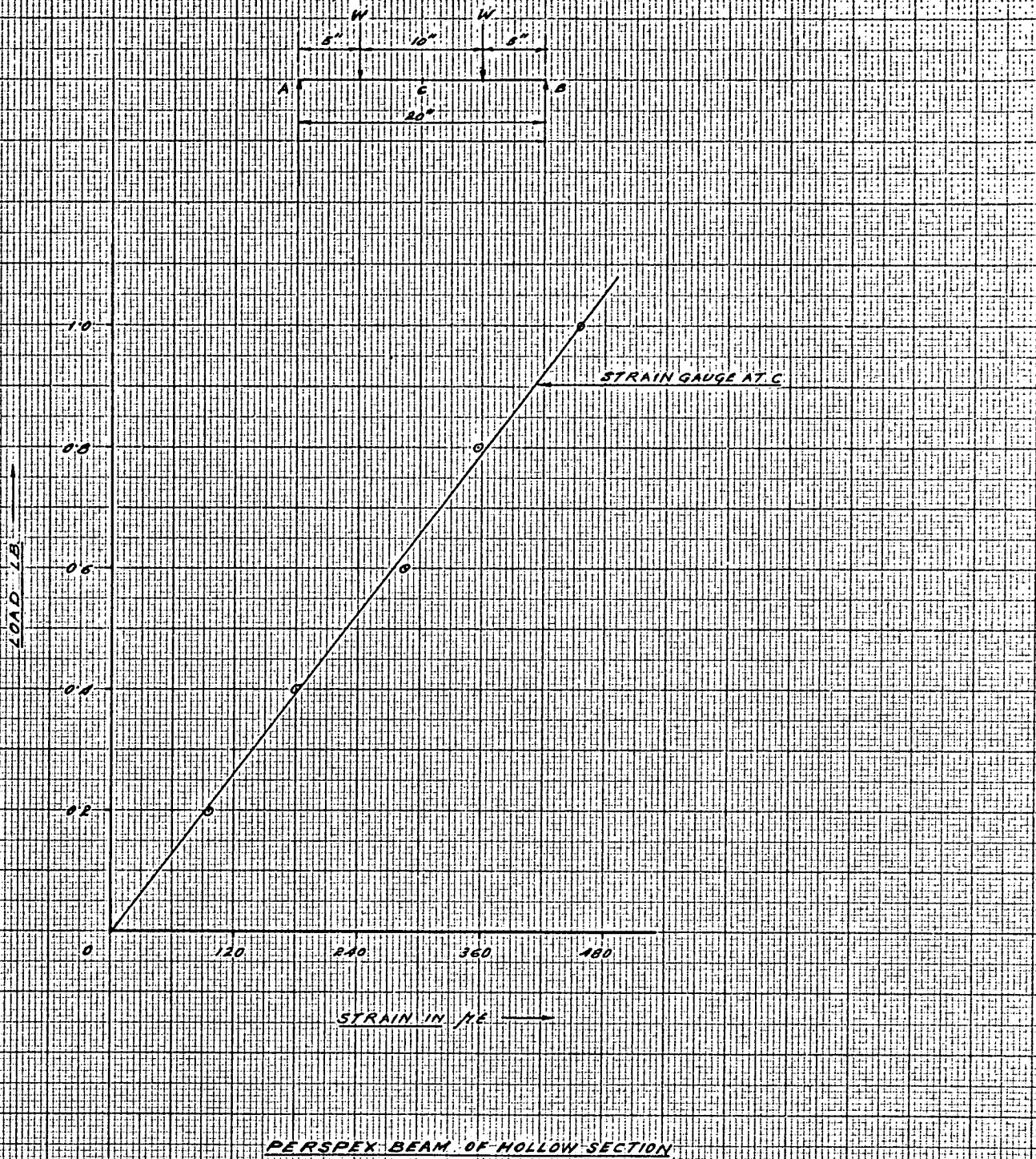

PERSPEX BEAM OF HOLLOW SECTION

FIGURE: 2-36

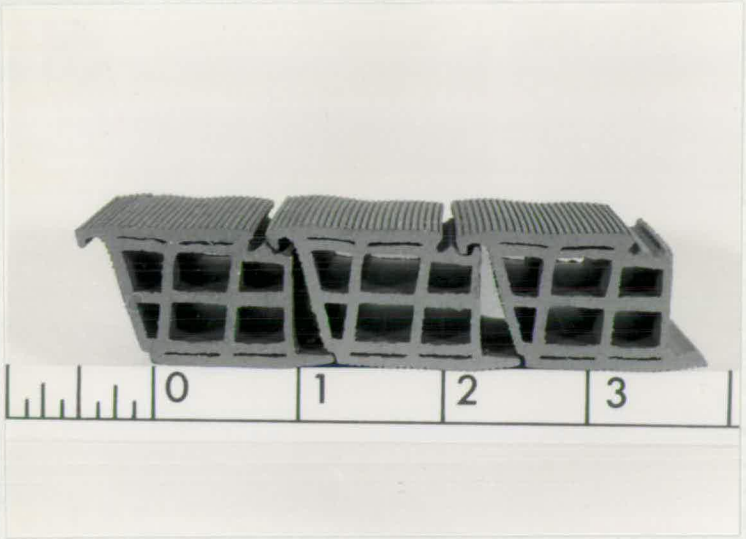

Plate: 2-14

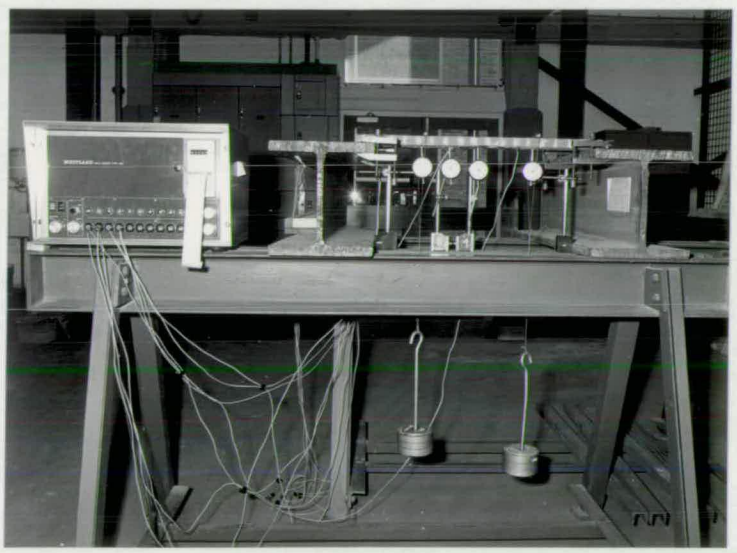

Plate: 2-15

27 in. approximately. The above two types of beams were built and tested in order to take care of the difference in bending rigidity of the plates in two directions. Plain clay blocks were used for fixing the strain gauges.

EI values were determined by applying two point loads at the quarter spans. (Plates 2.15 to 17). The experiments were repeated three times to determine if creep was present. Since the section of the beams are not perfectly symmetrical, EI values were also determined by testing the beams after turning them upside down. The lower value of the two is used for calculation. Figure (2.37).

EI Values (minimum) found by experiment are as follows:

(a) EI value for the first type of beam = 2.74×10^5 lb.in^2

(b) EI value for the second type of beam = 2.54×10^5 lb.in^2

Therefore $EI_{1st}/EI_{2nd} = 1.08$

2.2.6 CONCLUSIONS

2.2.6a. PERSPEX PLATE

i) The values of deflections, moments and stresses obtained by Navier's method and Finite difference method are in good agreement although there are minor differences at the central zone and near the boundaries. The values obtained by Navier's method at the central zone are a little higher than those obtained by Finite difference method but the reverse is true near the boundaries. In Navier's method only three terms of the trigonometric series was used and this might be one of the reasons for the higher values at the central zone. The discrepancy near the boundaries might be due to the reason

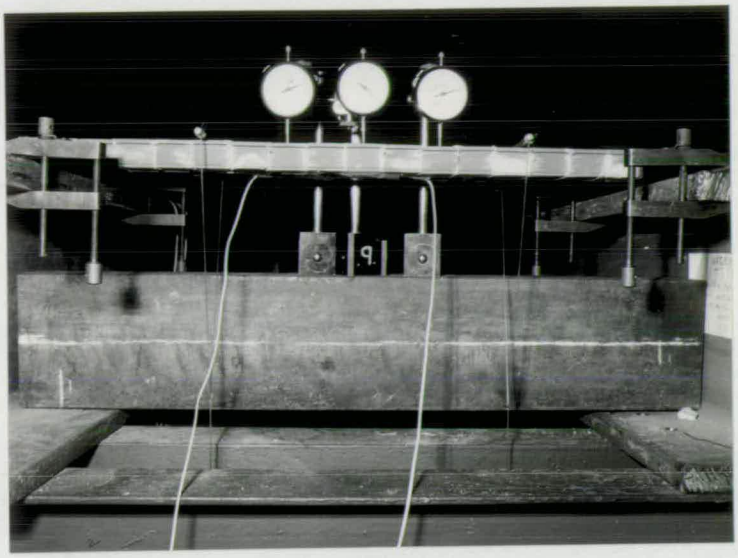

Plate: 2-16

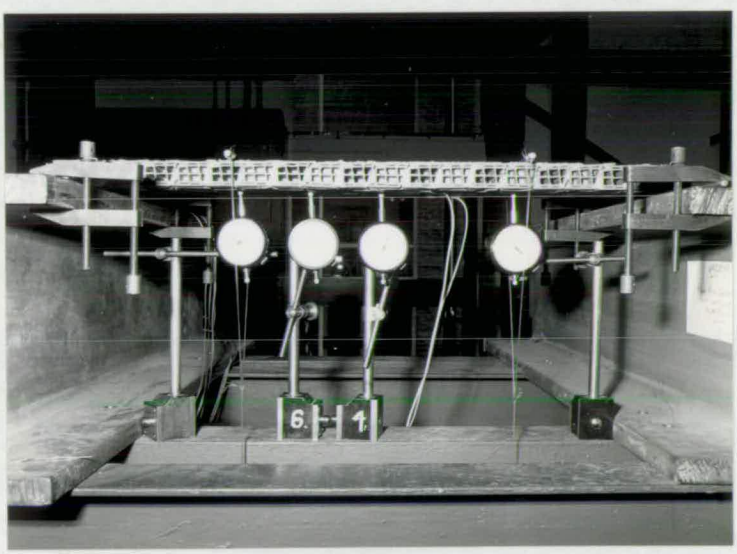

Plate: 2-17

BEAM BUILT OF CLAY BLOCKS

FIGURE: 2-37

mentioned above and also due to the mesh-size and presence of fictitious points in Finite difference method. Use of higher terms in Navier's method and use of smaller mesh size in Finite difference method would reduce the discrepancies.

ii) The comparison of the values of strains obtained by the theoretical calculations and by experiments are in close agreement. The probable reasons for slight discrepancies might be due to (1) variation of bending rigidity at different sections of the plate due to cementing of the strips and also workmanship (2) possible faults in the supports used during the tests and (3) method of loading. The discrepancies in the case of a plate supported at all four courners are of an opposite nature to those of simply supported at the edges condition. This might also be due to the reasons mentioned above.

2.2.6b. PLATE BUILT OF HOLLOW CLAY BLOCKS

Here also the experimental results are in close agreement with the theoretical results. The slight discrepancies might be due to (1) Workmanship (2) Support conditions and (3) Method of loading during the test.

2.2.6c. It has been shown that the theoretical expression for plates of hollow cross section are in good agreement with the experimental results for the model tested. It would have been interesting to compare the results obtained from full scale tests but the author was unable to find any published results for comparison.

Note: In all theoretical computations for perspex plate a value of Young's Modulus (E) was taken as 4.2×10^5 lb/in^2 as specified by the manufacturer. Since by testing a beam of hollow cross section the value of E was found as 3.9×10^5 lb/in^2 the theoretical results were corrected accordingly while comparing with the experimental results.

APPENDIX : 2-2

PLATE SIMPLY SUPPORTED /NAVIER S METHOD

COMPUTER PROGRAM

```
begin
integer i,j,m,n
real E,M,B1,B2,B3,T1,T2,a,b,xa,yb,A,B,C,P,W,MX,MY,SX,SY
realarray  K(1:14)

i= 0
j= 0
m= 0
n= 0
K(1)= 0

read(E,M,B1,B2,B3,T1,T2,a,b,P)

K(1)= (2E*(T2↑3 - T1↑3))/3
K(2)= 2E*T1↑3*B2/3B1
K(3)= 2E*T1↑3*B3/3B1
K(4)= K(1) + K(2)
K(5)= K(1) + K(3)
K(6)= K(1)/(1-M²)
K(7)= K(6) + K(2)
K(8)= K(6) + K(3)
K(9)= K(7)/K(6)
K(10)= K(8)/K(6)
K(11)= 16P/(π↑4*K(6))
K(12)= K(11)/π²
K(13)=( T2/K(4))*E
K(14)=( T2/K(5))*E


caption ## K(1) $$ to $$ K(14) ##
cycle i= 1,1,14
print fl(K(i),6)
newline
repeat
newlines(3)


cycle i= 0,1,12
     xa= i/12
cycle j= 0,1,12
     yb= j/12

    W= 0
    MX= 0
    MY= 0
    SX= 0
    SY= 0
```

```
cycle m= 1,2,5
cycle n= 1,2,5

A= (sin(m*π*xa)*sin(n*π*yb))/(m*n*(K(9)*((m/a)↑4) + 2*((m*n)/(a*b))↑2 + K(10)*((n/b)↑4)))

    B= A*(K(9)*(m/a)↑2 + M*(n/b)↑2)*K(6)

    C= A*(M*(m/a)↑2 + K(10)*(n/b)↑2)*K(6)


   W = W + A
   MX= MX + B
   MY= MY + C


    repeat
    repeat

 caption  xa $$$$$$$ yb $$$$$$$ W $$$$$$$ MX $$$$$$$ MY $$$$$$$ SX $$$$$$$ SY  nn

  print(xa,1,3)
  spaces(2)

  print(yb,1,3)
  spaces(2)

  printfl(K(12)*W,6)
  spaces(2)

  printfl(K(11)*MX,6)
  spaces(2)

  printfl(K(11)*MY,6)
  spaces(2)

  printfl(K(13)*K(11)*MX,6)
  spaces(2)

  printfl(K(14)*K(11)*MY,6)
  newlines(2)

repeat
repeat

end of program


420000  0.35  1.0  0.125  0.0  0.0625  0.125  12.0  12.0  1.0

***Z
```

APPENDIX : 2-3

COMPUTER PROGRAM FOR STRESSES & STRAINS FOR SIMPLY SUPPORTED PLATE BY FINITE DIFFERENCE METHOD

```
begin
integer i,j
array A(1:14),MX,MY,M,BX,BY,BXY,CX,CY,CXY(1:49),W(1:36)
real a,b,c,d,e,f,D,D1,D2,b1,b2,b3,t1,t2,d1,d2,h,PR,E,G,L,p


caption ## L is the length of the plate (square)
caption ## h is the mesh length
caption # MX,MY,M are the moments
caption # BX,BY,BXY are the stresses
caption # CX,CY,CXY are the strains
caption # E & G are the youngs & rigidity modulus ##


cycle  i=1,1,49

MX(i)= 0
MY(i)= 0
M(i) = 0
BX(i)= 0
BY(i)= 0
BXY(i)= 0
CX(i)= 0
CY(i)= 0
CXY(i)= 0


repeat


read ( h,PR,E,b1,b2,b3,t1,t2,p)


d= p*(h↑4)


cycle i= 1,1,36

read (W(i))

W(i)= d*(W(i))

caption # W #
print fl(W(i),5)
newline

repeat
```

```
D= (E/(1 - PR²))*(2/3)*((t2)↑3 - (t1)↑3)
D1= D+ E*(2/3)*(b2/b1)*((t1)↑3)
D2= D + E*(2/3)*(b3/b1)*((t1)↑3)
d1= D1/D
d2= D2/D

a = d1
b = PR
c = 2*(d1 + PR)
d = p*(h↑4)
e = d2
f = 2*(d2 + PR)
G = E/(2*(1 + PR))

A(1)= D
A(2)= D1
A(3)= D2
A(4)= d1
A(5)= d2
A(6)= b
A(7)= c

A(8)= d
A(9)= e
A(10)= f
A(11)= G
A(12)= (2/3)*((t2)↑3 - (t1)↑3)/(t2)
A(13)= A(12) + (2/3)*(b2/b1)*((t1)↑3)/(t2)
A(14)=  A(12) + (2/3)*(b3/b1)*((t1)↑3)/(t2)


caption ### A(1) # to A(14) ###

cycle i= 1,1,14
print fl(A(i),6)
newline

repeat

newlines(4)


MX(1)=2*a*W(3) + 2*b*W(2) - c*W(1)
MX(2)=2*a*W(5) + b*(W(4) + W(1)) - c*W(2)
MX(3)=a*(W(6) + W(1)) + 2*b*W(5) - c*W(3)
.....................
.....................
MX(35)=a*W(32) + b*(W(36) + W(33)) - c*W(35)
MX(36)=a*W(34) + b*W(35) - c*W(36)
```

```
MY(1)=2*e*W(2) + 2*b*W(3) - f*W(1)
MY(2)=e*(W(4) + W(1)) + 2*b*W(5) - f*W(2)
MY(3)=2*e*W(5) + b*(W(6) + W(1)) - f*W(3)
.....................................
.....................................
MY(34)=e*W(32) + b*(W(36) + W(31)) - f*W(34)
MY(35)=e*(W(36) + W(33)) + b*W(32) - f*W(35)
MY(36)=e*W(35) + b*W(34) - f*W(36)


M(5)= W(13) - W(4) + W(1) - W(6)
M(8)= W(13) - W(7) + W(2) - W(9)
M(9)= W(19) - W(8) + W(3) - W(10)
.............................
.............................
M(47)= 2*W(31) - 2*W(36)
M(48)= 2*W(34)
M(49)= 4*W(36)


cycle i=1,1,49

MX(i)= -MX(i)/h²
MY(i)= -MY(i)/ h²
M(i)= -(1-PR)*M(i)/ h²

repeat


cycle i= 1,1,49

BX(i)= MX(i)/A(13)
BY(i)= MY(i)/A(14)
BXY(i)= M(i)/A(12)

repeat


cycle i=1,1,49

CX(i)= 1/E*(BX(i) - PR*BY(i))
CY(i)= 1/E*(BY(i) - PR*BX(i))
CXY(i)= BXY(i)/G

repeat


caption nn MX ########## MY ########## M ########## BX ########## BY ########## BXY ###
```

```
cycle i= 1,1,49

print fl(MX(i),4)
spaces(3)


print fl(MY(i),4)
spaces(3)

print fl(M(i),4)
spaces(3)


print fl(BX(i),4)
spaces(3)

print fl(BY(i),4)
spaces(3)

print fl(BXY(i),4)
newlines(2)

repeat

newlines(4)


caption ### CX ########## CY ########## CXY ####


cycle i= 1,1,49

print fl(CX(i),4)
spaces(3)

print fl(CY(i),4)
spaces(3)

print fl(CXY(i),4)
newlines(2)

repeat

newlines(4)


end of program


d a t a

***Z
```

APPENDIX 2-4

STRENGH OF HOLLOW CLAY BLOCKS AND MORTAR CUBES

(a) Hollow Clay Blocks

A number of tests were carried out to find out the crushing strength of blocks along the longitudinal direction. Arrangement of tests is shown in Plate (2-18) and Table (2-4) shows the results obtained. For some of the tests the ends of the blocks were machined whilst the remainder were tested as supplied. Tests were conducted with and without a layer of plywood at the top and bottom of the block.

The high crushing strength might possibly be due to the fine grinding of the clay necessary for the manufacture of the model blocks and those high values may not be obtained for the full size blocks.

(b) Mortar

Table (2-5) shows the crushing test results on 1 inch cube mortar after 28 days.

Plate: 2-18

T A B L E 2-4

CRUSHING STRENGTH OF CLAY BLOCKS

Serial No.	Crushing load in Tons		
	Machined		Unmachined
	With plywood	Without plywood	With plywood
1	4.53	5.3	3.8
2	5.20	1.1	4.84
3	5.30		5.1
4			4.4
5			4.4
6			5.7
7			3.5
8			5.5
9			4.5
10			4.7

T A B L E 2-5

CRUSHING STRENGTH OF MORTAR CUBES

Serial Number	Size of Cubes	Crushing load in Tons
1	1in x 1in x 1in	1.25
2	"	1.31
3	"	1.46
4	"	1.37
5	"	1.52
6	"	2.1
7	"	2.05
8	"	2.3
9	"	1.15
10	"	1.63

CHAPTER 3

THEORY FOR CYLINDRICAL SHELLS OF HOLLOW CROSS SECTION

3.1 INTRODUCTION

The shell problem is a three dimensional one and the theory of elasticity will be used for the solution. There are a number of theories for such a problem developed by different authors. As the different authors develop their theories making assumptions and approximations at different stages it is very difficult to compare the theories and to assess the relative effect of the assumptions and approximations on the theories.

However, Davies (12) compares the theories of cylindrical shells developed by Love, Flügge, Timoshenko and Donnell. He consideres all the five relations viz. (1) Strain-Displacement, (2) Parallel-Surface Strains to Middle Surface Strains, (3) Stress-Strain, (4) Force-Moments and (5) Equations of Equilibrium which are being used by all the authors and compares each of the above relations at various stages to assess the effect on them due to the assumptions and approximations by the authors.

From his comparison it appears that (1) Strain-Displacement relationship used by Flügge is more accurate than other authors, on the other hand (2) Parallel Surface Strains to Middle Surface Strains and (3) Stress-Strain relations used by Love are more accurate that Flügge and other authors. Both Love and Flügge use the same expressions for (4) Force-Moment and (5) Equilibrium Equations which are more accurate than those used by Timoshenko or Donnell.

Zienkiewicz (55) discusses the relative accuracy of the Displacement Equations developed by (1) Flügge, (2) Timoshenko and (3) Donnell-Karman-

Jenkins. After thorough examination he concludes that though D.K.J.'s equations are used extensively in Britain due to their simplicity and though both D.K.J.'s and Timoshenko's equations are used as a basis for American Society of Civil Engineers' Manual but equations developed by Flügge are the most complete and accurate.

It is to be noted that equations derived by Donnell are the simplified version of the equations developed by Flügge.

McNamee (31) discusses the theories developed by Dischinger, Aas-Jakobsen, B.R.S., D.K.J., Finsterwalder and Schorer. Though the equations derived by Finsterwalder and Schorer are simple and easy to work with but unfortunately these have a very limited range of application.

Application of a theory to a cylindrical shell of hollow cross section will be complicated due to the differential properties along the longitudinal and transverse directions due to its hollow cross section. Therefore, though Flugge's theory seems to be complete and more accurate due to the possible complication mentioned above the simplest theory, i.e. Donnell's theory, will be used in this chapter.

3.2 DEVELOPMENT OF THEORY OF THIN CYLINDRICAL SHELLS OF HOLLOW CROSS SECTION AS USED BY AUTHOR

In order to develop a theory it is essential to make some assumptions. The following are the assumptions made by the author while developing the theory for cylindrical shells of hollow cross section.

1) Overall thickness of the shell is small compared to the radius.
2) Plane sections normal to the middle surface remain plane during the process of deformation and remain normal to it.

3) For all kinematic relations the distance z of a point from the middle surface may be considered as unaffected by the deformation of the shell.

4) Normal stresses on planes parallel to the middle surface are neglected in comparison with other stresses.

5) All displacements are small and they are negligible compared with the radii of the curvature of the middle surface.

6) The ratio z/R can be neglected compared with Unity.

Having made the above assumptions the next step to develop the theory is to obtain the relationships connecting

1) Middle surface strains and changes of curvature with the displacements of the middle surface.

2) Parallel surface strains with middle surface strains and changes of curvature.

3) Normal and shear stresses with parallel surface strains.

4) Forces and moments with normal and shear stresses.

5) Forces and moments in the form of the equilibrium equations.

Three partial differential equations connecting the displacements of the middle surface and external forces are obtained by successive substitution of one relation to another, mentioned above. An eighth order differential equation in terms of displacement 'W' can be obtained from the three displacement equations by successive differentiation and substitution of one into others (Appendix 3-1).

Strain-Displacement Equations

Figure(3-I)shows a longitudinal section of a shell element where a normal fibre 'aa' extended by direct stresses to 'bb' and rotated due to bending to 'cc'.

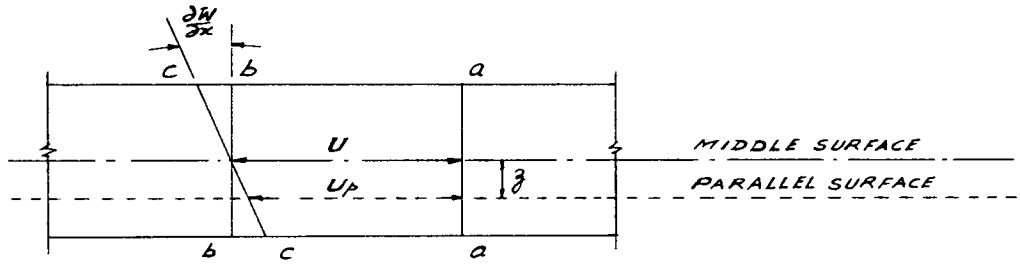

$$U_p = U - z \cdot \frac{\partial w}{\partial x}$$

FIGURE : 3-1

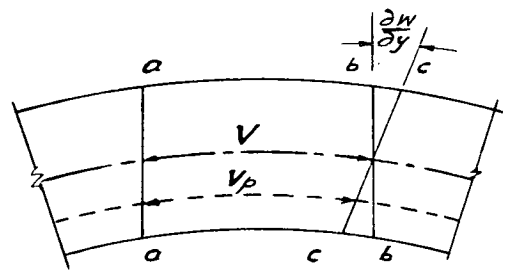

$$V_p = V - z \cdot \frac{\partial w}{\partial y}$$

FIGURE : 3-2

Due to the assumption $z/R \simeq 0$ i.e. z/R is neglected, Figure(3-2) shows the transverse section of a shell element.

From Figures (3-1 & 2.) the expressions for displacements of a parallel surface are:

$$U_p = U - z(\partial W/\partial x) \qquad (3.1.1)$$

$$V_p = V - z(\partial W/\partial y) \qquad (3.1.2)$$

$$W_p = W \qquad (3.1.3)$$

where U_p, V_p and W_p are the displacements of a surface parallel to the middle surface.

Since

$$\epsilon_x = \partial U_p/\partial x \qquad (3.2.1)$$

$$\epsilon_y = (\partial V_p/\partial y) - (W_p/R) \qquad (3.2.2)$$

$$\gamma_{xy} = (\partial V_p/\partial x) + (\partial U_p/\partial y) \qquad (3.2.3)$$

Therefore, substituting for U_p, V_p and W_p from equations (3.1.1 to 3.1.3) to (3.2.1 to 3.2.3), the expressions for parallel surface strains in terms of middle surface strains reduce to:

$$\epsilon_x = (\partial U/\partial x) - z(\partial^2 W/\partial x^2) \qquad (3.3.1)$$

$$\epsilon_y = (\partial V/\partial y) - z(\partial^2 W/\partial y^2) - W/R \qquad (3.3.2)$$

$$\gamma_{xy} = (\partial U/\partial y) + (\partial V/\partial x) - 2z(\partial^2 W/\partial x \partial y) \qquad (3.3.3)$$

Now using the assumption (4) i.e. the stress $\sigma_z = 0$ and using Hooke's Law the stress-strain relations follow:

$$\sigma_x = (E/(1-\mu^2))(\epsilon_x + \mu \epsilon_y) \qquad (3.4.1)$$

$$\sigma_y = (E/(1-\mu^2))(\epsilon_y + \mu \epsilon_x) \qquad (3.4.2)$$

$$T_{xy} = T_{yx} = G\gamma_{xy} \qquad (3.4.3)$$

where $G = E/2(1+\mu)$

For the slabs Hooke's law is represented by the equations (3.4.1 to 3.4.3) but for the ribs we have simply,

$$\sigma_x = E \epsilon_x \qquad (3.4.4)$$

$$\sigma_y = E \epsilon_y \qquad (3.4.5)$$

It is to be noted that due to the difference of the elastic laws for the one-dimensional and the two dimensional parts of the shell normal stresses σ_x or σ_y along two adjacent fibres of the rib and the slab will not be the same.

The forces Q_x and Q_y can be eliminated from the equations of equilibrium. Since Q_x and Q_y are related to stresses T_{xz} and T_{yz}, therefore T_{xz} and T_{yz} (Figure 3-3) are not required to derive the displacement equations.

Consider a section y = constant of the shell (Figure 3-4). Let b_1 be the length of the periodic repetition of the shaded part and b' be the width of the rib. As normal stresses are present in both the slabs and ribs, N_y and M_y are integrals of the normal stresses over the combined cross sections of the slabs and the rib. In order to distinguish them the notations 's' for slab and 'r' for rib to the lower end of the integral sign are used. Therefore, we have:

$$N_y = \int_s \sigma_y \, dz + \int_r \sigma_y (b'/b_1) dz \qquad (3.5.1)$$

and

$$M_y = \int_s \sigma_y \, z \, dx + \int_r \sigma_y (b'/b_1) z \, dz \qquad (3.5.2)$$

Now consider the section x = constant (Figure 3-5). As before let b_2 be the distance of the adjacent ribs and measured on the middle surface and b" be the width of the rib. The notations 's' and 'r' to the integral sign are used as before.

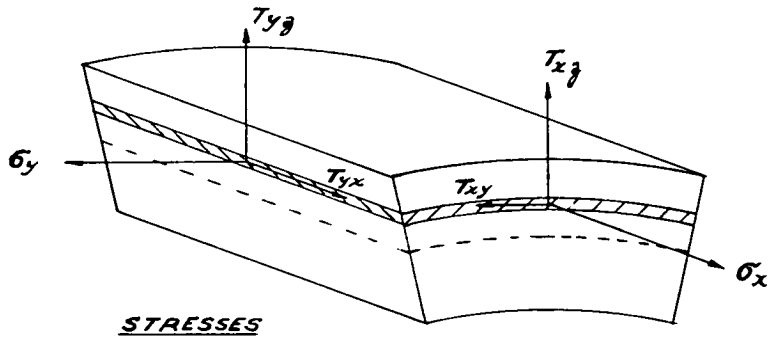

FIGURE : 3-3.

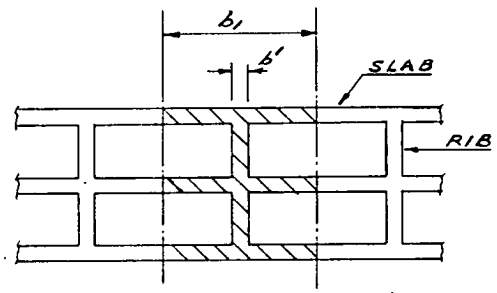

FIGURE : 3-4.

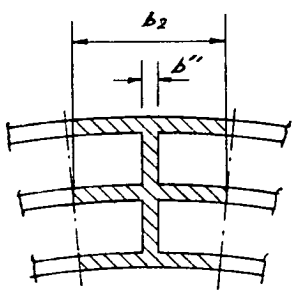

FIGURE : 3-5.

As z/R is considered to be small and hence neglected; then:

$$N_x = \int_s \sigma_x \, dz + \int_r \sigma_x (b''/b_2) \, dz \qquad (3.5.3)$$

and

$$M_x = \int_s \sigma_x \, z \, dz + \int_r \sigma_x (b''/b_2) z \, dz \qquad (3.5.4)$$

Since there are no shearing stresses on the lateral surface of the ribs, there will be no shear stress T_{xy} or T_{yx} in the cross section of the ribs and all the tangential shear will be carried by the slabs only. Therefore expressions for shearing forces and twisting moments are; (assuming z/R = 0):

$$N_{xy} = N_{yx} = \int_s T_{xy} \, dz \qquad (3.5.5)$$

$$M_{xy} = M_{yx} = \int_s T_{xy} \, z \, dz \qquad (3.5.6)$$

The stresses in terms of the strains can now be obtained using Hooke's Law and then using the kinematic relations, the strains are obtained in terms of U, V and W.

Following this procedure in detail and using equations (3.3.1 to 3.3.3), (3.4.1. to 3.4.5) and (3.5.1 to 3.5.6) the forces and moments can be expressed in terms of the middle surface displacements.

$$N_x = D_x(\partial U/\partial x) + \mu D(\partial V/\partial y - W/R) - S_x(\partial^2 W/\partial x^2) - \mu S(\partial^2 W/\partial y^2) \qquad (3.6.1)$$

$$N_y = D_y(\partial V/\partial y - W/R) + \mu D(\partial U/\partial x) - S_y(\partial^2 W/\partial y^2) - \mu S(\partial^2 W/\partial x^2) \qquad (3.6.2)$$

$$N_{xy} = N_{yx} = \frac{D}{2}(1 - \mu)(\partial U/\partial y + \partial V/\partial x) - S(1 - \mu)(\partial^2 W/\partial x \, \partial y) \qquad (3.6.3)$$

$$M_x = S_x(\partial U/\partial x) - K_x(\partial^2 W/\partial x^2) + \mu S(\partial V/\partial y) - \mu K(\partial^2 W/\partial y^2) - \mu S(W/R) \qquad (3.6.4)$$

$$M_y = S_y(\partial V/\partial y - W/R) - K_y(\partial^2 W/\partial y^2) + \mu S(\partial U/\partial x) - \mu K(\partial^2 W/\partial x^2) \qquad (3.6.5)$$

$$M_{xy} = M_{yx} = \frac{S}{2}(1-\mu)(\partial U/\partial y + \partial V/\partial x) - K(1-\mu)(\partial^2 W/\partial x \partial y) \qquad (3.6.6)$$

where D, D_x and D_y are the extensional rigidities and defined by:

$$D = E/(1-\mu^2) \int_s dz \qquad (3.7.1)$$

$$D_x = E/(1-\mu^2) \int_s dz + E \int_r \left(\frac{b''}{b_2}\right) dz \qquad (3.7.2)$$

$$D_y = E/(1-\mu^2) \int_s dz + E \int_r \left(\frac{b'}{b_1}\right) dz \qquad (3.7.3)$$

S, S_x and S_y are the rigidity moments and defined by:

$$S = E/(1-\mu^2) \int_s z\, dz \qquad (3.7.4)$$

$$S_x = E/(1-\mu^2) \int_s z\, dz + E \int_r \left(\frac{b''}{b_2}\right) z\, dz \qquad (3.7.5)$$

$$S_y = E/(1-\mu^2) \int_s z\, dz + E \int_r \left(\frac{b'}{b_1}\right) z\, dz \qquad (3.7.6)$$

K, K_x and K_y are the bending rigidities and defined by:

$$K = E/(1-\mu^2) \int_s z^2\, dz \qquad (3.7.7)$$

$$K_x = E/(1-\mu^2) \int_s z^2\, dz + E \int_r \left(\frac{b''}{b_2}\right) z^2\, dz \qquad (3.7.8)$$

$$K_y = E/(1-\mu^2) \int_s z^2\, dz + E \int_r \left(\frac{b'}{b_1}\right) z^2\, dz \qquad (3.7.9)$$

If a symmetrical section of the shell element is assumed then the rigidity moments S, S_x and S_y all become zero. Thus the assumption of a symmetrical cross-section of shell element reduces the forces and moments to the following expressions:

$$N_x = D_x(\partial U/\partial x) + \mu D(\partial V/\partial y - W/R) \qquad (3.8.1)$$

$$N_y = D_y(\partial V/\partial y - W/R) + \mu D(\partial U/\partial x) \qquad (3.8.2)$$

$$N_{xy} = N_{yx} = \frac{D}{2}(1 - \mu)(\partial U/\partial y + \partial V/\partial x) \qquad (3.8.3)$$

$$M_x = -(K_x(\partial^2 W/\partial x^2) + \mu K(\partial^2 W/\partial y^2)) \qquad (3.8.4)$$

$$M_y = -(K_y(\partial^2 W/\partial y^2) + \mu K(\partial^2 W/\partial x^2)) \qquad (3.8.5)$$

$$M_{xy} = M_{yx} = -K(1 - \mu)(\partial^2 W/\partial x \partial y) \qquad (3.8.6)$$

From Figures (3-6 & 7) the equations of equilibrium can be written as follows:

Equilibrium of Forces

In the x-direction, $\partial/\partial x(N_x) + \partial/\partial y(N_{yx}) + P_x = 0$ (3.9.1)

In the y-direction, $\partial/\partial y(N_y) + \partial/\partial x(N_{xy}) + P_y = 0$ (3.9.2)

In the z-direction, $\partial/\partial x(Q_x) + \partial/\partial y(Q_y) + N_y/R + P_z = 0$ (3.9.3)

Equilibrium of Moments

About the x-axis, $\partial/\partial y(M_y) + \partial/\partial x(M_{xy}) - Q_y = 0$ (3.10.1)

About the y-axis, $\partial/\partial y(M_x) + \partial/\partial y(M_{yx}) - Q_x = 0$ (3.10.2)

In the equation (3.9.2) the term $Q_{y/R}$ is neglected as already mentioned before.

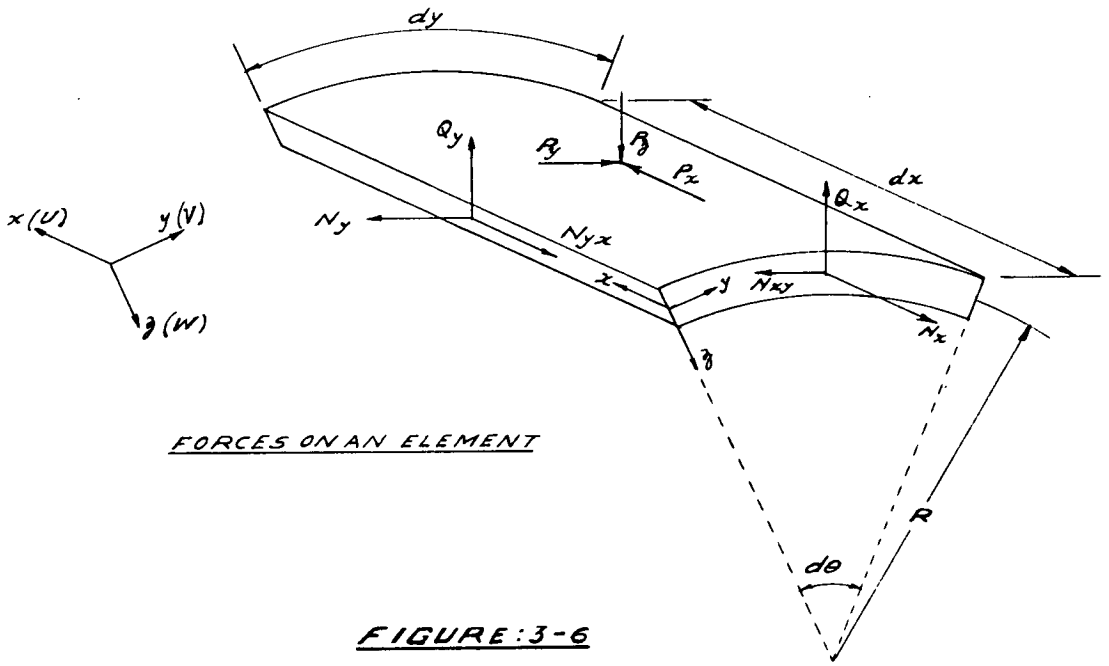

FORCES ON AN ELEMENT

FIGURE : 3-6

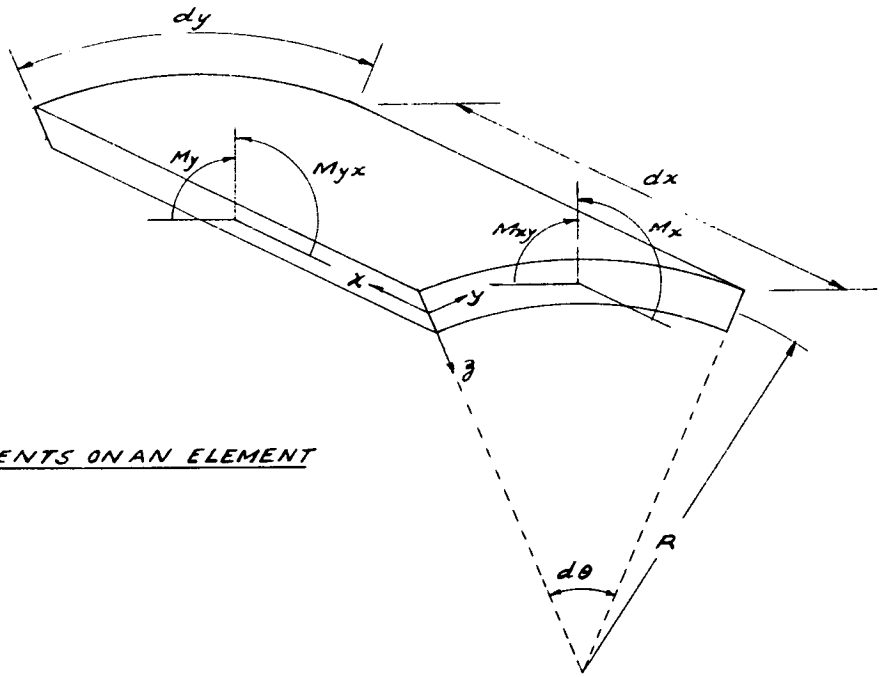

MOMENTS ON AN ELEMENT

FIGURE : 3-7

From the equations (3.10.1 and 3.10.2) Q_x and Q_y are obtained in terms of M_x, M_y and M_{xy} and substituting these values of Q_x and Q_y in the equation (3.9.3), the equations of equilibrium reduce to three as follows:

$$\partial/\partial x(N_x) + \partial/\partial y(N_{yx}) + P_x = 0 \qquad (3.11.1)$$

$$\partial/\partial y(N_y) + \partial/\partial x(N_{xy}) + P_y = 0 \qquad (3.11.2)$$

$$\partial^2/\partial x^2(M_x) + 2(\partial^2/\partial x \partial y)(M_{xy}) + \partial^2/\partial y^2(M_y) + N_y/R + P_z = 0 \qquad (3.11.3)$$

Substituting the values of N_x, N_y, N_{xy}, M_x, M_y and M_{xy} from the equations (3.8.1 to 3.8.6) to (3.11.1 to 3.11.3), the three equations of equilibrium are expressed in terms of three displacements U, V and W as follows:

$$D_x(\partial^2 U/\partial x^2) + \frac{D}{2}(1+\mu)(\partial^2 V/\partial x \partial y) + \frac{D}{2}(1-\mu)(\partial^2 U/\partial y^2) - (\mu D/R)(\partial W/\partial x) + P_x = 0 \qquad (3.12.1)$$

$$\frac{D}{2}(1-\mu)(\partial^2 V/\partial x^2) + \frac{D}{2}(1+\mu)(\partial^2 U/\partial x \partial y) + D_y(\partial^2 V/\partial y^2) - (D_y/R)(\partial W/\partial y) + P_y = 0 \qquad (3.12.2)$$

$$(\mu D/R)(\partial U/\partial x) + (D_y/R)(\partial V/\partial y) - (D_y/R^2)W - K_x(\partial^4 W/\partial x^4) - 2K(\partial^4 W/\partial x^2 \partial y^2) - K_y(\partial^4 W/\partial y^4) + P_z = 0 \qquad (3.12.3)$$

These are the three basic equations of equilibrium in terms of three displacements U, V and W, for shells of hollow cross section. To get a clear idea about the ratio of strength along two directions (x and y) and for the convenience of computation,

Let: $D_x = d' \cdot D$

$D_y = d'' \cdot D$

$K_x = k' \cdot K$

$K_y = k'' \cdot K$

and $D/K = \alpha$

Substituting the above values of D_x, D_y, K_x and K_y in the equations (3.12.1 to 3.12.3) and dividing the equations (3.12.1 and 3.12.2) by D and the equation (3.12.3) by K the equations of equilibrium reduce to:

$$d'(\partial^2 U/\partial x^2) + ((1+\mu)/2)(\partial^2 V/\partial x\,\partial y) + ((1-\mu)/2)(\partial^2 U/\partial y^2) - (\mu/R)(\partial W/\partial x) + P_x/D = 0 \qquad (3.13.1)$$

$$((1-\mu)/2)(\partial^2 V/\partial x^2) + ((1+\mu)/2)(\partial^2 U/\partial x\,\partial y) + d''(\partial^2 V/\partial y^2) - (d''/R)(\partial W/\partial y) + P_y/D = 0 \qquad (3.13.2)$$

$$(\mu\alpha/R)(\partial U/\partial x) + (d''\alpha/R)(\partial V/\partial y) - (d''\alpha/R^2)W - k'(\partial^4 W/\partial x^4) - 2(\partial^4 W/\partial x^2\,\partial y^2) - k''(\partial^4 W/\partial y^4) + P_z/K = 0 \qquad (3.13.3)$$

These displacement equations apply to cylindrical shells of hollow cross section and are the equations used in Chapter 4 for obtaining solutions by application of the finite difference/computer method of analysis.

For cylindrical shells of solid cross section previous authors have followed two approaches. Their equations have been expressed either in a form similar to the displacement equations shown above or as a single eighth order differential equation in one variable (usually the radial displacement). Since the equivalent eighth order equation has not been previously derived for shells of hollow section a derivation is given in the appendix.

A P P E N D I X 3-1

DERIVATION OF EIGHTH ORDER DIFFERENTIAL EQUATION FOR CYLINDRICAL SHELL OF HOLLOW CROSS SECTION

Let $A = -(\mu/R)(\partial W/\partial x) + P_x/D$

$B = -(d''/R)(\partial W/\partial y) + P_y/D$

and $C = -\left(k' (\partial^4 W/\partial x^4) + 2(\partial^4 W/\partial x^2 \partial y^2) + k''(\partial^4 W/\partial y^4) + (d''\alpha/R^2)W - P_z/K \right)$

Substituting A, B and C in the equations (3.13.1 to 3.13.3) and differentiating the equation (3.13.1) with respect to y:

$$d'(\partial^3 U/\partial x^2 \partial y) + ((1 + \mu)/2)(\partial^3 V/\partial x \partial y^2) + ((1 - \mu)/2)(\partial^3 U/\partial y^3) + \partial A/\partial y = 0 \qquad (3.14.1)$$

Differentiating the equation (3.13.1) with respect to x:

$$d'(\partial^3 U/\partial x^3) + ((1 + \mu)/2)(\partial^3 V/\partial x^2 \partial y) + ((1 - \mu)/2)(\partial^3 U/\partial x \partial y^2) + \partial A/\partial x = 0 \qquad (3.14.2)$$

and $\partial^2/\partial x \partial y$ (equation 3.13.3):

$$(\mu\alpha/R)(\partial^3 U/\partial x^2 \partial y) + (d''\alpha/R)(\partial^3 V/\partial x \partial y^2) + (\partial^2 C/\partial x \partial y) = 0 \qquad (3.15.1)$$

Multiplying the equation (3.15.1) by $(1 + \mu)/2$ and the equation (3.14.1) by $(d''\alpha/R)$ and subtracting one from other:

$$[(d'd''\alpha/R) - ((1 + \mu)/2)(\mu\alpha/R)](\partial^3 U/\partial x^2 \partial y) + (d''\alpha/R)((1 - \mu)/2)(\partial^3 U/\partial y^3) + (d''\alpha/R)(\partial A/\partial y) - ((1 + \mu)/2)(\partial^2 C/\partial x \partial y) = 0 \qquad (3.16.1)$$

Now by $\partial/\partial x$ (3.14.2), $\partial/\partial y$ (3.14.1) and $\partial^2/\partial x\partial y$ (3.13.2):

$$d'(\partial^4U/\partial x^4) + ((1+\mu)/2)(\partial^4V/\partial x^3\partial y) + ((1-\mu)/2)(\partial^4U/\partial x^2\partial y^2) + \partial^2A/\partial x^2 = 0 \quad (3.17.1)$$

$$d'(\partial^4U/\partial x^2\partial y^2) + ((1+\mu)/2)(\partial^4V/\partial x\partial y^3) + ((1-\mu)/2)(\partial^4U/\partial y^4) + \partial^2A/\partial y^2 = 0 \quad (3.17.2)$$

$$((1-\mu)/2)(\partial^4V/\partial x^3\partial y) + ((1+\mu)/2)(\partial^4U/\partial x^2\partial y^2) + (d'')(\partial^4V/\partial x\partial y^3) + \partial^2B/\partial x\partial y = 0 \quad (3.18.1)$$

Multiplying the equation (3.17.1) by $(1-\mu)$ and (3.18.1) by $(1+\mu)$ and subtracting one from other:

$$((1-\mu)d')(\partial^4U/\partial x^4) - (2\mu)(\partial^4U/\partial x^2\partial y^2) - ((1+\mu)\,d'')(\partial^4V/\partial x\partial y^3) + (1-\mu)(\partial^2A/\partial x^2) - (1+\mu)(\partial^2B/\partial x\partial y) = 0 \quad (3.19.1)$$

Multiplying the equation (3.17.2) by $2d''$ and adding to (3.19.1):

$$((1-\mu)d')(\partial^4U/\partial x^4) + (2(d'd''-\mu))(\partial^4U/\partial x^2\partial y^2) + (d''(1-\mu))(\partial^4U/\partial y^4) + (1-\mu)(\partial^2A/\partial x^2) + (2d'')(\partial^2A/\partial y^2) - (1+\mu)(\partial^2B/\partial x\partial y) = 0 \quad (3.20.1)$$

Let $E = (1-\mu)(\partial^2A/\partial x^2) + (2d'')(\partial^2A/\partial y^2) - (1+\mu)(\partial^2B/\partial x\partial y)$ (3.21.1)

$F = (d''\alpha/R)(\partial A/\partial y) - ((1+\mu)/2)(\partial^2C/\partial x\partial y)$ (3.21.2)

$\beta = (d'd''\alpha/R) - ((1+\mu)/2)(\mu\alpha/R)$ (3.21.3)

$\zeta = (d''\alpha/R)(1-\mu)/2$ (3.21.4)

$\delta = (1-\mu)d'$ (3.21.5)

$\psi = 2(d'd''-\mu)$ (3.21.6)

$\xi = d''(1-\mu)$ (3.21.7)

Rewriting the equations (3.20.1) and (3.16.1):

$$\delta(\partial^4U/\partial x^4) + \psi(\partial^4U/\partial x^2\partial y^2) + \xi(\partial^4U/\partial y^4) + E = 0 \qquad (3.20.2)$$

$$\beta(\partial^3U/\partial x^2\partial y) + \zeta(\partial^3U/\partial y^3) + F = 0 \qquad (3.16.2)$$

Now $\partial^4/\partial x^4$ (equation 3.16.2):

$$\beta(\partial^7U/\partial x^6\partial y) + \zeta(\partial^7U/\partial x^4\partial y^3) + \partial^4F/\partial x^4 = 0 \qquad (3.22.1)$$

and $\partial^4/\partial y^4$ (equation 3.16.2):

$$\beta(\partial^7U/\partial x^2\partial y^5) + \zeta(\partial^7U/\partial y^7) + \partial^4F/\partial y^4 = 0 \qquad (3.22.2)$$

and $\partial^4/\partial x^2\partial y^2$ (equations 3.16.2):

$$\beta(\partial^7U/\partial x^4\partial y^3) + \zeta(\partial^7U/\partial x^2\partial y^5) + \partial^4F/\partial x^2\partial y^2 = 0 \qquad (3.22.3)$$

Again, $\partial^3/\partial x^2\partial y$ (equation 3.20.2):

$$\zeta(\partial^7U/\partial x^6\partial y) + \psi(\partial^7U/\partial x^4\partial y^3) + \xi(\partial^7U/\partial x^2\partial y^5) + \partial^3E/\partial x^2\partial y = 0 \qquad (3.23.1)$$

$\partial^3/\partial y^3$ (equation 3.20.2):

$$\delta(\partial^7U/\partial x^4\partial y^3) + \psi(\partial^7U/\partial x^2\partial y^5) + \xi(\partial^7U/\partial y^7) + \partial^3E/\partial y^3 = 0 \qquad (3.23.2)$$

Now multiplying equations (3.22.1) by δ and (3.23.1) by β and subtracting one from other:

$$(\delta\zeta - \beta\psi)(\partial^7U/\partial x^4\partial y^3) - \beta\xi(\partial^7U/\partial x^2\partial y^5) + \delta(\partial^4F/\partial x^4) - \beta(\partial^3E/\partial x^2\partial y) = 0 \qquad (3.24.1)$$

Multiply equation (3.22.2) by ξ and adding to equation (3.24.1):

$$(\delta\zeta - \beta\psi)(\partial^7U/\partial x^4\partial y^3) + \xi\zeta(\partial^7U/\partial y^7) + \delta(\partial^4F/\partial x^4) - \beta(\partial^3E/\partial x^2\partial y) + \xi(\partial^4F/\partial y^4) = 0 \qquad (3.25.1)$$

Multiply equation (3.23.2) by ζ and subtract from equation (3.25.1):

$$- \beta\psi\,(\partial^7 U/\partial x^4\,\partial y^3) - \zeta\psi(\partial^7 U/\partial x^2\,\partial y^5) + \delta(\partial^4 F/\partial x^4) - \beta(\partial^3 E/\partial x^2\,\partial y) + \xi(\partial^4 F/\partial y^4) - \zeta(\partial^3 E/\partial y^3) = 0 \qquad (3.26.1)$$

Multiply equation (3.22.3) by ψ and adding to (3.26.1):

$$\delta(\partial^4 F/\partial x^4) + \psi\,(\partial^4 F/\partial x^2\,\partial y^2) - \beta\,(\partial^3 E/\partial x^2\,\partial y) - \zeta(\partial^3 E/\partial y^3) + \xi(\partial^4 F/\partial y^4) = 0 \qquad (3.27.1)$$

Substituting for A, B, C, E, F, β, ζ, δ, ψ and ξ in the equation (3.27.1) and dividing by $(1+\mu)/2$ and rearranging:

$$(k'd'(1-\mu))(\partial^8 W/\partial x^8) + 2[d'(1-\mu) + k'(d'd''-\mu)](\partial^8 W/\partial x^6\,\partial y^2) + [d'(1-\mu)k'' + 4(d'd''-\mu) + d''(1-\mu)k'](\partial^8 W/\partial x^4\,\partial y^4) + 2[(d'd''-\mu)k'' + d''(1-\mu)](\partial^8 W/\partial x^2\,\partial y^6) + [d''(1-\mu)k''](\partial^8 W/\partial y^8) + [(\alpha(1-\mu)/R^2)(d'd''-\mu^2)](\partial^4 W/\partial x^4) = (1/K)[(d'(1-\mu)/2)(\partial^4 P_z/\partial x^4) + 2(d'd''-\mu)(\partial^4 P_z/\partial x^2\,\partial y^2) + d''(1-\mu)(\partial^4 P_z/\partial y^4)] - (\alpha/RD)[\mu(1+\mu)(\partial^3 P_x/\partial x^3) - d''(1-\mu)(\partial^3 P_x/\partial x\,\partial y^2) + \{2d'd''-\mu(1+\mu)\}(\partial^3 P_y/\partial x^2\,\partial y) + d''(1-\mu)(\partial^3 P_y/\partial y^3)] \qquad (3.28.1)$$

This is the eighth order differential equation in terms of deflection 'W' for a cylindrical shell of hollow cross section.

For a cylindrical shell of solid cross section assuming Poisson's ratio $\mu = 0$, $d' = 1$, $d'' = 1$, $k' = 1$, $k'' = 1$, and $\alpha = {}^{12}/t^2$ then equation (3.28.1) reduces to:

$$\partial^8 W/\partial x^8 + 4(\partial^8 W/\partial x^6\,\partial y^2) + 6(\partial^8 W/\partial x^4\,\partial y^4) + 4(\partial^8 W/\partial x^2\,\partial y^6) + \partial^8 W/\partial y^8 + (12/R^2 t^2)(\partial^4 W/\partial x^4) = (1/K)[(\partial^4 P_z/\partial x^4 + 2(\partial^4 P_z/\partial x^2\,\partial y^2) + \partial^4 P_z/\partial y^4) - (1/R)(2(\partial^3 P_y/\partial x^2\,\partial y) - \partial^3 P_x/\partial x\,\partial y^2 + \partial^3 P_y/\partial y^3)] \qquad (3.29.1)$$

Or in compact form:

$$\nabla^8 W + (12/R^2 t^2)(\partial^4 W/\partial x^4) = (12/Et^3)[\nabla^4 P_z - (2/R)(\partial^3 P_y/\partial x^2 \partial y) + (1/R)(\partial^3 P_x/\partial x \partial y^2) - (1/R)(\partial^3 P_y/\partial y^3)] \quad (3.29.2)$$

Which is the single eighth order differential equation in terms of displacement 'W' only for solid cylindrical shells in the form derived by Jenkins.

CHAPTER 4

ANALYTICAL SOLUTIONS OF CYLINDRICAL SHELL OF HOLLOW CROSS SECTION

4.1 INTRODUCTION

In chapter 3 the governing equations for a cylindrical shell in terms of the three displacements U, V and W have been derived and a single eighth order equation in terms of 'W' only is also derived. The eighth order equation is unsuitable for the application of numerical methods for approximate solution. Unless the equations are expressed mathematically within the form of fourth order differential equations these are not suitable for solution by numerical methods. Therefore in this chapter three governing equations in terms of U, V and W of which two are second order and one fourth order are used for numerical solutions.

Using the finite difference approximations the differential equations are reduced to a finite number of linear simultaneous equations. These simultaneous equations are solved using a computer.

In this chapter three types of problems are solved:

a) Fixed at the edges and at the end-arches; the length of shell is equal to twice the width, (for a model shell of perspex). (Figure 4-1).

b) Fixed at the edges and free at the end-arches; length = 2 x width; (for a model shell of perspex). (Figure 4-2).

c) Fixed at the edges and free at the end-arches; length:width any quantity; (for a shell of model hollow clay blocks). (Figure 4-3).

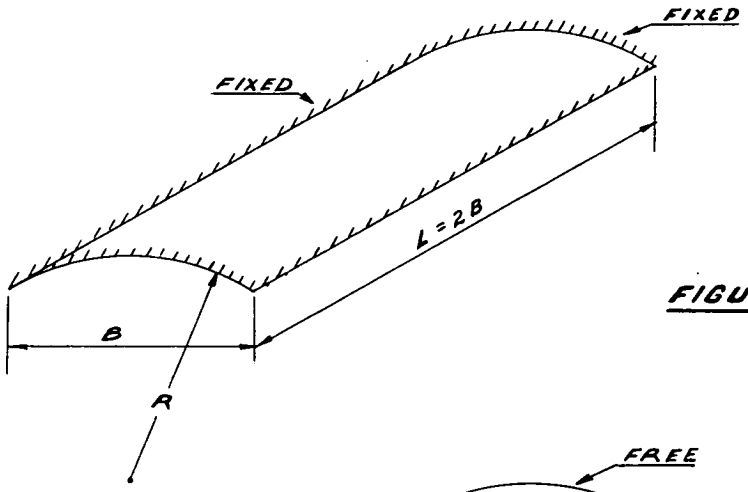

FIGURE : 4-1.

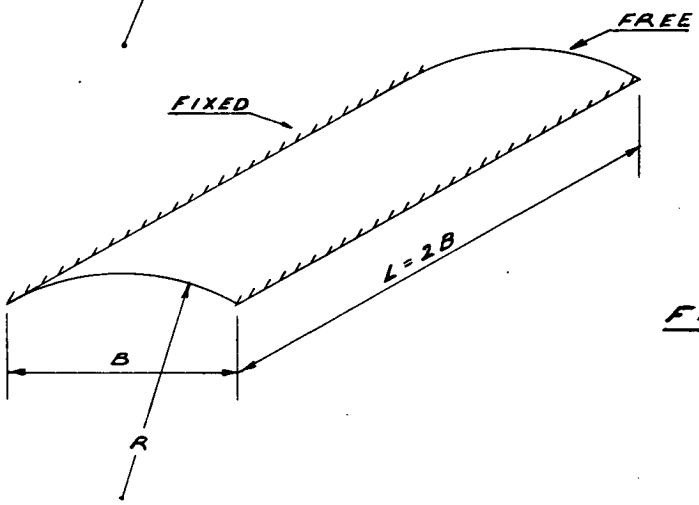

FIGURE: 4-2.

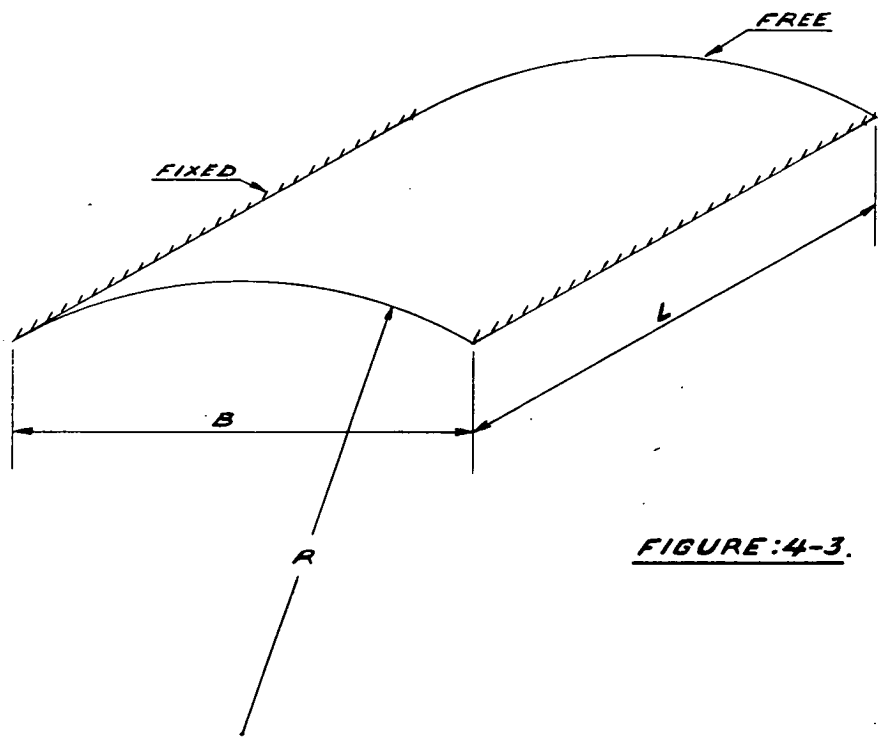

FIGURE :4-3.

4.2 FINITE DIFFERENCE APPROXIMATIONS

For convenience the displacement equations are expressed in non-dimensional form and then expressed in finite difference form, using the finite difference expressions included in Appendix 2-1. The non-dimensional displacement quantities $\bar{U}$, $\bar{V}$ and $\bar{W}$ are defined by:

$$\bar{U} = U/B$$

$$\bar{V} = V/B$$

$$\bar{W} = W/B$$

where B is any convenient dimension, here the width of shell.

The non-dimensional displacement equations are:

$$d'\left(\partial^2\bar{U}/\partial x^2\right) + \left((1-\mu)/2\right)\left(\partial^2\bar{U}/\partial y^2\right) + \left((1+\mu)/2\right)\left(\partial^2\bar{V}/\partial x\,\partial y\right) - \left(\mu B/R\right)\left(\partial\bar{W}/\partial x\right) = 0 \qquad (4.1.1)$$

$$\left((1-\mu)/2\right)\left(\partial^2\bar{V}/\partial x^2\right) + d''\left(\partial^2\bar{V}/\partial y^2\right) + \left((1+\mu)/2\right)\left(\partial^2\bar{U}/\partial x\,\partial y\right) - \left(d''B/R\right)\left(\partial\bar{W}/\partial y\right) + \left(P_y/D\right)B = 0 \qquad (4.1.2)$$

$$k'\left(\partial^4\bar{W}/\partial x^4\right) + 2\left(\partial^4\bar{W}/\partial x^2\partial y^2\right) + k''\left(\partial^4\bar{W}/\partial y^4\right) - \left(\mu\alpha B^3/R\right)\left(\partial\bar{U}/\partial x\right) - \left(d''\alpha B^3/R\right)\left(\partial\bar{V}/\partial y\right) + \left(d''\alpha B^4/R^2\right)\bar{W} - \left(P_z/K\right)B^3 = 0 \qquad (4.1.3)$$

The bar denoting a non-dimensional displacement will no longer be used, true values of U, V and W will be obtained by multiplying the computed values of $\bar{U}$, $\bar{V}$ and $\bar{W}$ by B. If a' and b' are the actual grid lengths along x and y directions respectively then a = a'/B and b = b'/B are the non-dimensional grid lengths (Figure 4-4). The above displacement equations, at a mesh point O, in finite difference expressions become:

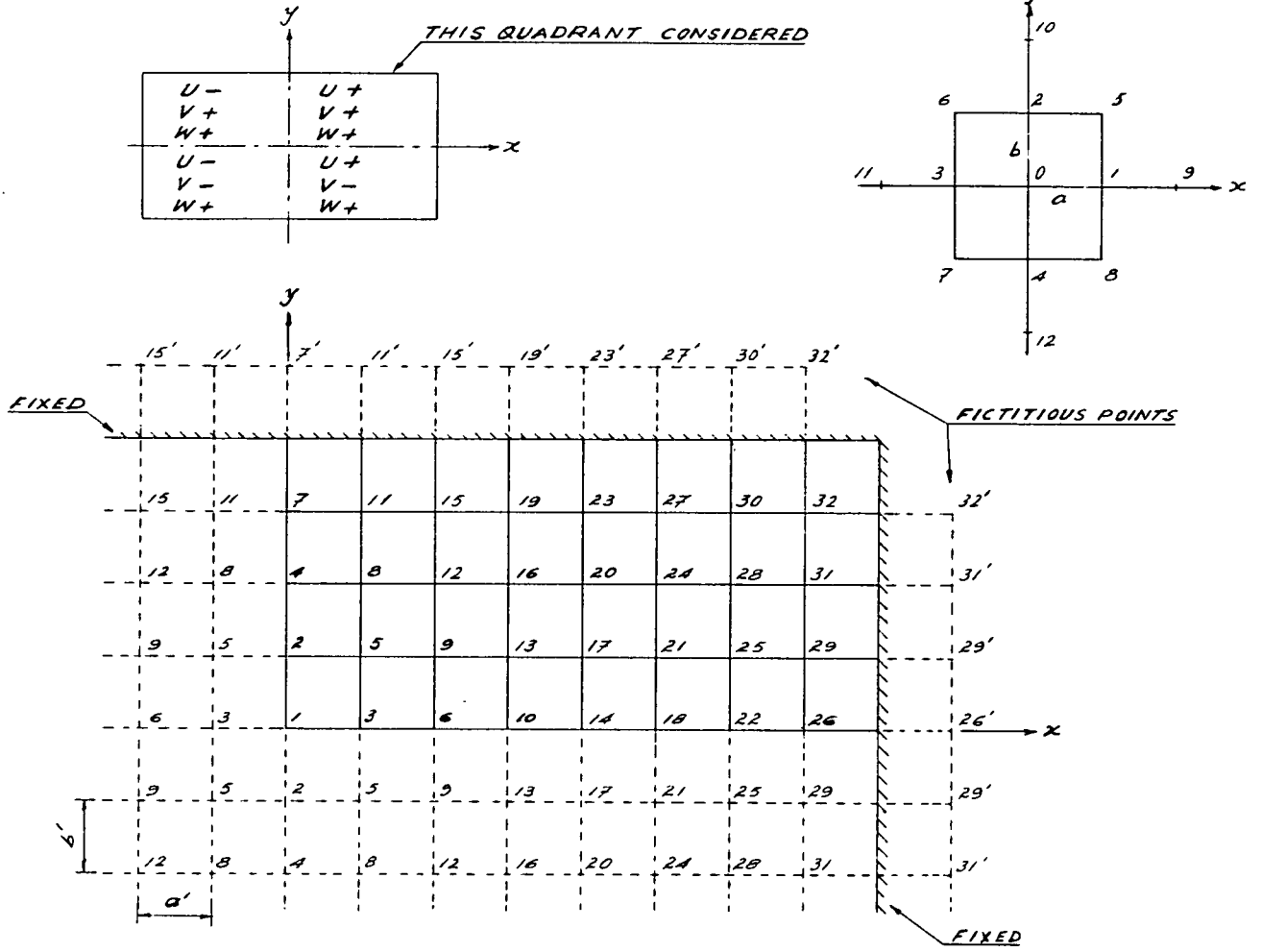

FIGURE : 4-4

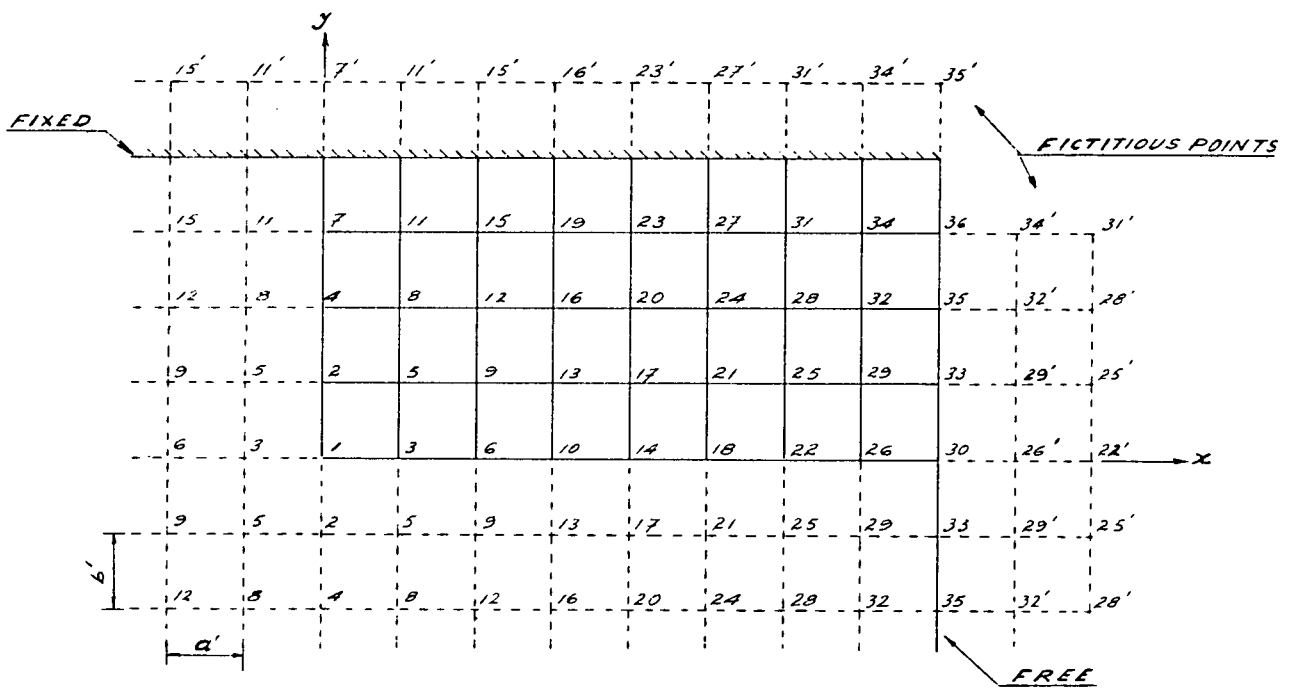

FIGURE : 4-5

$$(d'/a^2)(U_1 - 2U_0 + U_3) + ((1 - \mu)/2b^2)(U_2 - 2U_0 + U_4) + ((1 + \mu)/8ab)(V_5 - V_6 + V_7 - V_8) - (\mu B/2Ra)(W_1 - W_3) = 0 \qquad (4.2.1)$$

$$((1 - \mu)/2a^2)(V_1 - 2V_0 + V_3) + (d''/b^2)(V_2 - 2V_0 + V_4) + ((1 + \mu)/8ab)(U_5 - U_6 + U_7 - U_8) - (d''B/2Rb)(W_2 - W_4) + (P_y/D)B = 0 \qquad (4.2.2)$$

$$(k'/a^4)(6W_0 - 4W_1 - 4W_3 + W_9 + W_{11}) + (2/a^2b^2)(4W_0 - 2W_1 - 2W_2 - 2W_3 - 2W_4 + W_5 + W_6 + W_7 + W_8) + (k''/b^4)(6W_0 - 4W_2 - 4W_4 + W_{10} + W_{12}) - (\mu\alpha B^3/2Ra)(U_1 - U_3) - (d''\alpha B^3/2Rb)(V_2 - V_4) + (d''\alpha B^4/R^2)W_0 - (P_z/K)B^3 = 0 \qquad (4.2.3)$$

Let $a/b = c$ and multiplying equations (4.2.1) by b^2, (4.2.2) by a^2 and (4.2.3) by a^2b^2 and re-arranging:

$$-(1 - \mu + 2d'/c^2)U_0 + (d'/c^2)U_1 + ((1 - \mu)/2)U_2 + (d'/c^2)U_3 + ((1 - \mu)/2)U_4 + ((1 + \mu)/8c)(V_5 - V_6 + V_7 - V_8) - (\mu Bb/2Rc)(W_1 - W_3) = 0 \qquad (4.3.1)$$

$$-(1 - \mu + 2d''c^2)V_0 + ((1 - \mu)/2)V_1 + d''c^2V_2 + ((1 - \mu)/2)V_3 + d''c^2V_4 + ((1 + \mu)c/8)(U_5 - U_6 + U_7 - U_8) - (d''Bbc^2/2R)(W_2 - W_4) = -(P_y/D)Bb^2c^2 \qquad (4.3.2)$$

$$(6k'/c^2 + 6k''c^2 + 8 + (d''\alpha/R^2)B^4c^2b^4)W_0 - 4(k'/c^2 + 1)W_1 - 4(k''c^2 + 1)W_2 - 4(k'/c^2 + 1)W_3 - 4(k''c^2 + 1)W_4 + 2(W_5 + W_6 + W_7 + W_8) + (k'/c^2)W_9 + k''c^2W_{10} + (k'/c^2)W_{11} + k''c^2W_{12} - (\mu\alpha/2R)B^3cb^3(U_1 - U_3) - (d''\alpha/2R)B^3c^2b^3(V_2 - V_4) = (P_z/K)B^3c^2b^4 \qquad (4.3.3)$$

4.3 METHOD OF SOLUTION

The method of solution of the above equations are similar for all the boundary conditions (a), (b) and (c) except that some of the coefficients are different for the different boundary conditions. The solution of each individual problem is discussed separately.

The developed surface of the shell is partitioned into a number of grids of convenient length. Since the shell is symmetrical in both the x and y directions, only one quadrant of the shell is considered for solution.

Though by inspection it could be seen that U = 0 along x = 0, and V = 0 along y = 0, initially, values of U and V along x and y respectively were not assumed as zero. But from the results it was found that the values were nearly equal to zero, fractional values of U and V along x = 0 and y = 0 respectively might be due to the discrepancies arising due to the approximations assumed to eliminate the fictitious values. However in final computations the values of U along x = 0 and V along y = 0 were taken as zero.

Each nodal point is numbered starting from the ordinate. As the local computer has a small storage capacity, care is taken to minimise the amount of storage required and also the amount of typing. After a few trials the system of numbering shown in Figures (4-4 & 5) proved to be worthwhile.

Although the three displacement equations contain U, V and W terms, it is convenient to refer to the first as the U-equation, the second as the V-equation and the third as the W-equation. At each nodal point the equations (4.3.1 to 4.3.3) are applied and three linear equations are obtained for each point. Therefore for n-number of nodal points there are 3 n-number of equations, n-number of equations for each of U, V and W equations. The equations for the interior points of the shell can be written down by inspection. But the difficulty arises at points near the boundary which

are to be obtained by considering the boundary conditions of the individual problem. However, the sets of equations can be written in the form:

U-equations:

$$\begin{bmatrix} a_{11} & a_{12} & \cdots & a_{1n} \\ \vdots & & & \\ a_{n1} & & & a_{nn} \end{bmatrix} U + \begin{bmatrix} b_{11} & b_{12} & \cdots & b_{1n} \\ \vdots & & & \\ b_{n1} & & & b_{nn} \end{bmatrix} V + \begin{bmatrix} c_{11} & c_{12} & \cdots & c_{1n} \\ \vdots & & & \\ c_{n1} & & & c_{nn} \end{bmatrix} W = \begin{bmatrix} 0 \\ \\ \\ 0 \end{bmatrix} \quad (4.4.1)$$

V-equations:

$$\begin{bmatrix} d_{11} & d_{12} & \cdots & d_{1n} \\ \vdots & & & \\ d_{n1} & & & d_{nn} \end{bmatrix} U + \begin{bmatrix} e_{11} & e_{12} & \cdots & e_{1n} \\ \vdots & & & \\ e_{n1} & & & e_{nn} \end{bmatrix} V + \begin{bmatrix} f_{11} & f_{12} & \cdots & f_{1n} \\ \vdots & & & \\ f_{n1} & & & f_{nn} \end{bmatrix} W = \begin{bmatrix} p_{y_1} \\ \\ \\ p_{y_n} \end{bmatrix} \quad (4.4.2)$$

W-equations:

$$\begin{bmatrix} g_{11} & g_{12} & \cdots & g_{1n} \\ \vdots & & & \\ g_{n1} & & & g_{nn} \end{bmatrix} U + \begin{bmatrix} h_{11} & h_{12} & \cdots & h_{1n} \\ \vdots & & & \\ h_{n1} & & & h_{nn} \end{bmatrix} V + \begin{bmatrix} k_{11} & k_{12} & \cdots & k_{1n} \\ \vdots & & & \\ k_{n1} & & & k_{nn} \end{bmatrix} W = \begin{bmatrix} p_{z_1} \\ \\ \\ p_{z_n} \end{bmatrix} \quad (4.4.3)$$

where $a_{11}, a_{12}\cdots$, $b_{11}, b_{12}\cdots$, $c_{11}, c_{12}\cdots$, etc., are the coefficients of U, V, W and p_{y_1}., p_{z_1}., etc., are the load terms.

In compact form,

$$AU + BV + CW = 0 \quad (4.5.1)$$

$$DU + EV + FW = P_Y \quad (4.5.2)$$

$$GU + HV + KW = P_Z \quad (4.5.3)$$

For convenience of solution U-terms in U-equations, V-terms in V-equations and W-terms in W-equations are kept on the left hand side and the remaining

terms are transferred to the right hand side.

$$AU = -BV - CW \tag{4.6.1}$$

$$EV = P_Y - DU - FW \tag{4.6.2}$$

$$KW = P_Z - GU - HV \tag{4.6.3}$$

Since the W-equations contain the largest component of the load and the W-displacements are the largest, they are considered first while solving the above equations. Initially W-equations are solved by assuming U = V = 0. Substituting the values of 'W' thus obtained and assuming V = 0 in the U-equations, values of 'U' are obtained. Finally values of 'V' are obtained by solving the V-equations after substituting the values of 'W' and 'U' already obtained. Thus the first cycle is completed.

In the second cycle the values of U, V and W obtained from the first cycle are used and more accurate values of U, V and W are obtained.

Thus the accuracy of the values of U, V and W can be increased by increasing the number of cycles.

The whole operation of computation is performed by using a combination of standard programs which were first suitably modified for a KDF 9 computer.

It is to be noted that in order to use the computer program the eqatuions (4.6.3, 4.6.1 and 4.6.2) are written in the following form:

$$[C]W = [D] \tag{4.7.3}$$

$$[E]U = [F] \tag{4.7.1}$$

$$[G]V = [H] \tag{4.7.2}$$

where $[C] = K$

$[E] = A$

$[G] = E$

$$[D] = P_Z - GU - HV \tag{4.8.1}$$

$$[F] = -BV - CW \qquad (4.8.2)$$

$$[G] = P_Y - DU - FW \qquad (4.8.3)$$

This method of solution of the equations is adopted in all the three problems.

4.4 BOUNDARY CONDITONS

The state of stress in a shell can not be completely obtained by solving the differential equations in terms of displacements U, V and W unless they are subject to boundary conditions. In other words, stresses cannot be obtained, until certain number of relations between the forces, moments, and displacements of the elements at the supporting edges of the shell are specified. The interaction of the boundary elements with the shell is one of the most difficult problems of the shell theory. Not much work has yet been done on this aspect. In most of the cases the shell slab and the supporting members are treated separately. While determining the moments in the shell, the supporting edges are considered clamped and the moments and shears on the egde beams determined treating the entire load on the shell to be transferred to the beam as transverse shear forces.

However, in this chapter, keeping in mind the amount of analytical work and available facilities of testing, two boundary conditions viz. (a) Fixed at the edges and free at the end-arches, and (b) Fixed at the edges and at the end-arches, are considered.

4.5 CYLINDRICAL SHELLS HAVING A LENGTH/WIDTH RATIO OF TWO

The method discussed below is applicable to any cylindrical shell which has a length/width ratio of two and the assumed boundary conditions.

The plan of the shell is divided into 128 square mesh, 32 in each

quadrant, thus making mesh lengths a' = b' and hence a = b and $^{a}/_{b}$ = c = 1. (Figure 4-4). Therefore the non-dimensional displacement equations (4.3.1 to 4.3.3) in finite difference form for a nodal point 0 become:

$$-(1-\mu+2d')U_o + d'U_1 + ((1-\mu)/2)U_2 + d'U_3 + ((1-\mu)/2)U_4 + ((1+\mu)/8)(V_5 - V_6 + V_7 - V_8) - (\mu Ba/2R)(W_1 - W_3) = 0 \qquad (4.9.1)$$

$$-(1-\mu+2d'')V_o + ((1+\mu)/2)V_1 + d''V_2 + ((1-\mu)/2)V_3 + d''V_4 + ((1+\mu)/8)(U_5 - U_6 + U_7 - U_8) - (d''Ba/2R)(W_2 - W_4) = (-P_y/D)Ba^2 \qquad (4.9.2)$$

$$(6k' + 6k'' + 8 + (d''\alpha/R^2)B^4a^4)W_o - 4(k'+1)W_1 - 4(k''+1)W_2 - 4(k'+1)W_3 - 4(k''+1)W_4 + 2(W_5 + W_6 + W_7 + W_8) + k'W_9 + k''W_{10} + k'W_{11} + k''W_{12} - (\mu\alpha/2R)(B^3a^3)(U_1 - U_3) - (d''\alpha B^3a^3/2R)(V_2 - V_4) = (P_z/K)B^3a^4 \qquad (4.9.3)$$

4.5a <u>Fixed at the edges and at the end-arches (Figure 4-4)</u>

For the above boundary conditions at the edges and at the end-arches:

1. $W = 0$ (4.10.1)
2. $U = 0$ (4.10.2)
3. $V = 0$ (4.10.3)
4. $\partial W/\partial x = 0$ (4.10.4a)

   $\therefore W_1 = W_3$ (4.10.4b)
5. $\partial W/\partial y = 0$ (4.10.5a)

   $\therefore W_2 = W_4$ (4.10.5b)

Substituting the values of the fictitious points, the sets of U, V and W equations are written down in the form of the equations (4.4.1 to 4.4.3) and the solutions obtained using a computer. The computer program is included

in Appendix 4-4

The program is written in a general form so that cylindrical shells of any size having the length equal to twice the width, of any cross-section, material & Poisson's ratio, under any load intensity can be solved by this program only by changing the appropriate data.

For the perspex shell the following data was used. (Figure 4-6).

Length	=	30 in.
Width	=	15 in.
Radius	=	15 in.
Mesh Size	=	1.875 in. square
t_1	=	0.125 in.
t_2	=	0.1875 in.
b_1	=	1.00 in.
b_2	=	0.0 in.
b_3	=	0.125 in.
Poisson's Ratio	=	0.35
Young's Modulus	=	1 lb/sq. in.
Load	=	1 unit load/sq.in.

In order to obtain the true displacements the values obtained from the program must be multiplied by (applied load/sq.in)/Young's Modulus.

The displacements U,V and W at different nodal points due to a unit load/sq.in. with Young's Modulus = 1 lb/sq.in. are shown in Figures (4-7 & 8)

4.5b Fixed at the edges and free at the end-arches (Figure 4-5)

This problem is more complicated than the previous one though the procedure of solution is the same. In the x-direction, for each displacement equation there will be 3 fictitious points one mesh length outside the free

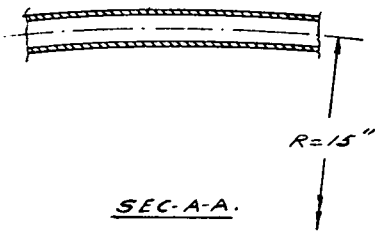

SEC-A-A.

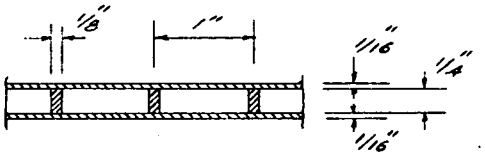

SEC-B-B.

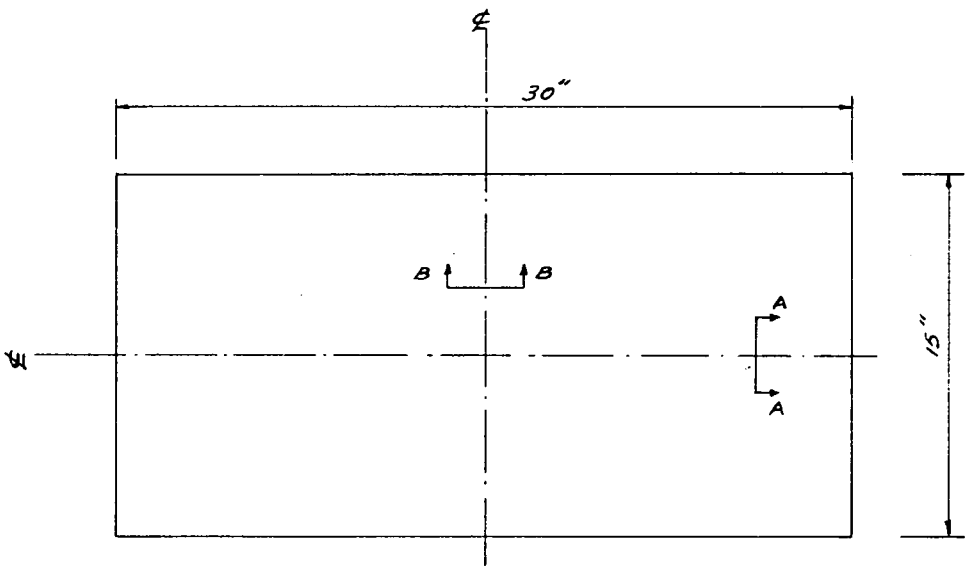

PLAN

DETAILS OF PERSPEX MODEL : SHELL.

FIGURE : 4-6

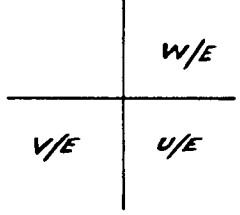

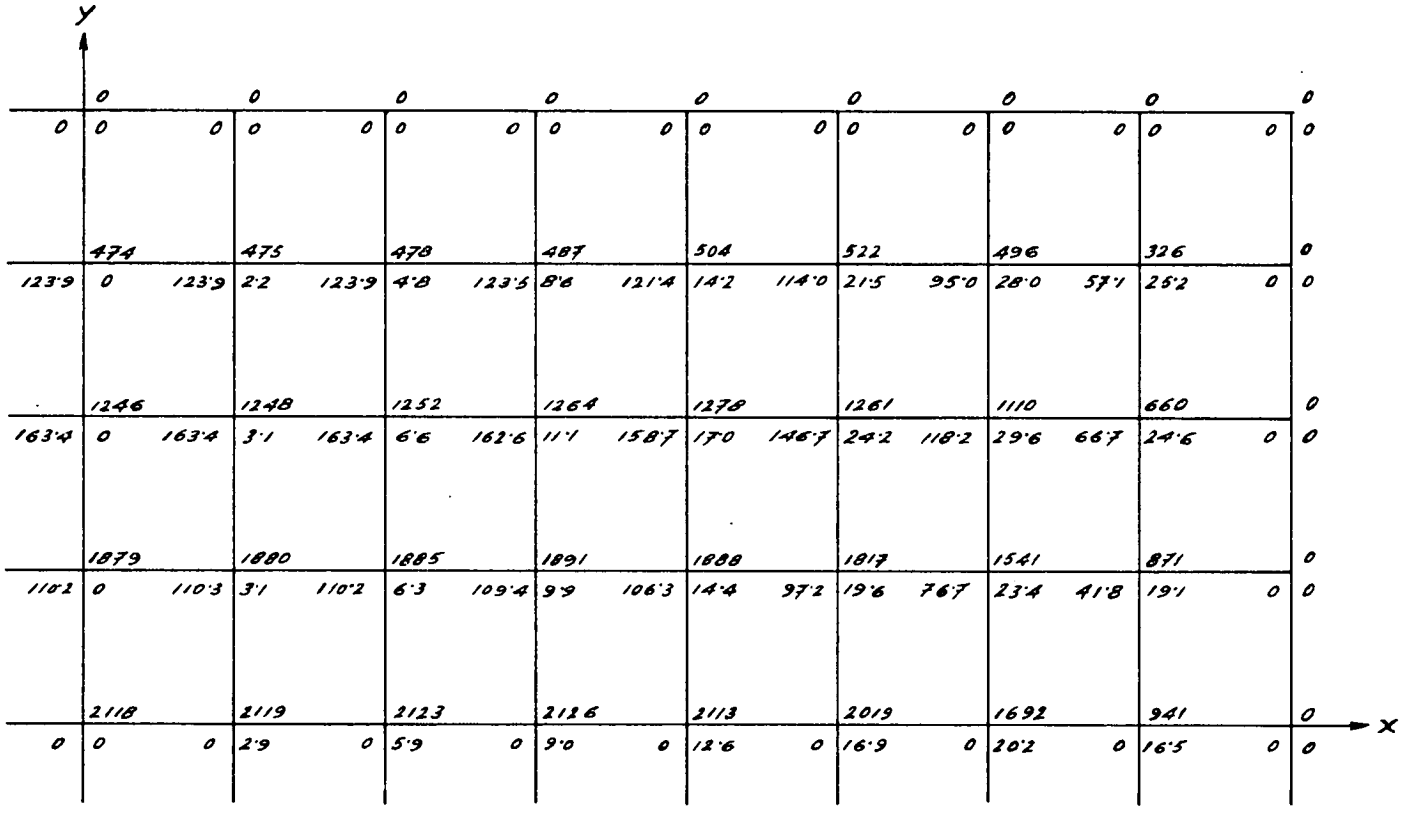

U.D.LOAD = 1 lb/in^2.

μ = 0·35.

DISPLACEMENTS.(INCH.) AT 12TH CYCLE.

CASE-(a): PERSPEX CYLINDRICAL SHELL FIXED AT EDGES & END-ARCHES.

FIGURE: 4-7.

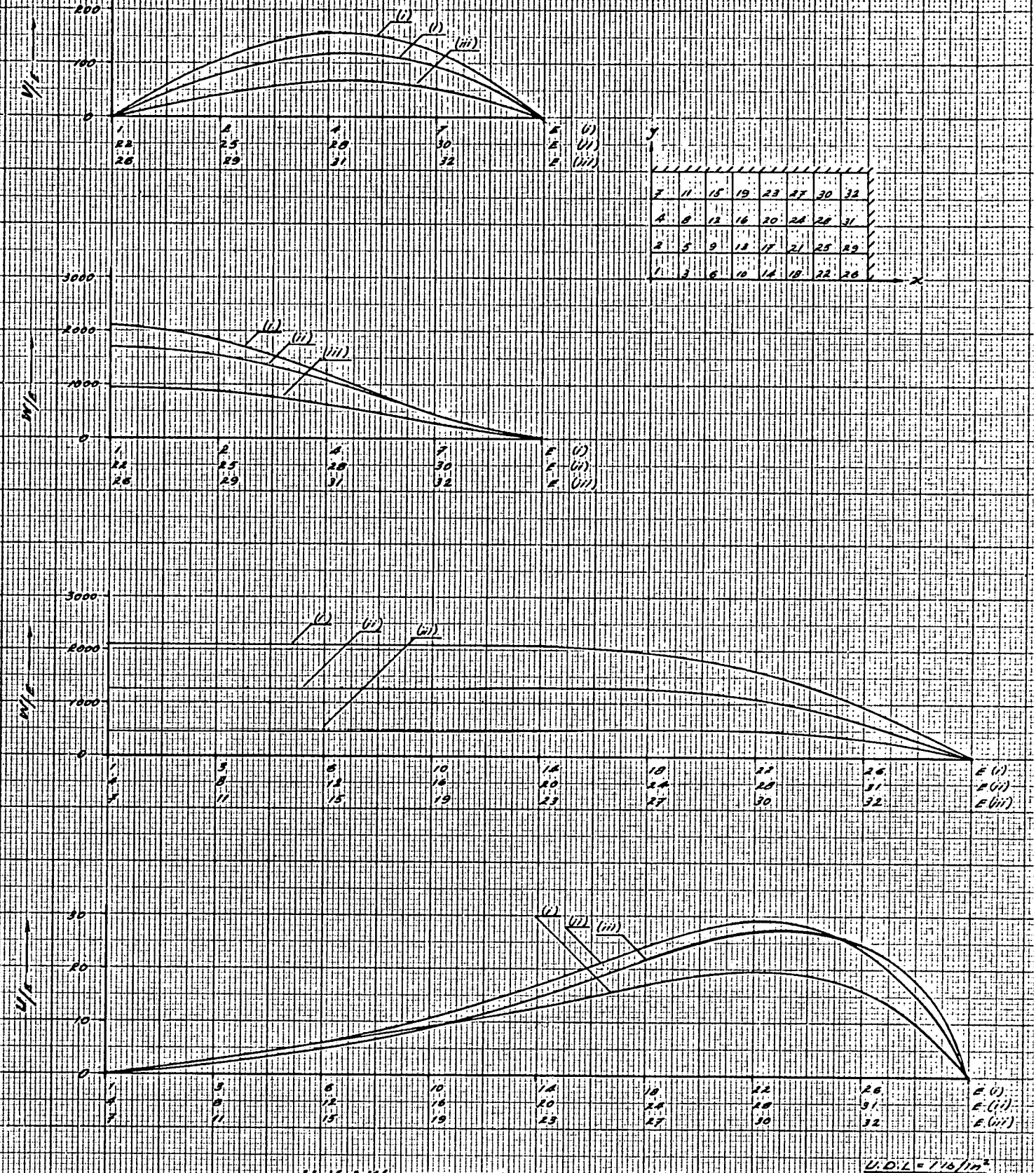

U.D.L = 1 lb/in²

U, V & W- DISPLACEMENTS FOR CASE (a)

FIGURE: 4-8

edge and 1 fictitious point two mesh lengths outside the free edge. The fictitious values are obtained as follows:

At the fixed edges:

1. $W = 0$ (4.11.1)

2. $U = 0$ (4.11.2)

3. $V = 0$ (4.11.3)

4. $\partial W/\partial y = 0$ (4.11.4a)

$\therefore W_2 = W_4$ (4.11.4b)

At the free edges:

1. $N_x = 0$ (4.12.1)

2. $N_{xy} = 0$ (4.12.2)

3. $M_x = 0$ (4.12.3)

4. $M_{xy} = 0$ (4.12.4)

5. $Q_x = 0$ (4.12.5)

The above five conditions are not independent. M_{xy} can be coupled with Q_x to give $Q_x + \partial/\partial y(M_{xy}) = 0$, and with N_{xy} to give $N_{xy} - M_{xy}/R = 0$

Therefore, the five conditions can be reduced to the following four boundary conditions:

$N_x = 0$ (4.13.1)

$N_{xy} - M_{xy}/R = 0$ (4.13.2)

$M_x = 0$ (4.13.3)

$Q_x + \partial/\partial y(M_{xy}) = 0$ (4.13.4)

Neglecting the term M_{xy}/R, since it is very small compared to N_{xy}, and expressing the above equations in terms of displacements:

$$D_x(\partial U/\partial x) + \mu D(\partial V/\partial y - W/R) = 0 \qquad (4.14.1)$$

$$(D(1-\mu)/2)(\partial U/\partial y + \partial V/\partial x) = 0 \qquad (4.14.2)$$

$$-K_x(\partial^2 W/\partial x^2) - \mu K(\partial^2 W/\partial y^2) = 0 \qquad (4.14.3)$$

$$-K_x(\partial^3 W/\partial x^3) - (2-\mu)K(\partial^3 W/\partial x \partial y^2) = 0 \qquad (4.14.4)$$

Dividing the equations (4.14.1 and 4.14.2) by 'D' and equations (4.14.3 and 4.14.4) by 'K' and expressing these in finite difference form:

$$(d'/2a)(U_1 - U_3) + (\mu/2a)(V_2 - V_4) - (\mu/R)W_o = 0 \qquad (4.15.1)$$

$$(1/2a)(U_2 - U_4) + (1/2a)(V_1 - V_3) = 0 \qquad (4.15.2)$$

$$(k'/a^2)(W_1 + W_3 - 2W_o) + (\mu/a^2)(W_2 + W_4 - 2W_o) = 0 \qquad (4.15.3)$$

$$(k'/2a^3)(W_9 - 2W_1 + 2W_3 - W_{11}) + ((2-\mu)/2a^3)(W_5 - W_6 - 2W_1 + 2W_3 + W_8 - W_7) = 0 \qquad (4.15.4)$$

Therefore re-arranging the terms in the above equations the following fictitious points are obtained:

From eqn.(4.15.1), $$U_1 = U_3 - (\mu/d')(V_2 - V_4) + (2a\mu/Rd')W_o \qquad (4.16.1)$$

From eqn.(4.15.2), $$V_1 = V_3 - U_2 + U_4 \qquad (4.16.2)$$

From eqn.(4.15.3),

Origin at O, $$W_1 = (2(k'+\mu)/k')W_o - W_3 - (\mu/k')(W_2 + W_4) \qquad (4.16.3a)$$

Origin at 2, $$W_5 = (2(k'+\mu)/k')W_2 - W_6 - (\mu/k')(W_o + W_{10}) \qquad (4.16.3b)$$

Origin at 4, $$W_8 = (2(k'+\mu)/k')W_4 - W_7 - (\mu/k')(W_o + W_{12}) \qquad (4.16.3c)$$

From equation (4.15.4):

$$W_9 = (2(k'+2-\mu)/k')(W_1 - W_3) - ((2-\mu)/k')(W_5 - W_6 + W_8 - W_7) + W_{11} \qquad (4.16.4a)$$

In this expression for W_9, a fictitious value two mesh lengths outside the free edge, values of W_1, W_5 and W_8 are the fictitious values. Substituting for W_1, W_5 and W_8 already obtained, the fictitious value of W_9 becomes:

$$W_9 = W_{11} + ((4k'^2 + 8k' + 12\mu - 6\mu^2)/k'^2)W_o + ((4\mu^2 - 8\mu - 4k')/k'^2)(W_2 + W_4) + (4\mu - 4k' - 8)W_3 + (2(2-\mu)/k')(W_6 + W_7) + ((2\mu - \mu^2)/k'^2)(W_{10} + W_{12}) \quad (4.16.4b)$$

After obtaining the fictitious values, the displacement equations for each mesh point in finite difference form are written down in the form of the equations (4.4.1 to 4.4.3). The solutions of the above equations were obtained using a computer program similar to the previous example.

Data used in the previous example are used in this example also.

The displacements U, V and W at different nodal points are shown in Figures (4. 9 & 10).

Figures (4. 11 to 4. 13) show the comparison between the displacements for case (a) and (b).

For a concentrated load at any point, the load is considered as uniformly distributed over a single mesh area. Only the equations at the surrounding node contain a non-zero value for the load terms.

Data used in this case also are the same as the previous example except that here unit concentrated load is assumed at the central point.

The displacements U, V and W at different nodal points are shown in Figure (4-14).

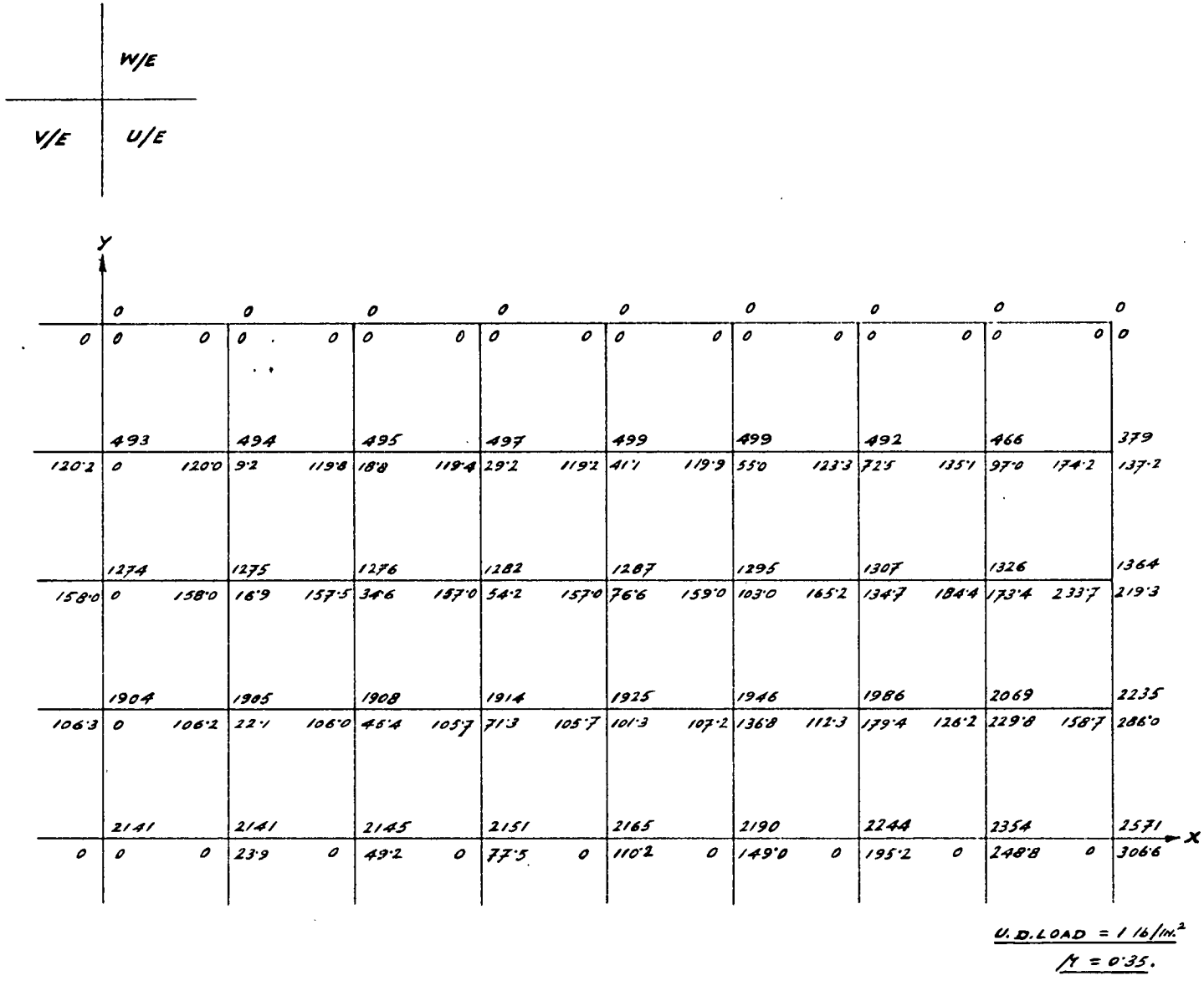

U.D.LOAD = 1 16/in.²

1/M = 0·35.

DISPLACEMENTS AT 12TH CYCLE.

CASE-(6): PERSPEX CYLINDRICAL SHELL FIXED AT EDGES, FREE AT END-ARCHES.

FIGURE: 4-9.

V & W - DISPLACEMENTS FOR CASE (6)

FIGURE: 4-10

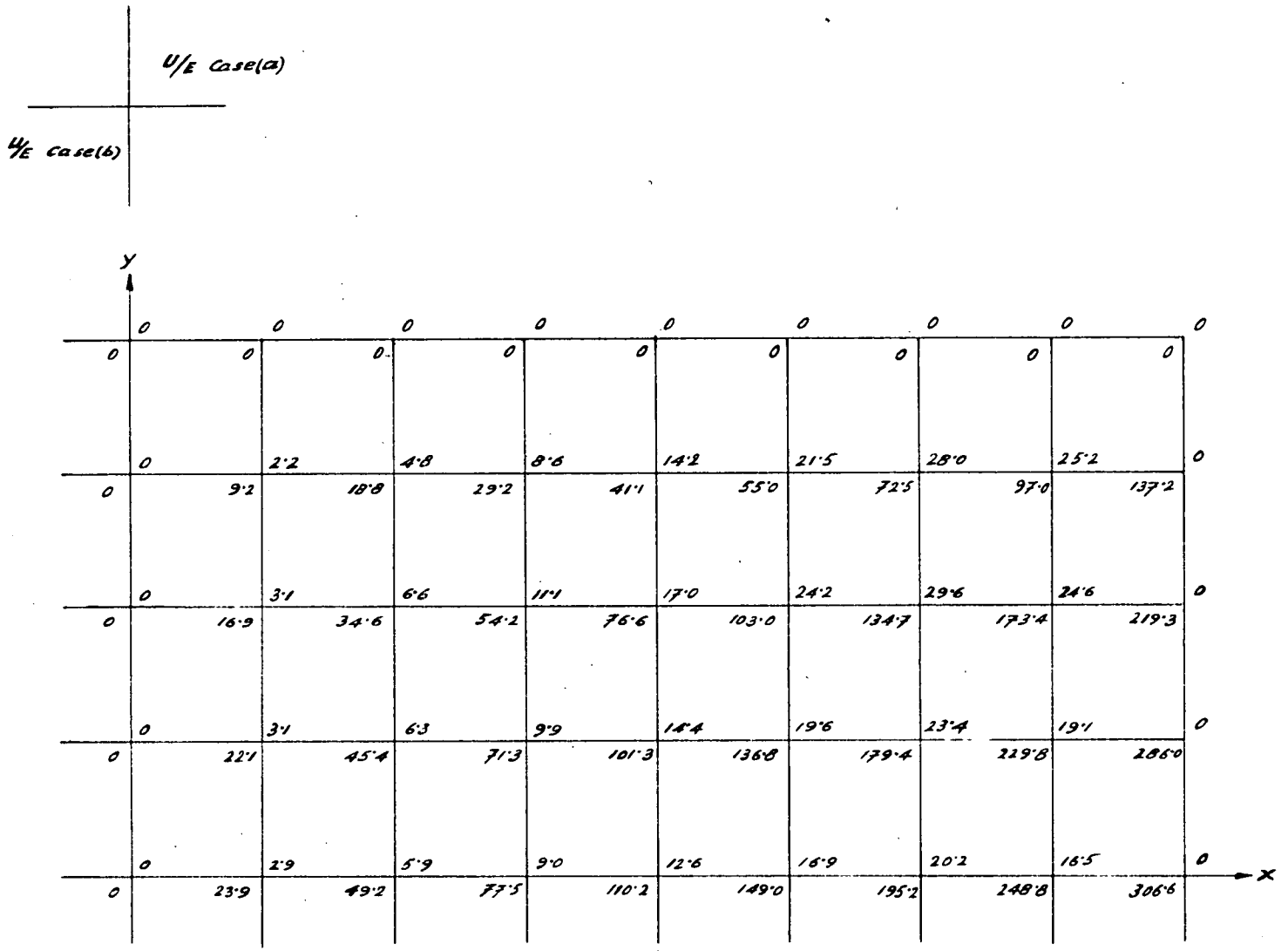

U.D.L. = 1 lb/in.²

μ = 0·35.

COMPARISON OF U-DISPLACEMENTS : CASES-(a) & (b).

FIGURE : 4-11.

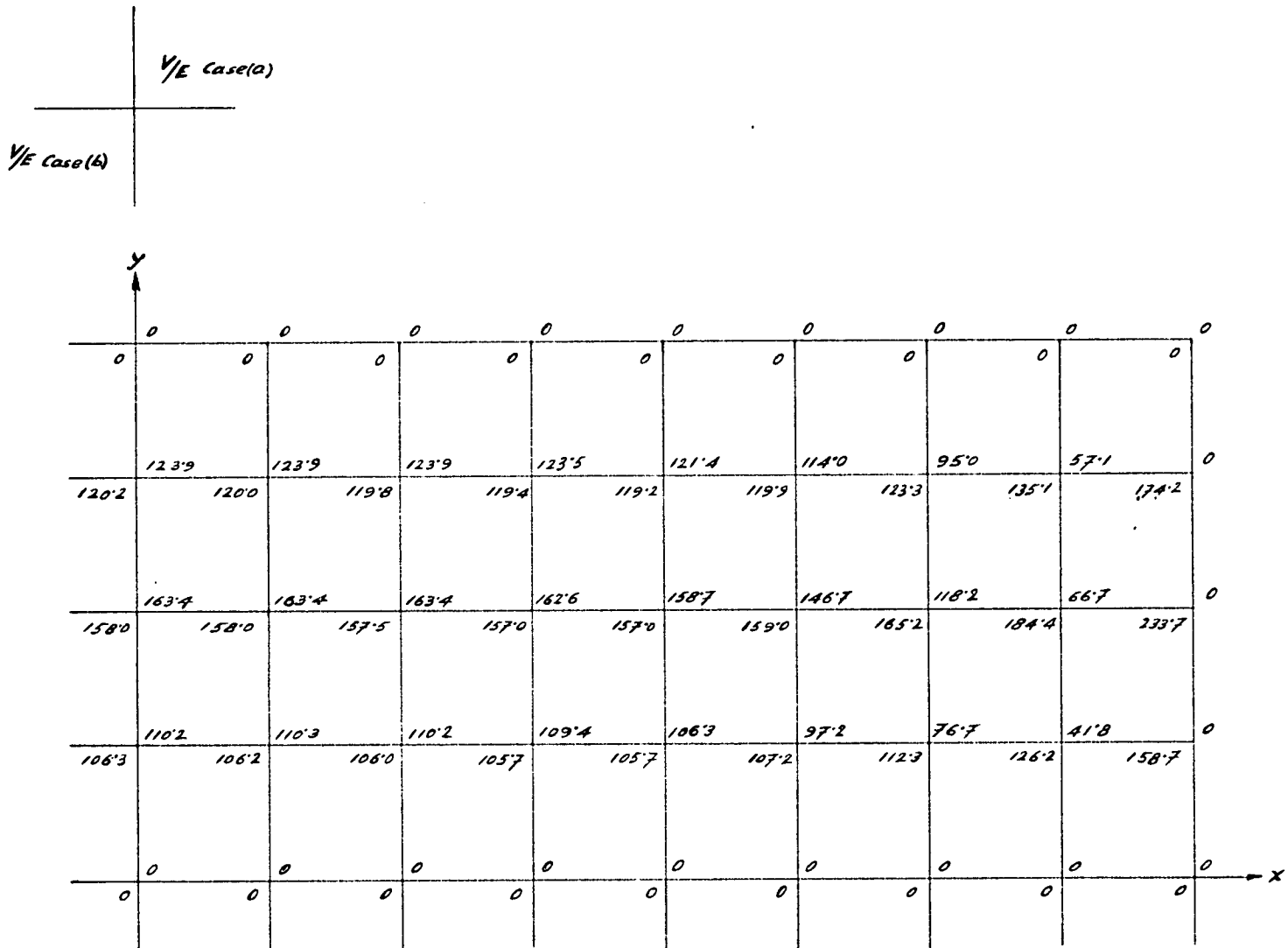

U.D.L. = 1 lb/in².

μ = 0·35.

COMPARISON OF V- DISPLACEMENTS : CASES-(a) & (b).

FIGURE : 4-12.

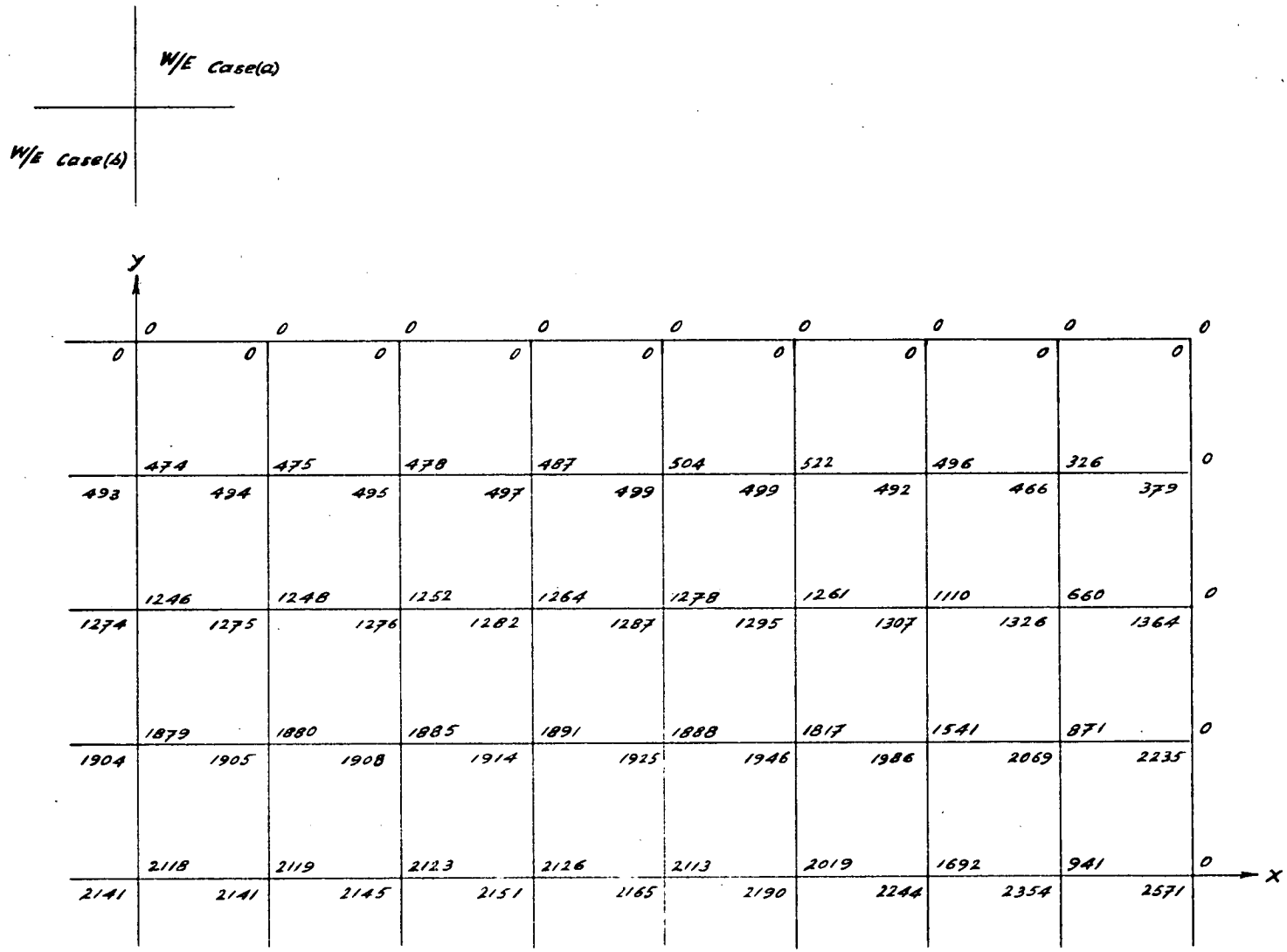

U.D.L. = 1 lb/in.^{2}

$\mu = 0.35$.

COMPARISON OF W-DISPLACEMENTS: CASES-(a) & (b).

FIGURE: 4-13.

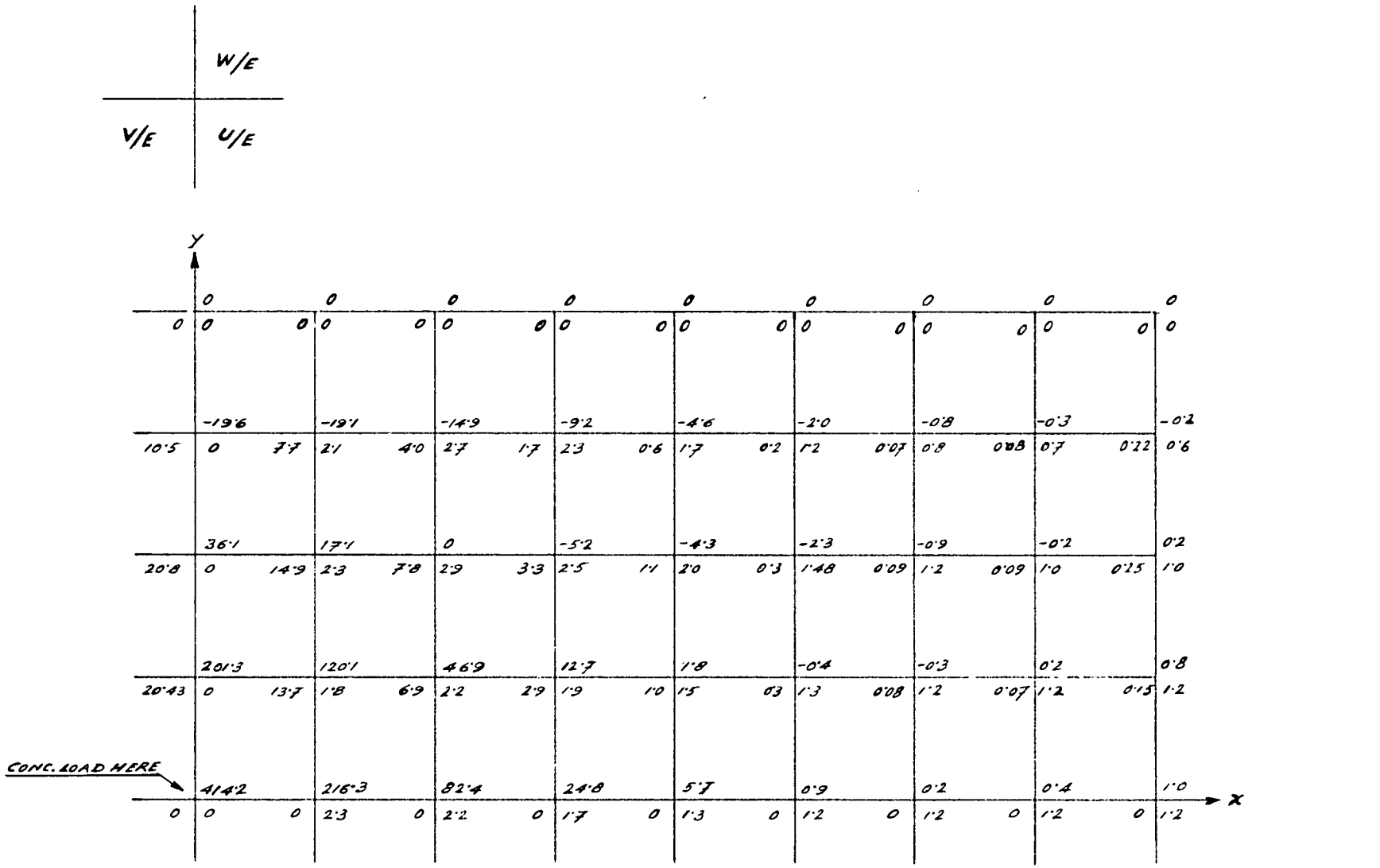

CONC. LOAD OF 1·0 LB AT THE CENTRE.

$\nu = 0.35$.

DISPLACEMENTS. (INCH.). AT 11TH CYCLE. CASE-(b).

FIGURE : 4-14.

4.6 CYLINDRICAL SHELL OF ANY LENGTH/WIDTH RATIO: (MODEL:HOLLOW CLAY BLOCKS)

4.6a Fixed at the edges and free at the end-arches

For a shell of arbitrary size a solution can be obtained by assuming a ratio between the grid lengths a' and b' and hence the ratio between a and b equal to c. Several tests were done to determine the Poisson's ratio of hollow clay structures and this was found to be nearly zero. It is also usual practice to assume Poisson's ratio for brick structures or concrete structures as zero. In the present case therefore Poisson's ratio is taken as zero. The solution of this problem is similar to the previous examples.

The assumption that Poisson's ratio equals to zero reduces the displacement equations to:

$$d'(\partial^2U/\partial x^2) + \tfrac{1}{2}(\partial^2U/\partial y^2) + \tfrac{1}{2}(\partial^2V/\partial x\partial y) = 0 \quad (4.17.1)$$

$$\tfrac{1}{2}(\partial^2V/\partial x^2) + d''(\partial^2V/\partial y^2) + \tfrac{1}{2}(\partial^2U/\partial x\partial y) - (d''B/R)(\partial W/\partial y) + (P_y/D)B = 0 \quad (4.17.2)$$

$$k'(\partial^4W/\partial x^4) + 2(\partial^4W/\partial x^2\partial y^2) + k''(\partial^4W/\partial y^4) - (d''\alpha/R)B^3(\partial V/\partial y) + (d''\alpha/R^2).B^4W - (P_z/K)B^3 = 0 \quad (4.17.3)$$

Expressing these equations in finite difference form and re-arranging:

$$-(1 + 2d'/c^2)U_o + (d'/c^2)U_1 + \tfrac{1}{2}U_2 + (d'/c^2)U_3 + \tfrac{1}{2}U_4 + (1/8c)(V_5 - V_6 + V_7 - V_8) = 0 \quad (4.18.1)$$

$$-(1 + 2d''c^2)V_o + \tfrac{1}{2}V_1 + d''c^2V_2 + \tfrac{1}{2}V_3 + d''c^2V_4 + (c/8)(U_5 - U_6 + U_7 - U_8) - (d''B/2R)\,c^2b\,(W_2 - W_4) = -(P_y/D)\,Bb^2c^2 \quad (4.18.2)$$

$$(6(k'/c^2) + 6k''c^2 + 8 + (d''\alpha/R^2)B^4c^2b^4)W_o - 4(k'/c^2 + 1)W_1 - 4(k''c^2 + 1)W_2 - 4(k'/c^2 + 1)W_3 - 4(k''c^2 + 1)W_4 + 2(W_5 + W_6 + W_7 + W_8) + (k'/c^2)W_9 + k''c^2W_{10} + (k'/c^2)W_{11} + k''c^2W_{12} - (d''\alpha/2R)\,B^3c^2b^3\,(V_2 - V_4) = (P_z/K)\,B^3c^2b^4 \quad (4.18.3)$$

Determination of values of fictitious points (Figure 4-15)

At the fixed edges, the boundary conditions:

1. $W = 0$ (4.19.1)

2. $U = 0$ (4.19.2)

3. $V = 0$ (4.19.3)

4. $\partial W/\partial y = 0$ (4.19.4a)

$\therefore W_2 = W_4$ (4.19.4b)

At the free edges, the boundary conditions, from equations (4.14.1 to 4.14.4)

1. $D_x(\partial U/\partial x) = 0$ (4.20.1a)

$\therefore U_1 = U_3$ (4.20.1b)

2. $\partial U/\partial y + \partial V/\partial x = 0$ (4.20.2a)

or, $(1/2b)(U_2 - U_4) + (1/2a)(V_1 - V_3) = 0$ (4.20.2b)

$\therefore V_1 = V_3 - c(U_2 - U_4)$ (4.20.2c)

3. $K_x(\partial^2 W/\partial x^2) = 0$ (4.20.3a)

$\therefore W_1 = 2W_o - W_3$ (4.20.3b)

similarly,

$W_5 = 2W_2 - W_6$ (4.20.3c)

$W_8 = 2W_4 - W_7$ (4.20.3d)

4. $K_x(\partial^3 W/\partial x^3) + 2k(\partial^3 W/\partial x \partial y^2) = 0$ (4.20.4a)

Dividing by K, expressing in finite difference approximations, substituting the values of fictitious points one mesh length outside the free edge and re-arranging the fictitious value two mesh lengths outside the free edge becomes:

$$W_9 = W_{11} + 4(1 + 2c^2/k')W_o - (4c^2/k')W_2 - 4(1 + 2c^2/k')W_3 - (4c^2/k')(W_4 - W_6 - W_7) \quad (4.20.4b)$$

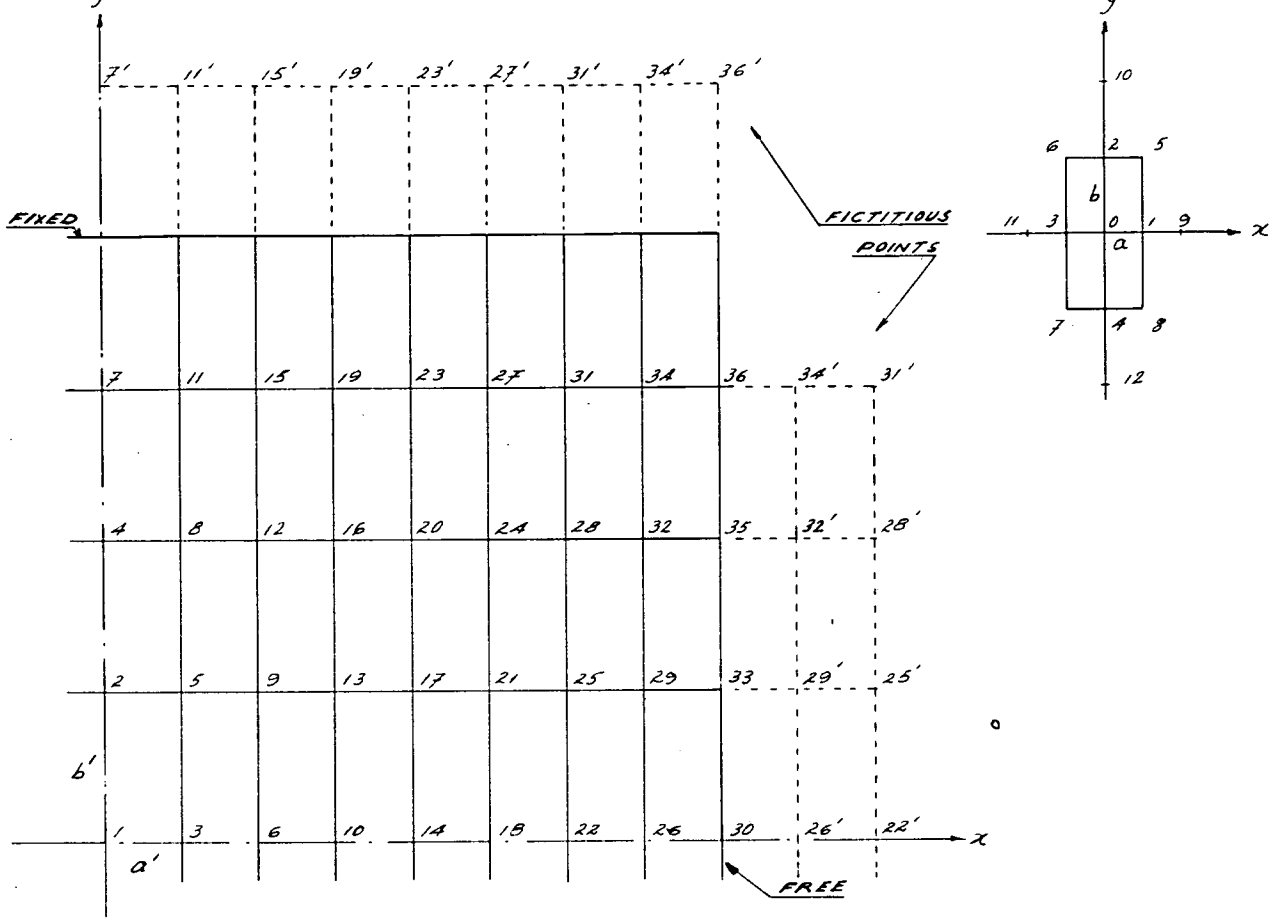

FIGURE: 4-15.

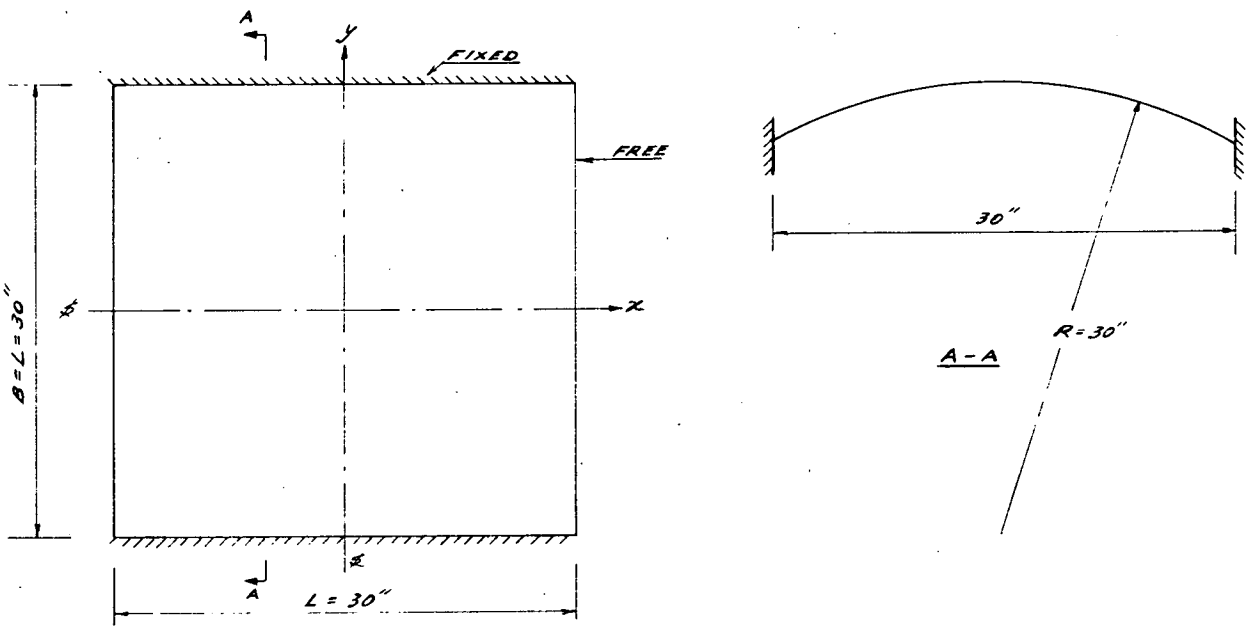

DIMENSIONS OF CLAY-BLOCK SHELL.

FIGURE: 4-16.

Therefore substituting the values of the fictitious points, the sets of U, V and W-equations are written down in the form of the equations (4.4.1 to 4.4.3). These equations were solved using a computer program similar to the previous examples.

The program is written in a general form so that this can be used to solve shell built of hollow clay blocks of any size and cross section under any load intensity using the appropriate data.

The data for the model shell constructed in the laboratory were as follows: (Figure 4-16).

1.	Length	=	30 in.
2.	Width	=	30 in.
3.	Radius	=	30 in.
4.	Mesh Lengths a'	=	1.875 in.
	b'	=	3.75 in.
5.	Load	=	1 lb/in^2
6.	EA	=	1.57 x 10^5 lbs.
7.	EA_x	=	1.57 x 10^5 lbs.
8.	EA_y	=	1.7 x 10^5 lbs.
9.	EI	=	6.57 x 10^4 lb.in^2
10.	EI_x	=	6.57 x 10^4 lb.in^2
11.	EI_y	=	7.1 x 10^4 lb.in^2

In order to obtain the true displacements, the computed values are to be multiplied by 'B' to make them dimensional and then by the applied load/in^2.

The Figure (4.17) shows the displacements V and W at different nodal points.

Note: In the above case D = EA, $D_x = EA_x$, $D_y = EA_y$, K = EI, $K_x = EI_x$ and $K_y = EI_y$. However, a program is also written in which D, D_x, D_y, K

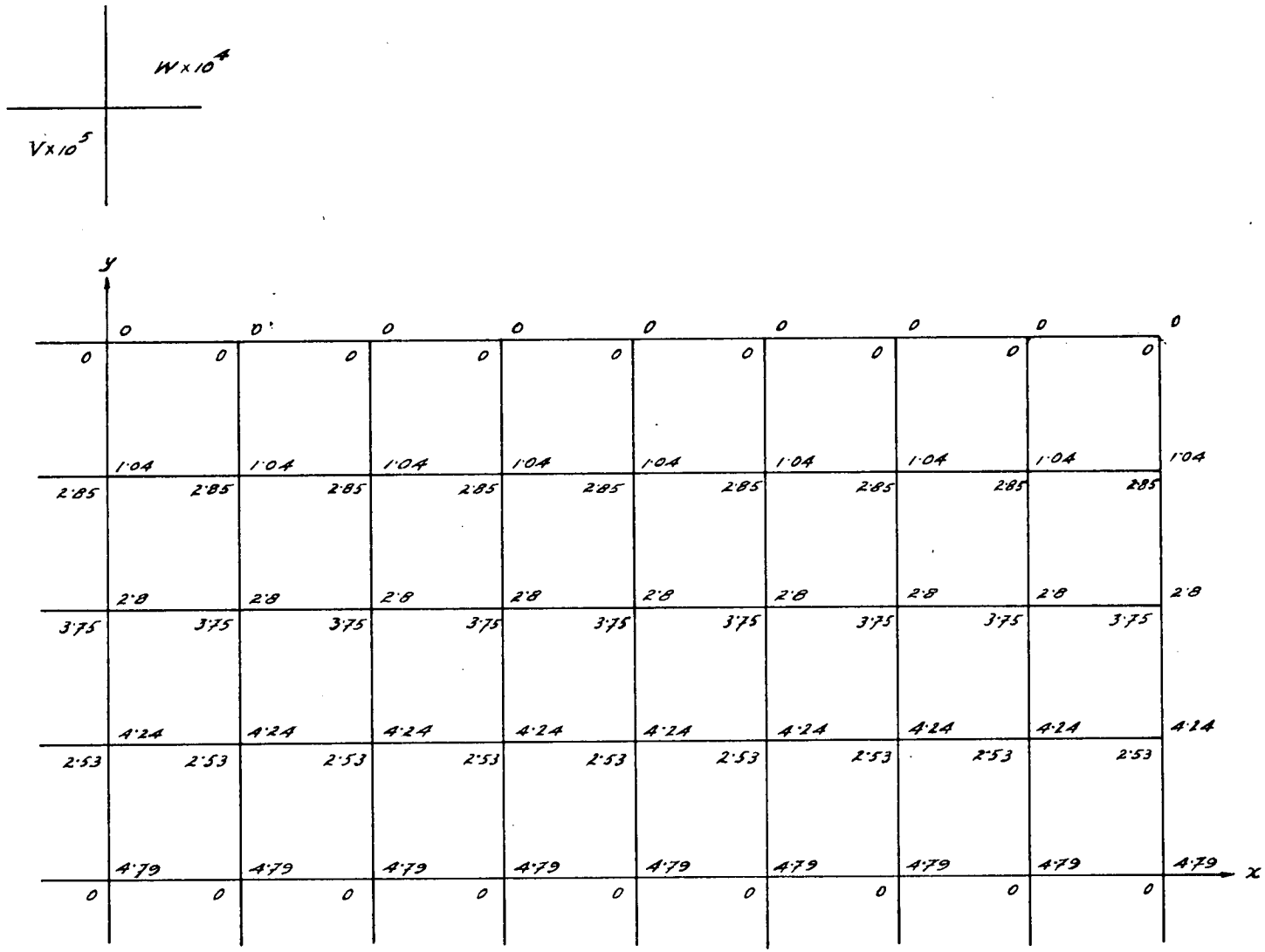

LOAD = 1 lb/in.^{2}

$\mu = 0$.

DISPLACEMENTS (INCH)

CYLINDRICAL SHELL BUILT OF HOLLOW CLAY BLOCKS.

FIGURE: 4-17

K_x and K_y are expressed in terms of b_1, b_2, b_3, t_1, t_2 and E. This program is used to compare the analytical results of shell obtained in (4.5b) taking Poisson's ratio equals to zero.

4.7 DETERMINATION OF STRESSES AND STRAINS:

Once the values of U, V and W are obtained, the values of Forces and Moments at the nodal points can easily be calculated by substituting the finite difference approximations into the equations (3.8.1 to 3.8.6):

$$(N_x)_o = D((d'/2a)(U_1 - U_3) + (\mu/2b)(V_2 - V_4) - (\mu/R)W_o)) \quad (4.21.1)$$

$$(N_y)_o = D((d''/2b)(V_2 - V_4) - (d''/R)W_o + (\mu/2a)(U_1 - U_3)) \quad (4.21.2)$$

$$(N_{xy})_o = (D(1-\mu)/4)(\tfrac{1}{b}(U_2 - U_4) + \tfrac{1}{a}(V_1 - V_3)) \quad (4.21.3)$$

$$(M_x)_o = -K((k'/a^2)(W_1 + W_3) - 2(k'/a^2 + \mu/b^2)W_o + (\mu/b^2)(W_2 + W_4)) \quad (4.21.4)$$

$$(M_y)_o = -K((k''/b^2)(W_2 + W_4) - 2(k''/b^2 + \mu/a^2)W_o + (\mu/a^2)(W_1 + W_3)) \quad (4.21.5)$$

$$(M_{xy})_o = (-K(1-\mu)/4ab)(W_5 - W_6 + W_7 - W_8) \quad (4.21.6)$$

The Combined stresses are given by:

$$\sigma_x = N_x/A_x \pm (M_x/I_x)(t_2/2) \quad (4.22.1)$$

$$\sigma_y = N_y/A_y \pm (M_y/I_y)(t_2/2) \quad (4.22.2)$$

$$T_{xy} = N_{xy}/A \pm (M_{xy}/I)(t_2/2) \quad (4.22.3)$$

where, A_x, A_y and A are the areas of cross sections

I_x, I_y and I are the moments of Inertia of sections

t_2 is the overall thickness of the shell.

And the strains are obtained from the expressions:

$$\epsilon_x = (1/E)(\sigma_x - \mu\sigma_y) \qquad (4.23.1)$$

$$\epsilon_y = (1/E)(\sigma_y - \mu\sigma_x) \qquad (4.23.2)$$

$$\gamma_{xy} = T_{xy}/G \qquad (4.23.3)$$

The values of Forces, Moments and Stresses at different nodal points have been computed and these are shown in Figures (4.18 to 4.34).

Note: It is to be noted that while writing down all the computer programs of this chapter some of the notation is changed for convenience.

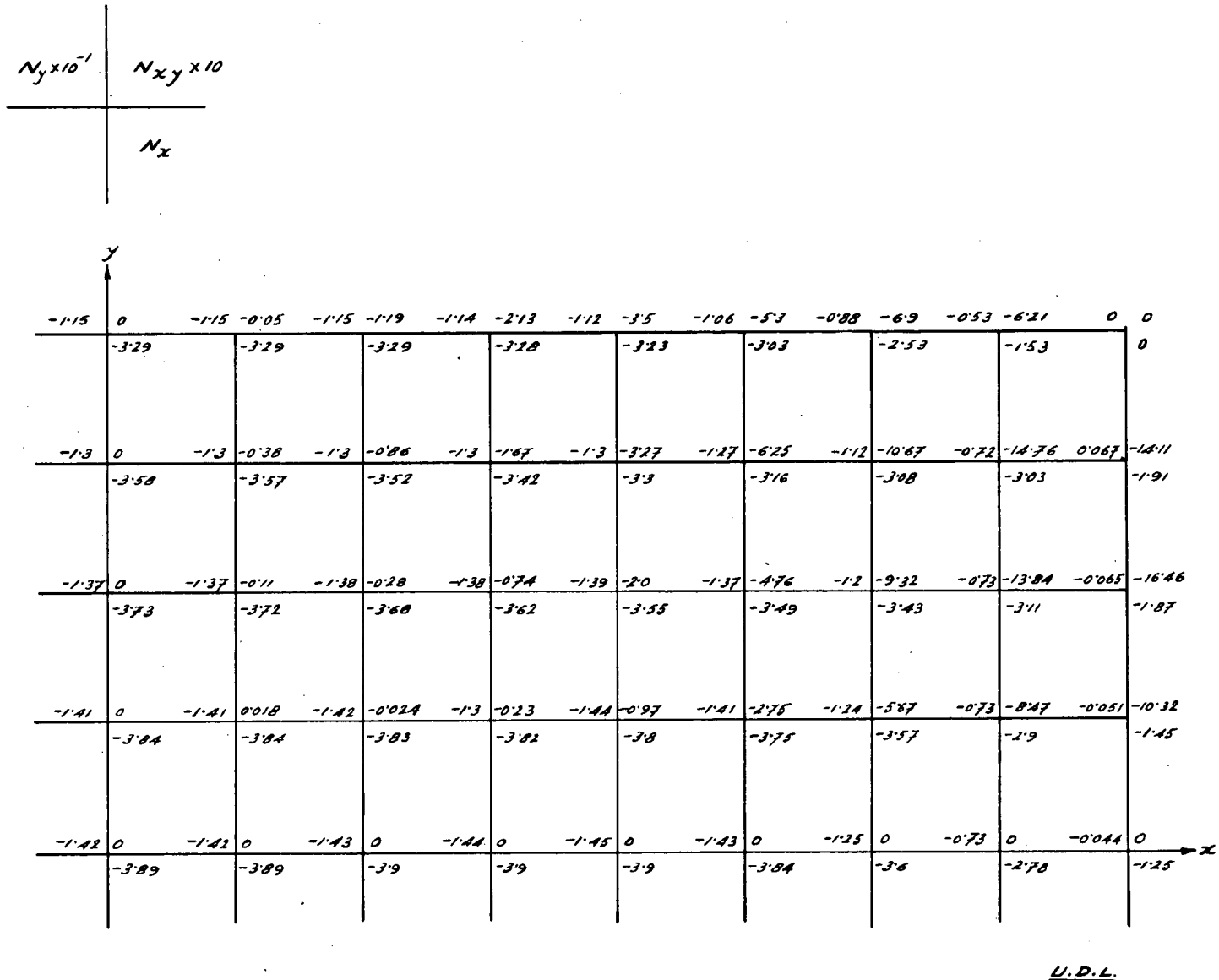

U.D.L.

FORCES (LBS).

CASE-(a): PERSPEX CYL. SHELL FIXED AT EDGES & END-ARCHES.

FIGURE: 4-18.

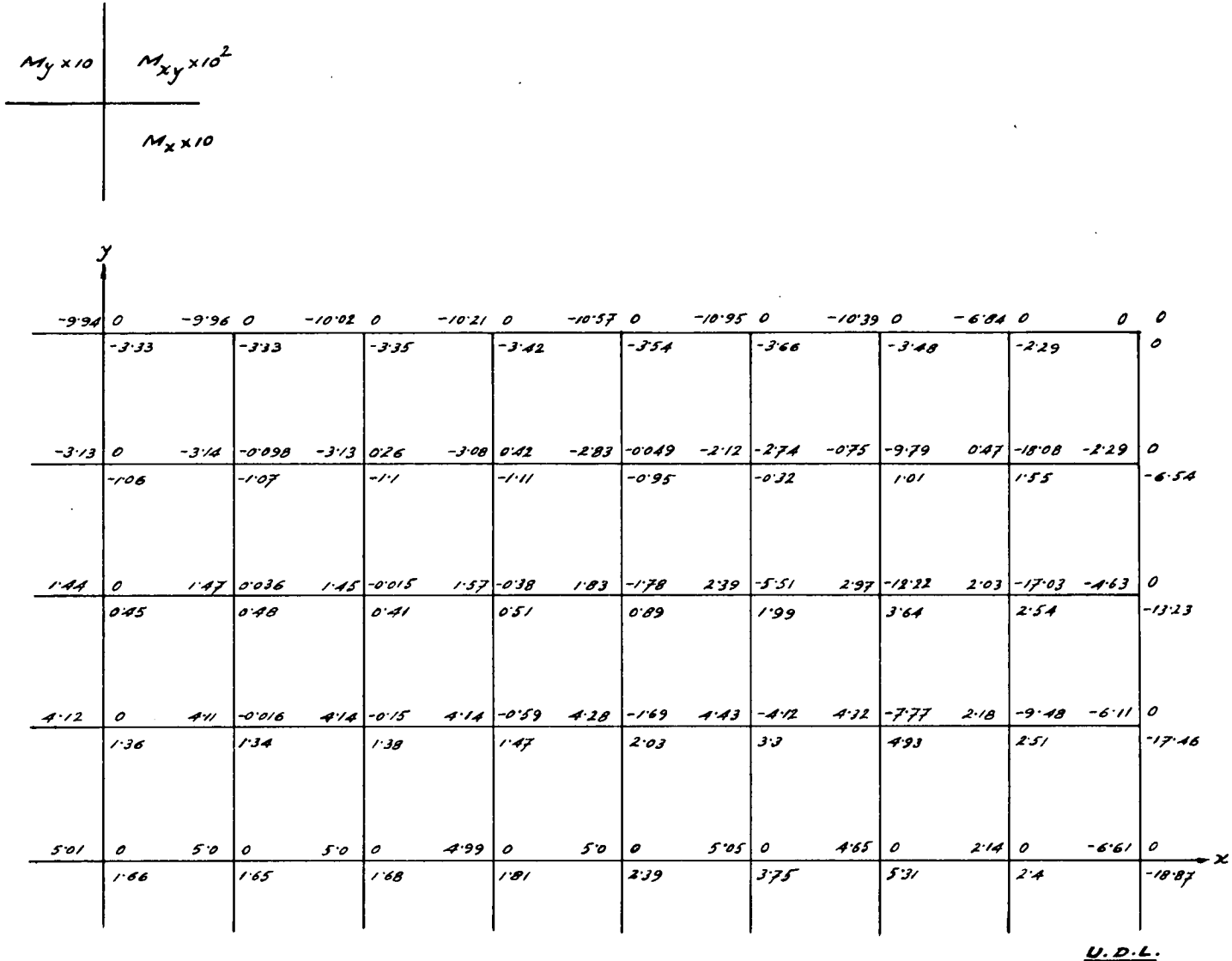

U.D.L.

MOMENTS (LB.IN).

CASE-(a).

FIGURE: 4.9.

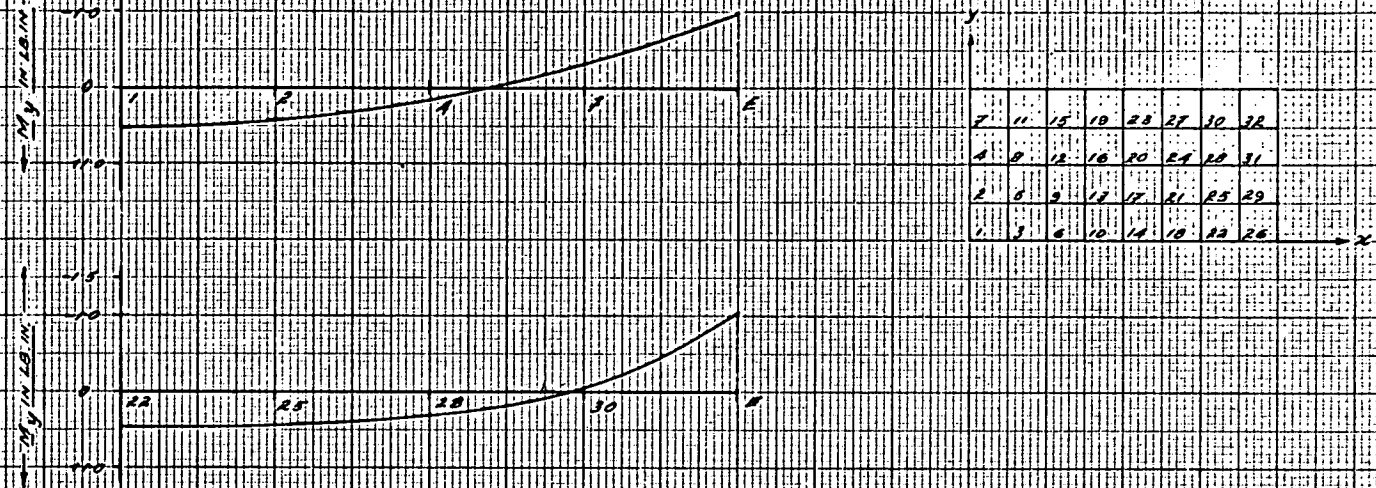

MOMENTS 'My' FOR CASE (a)

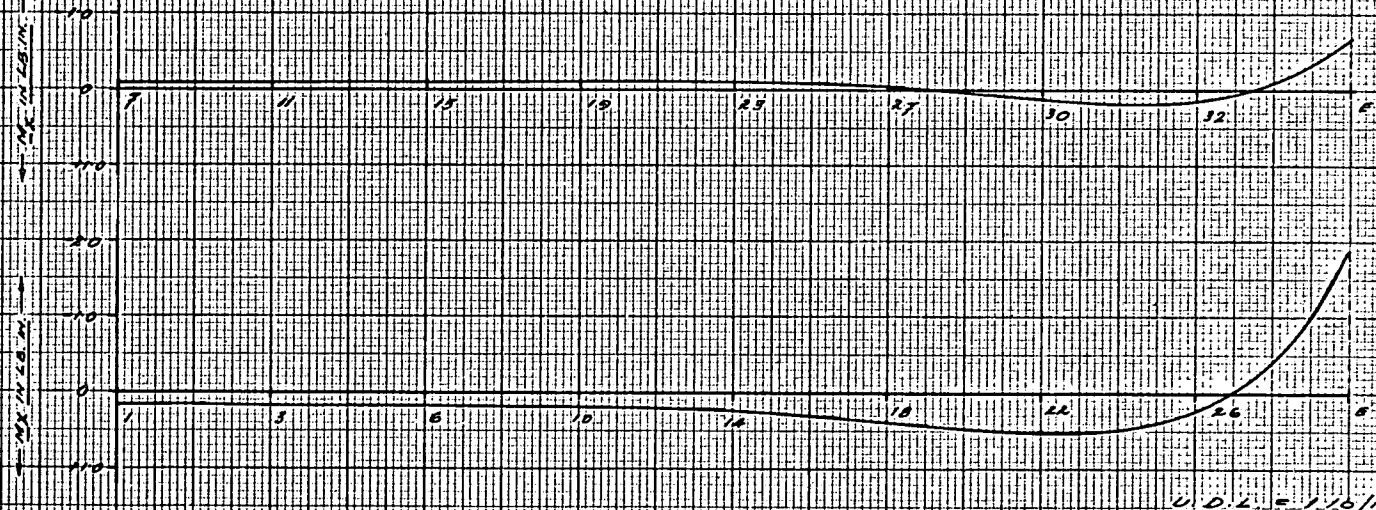

MOMENTS Mx FOR CASE (a)

FIGURE: 4-20

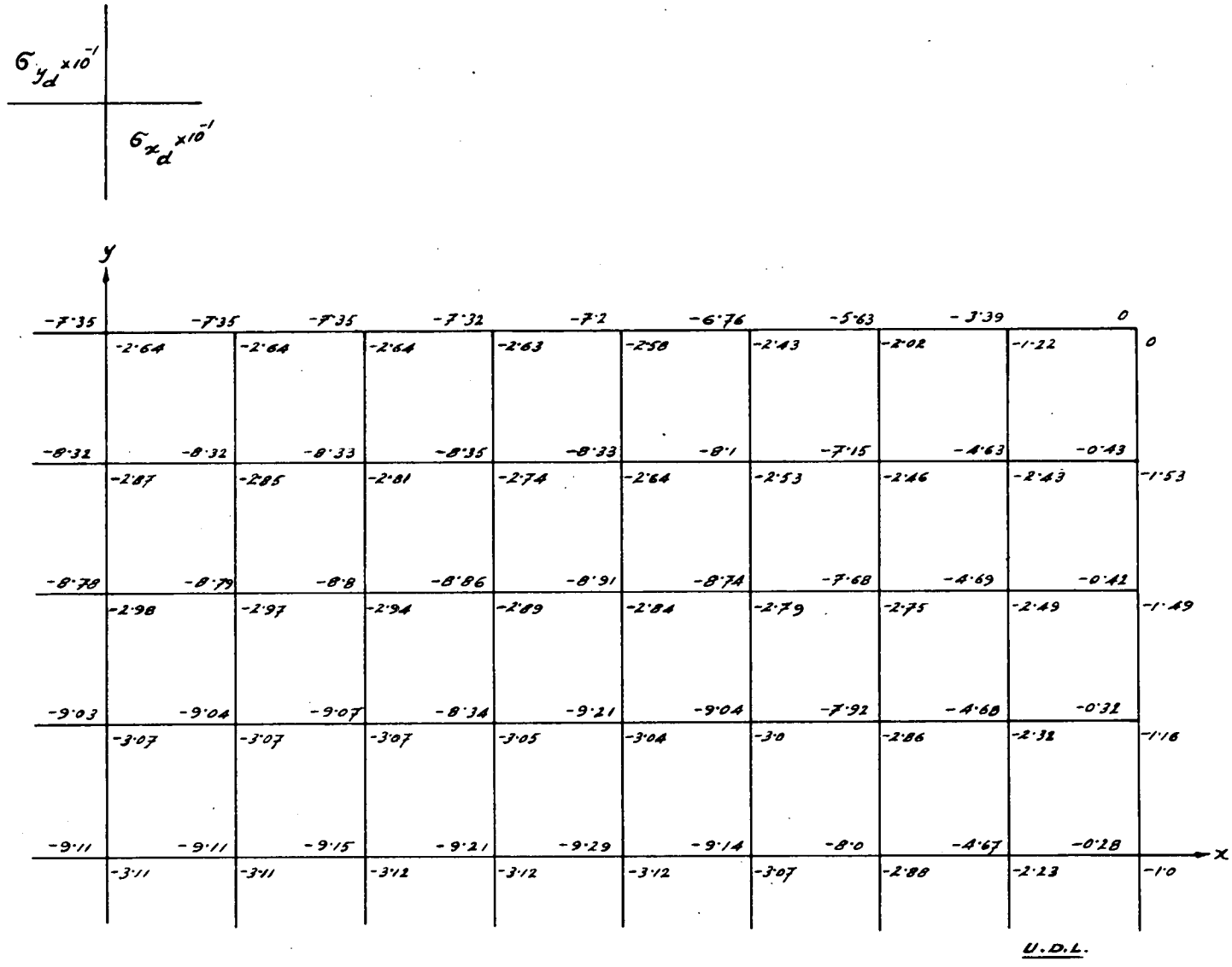

DIRECT STRESSES (LB/IN.^{2}).

CASE-(a).

FIGURE : 4-21.

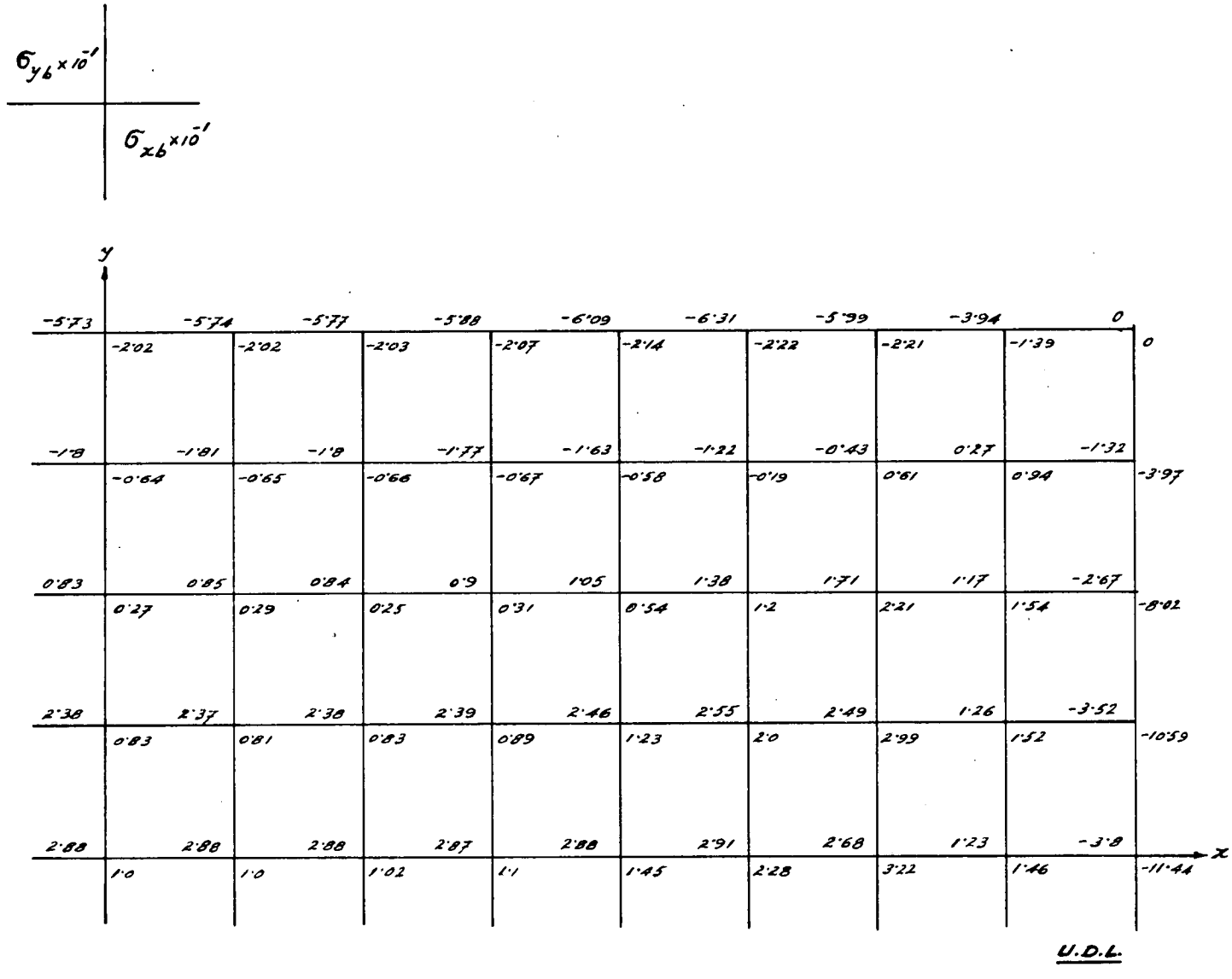

BENDING STRESSES (LB/IN.²).

CASE: (a).

FIGURE: 4-22.

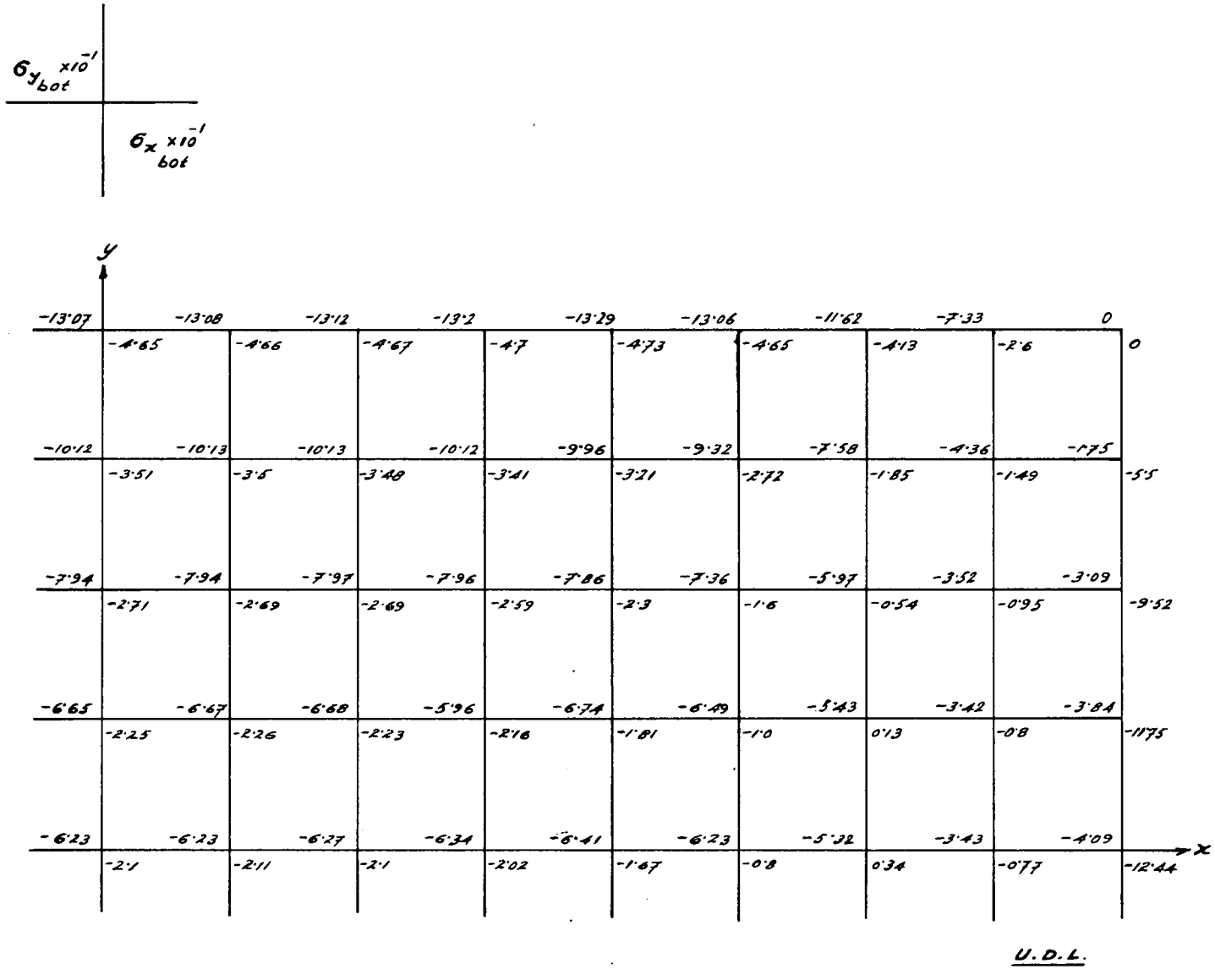

U.D.L.

RESULTANT STRESSES (LB/IN.^{2}).

CASE-(a): BOT. SURFACE.

FIGURE: 4-23.

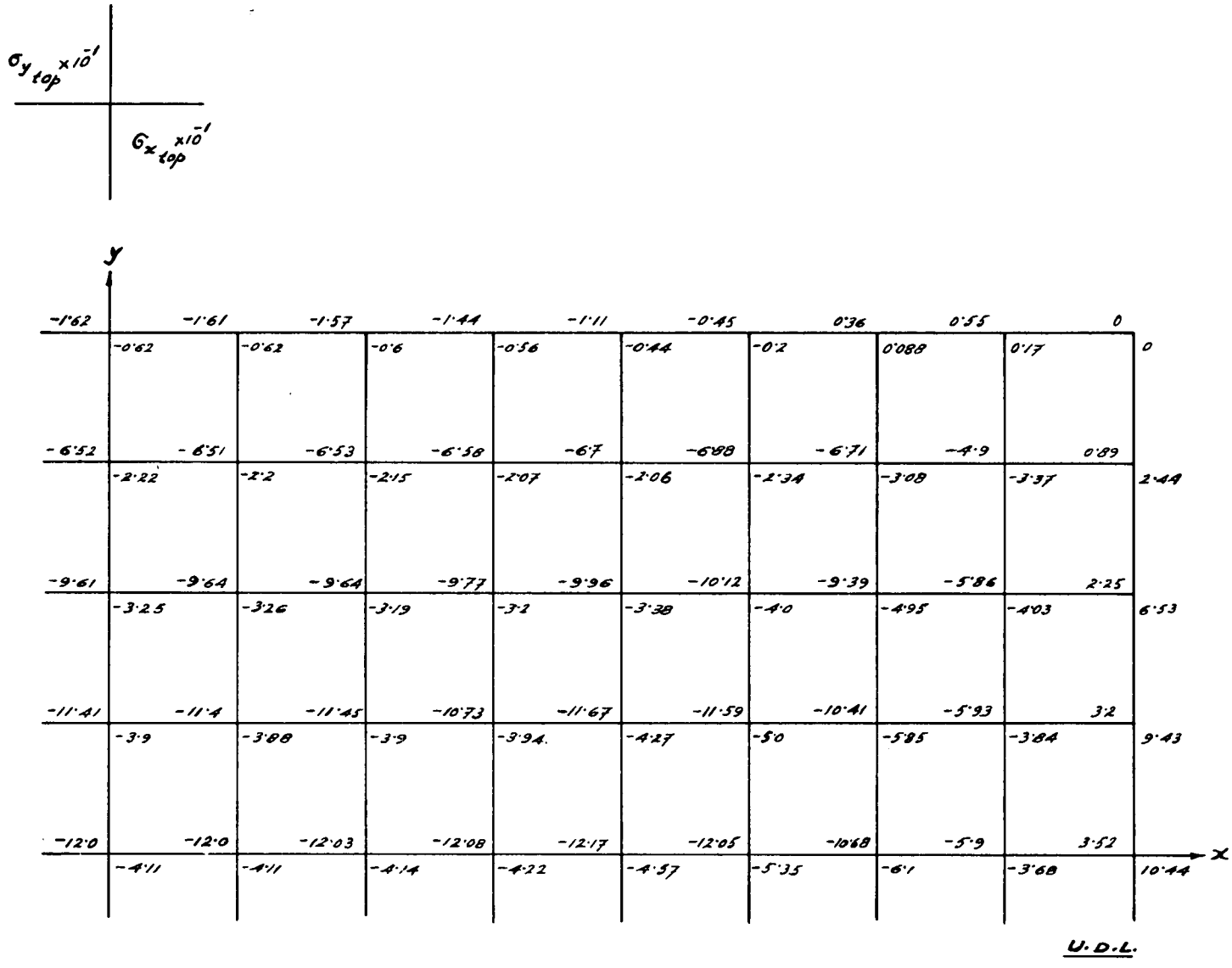

RESULTANT STRESSES (LB/IN.^{2}).

CASE-(a) : TOP SURFACE.

FIGURE : 4-24.

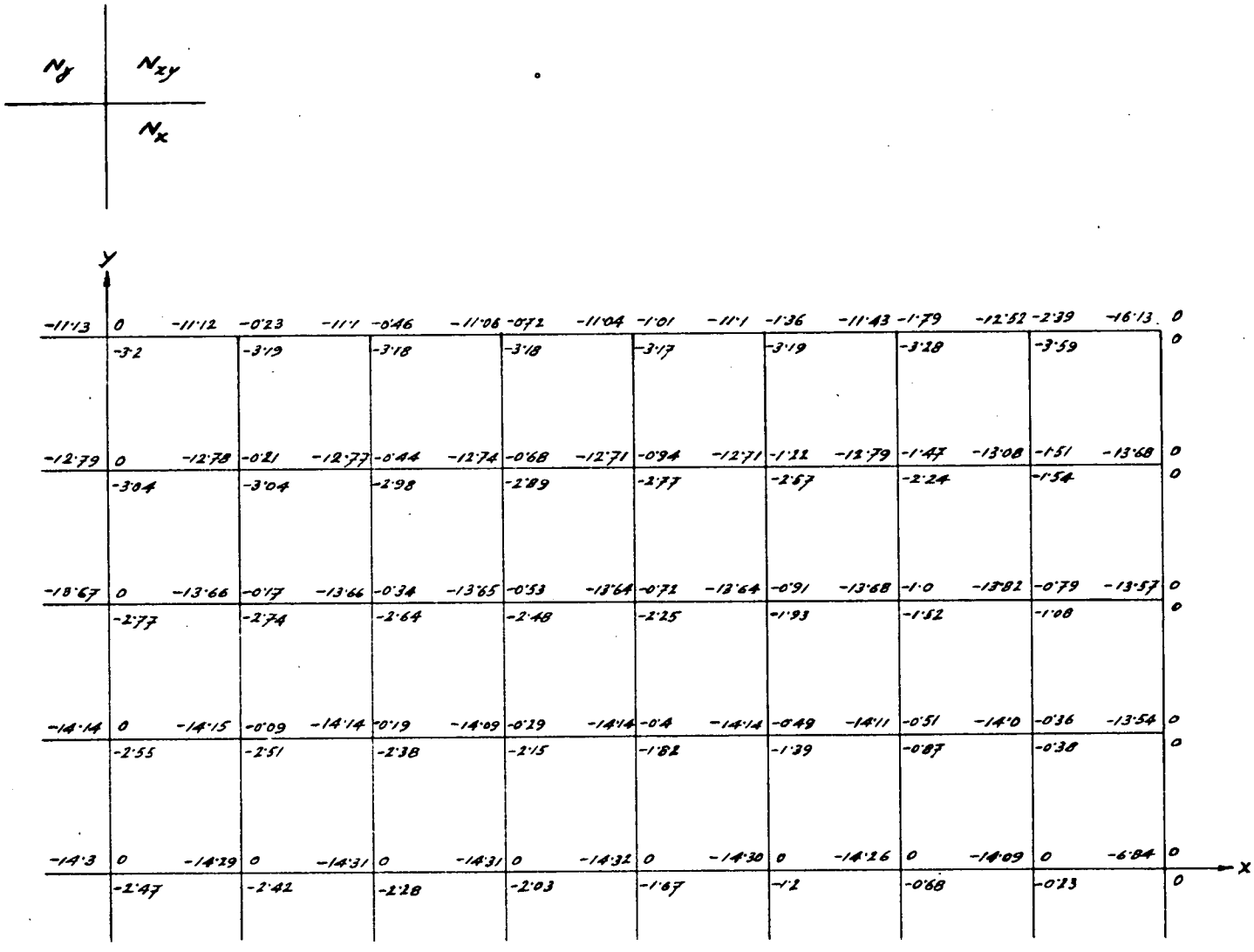

FORCES (LBS). U.D.L.

CASE-(6) : PERSPEX CYLINDRICAL SHELL FIXED AT EDGES & FREE AT END-ARCHES.

FIGURE : 4-25.

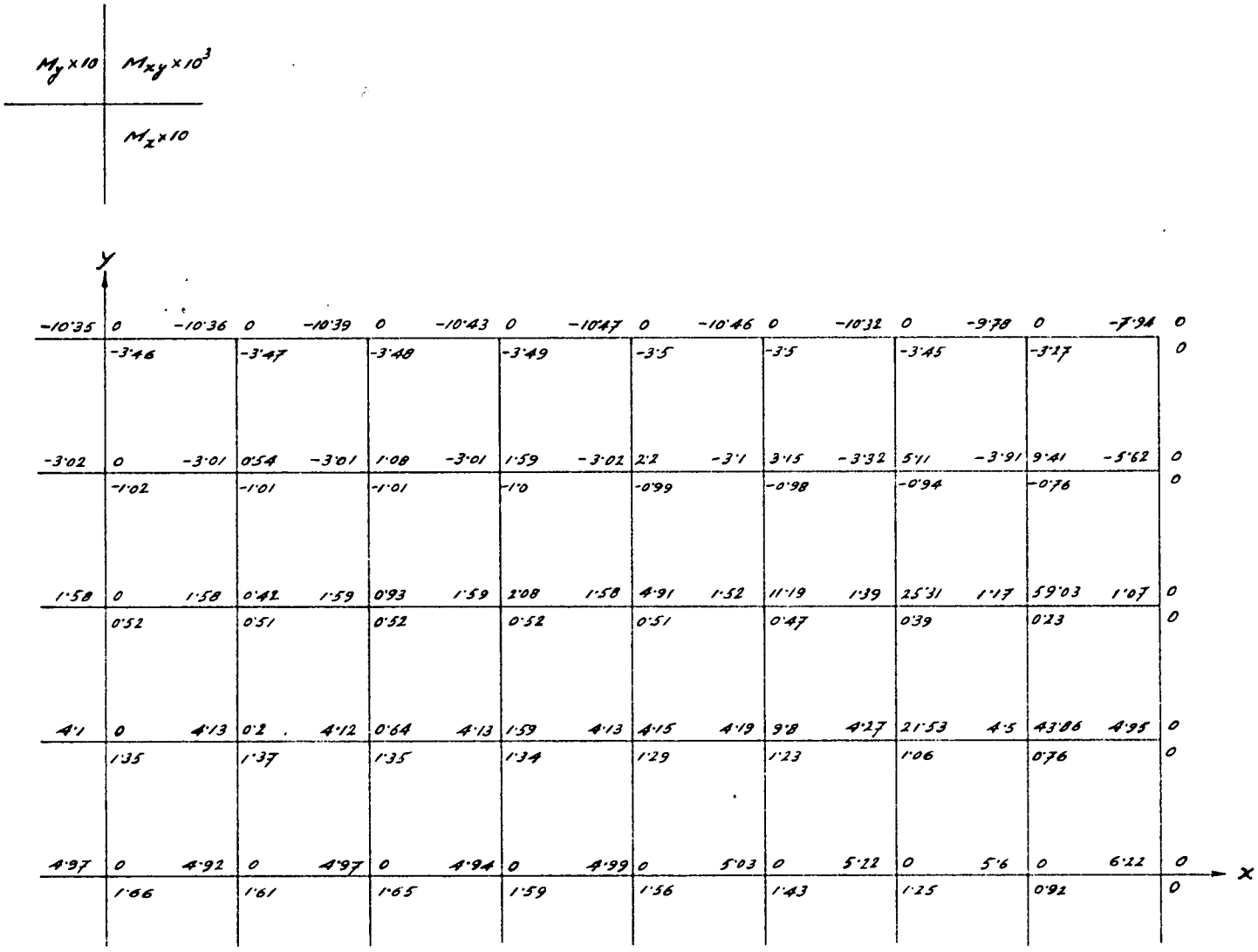

U.D.L.

MOMENTS (LB.IN.).

CASE-(b)

FIGURE: 4-26.

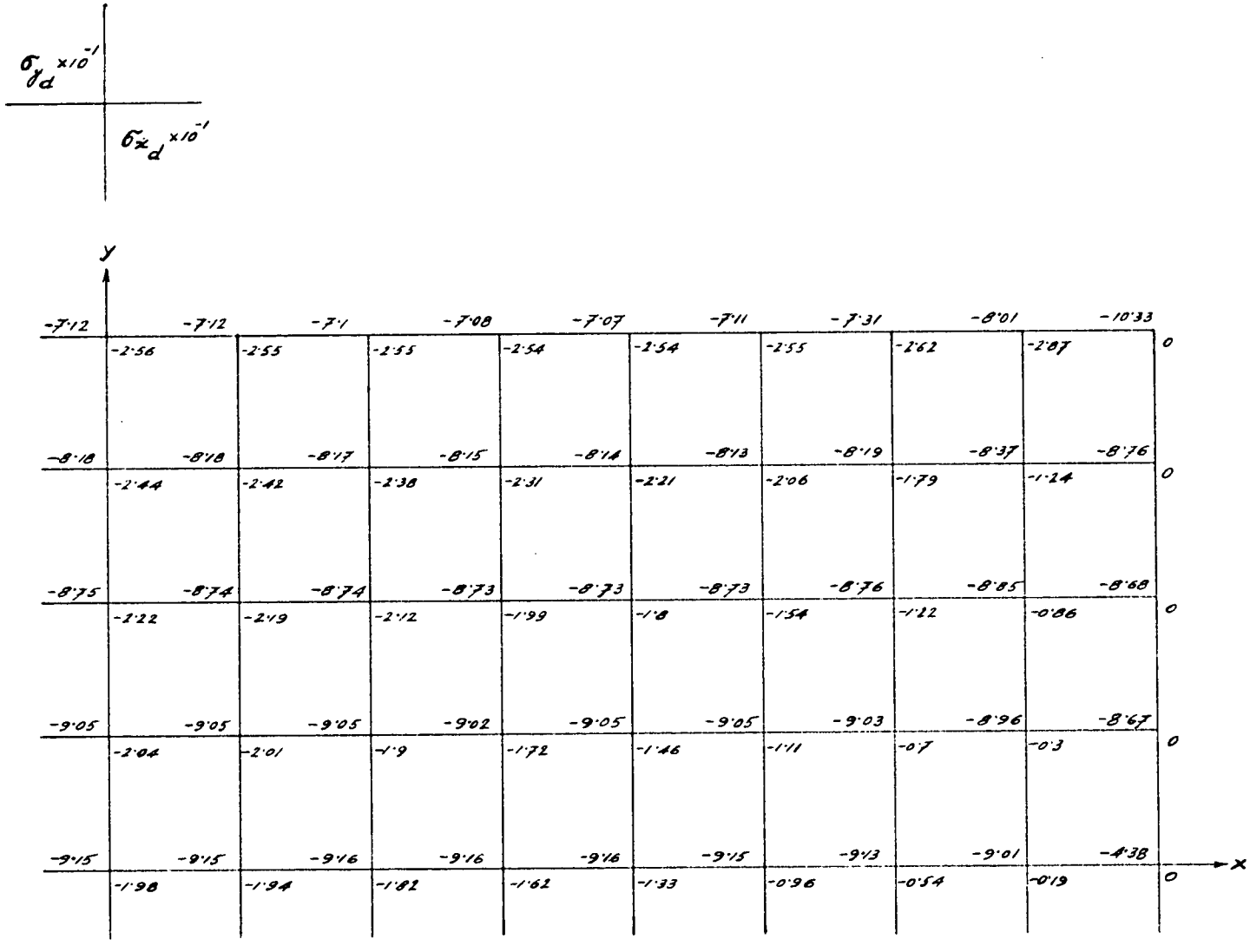

U.D.L.

DIRECT STRESSES (LB./IN.²).

CASE-(b).

FIGURE : 4-27.

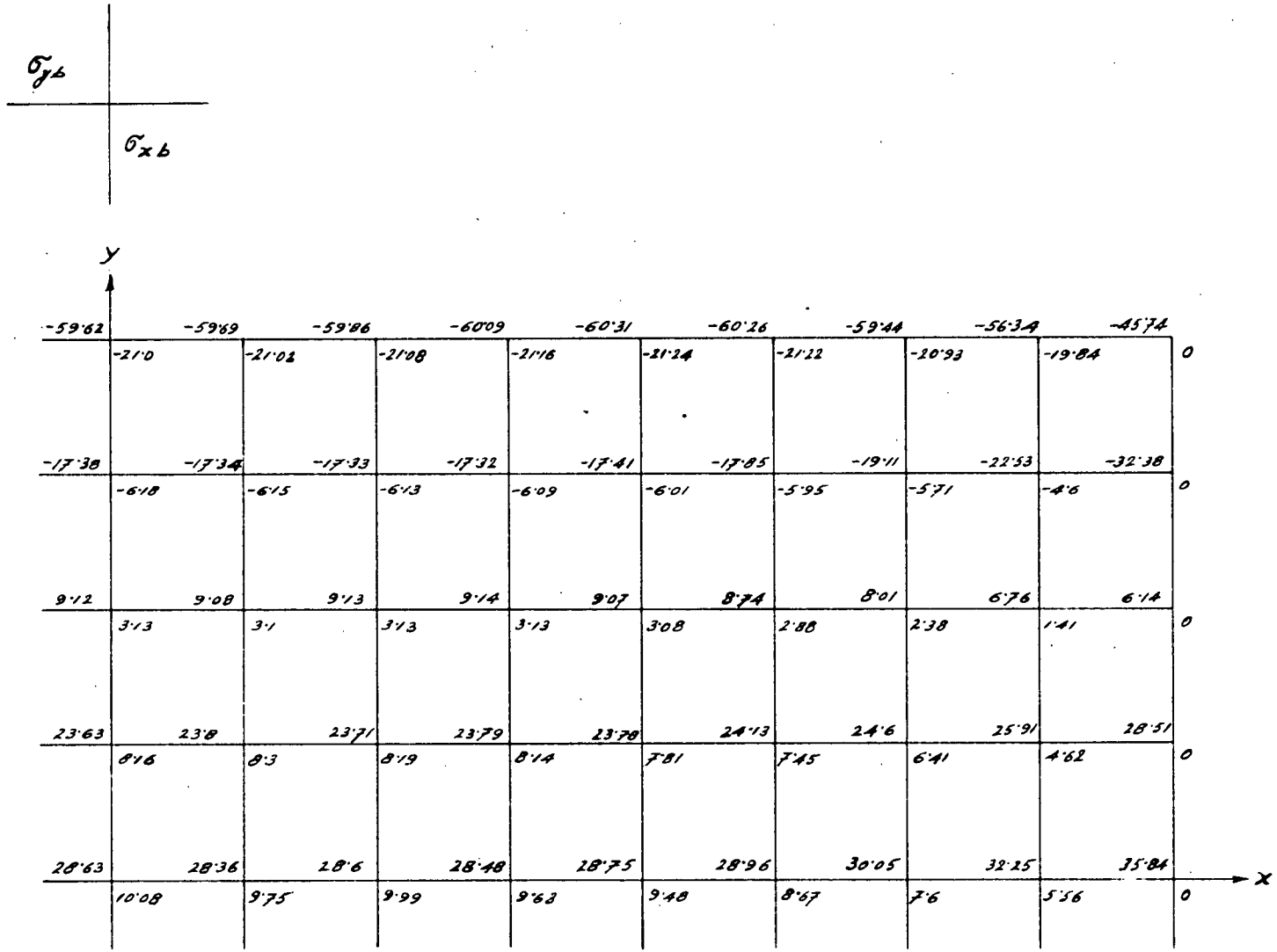

U.D.L.

BENDING STRESSES. (LB/IN^2).

CASE-(b).

FIGURE : 4-28.

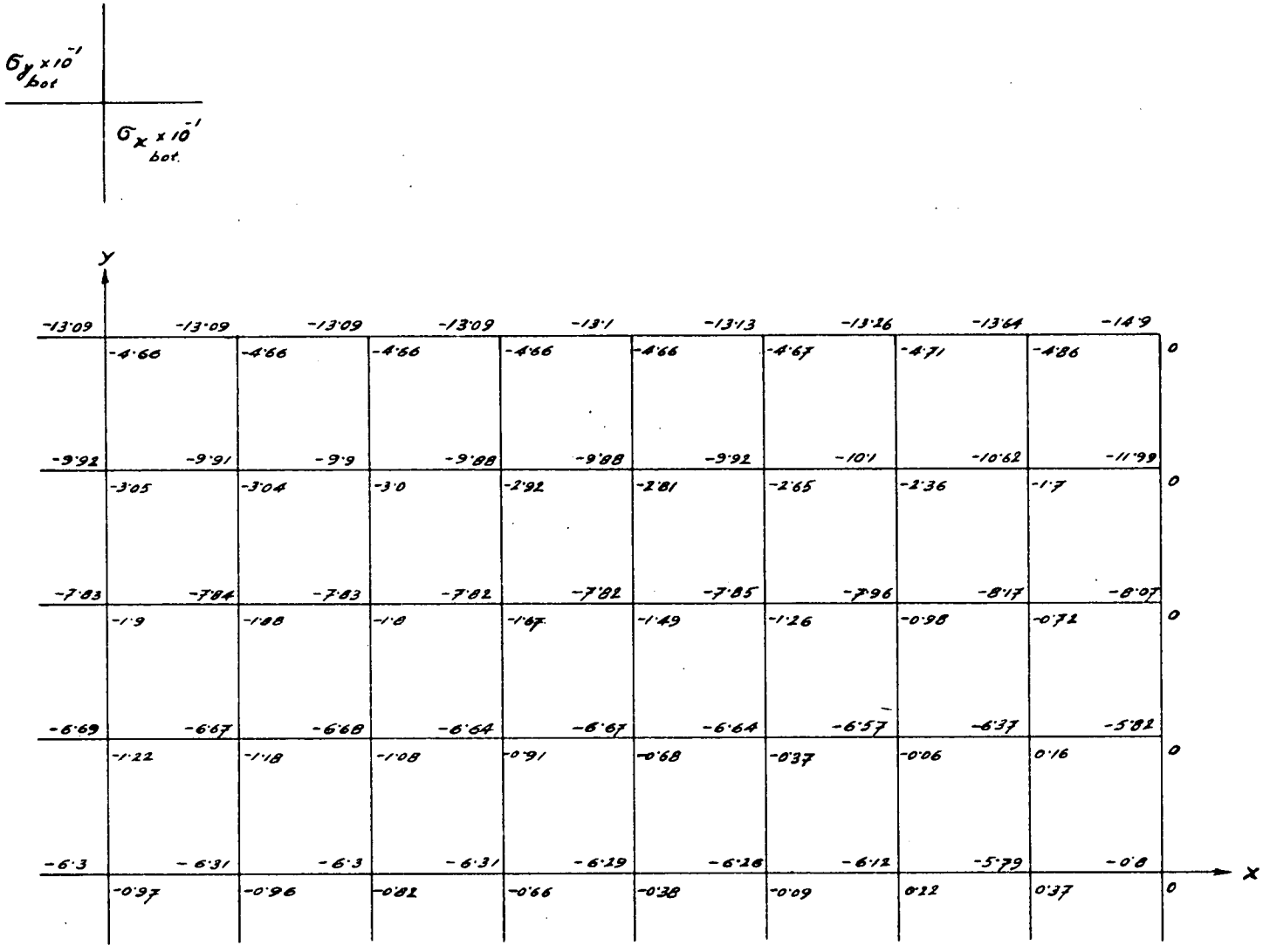

U.D.L.

RESULTANT STRESS (LB/IN.^{2})

CASE-(6). BOT. SURFACE.

FIGURE: 4-29.

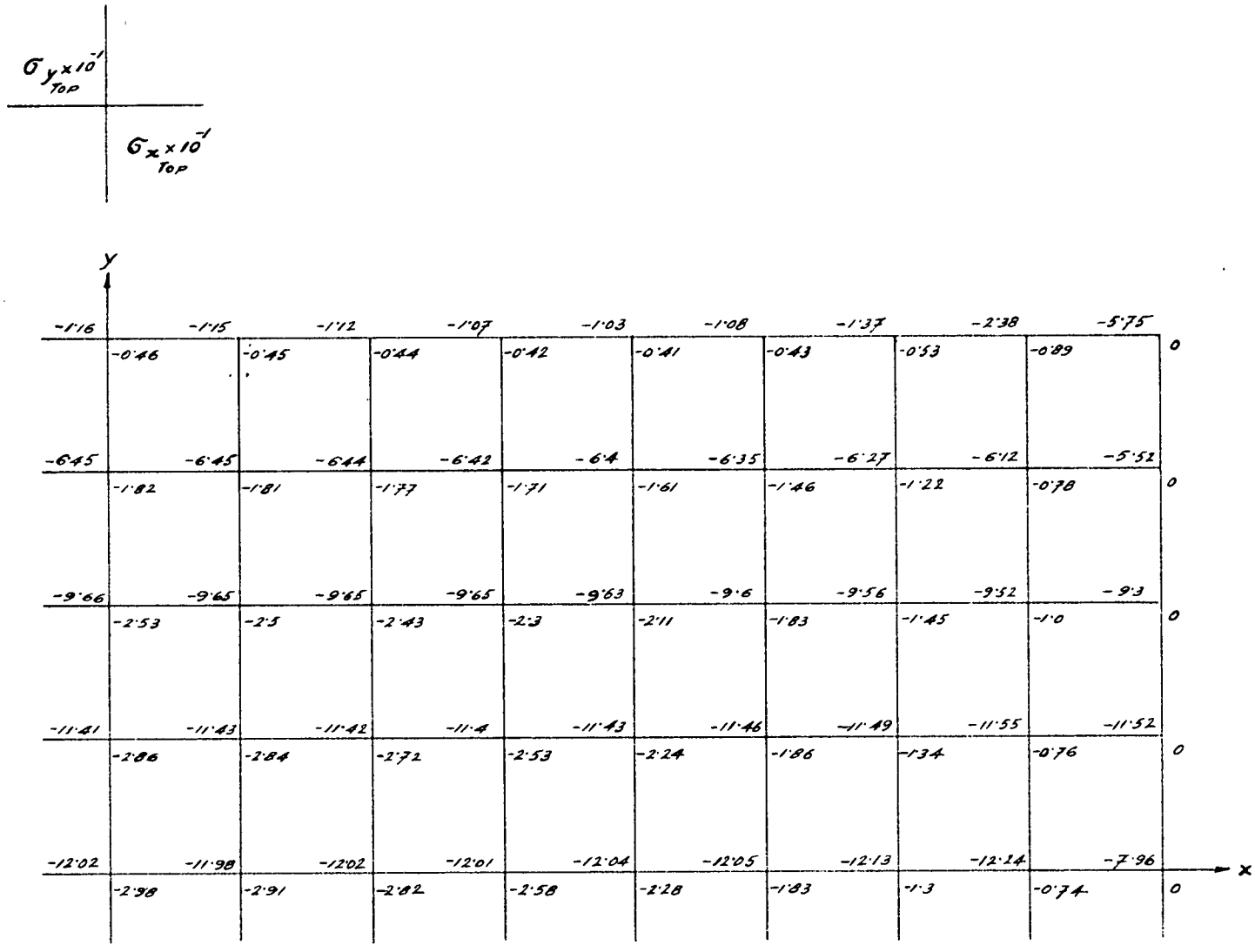

U.D.L.

RESULTANT STRESSES (LB/IN^2).

CASE-(b). TOP SURFACE.

FIGURE: 4-30.

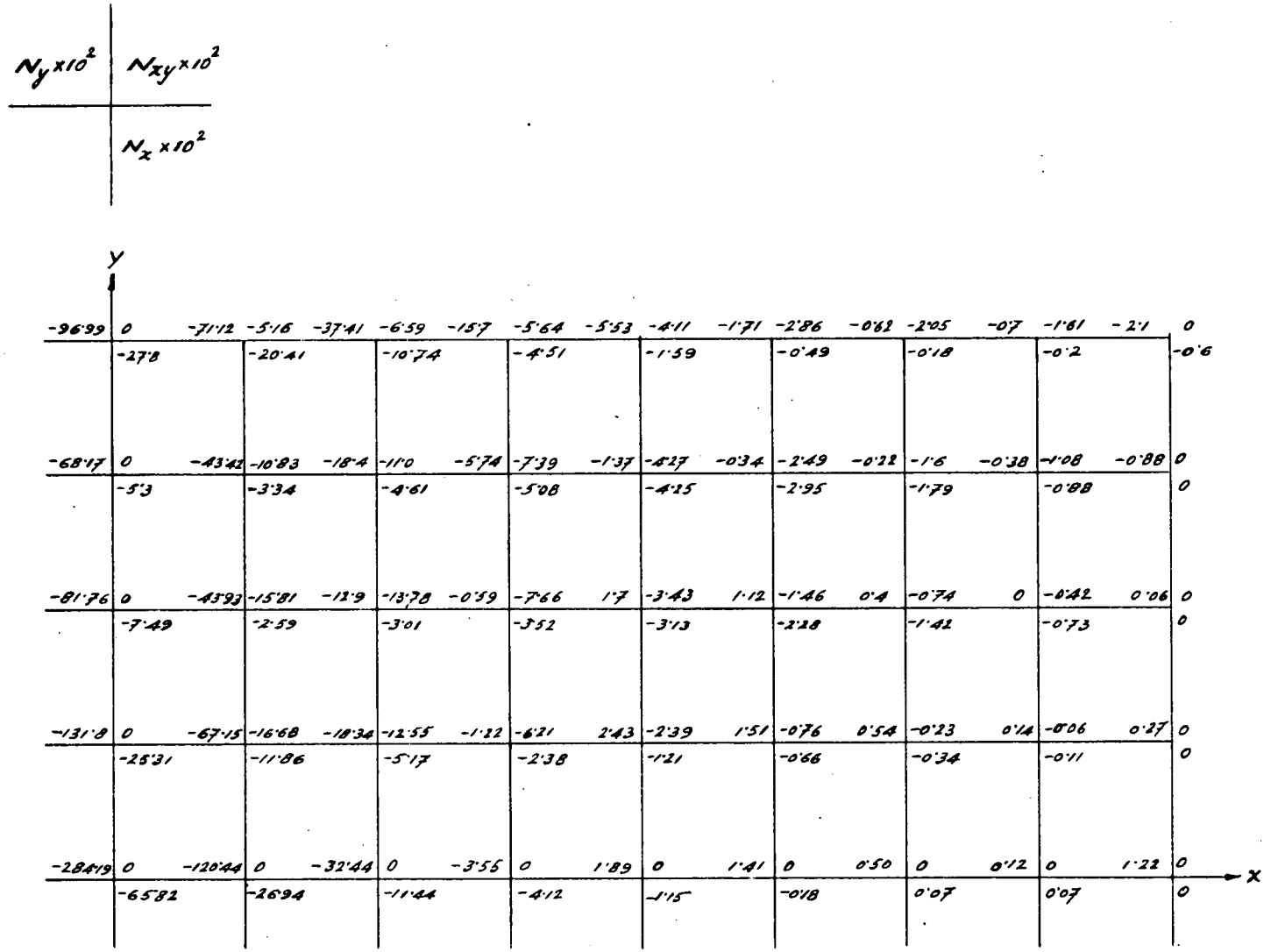

CONC. LOAD OF 1 LB AT M.P. ①.

FORCES (LBS.).

CASE - (6).

FIGURE: 4-31.

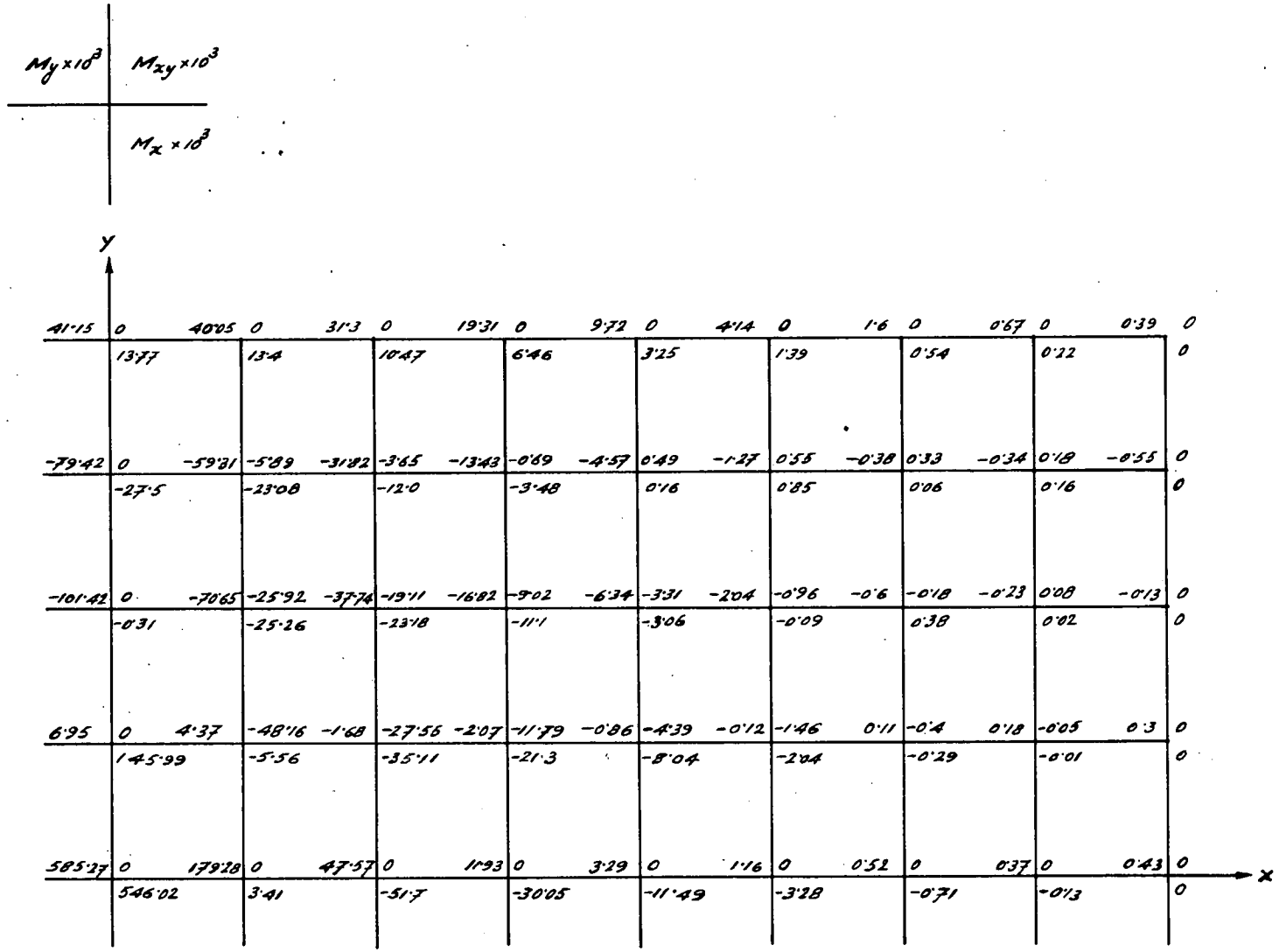

CONC. LOAD.

MOMENTS (LB.IN).

CASE -(b).

FIGURE: 4-32.

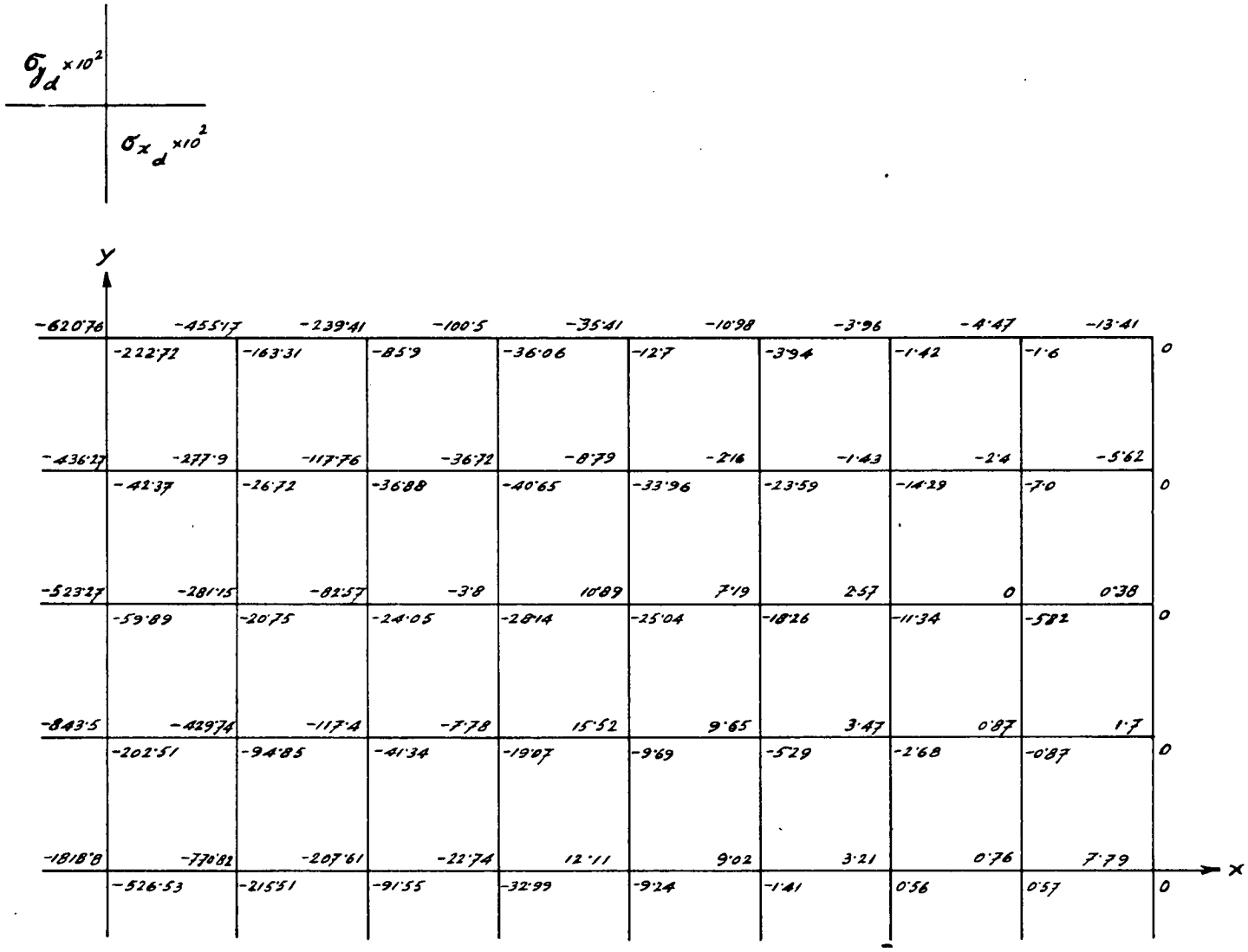

CONC. LOAD.

DIRECT STRESSES (LB/IN.^{2}).

CASE-(b).

FIGURE: 4-33.

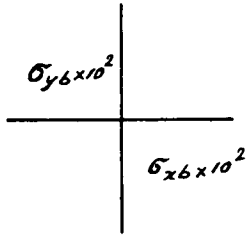

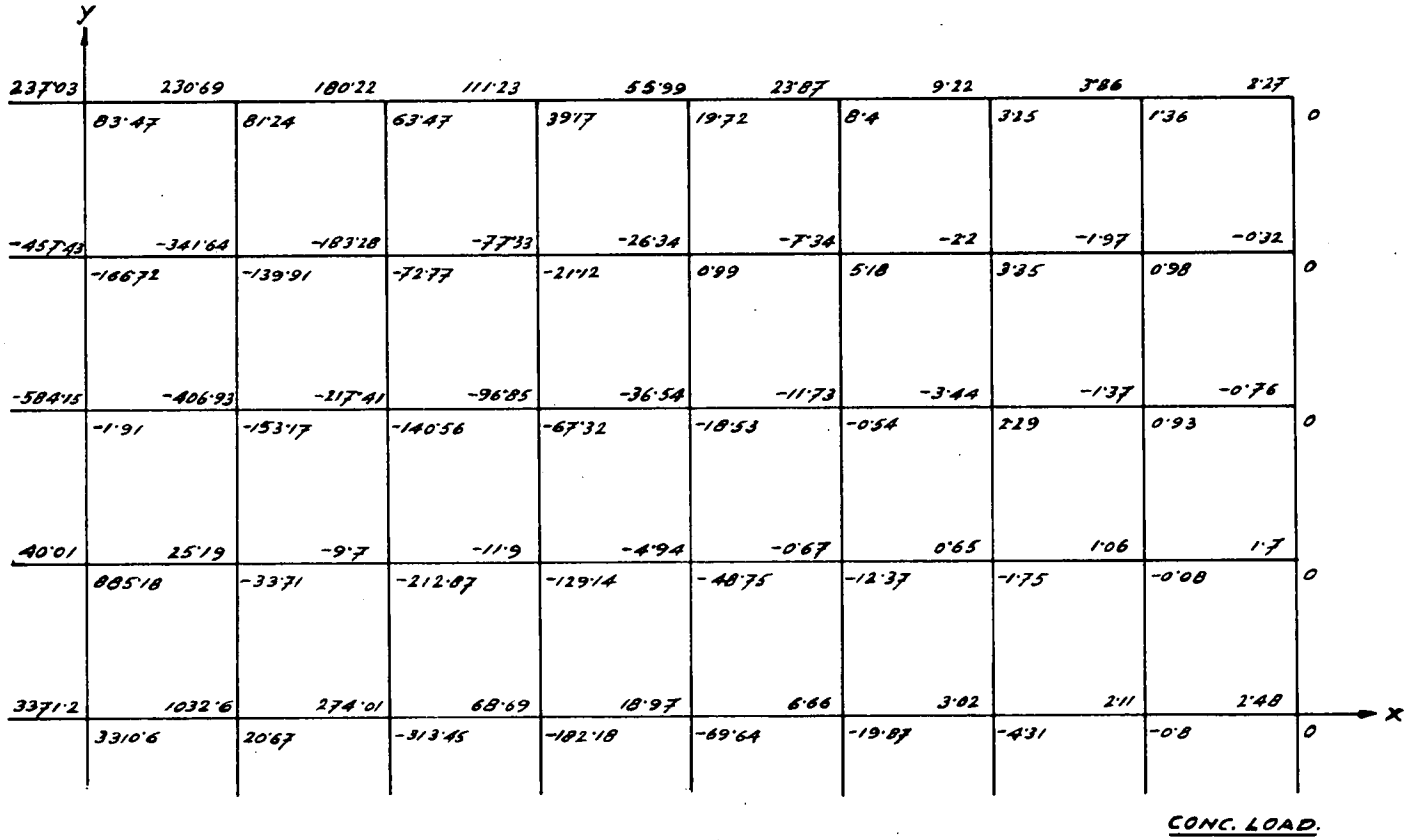

CONC. LOAD.

BENDING STRESSES (LB/IN.^{2}).

CASE - (6).

FIGURE : 4-34.

APPENDIX 4-1

COMPARISON OF THEORETICAL RESULTS WITH PUBLISHED RESULTS

Having written the computer program for a cylindrical shell of hollow cross section with the boundary conditions, fixed at the edges and at the end-arches it was decided to check the results. Unfortunately there are no published results for the cylindrical shell of hollow cross section. Holman's (25) analysis for a shell of solid cross section was taken for comparison. Holman analysed a cylindrical shell having a size of length = 2.5 x width whereas the size of one of the shells analysed in this chapter was length = 2 x width. There should be difference in deflections due to the difference of size but at the central zone the difference should not be much, however this would give some idea about the validity of the theory. In order to do so appropriate data were fed into the computer to simulate the shell analysed by Holman. The solid section was obtained from the expression for hollow section using t_2 = thickness of the shell and $t_1 = 0$. The size of the shell analysed here was 80 ft. x 40 ft. against Holman's shell size = 100 ft. x 40 ft., the other data remaining the same. The displacements at different nodal points for both the cases are shown in Figures (4.35). The comparison shows that at the central zone deflections for both cases are nearly equal which shows that the theoretical results are in close agreement with the published results.

$\frac{W}{E} \times 10^{-3}$

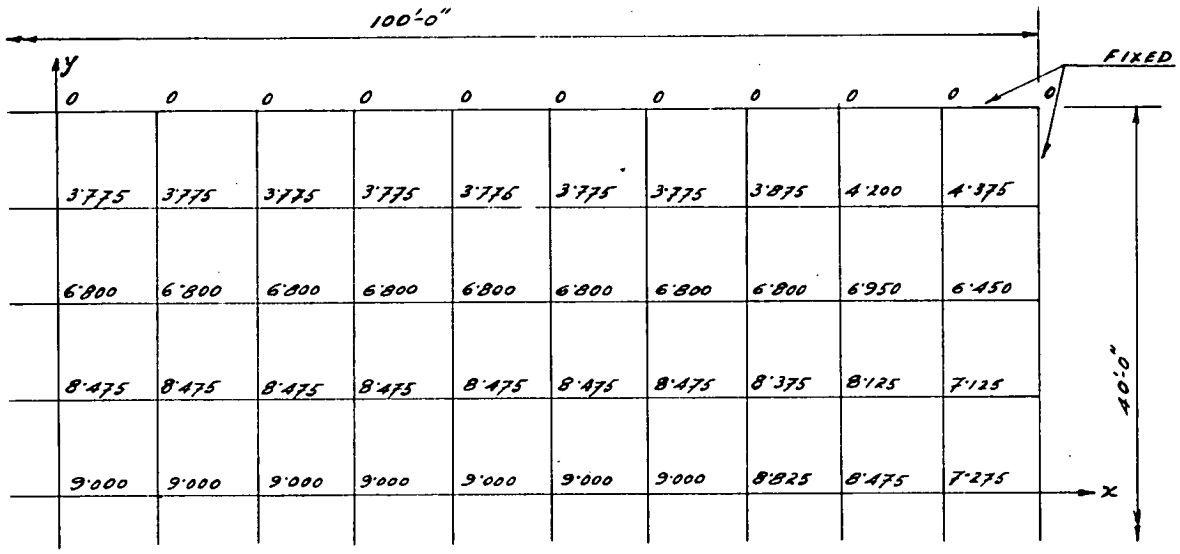

HOLMAN'S

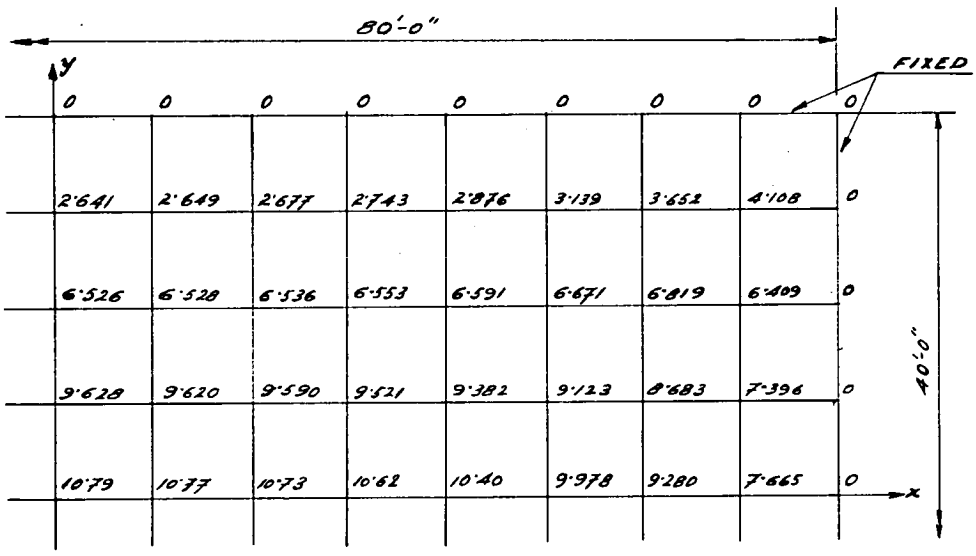

AUTHOR'S

THICKNESS = 3 IN.
RADIUS = 40'-0"
POISSON'S RATIO = 0.
LOAD = 1 LB/FT.^{2}

DISPLACEMENTS 'W.'

FIGURE: 4-35.

APPENDIX 4-2

INFLUENCE OF POISSON'S RATIO ON SHELL DISPLACEMENTS

While computing the displacements for a perspex cylindrical shell with Poisson's ratio = 0.35 and a concrete cylindrical shell with Poisson's ratio = 0, a change in sign for most of the U-values were observed. It was therefore decided to study the effect of the Poisson's ratio on the deflections and hence on the stresses of cylindrical shell. Deflections U, V and W for a cylindrical shell of 80 ft. x 40 ft. size having a radius of 40 ft. and thickness of 3 in. are computed with Poisson's ratios equal to 0.0, 0.2, 0.35 and 0.5 respectively. The values of U, V and W are shown in Figures (4. 36 - 42).

It is found that V and W values decrease with the increase of Poisson's ratio whereas the U-values increase with the increase of Poisson's ratio.

$\mu_Y = 0.2$	$\mu_X = 0$
$\mu_X = 0.35$	$\mu_1 = 0.5$

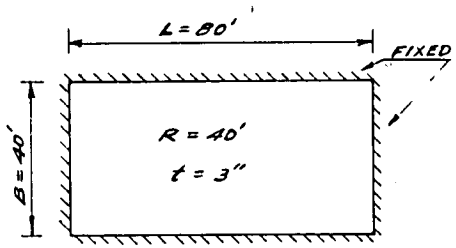

Y

0	0	0	0	0	0	0	0	0	0	0	0	0	0	0	0	0	0	0
0	0	0	0	0	0	0	0	0	0	0	0	0	0	0	0	0	0	0
0	0	1.96	-1.59	5.075	-2.19	10.64	-.07	20.16	4.02	35.14	12.6	55.98	23.42	72.37	27.81	0	0	
0	0	4.74	7.33	10.68	15.86	19.22	27.04	32.13	42.82	51.5	65.74	78.84	97.55	101.0	120.6	0	0	
0	0	-.045	-7.57	-.0129	-14.7	1.88	-20.82	6.69	-25.16	15.49	-27.1	29.36	-26.58	43.75	-22.32	0	0	
0	0	5.24	10.63	11.42	22.32	19.65	36.27	31.21	53.9	47.68	76.96	70.37	106.0	88.53	122.2	0	0	
0	0	-5.03	-14.98	-10.36	-30.79	-16.06	-47.93	-21.53	-65.94	-24.44	-82.31	-18.28	-90.07	5.48	-72.92	0	0	
0	0	3.05	10.8	6.14	21.92	94.46	33.75	13.63	47.0	20.79	63.38	36.4	86.24	60.42	104.9	0	0	
0	0	-7.28	-18.32	-15.39	-38.1	-24.87	-60.3	-35.23	-84.52	-43.3	-107.0	-39.61	-117.1	-10.64	-92.73	0	0	X
0	0	1.75	10.42	3.07	20.79	3.72	31.13	4.16	41.86	7.03	54.99	20.21	75.62	48.28	96.78	0	0	

LOAD = 1 LB/FT.^{2}

U - DISPLACEMENTS, (U/E)

FIGURE: 4-36

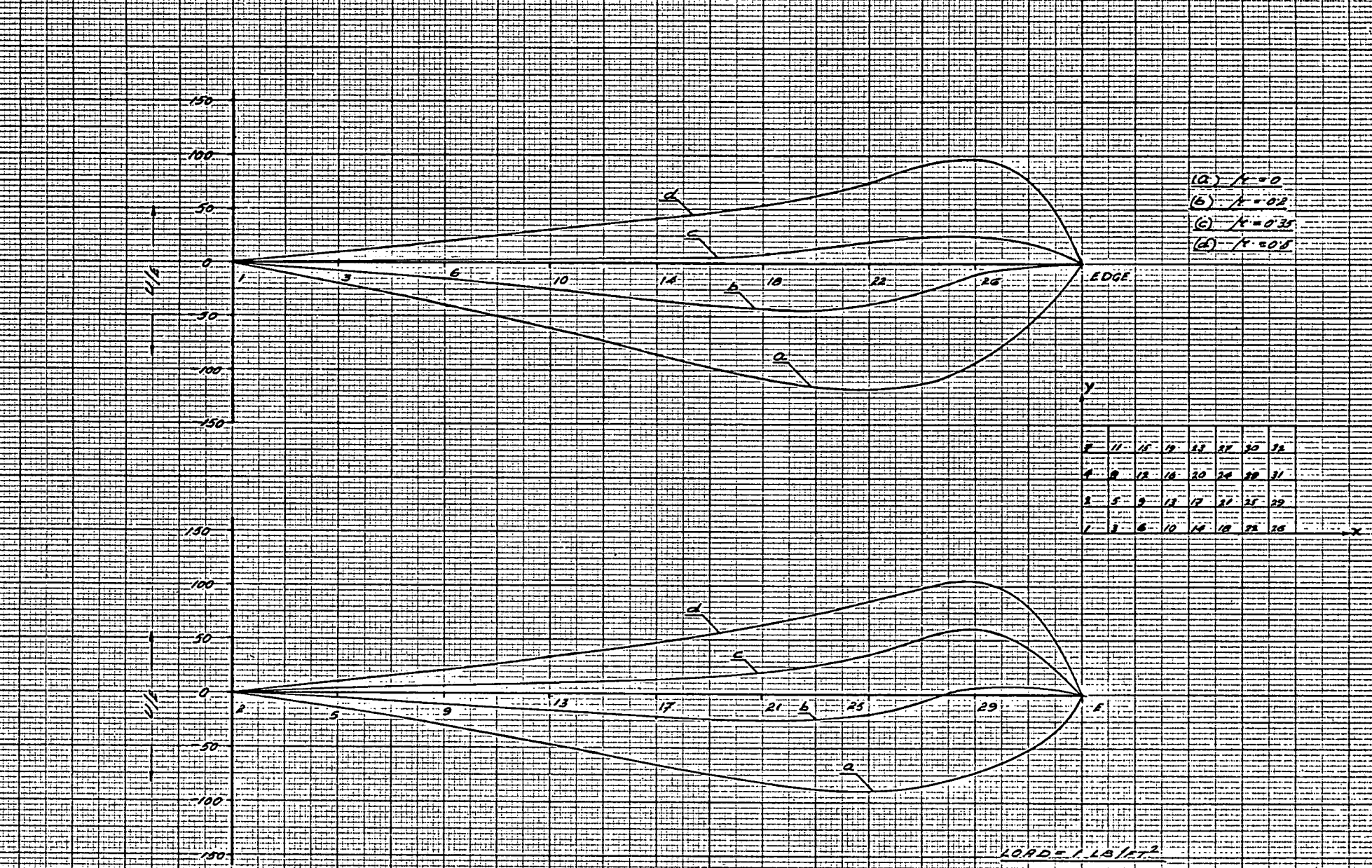

U - DISPLACEMENTS

FIGURE: 4-37

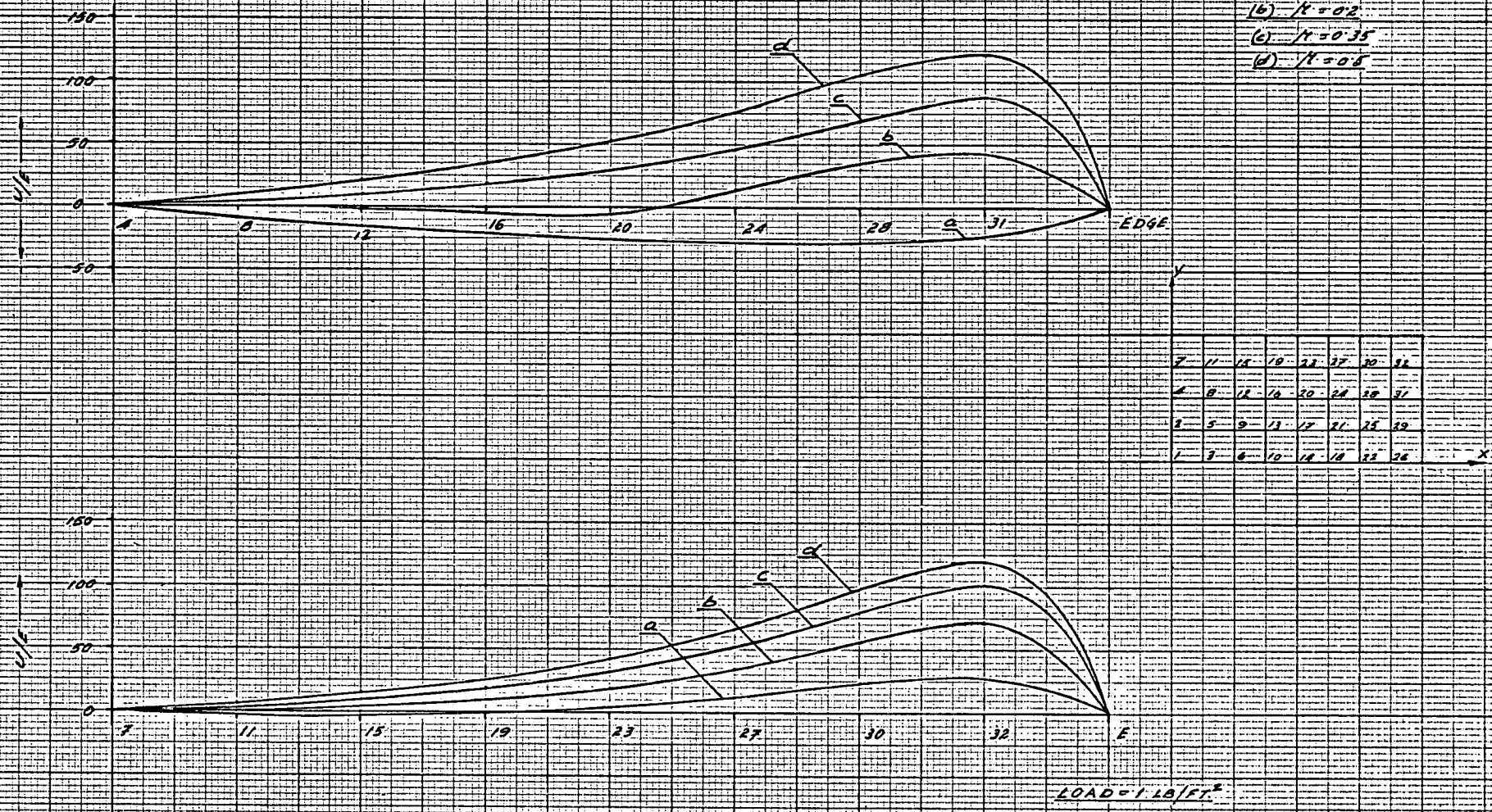

U - DISPLACEMENTS

FIGURE: 4-38

$\mu = 0.2$	$\mu = 0$
$\mu = 0.35$	$\mu = 0.5$

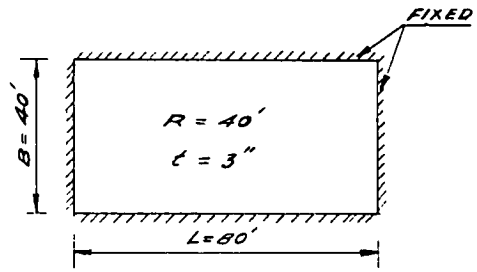

y

0	0	0	0	0	0	0	0	0	0	0	0	0	0	0	0	0	0
0	0	0	0	0	0	0	0	0	0	0	0	0	0	0	0	0	0
6·068	6·352	6·06	6·34	6·031	6·298	5·963	6·204	5·82	6·018	5·528	5·659	4·925	4·958	3·52	3·435	0	0
5·53	4·714	5·525	4·712	5·506	4·703	5·46	4·678	5·357	4·616	5·134	4·468	4·639	4·106	3·401	3·098	0	0
7·873	8·252	7·859	8·23	7·807	8·153	7·683	7·98	7·414	7·628	6·863	6·961	5·769	5·704	3·655	3·489	0	0
7·168	6·106	7·16	6·102	7·128	6·088	7·046	6·046	6·855	5·933	6·43	5·65	5·518	4·969	3·602	3·358	0	0
5·267	5·525	5·257	5·508	5·216	5·447	5·118	5·309	4·902	5·026	4·461	4·488	3·615	3·536	2·141	2·018	0	0
4·793	4·081	4·787	4·079	4·763	4·068	4·699	4·036	4·545	3·945	4·203	3·716	3·491	3·177	2·135	2·019	0	0
0	0	0	0	0	0	0	0	0	0	0	0	0	0	0	0	0	0
0	0	0	0	0	0	0	0	0	0	0	0	0	0	0	0	0	0

x

LOAD = 1 LB/FT.^{2}

V-DISPLACEMENTS ($V/E \times 10^{-2}$)

FIGURE: 4-39

V- DISPLACEMENTS

FIGURE: 4.40

$\mu = 0.2$	$\mu = 0$
$\mu = 0.35$	$\mu = 0.5$

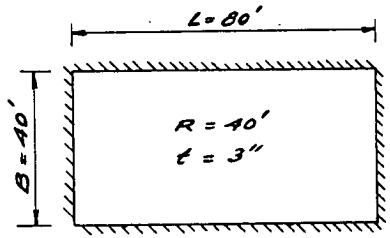

y																					
0	0	0	0	0	0	0	0	0	0	0	0	0	0	0	0	0	0	0	0	0	0
0	0	0	0	0	0	0	0	0	0	0	0	0	0	0	0	0	0	0	0	0	0
2·556	2·641	2·562	2·649	2·584	2·677	2·636	2·743	2·744	2·876	2·969	3·139	3·422	3·652	3·805	4·108	0	0				
2·357	2·04	2·361	2·043	2·378	2·057	2·418	2·085	2·505	2·151	2·693	2·294	3·072	2·572	3·333	2·671	0	0				
6·267	6·526	6·269	6·528	6·275	6·536	6·291	6·553	6·325	6·591	6·4	6·671	6·547	6·819	6·136	6·409	0	0				
5·746	4·942	5·747	4·944	5·754	4·952	5·769	4·967	5·801	4·997	5·872	5·06	5·998	5·143	5·54	4·617	0	0				
9·216	9·628	9·21	9·62	9·189	9·59	9·141	9·521	9·037	9·382	8·837	9·133	8·473	8·683	7·227	7·396	0	0				
8·429	7·232	8·426	7·231	8·414	7·228	8·383	7·216	8·314	7·181	8·17	7·096	7·871	6·856	6·645	5·666	0	0				
10·32	10·79	10·31	10·77	10·27	10·73	10·2	10·62	10·03	10·4	9·697	9·978	9·107	9·28	7·542	7·665	0	0	x			
9·428	8·084	9·423	8·082	9·403	8·074	9·351	8·049	9·234	7·984	8·99	7·831	8·501	7·445	6·975	5·992	0	0				

LOAD = 1 LB/FT.^{2}

W- DISPLACEMENTS $(W/E \times 10^{-3})$.

FIGURE : 4-41.

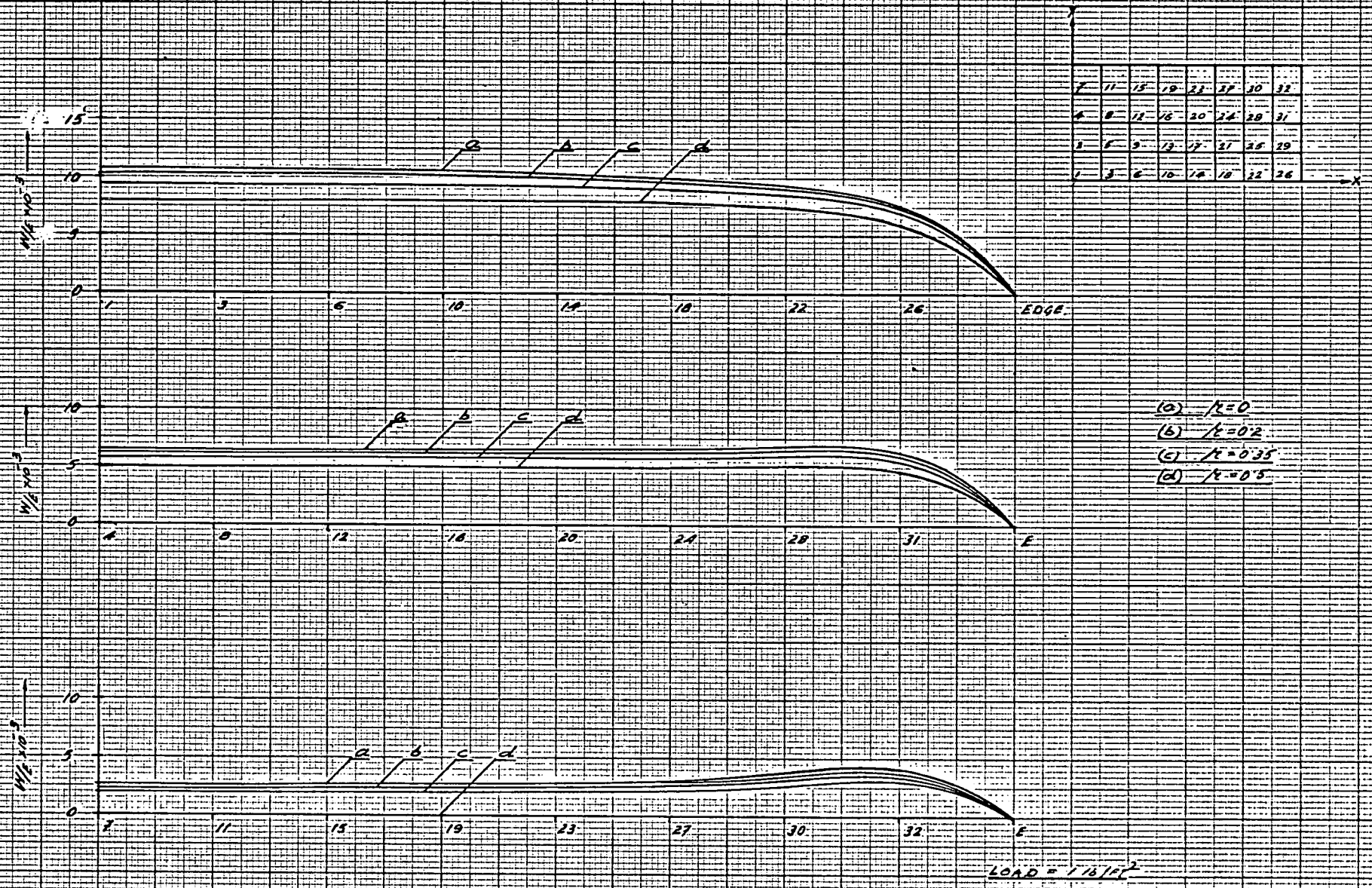

W - DISPLACEMENTS

FIGURE: 4-42

APPENDIX 4-3

EFFECT OF VARIATION OF THICKNESS OF SHELL ON THE VALUES OF DISPLACEMENTS AND MOMENTS

Due to the introduction of hollow cross section the rigidities of a shell increase compared to a solid section of the equivalent effective thickness and hence the reduction in the values of displacements and moments. The increase in the distance between the slabs increases the rigidities of a shell. Therefore, in order to study the effect of the variation of the distance between the slabs on the values of displacements and moments a shell having length = 100 ft, breadth = 40 ft, radius = 40 ft and Poisson's ratio = 0, fixed at the edges and free at the end-arches subject to a UDL of 1 lb/ft^2 is considered. Width of the ribs b_3 along the y-axis is taken as 1½in. spaced at 1 ft. c/c and no rib along the x-axis ($b_2 = 0$). The effective thickness (i.e. $T_2 - T_1$) is taken as 1½in. and the values of T_1, the distance between the slabs are varied from 0" to 7".

The values of V, W and M_y are shown in Tables (4-1 & 2) and Figures (4-43 to 47). It can be seen from Figures (4-45 to 47) that between 'a' and 'b' there is a sharp drop in the values of V, W and M_y due to the introduction of the hollow section. After 'b' the reduction in the values of V and W are nearly at constant rate and M_y at the centre reduce rapidly between 'd' and 'f'. On the other hand the reduction in the values of M_y at the edges is at a lower rate, the slope being nearly horizontal at 'f'. Therefore, it appears that after a particular stage the values of M_y at the edges which predominate over those values at the centre do not decrease considerably with the increase in the distance between the slabs.

T A B L E 4-1

W - DISPLACEMENTS

Section / Mesh Points	$\delta_1 = 12''$ $\delta_2 = 0$ $\delta_3 = 1\frac{1}{2}''$	W/E					
		(a)	(b)	(c)	(d)	(e)	(f)
	T_1	0	3"	4"	5"	6"	7"
	T_2	$1\frac{1}{2}$"	$4\frac{1}{2}$"	$5\frac{1}{2}$"	$6\frac{1}{2}$"	$7\frac{1}{2}$"	$8\frac{1}{2}$"
1,3,6,10,14, 18,22,26,30.		19,800	16,352	15,480	14,676	13,920	13,212
2,5,9,13,17, 21,25,29,33.		18,248	14,864	14,000	13,212	12,484	11,812
4,8,12,16,20, 24,28,32,35.		13,528	10,572	9,804	9,132	8,540	8,012
7,11,15,19,23, 27,31,34,36.		6,332	4,544	4,100	3,729	3,423	3,165

T A B L E 4-2

V - DISPLACEMENTS

Section / Mesh Points	$\delta_1 = 12''$ $\delta_2 = 0$ $\delta_3 = 1\frac{1}{2}''$	W/E					
		(a)	(b)	(c)	(d)	(e)	(f)
	T_1	0	3"	4"	5"	6"	7"
	T_2	$1\frac{1}{2}$"	$4\frac{1}{2}$"	$5\frac{1}{2}$"	$6\frac{1}{2}$"	$7\frac{1}{2}$"	$8\frac{1}{2}$"
1,3,6,10,14, 18,22,26,30.		0	0	0	0	0	0
2,5,9,13,17, 21,25,29,33.		940	808	775	742	710	678
4,8,12,16,20, 24,28,32,35.		1462	1235	1176	1121	1067	1016
7,11,15,19,23, 27,31,34,36.		1190	977	922	872	825	781

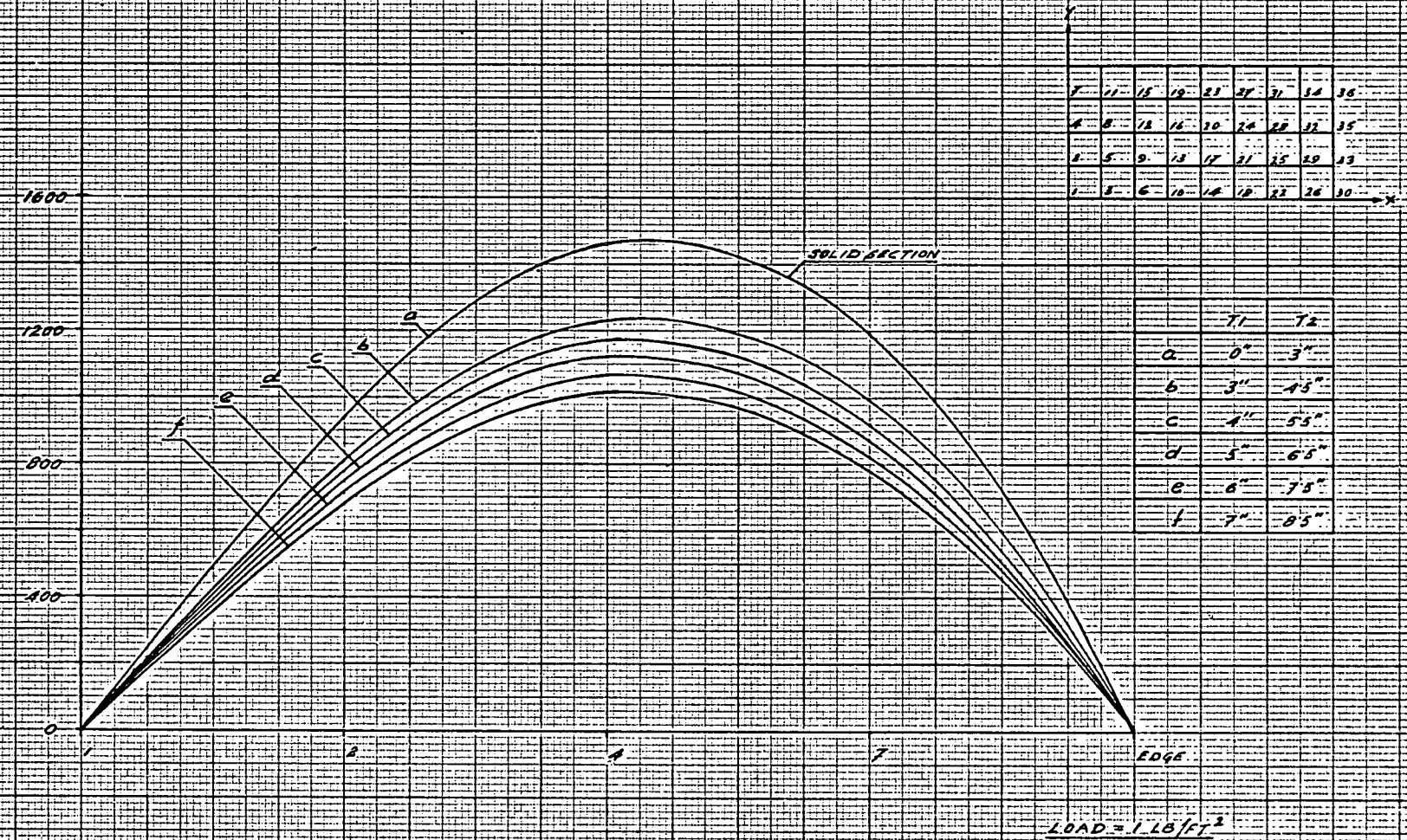

7	11	15	19	23	27	31	34	36
4	8	12	16	20	24	28	32	35
2	5	9	13	17	21	25	29	33
1	3	6	10	14	18	22	26	30

	T1	T2
a	0"	3"
b	3"	4.5"
c	4"	5.5"
d	5"	6.5"
e	6"	7.5"
f	7"	8.5"

V- DISPLACEMENTS

FIGURE: 4-43

	T_1	T_2
a	0	1.5"
b	3"	4.5"
c	4"	5.5"
d	5"	6.5"
e	6"	7.5"
f	7"	8.5"

W - DISPLACEMENTS.

FIGURE 4-44

7	11	15	19	23	27	31	34	36
4	8	12	16	20	24	28	32	35
2	5	9	13	17	21	25	29	33
1	3	6	10	14	18	22	26	30

	T1	T2
a	0"	3"
b	3"	4.5"
c	4"	5.5"
d	5"	6.5"
e	6"	7.5"
f	7"	8.5"

V = DISPLACEMENTS

FIGURE 4-45

	T_1	T_2
a	0	1.5"
b	3"	4.5"
c	4"	5.5"
d	5"	6.5"
e	6"	7.5"
f	7"	8.5"

7	11	15	19	23	27	31	34	36
4	8	12	16	20	24	28	32	35
2	6	9	13	17	21	25	29	33
1	3	5	10	14	18	22	26	30

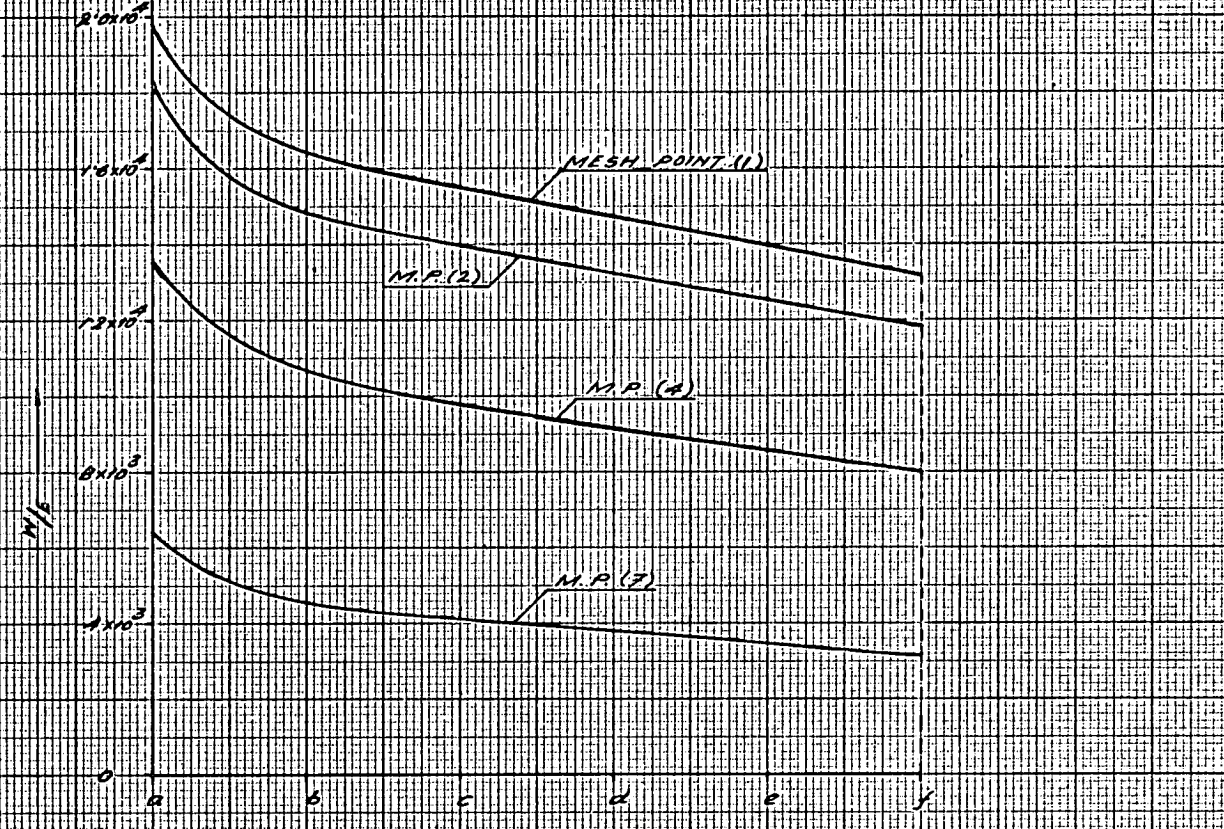

LOAD = 1 lb/ft.²

W = DISPLACEMENTS

FIGURE: 4-46

	MOMENT AT EDGE $M_y/(P_s/25E)$	MOMENT AT CENTRE $M_y/(P_s/15D)$
a	-12,664	+ 3,104
b	- 9088	+ 2,976
c	- 8,200	+ 2,960
d	- 7,458	+ 2,928
e	- 6,846	+ 2,872
f	- 6,330	+ 2,800

FIGURE : 4-47

APPENDIX : 4-4

COMPUTER PROGRAM FOR PERSPEX SHELL : CASE (a)

```
begin
real norm,  D1,D2,Kx,Ky,KK,K1,K2,DD,P1,h,PR,R,EM,b1,b2,b3,t1,t2,a,b,c,dd
integer i,j,k,l,m,n,p,q,ptr,ctr,x,ii,jj,kk,printc,printe,printe1,stepc,stepe,stepe1,c,
array K(1:14),A(1:20),d(1:10),pp(1:2),ZZ(1:10)


ii=0
jj=0
kk=0

....................
....................
....................
20: read(h, PR,R,EM,P1,b1,b2,b3,t1,t2)

DD=(EM/(1-PR↑2))*2*(t2-t1)
D1=DD+EM*(b2/b1)*2*t1
D2=DD+EM*(b3/b1)*2*t1
KK=(EM/(1-PR↑2))*(2/3)((t2)↑3-(t1)↑3)
Kx=KK+EM*(b2/b1)*(2/3)*((t1)↑3)
Ky=KK+EM*(b3/b1)*(2/3)*((t1)↑3)
K1=Kx/KK
K2=Ky/KK

d(1)=D1/DD
d(2)=D2/DD
d(3)=DD
d(4)=D1
d(5)=D2

d(6)=KK
d(7)=Kx
d(8)=Ky
d(9)=K1
d(10)=K2

a= h/R
b= (2*h)/R
c=(3*h)/R
dd= (4*h)/R

pp(1)=(P1/DD)*(h↑2)
pp(2)=(P1/KK)*(h↑4)

ZZ(1)= -pp(1)*(sin(0))
ZZ(2)= -pp(1)*(sin(a))
ZZ(3)= -pp(1)*(sin(b))
ZZ(4)= -pp(1)*(sin(c))
ZZ(5)= -pp(1)*(sin(dd))
```

```
ZZ(6)= pp(2)*(cos(0))
ZZ(7)= pp(2)*(cos(a))
ZZ(8)= pp(2)*(cos(b))
ZZ(9)= pp(2)*(cos(c))
ZZ(10)= pp(2)*(cos(dd))

K(1)=2*((PR-1)/2-d(1))
K(2)=(1-PR)/2
K(3)=DD/KK
K(4)=-(1+PR)/8
K(5)=(PR/R)*(h/2)

K(6)=0
K(7)=-(1+PR)/8
K(8)=2*((PR-1)/2-d(2))
K(9)=-(d(2)/R)*(1/(2*h))*(h↑2)
K(10)=-((PR*K(3))/R)*(1/(2*h))*(h↑4)

K(11)=-((K(3)*d(2))/R)*(1/(2*h))*(h↑4)
K(12)=8+6*(K1+K2)+((d(2)*K(3))/(R↑2))*(h↑4)
K(13)=4*(1+K1)
K(14)=4*(1+K2)

A(1)=K(12)
A(2)=-2*K(14)
A(3)=-2*K(13)
A(4)=2*K2
A(5)=2*K1

A(6)=-K(14)
A(8)=K2
A(7)=A(1)+A(8)
A(9)=-K(13)
A(11)=K1
A(10)=A(1)+A(11)

A(12)=A(1)+A(8)+A(11)
A(13)=K(1)
A(14)=2*K(2)
A(15)=2*d(1)

A(16)=K(2)
A(17)=d(1)
A(18)=K(8)
A(19)=2*d(2)
A(20)=d(2)
```

```
D(1,1)=ZZ(6)-K(10)(2*U(3))-K(11)(2*V(2))
D(2,1)=ZZ(7)+K(11)(V(1)-V(4))-K(10)(2*U(5))
D(3,1)=ZZ(6)+K(10)(U(1)-U(6))-K(11)(2*V(5))
D(4,1)=ZZ(8)+K(11)(V(2)-V(7))-K(10)(2*U(8))
D(5,1)=ZZ(7)+K(10)(U(2)-U(9))+K(11)(V(3)-V(8))

D(6,1)=ZZ(6)+K(10)(U(3)-U(10))-K(11)(2*V(9))
D(7,1)=ZZ(9)+K(11)(V(4))-K(10)(2*U(11))
D(8,1)=ZZ(8)+K(10)(U(4)-U(12))+K(11)(V(5)-V(11))
D(9,1)=ZZ(7)+K(10)(U(5)-U(13))+K(11)(V(6)-V(12))
D(10,1)=ZZ(6)+K(10)(U(6)-U(14))-K(11)(2*V(13))

D(11,1)=ZZ(9)+K(10)(U(7)-U(15))+K(11)(V(8))
D(12,1)=ZZ(8)+K(10)(U(8)-U(16))+K(11)(V(9)-V(15))
D(13,1)=ZZ(7)+K(10)(U(9)-U(17))+K(11)(V(10)-V(16))
D(14,1)=ZZ(6)+K(10)(U(10)-U(18))-K(11)(2*V(17))
D(15,1)=ZZ(9)+K(10)(U(11)-U(19))+K(11)(V(12))

D(16,1)=ZZ(8)+K(10)(U(12)-U(20))+K(11)(V(13)-V(19))
D(17,1)=ZZ(7)+K(10)(U(13)-U(21))+K(11)(V(14)-V(20))
D(18,1)=ZZ(6)+K(10)(U(14)-U(22))-K(11)(2*V(21))
D(19,1)=ZZ(9)+K(10)(U(15)-U(23))+K(11)(V(16))
D(20,1)=ZZ(8)+K(10)(U(16)-U(24))+K(11)(V(17)-V(23))

D(21,1)=ZZ(7)+K(10)(U(17)-U(25))+K(11)(V(18)-V(24))
D(22,1)=ZZ(6)+K(10)(U(18)-U(26))-K(11)(2*V(25))
D(23,1)=ZZ(9)+K(10)(U(19)-U(27))+K(11)(V(20))
D(24,1)=ZZ(8)+K(10)(U(20)-U(28))+K(11)(V(21)-V(27))
D(25,1)=ZZ(7)+K(10)(U(21)-U(29))+K(11)(V(22)-V(28))

D(26,1)=ZZ(6)+K(10)(U(22))-K(11)(2*V(29))
D(27,1)=ZZ(9)+K(10)(U(23)-U(30))+K(11)(V(24))
D(28,1)=ZZ(8)+K(10)(U(24)-U(31))+K(11)(V(25)-V(30))
D(29,1)=ZZ(7)+K(10)(U(25))+K(11)(V(26)-V(31))
D(30,1)=ZZ(9)+K(10)(U(27)-U(32))+K(11)(V(28))

D(31,1)=ZZ(8)+K(10)(U(28))+K(11)(V(29)-V(32))
D(32,1)=ZZ(9)+K(10)(U(30))+K(11)(V(31))
```

```
F(1,1)=0
F(2,1)=0
F(3,1)=-K(5)(W(1)-W(6))+K(4)(2*V(9)-2*V(2))
F(4,1)=0
F(5,1)=K(4)(V(1)-V(4)-V(6)+V(12))-K(5)(W(2)-W(9))

F(6,1)=-K(5)(W(3)-W(10))+K(4)(2*V(13)-2*V(5))
F(7,1)=0
F(8,1)=K(4)(V(2)-V(7)-V(9)+V(15))-K(5)(W(4)-W(12))
F(9,1)=K(4)(V(3)-V(8)-V(10)+V(16))-K(5)(W(5)-W(13))
F(10,1)=-K(5)(W(6)-W(14))+K(4)(2*V(17)-2*V(9))

F(11,1)=K(4)(V(4)-V(12))-K(5)(W(7)-W(15))
F(12,1)=K(4)(V(5)-V(11)-V(13)+V(19))-K(5)(W(8)-W(16))
F(13,1)=K(4)(V(6)-V(12)-V(14)+V(20))-K(5)(W(9)-W(17))
F(14,1)=-K(5)(W(10)-W(18))+K(4)(2*V(21)-2*V(13))
F(15,1)=K(4)(V(8)-V(16))-K(5)(W(11)-W(19))

F(16,1)=K(4)(V(9)-V(15)-V(17)+V(23))-K(5)(W(12)-W(20))
F(17,1)=K(4)(V(10)-V(16)-V(18)+V(24))-K(5)(W(13)-W(21))
F(18,1)=-K(5)(W(14)-W(22))+K(4)(2*V(25)-2*V(17))
F(19,1)=K(4)(V(12)-V(20))-K(5)(W(15)-W(23))
F(20,1)=K(4)(V(13)-V(19)-V(21)+V(27))-K(5)(W(16)-W(24))

F(21,1)=K(4)(V(14)-V(20)-V(22)+V(28))-K(5)(W(17)-W(25))
F(22,1)=-K(5)(W(18)-W(26))+K(4)(2*V(29)-2*V(21))
F(23,1)=K(4)(V(16)-V(24))-K(5)(W(19)-W(27))
F(24,1)=K(4)(V(17)-V(23)-V(25)+V(30))-K(5)(W(20)-W(28))
F(25,1)=K(4)(V(18)-V(24)-V(26)+V(31))-K(5)(W(21)-W(29))

F(26,1)=-K(5)(W(22))-K(4)(2*V(25))
F(27,1)=K(4)(V(20)-V(28))-K(5)(W(23)-W(30))
F(28,1)=K(4)(V(21)-V(27)-V(29)+V(32))-K(5)(W(24)-W(31))
F(29,1)=K(4)(V(22)-V(28))-K(5)(W(25))
F(30,1)=K(4)(V(24)-V(31))-K(5)(W(27)-W(32))

F(31,1)=K(4)(V(25)-V(30))-K(5)(W(28))
F(32,1)=K(4)(V(28))-K(5)(W(30))
```

```
H(1,1)=0
H(2,1)=ZZ(2)+K(9)(W(1)-W(4))+K(7)(2*U(8)-2*U(3))
H(3,1)=0
H(4,1)=ZZ(3)+K(9)(W(2)-W(7))+K(7)(2*U(11)-2*U(5))
H(5,1)=ZZ(2)+K(7)(U(1)-U(4)-U(6)+U(12))+K(9)(W(3)-W(8))

H(6,1)=0
H(7,1)=ZZ(4)+K(9)(W(4))-K(7)(2*U(8))
H(8,1)=ZZ(3)+K(7)(U(2)-U(7)-U(9)+U(15))+K(9)(W(5)-W(11))
H(9,1)=ZZ(2)+K(7)(U(3)-U(8)-U(10)+U(16))+K(9)(W(6)-W12))
H(10,1)=0

H(11,1)=ZZ(4)+K(7)(U(4)-U(12))+K(9)(W(8))
H(12,1)=ZZ(3)+K(7)(U(5)-U(11)-U(13)+U(19))+K(9)(W(9)-W(15))
H(13,1)=ZZ(2)+K(7)(U(6)-U(12)-U(14)+U(20))+K(9)(W(10)-W(16))
H(14,1)=      0
H(15,1)=ZZ(4)+K(7)(U(8)-U(16))+K(9)(W(12))

H(16,1)=ZZ(3)+K(7)(U(9)-U(15)-U(17)+U(23))+K(9)(W(13)-W(19))
H(17,1)=ZZ(2)+K(7)(U(10)-U(16)-U(18)+U(24))+K(9)(W(14)-W(20))
H(18,1)=0
H(19,1)=ZZ(4)+K(7)(U(12)-U(20))+K(9)(W(16))
H(20,1)=ZZ(3)+K(7)(U(13)-U(19)-U(21)+U(27))+K(9)(W(17)-W(23))

H(21,1)=ZZ(2)+K(7)(U(14)-U(20)-U(22)+U(28))+K(9)(W(18)-W(24))
H(22,1)=0
H(23,1)=ZZ(4)+K(7)(U(16)-U(24))+K(9)(W(20))
H(24,1)=ZZ(3)+K(7)(U(17)-U(23)-U(25)+U(30))+K(9)(W(21)-W(27))
H(25,1)=ZZ(2)+K(7)(U(18)-U(24)-U(26)+U(31))+K(9)(W(22)-W(28))

H(26,1)=0
H(27,1)=ZZ(4)+K(7)(U(20)-U( 28))+K(9)(W(24))
H(28,1)=ZZ(3)+K(7)(U(21)-U(27)-U(29)+U(32))+K(9)(W(25)-W(30))
H(29,1)=ZZ(2)+K(7)(U(22)-U(28))+K(9)(W(26)-W(31))
H(30,1)=ZZ(4)+K(7)(U(24)-U(31))+K(9)(W(28))

H(31,1)=ZZ(3)+K(7)(U(25)-U(30))+K(9)(W(29)-W(32))
H(32,1)=ZZ(4)+K(7)(U(28))+K(9)(W(31))
```

C - MATRIX

1001 1002 1003 1004 8 1005 0 0 0
1006 1007 4 1006 1003 0 1008 4 1005 0
1009 4 1010 0 1002 1009 0 1004 4 1011 0
1008 1006 0 1001 4 0 1006 1003 0 0 4 1005
2 1009 1006 2 1012 2 0 1006 1009 0 1008 2 1011

1011 0 1009 0 4 1001 0 0 1002 1009 0 1004 4 1011
0 1008 0 1006 0 0 1007 4 0 0 1003 0 0 0 1005
0 2 1008 1009 1006 0 2 1010 2 0 1006 1009 0 0 2 1011
0 1011 2 0 1009 1006 0 2 1007 2 0 1006 1009 0 1008 2 1011
0 1011 0 0 1009 0 0 4 1001 0 0 1002 1009 0 1004 4 1011

0 2 1008 0 1009 1006 0 0 1012 2 0 0 1009 0 0 0 1011
1011 2 1008 0 1009 1006 0 2 1001 2 0 1006 1009 0 0 2 1011
1011 2 0 0 1009 1006 0 2 1007 2 0 1006 1009 0 1008 2 1011
1011 0 0 0 1009 0 0 4 1001 0 0 1002 1009 0 1004 4 1011
1011 2 1008 0 1009 1006 0 0 1007 2 0 0 1009 0 0 0 1011

1011 2 1008 0 1009 1006 0 2 1001 2 0 1006 1009 0 0 2 1011
1011 2 0 0 1009 1006 0 2 1007 2 0 1006 1009 0 1008 2 1011
1011 0 0 0 1009 0 0 4 1001 0 0 1002 1009 0 1004 4 1011
1011 2 1008 0 1009 1006 0 0 1007 2 0 0 1009 0 0 0 1011
1011 2 1008 0 1009 1006 0 2 1001 2 0 1006 1009 0 0 2 1011

1011 2 0 0 1009 1006 0 2 1007 2 0 1006 1009 0 1008 2 1011
1011 0 0 0 1009 0 0 4 1001 0 0 1002 1009 0 1004 4 0
1011 2 1008 0 1009 1006 0 0 1007 2 0 0 1009 0 0 1011 0
1011 2 1008 0 1009 1006 0 2 1001 2 0 1006 1009 0 2 1011 0
1011 2 0 0 1009 1006 0 2 1007 2 0 1006 1009 1008 2 0

1011 0 0 0 1009 0 0 4 1010 0 0 1002 0 1004 0
1011 2 1008 0 1009 1006 0 0 1007 2 0 1009 0 1011
1011 2 1008 0 1009 1006 0 2 1001 2 1006 1009 2
1011 2 0 0 1009 1006 0 2 1012 0 1006 1008
0 1011 2 1008 0 1009 1006 0 1007 2 1009

0 1011 2 1008 0 1009 1006 2 1010 1006
0 0 0 1011 2 1008 1009 1006 1012

10000

E - MATRIX

1013 0 0 0 0
1016 1013 0 1016 0 0
1017 0 1013 0 1014 1017 0
0 1016 0 1013 0 0 1016 0
0 1017 1016 0 1013 0 0 1016 1017

0 1017 0 0 1013 0 0 1014 1017
0 1016 0 0 1013 0 0 0 0
1017 1016 0 0 1013 0 0 1016 1017
1017 1016 0 0 1013 0 0 1016 1017
1017 0 0 0 1013 0 0 1014 1017

1017 1016 0 0 1013 0 0 0 1017
1017 1016 0 0 1013 0 0 1016 1017
1017 1016 0 0 1013 0 0 1016 1017
1017 0 0 0 1013 0 0 1014 1017
1017 1016 0 0 1013 0 0 0 1017

1017 1016 0 0 1013 0 0 1016 1017
1017 1016 0 0 1013 0 0 1016 1017
1017 0 0 0 1013 0 0 1014 1017
1017 1016 0 0 1013 0 0 0 1017
1017 1016 0 0 1013 0 0 1016 1017

1017 1016 0 0 1013 0 0 1016 1017
1017 0 0 0 1013 0 0 1014 1017
1017 1016 0 0 1013 0 0 0 1017
1017 1016 0 0 1013 0 0 1016 1017
1017 1016 0 0 1013 0 0 1016 1017

1017 0 0 0 1013 0 0 1014 0
1017 1016 0 0 1013 0 0 1017 0
1017 1016 0 0 1013 0 1016 1017 0
1017 1016 0 0 1013 0 1016 0
0 1017 1016 0 1013 0 1017

0 1017 1016 0 1013 1016
0 0 1017 1016 1013

10000

G - MATRIX

1018 0 0 0 0
1020 1018 0 1020 1014 0
1016 0 1018 0 0 1016 0
0 1020 0 1018 0 0 1020 1014
0 1016 1020 0 1018 0 0 1020 1016

0 1016 0 0 1018 0 0 0 1016
0 1020 0 0 1018 0 0 0 1014
1016 1020 0 0 1018 0 0 1020 1016
1016 1020 0 0 1018 0 0 1020 1016
1016 0 0 0 1018 0 0 0 1016

1016 1020 0 0 1018 0 0 0 1016
1016 1020 0 0 1018 0 0 1020 1016
1016 1020 0 0 1018 0 0 1020 1016
1016 0 0 0 1018 0 0 0 1016
1016 1020 0 0 1018 0 0 0 1016

1016 1020 0 0 1018 0 0 1020 1016
1016 1020 0 0 1018 0 0 1020 1016
1016 0 0 0 1018 0 0 0 1016
1016 1020 0 0 1018 0 0 0 1016
1016 1020 0 0 1018 0 0 1020 1016

1016 1020 0 0 1018 0 0 1020 1016
1016 0 0 0 1018 0 0 0 1016
1016 1020 0 0 1018 0 0 0 1016
1016 1020 0 0 1018 0 0 1020 1016
1016 1020 0 0 1018 0 0 1020 1016

1016 0 0 0 1018 0 0 0 0
1016 1020 0 0 1018 0 0 1016 0
1016 1020 0 0 1018 0 1020 1016 0
1016 1020 0 0 1018 0 1020 0
0 1016 1020 0 1018 0 1016

0 1016 1020 0 1018 1020
0 0 1016 1020 1018

10000

data

CHAPTER 5

CYLINDRICAL SHELLS : MODEL EXPERIMENTS

5.1 INTRODUCTION

As for plates, in the case of cylindrical shells built of hollow clay blocks models were built of strips of perspex cemented together and tested to examine the validity of the theory developed in Chapter 3 for Cylindrical Shells. One model of a cylindrical shell using strips of perspex was built and tested under two boundary conditions viz. (a) fixed at the edges and free at the end-arches subject (1) to a uniformly distributed load and (2) to a concentrated load, and (b) fixed at both the edges and the end-arches and subject to a uniformly distributed load. After this one model of a cylindrical shell fixed at the edges and free at the end-arches of hollow clay blocks was built and tested under U.D.L. The above test results are compared with the behaviour of the shell of hollow cross sections as derived from the theory.

5.2 PERSPEX MODEL:

5.2a Construction of Model:

In order to give and maintain the proper profile of the shell a mould was made using plywood. Strips of plywood were fixed at the ends and at the edges to keep the alignment of the bottom slab of the shell. Two $\frac{3}{8}$in x $\frac{1}{8}$in flat steel bars were grooved and fixed along the edges of the mould to act as guides for the ribs of the shell. (Plate 5-I). One inch wide strips were cut from a 1/16in thick sheet of perspex. To facilitate the running of cement along the joints, the strips were champhered at both edges.

Plate: 5-1

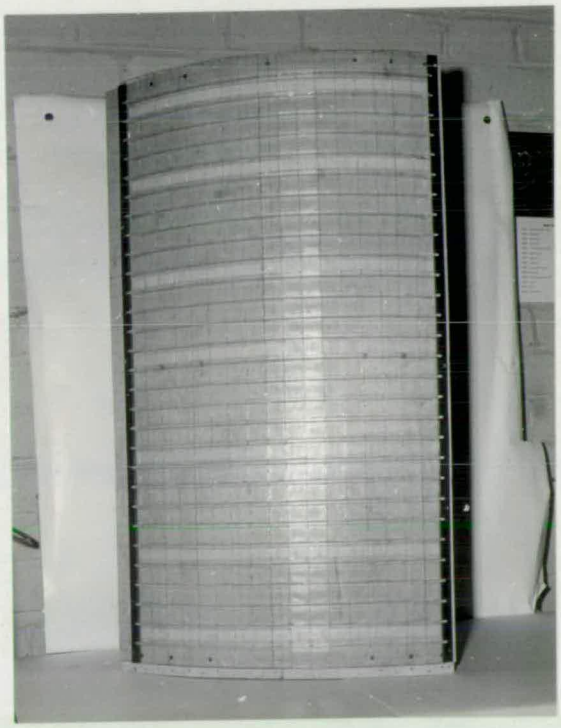

Plate: 5-2

These were used in building the upper and lower surfaces. For ribs $\frac{1}{4}$in. deep circular arches of 15in radius were cut from a $\frac{1}{8}$in thick perspex sheet. While cutting the arches an aluminium template was used to maintain the regularity and uniformity. The arches were cut larger than required by a bend-saw and afterwards using the template these were machined to proper size.

Transverse lines at intervals of 1 in were drawn on the mould to guide the positioning of the ribs. Seven strips of double faced cellotape were spread transversely to keep the perspex strips of the lower slab in position, these can be seen in Plate(5-2.) Strips of ordinary single faced cellotape were used under the longitudinal joints to prevent the flowing down of the cement. Cementing was started from the central strip. This was done in order to cut the strips at the edge to the required width depending on the spaces left between the penultimate strips and the edge guides. The depressions developed along the joints due to shrinkage of cement after the first run were roughened by using a triangular file and sand paper. The cement was run for the second time along the joints. After the cement dried the joints were brought down to level by using sand-paper. Before cementing the ribs to the bottom slab each of these were filed and checked so that there was proper contact between the slab and the rib. The surface of contact was roughened by rubbing with sandpaper. Cement was run on the slab and also on the rib and the rib was placed in position and a steady pressure was applied. This was done by stretching strips of cellotape across the rib and slab. Similarly all the ribs were fixed initially. Excess cement was removed and joints were cleaned. The mould was kept vertical so that the joints of the ribs are nearly horizontal (Plate 5-2). The cement was run along the joints to fill up any

gaps. The other face of the joint was treated similarly by turning the mould upside down. Plates (5-1& 2)show the detail of the moulds, edge-guides, guides for ribs and the shell with bottom slab and ribs. The guides for the ribs were removed before the construction of the top slab was undertaken.

Before taking up the building of the top slab the level of the top of the ribs was checked. The ribs were filed and rubbed with sandpaper to an even level. These were thoroughly cleaned with Acetone. Like the bottom slab here also cementing was started from the centre. Cememt was run on the ribs only for an approximate length of contact with the 1 inch wide strip. Cement was also run on the 1 inch wide strip at places were to be in contact, after which the later strip was placed in position and kept under constant pressure till the cement dried. Excess cement at the joints were chipped out and cleaned. Similar procedure was followed for the rest of the strips. The V-notches formed at the joints between the 1 inch strips were cleaned and cement was run along the joints. The following day after rubbing and cleaning the depressions cement was run again to fill up the joints. Plate (5-3)shows the shell without edge beams. The fixing of the edge beams is discussed under Testing Procedure since this depends on the boundary conditions.

It is to be noted that before applying cement at any place, it was roughened by sand paper and thoroughly cleaned with Acetone. I.C.I.'s 'Tensol' cement No. 7 was used throughout.

5.2b Strain and Deflection Measurements

Electric resistance strain gauages of PL-10 type of 120 Ω having 10mm gauge length were used for measuring strains. The surface of the shell was roughened by rubbing fine sand paper and cleaned with Acetone.

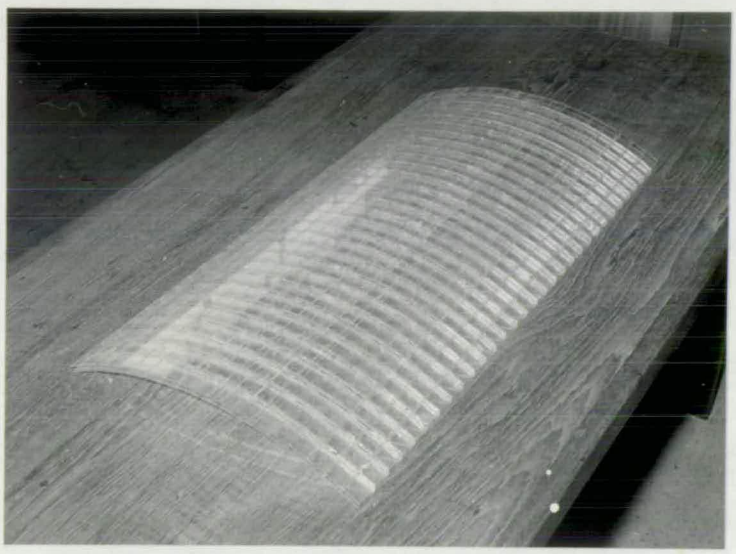

Plate: 5-3

The strain gauges were fixed with CN adhesive as recommended by the manufacturer. The strain gauges can be seen in Plate (5-6). An equal number of PL-10 strain gauges were fixed on another perspex shell of hollow cross section with CN adhesive to act as compensating gauges. The strain gauges were covered with polythene sheets to prevent the gauges from drift. For recording the strains a 10 channel Westland Data Logger, and Savage & Parsons Strain Recorder were used. In each of the instruments a voltage of 5 volts was applied across the bridge. Besides strains it was also decided to measure deflections. The sensitivity of the dial gauges were 10^{-4}in.

5.2c Testing Procedure

A frame was made using 2in x 2in x $\frac{1}{4}$in machined angles details of which are shown in Plates (5-4 & 5). The inside dimensions of the frame were made just to accommodate the shell with its edge beams. In order to minimise the initial stress due to fixing of the shell to the frame, the following procedure was adopted; $\frac{3}{8}$in thick perspex used as edge beams were cut to proper sizes and fixed to the frame using BA No.2 bolts. Two rows of holes were drilled on the upstand legs of the steel angles for the bolts. Similar holes were drilled on the perspex beams by clamping them with the corresponding upstand legs. Before fixing the beams the inside faces where shell would be cemented they were roughened by using sand paper. The edges of the shell and the ends of the ribs were filed to the correct alignment. Top and bottom of the shell edges and ends were roughened by sand paper. The shell was then placed inside the frame and kept at proper position and level by using blocks, cut to required sizes.

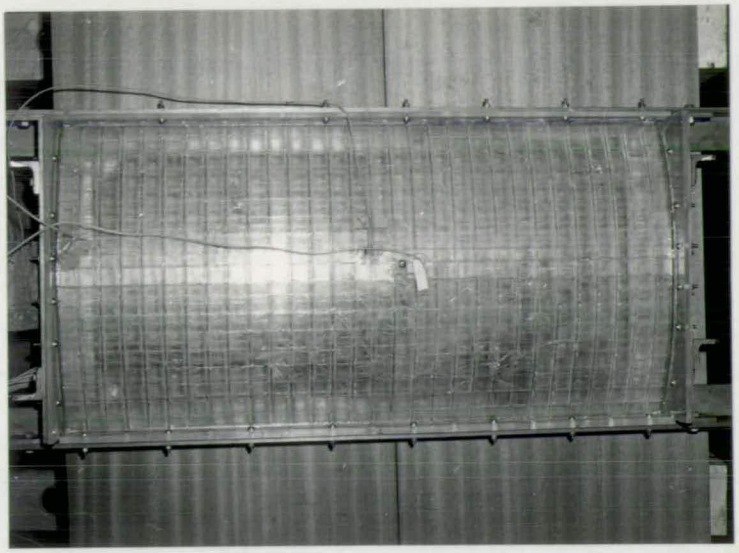

Plate: 5-4

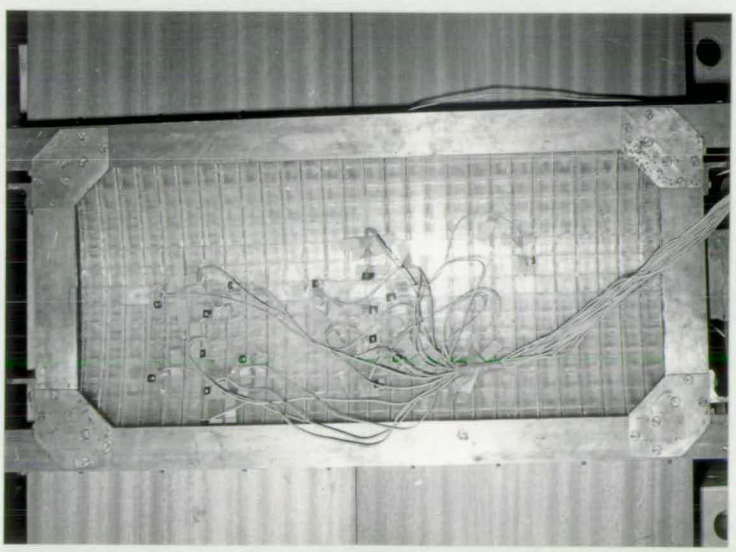

Plate: 5-5

5.2d Fixed at the edges and free at the end-arches:

To obtain the fixed at the edges and free at the end-arches boundary conditions the two edges of the shell were cemented to the edge beams which in turn were fixed to the frame. Cement was run along the edges to fill up the gaps between the top slab of the shell and the edge beams. To prevent the cement from running down the gap, before applying, it was thickened by allowing a few minutes to elapse after it was prepared. After the cement dried the joints were roughened by using sand paper and cleaned. Fresh cement was run along the joints. Several runs of cement were applied to make the joint strong. Due to the horizontal legs of the angles of the frame it was not possible to run cement along the joints between the bottom slab of the shell and the edge beams. The shell was taken out and turned upside down. In order to prevent running down of cement the shell was kept inclined along its transverse axis but keeping the joint horizontal. The cement was run along the joints to fill up the gap. Repeated runs of cement were applied to make the joint strong. Plate (5-6) shows the details of the shell with edge beams and strain gauges.

A test rig was erected on a strong floor shown in Plate (5-7) and the steel frame was placed on the rig and clamped tightly using steel shims as packing to fill up the gaps between the horizontal faces of the frame and the horizontal beams of the rig. The shell was placed inside the frame and bolted. It was observed that there developed some initial stresses in the shell when the bolts were tightened. In order to avoid such stresses the bolts were removed and solution of Polycell filler was injected through the holes keeping other end of holes closed to fill up the gaps between the vertical legs of the frame and the perspex edge beams. When the solution dried up the bolts were replaced and

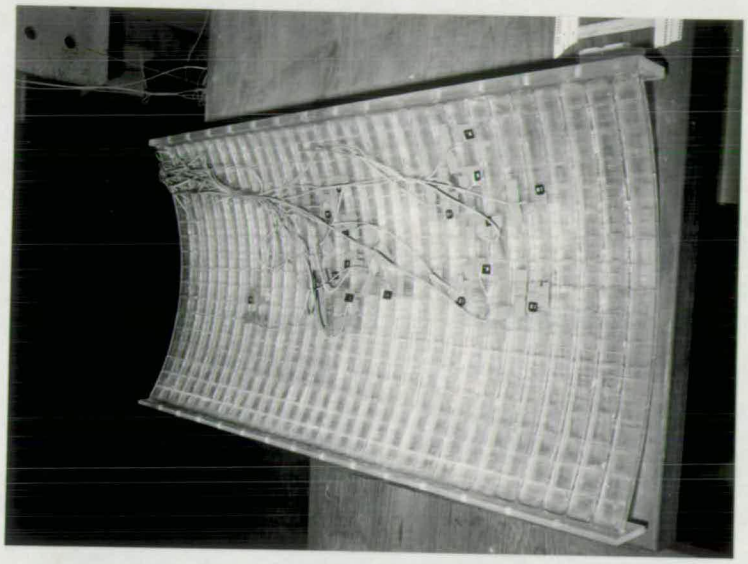

Plate: 5-6

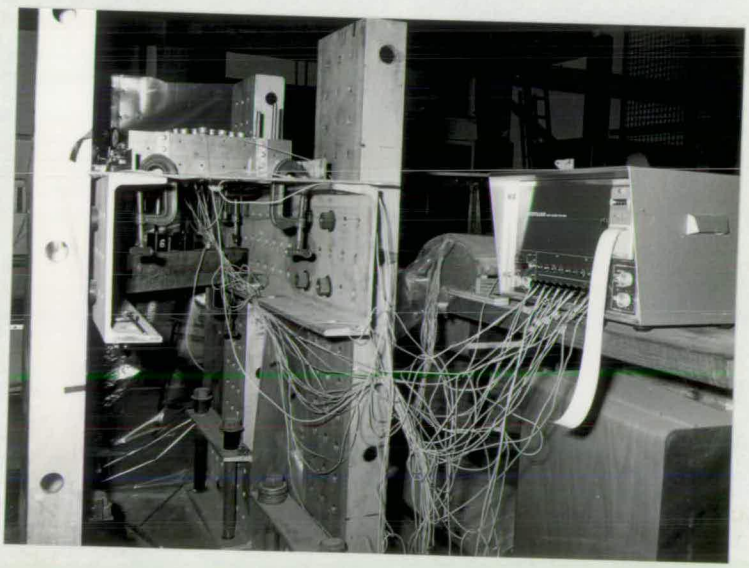

Plate: 5-7

tightened during which no initial stress in shell was observed. During the initial tests, particularly at final load stage, a little horizontal movement of the edge beams was observed which was prevented by using clamps at closer intervals.

Plates (5-7 & 8) show the general arrangement of the test, where strains at 10 places and deflections at 3 points were measured. Four dial gauges were used to measure the vertical and horizontal movements of the edge beams (Plate 5-9).

For uniformly distributed loads 600-linch diam x $\frac{1}{2}$in thick lead weights each weighing approximately 0.2 lbs. were cast. These were drilled through the diameter. Each ten of these were threaded by nylon thread to make a chain 15 in long. Each of these were placed on the shell transversely and lead weights were distributed evenly to produce uniformly distributed loads. Loads of 20 lbs or 40 lbs at each stage and up to a maximum of 120 lbs distributed over the surface of the shell were applied. Before placing the loads a sheet of foam rubber was spread on the top of the shell so that the loads were evenly distributed.

For concentrated loads cast iron weights were used. Loads were applied at the centre of the shell and up to a maximum load of 7 lbs.

All the strain gauges were balanced i.e. readings of the strain recorder were brought to zero and the initial readings of the dial gauges were noted before starting the experiment. Readings were taken twice at every load stage, once just after applying the loads and the next one 20 minutes after applying the loads, to allow for creep. The test was repeated for several times on subsequent days until all the readings were steady for most of the tests.

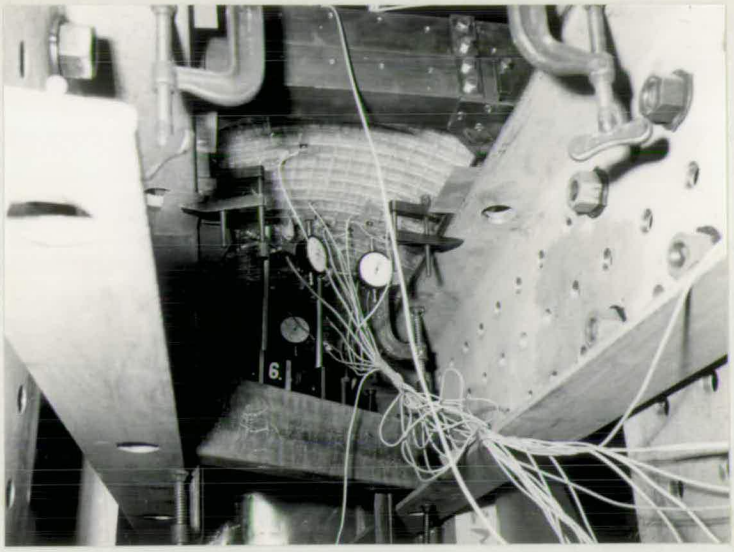

Plate: 5-8

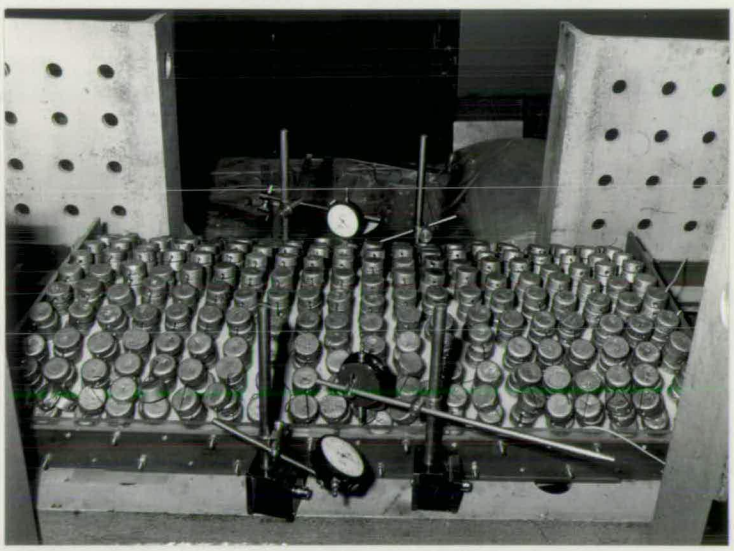

Plate: 5-9

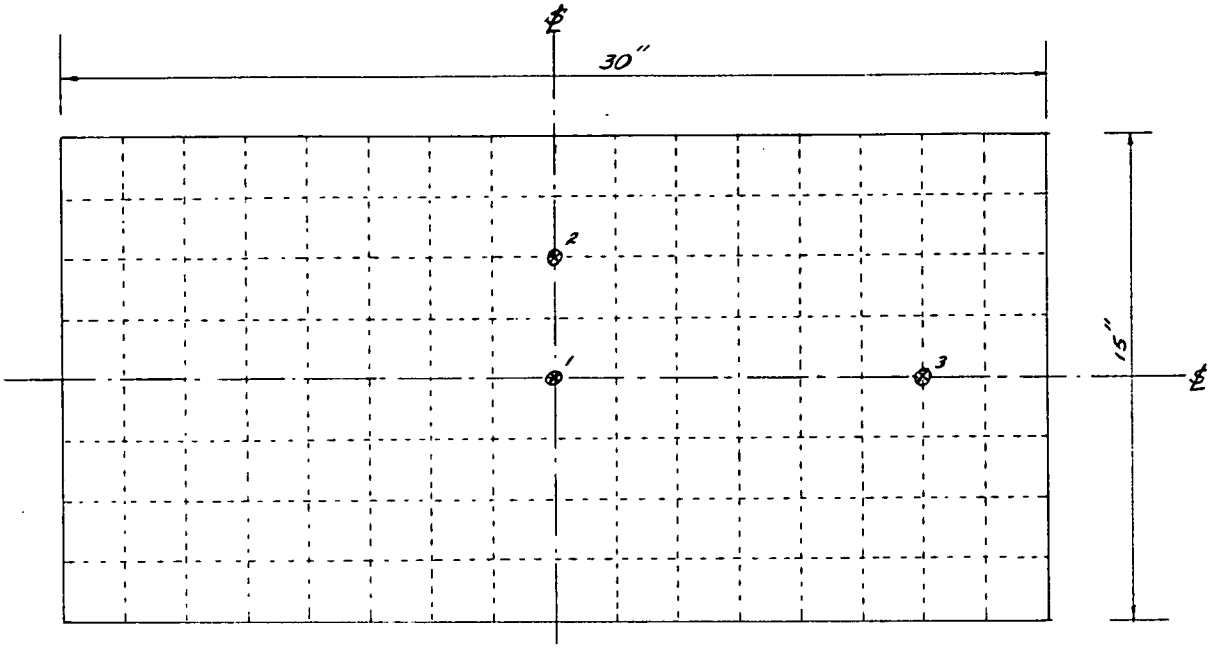

LOCATION OF DIAL GAUGES

FIGURE: 5-1

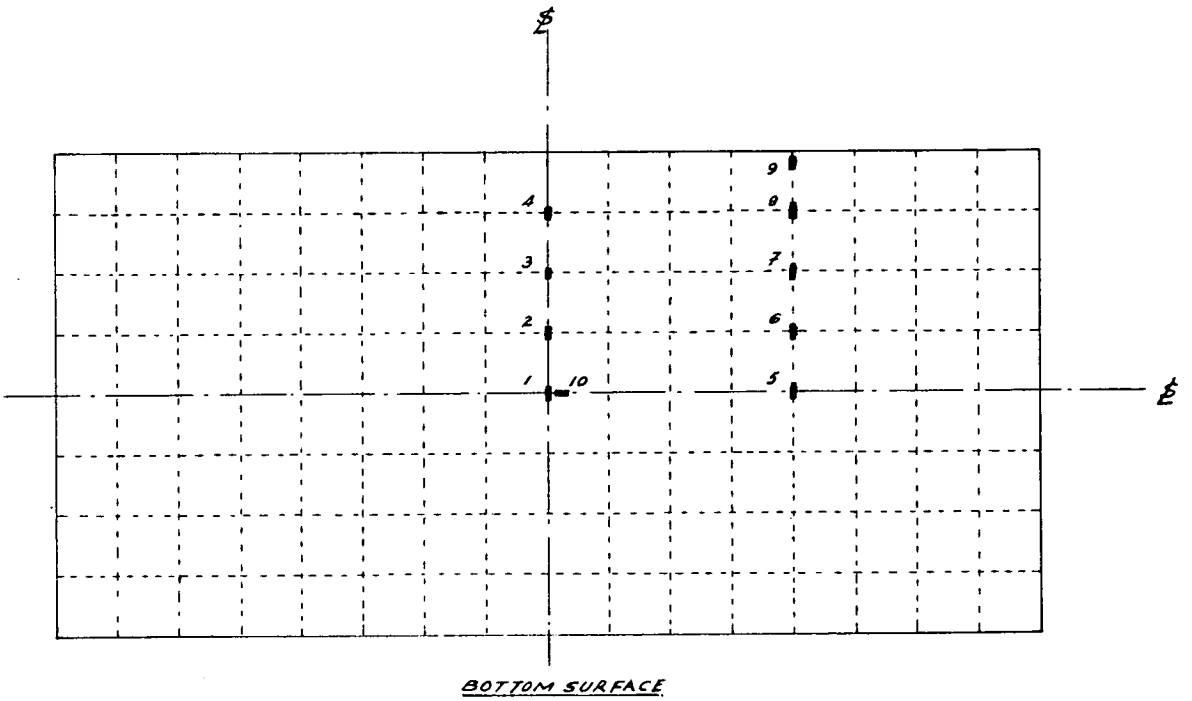

LOCATION OF STRAIN GAUGES.

FIGURE: 5-2

PERSPEX SHELL: FIXED AT EDGES & FREE AT END-ARCHES: U.D.L. & CONC. LD.

The deflections and the strains different load intervals are plotted in Figures (5-3 to 6).

Tables (5-1 to 4) and Figures (5-7 to 9) show the comparison between the theoretical and experimental results.

5.2e Fixed at the edges and at end-arches

To attain these boundary conditions the shell was cemented at the end-arches as well. The frame was removed from the rig. The perspex beams used as end-gables were placed between the shell and the frame. In order to prevent running down of the cement the shell was kept nearly vertical (i.e. its longitudinal axis nearly vertical) making the line of joint nearly horizontal. The cement was run along the joint to fill up the gap between the top of the slab of the shell at the end-arch and the end-gable beam. When the gap was filled up the angle of inclination of the shell was lowered and cement was run for several times until the joint was strong enough. Similarly other joints were cemented.

The frame was placed on the test-rig. The frame was clamped properly and the shell was placed inside the frame. Before bolting the gaps between the edge beams and the vertical legs of the frame were filled up by injecting solution of Polycell filler as in the previous case. Then the bolts were tightened during which no initial stress in the shell was observed.

During the test both vertical and horizontal movement of the frame was observed. To prevent the vertical deflection ten $\frac{3}{4}$in diam bolts with nuts were used as jacks between the 2in x 2in steel bars to which the frame was clamped and the horizontal beams of the main rig. To prevent the horizontal movement, which was mostly at the central portion of the frame, two

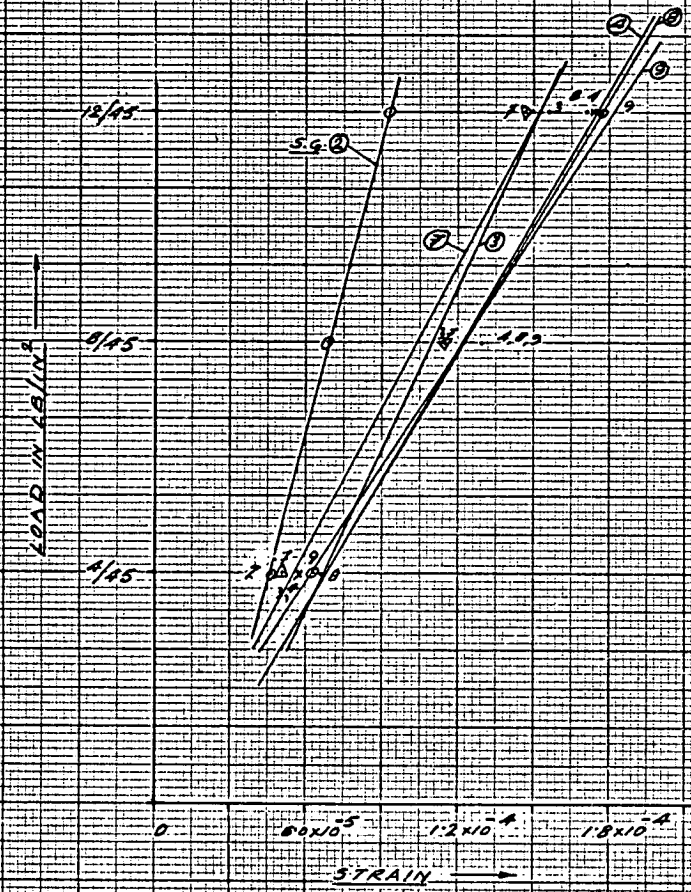

FIGURE : 5-3

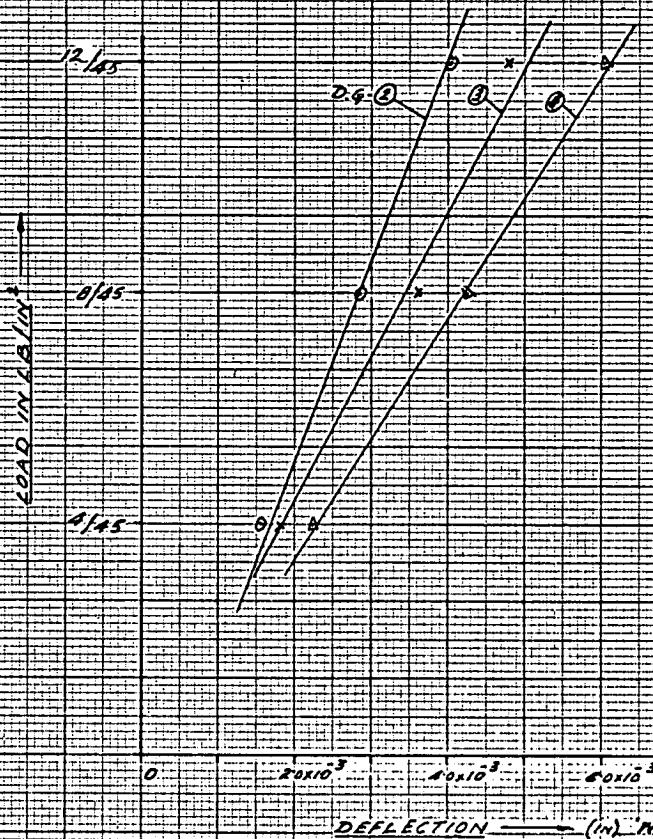

FIGURE : 5-4

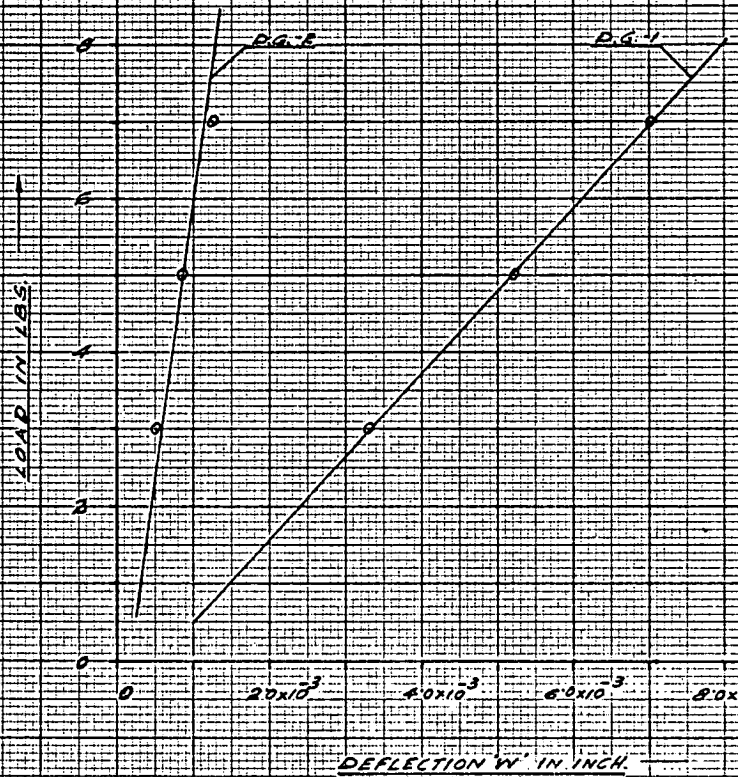

FIGURE : 5-5

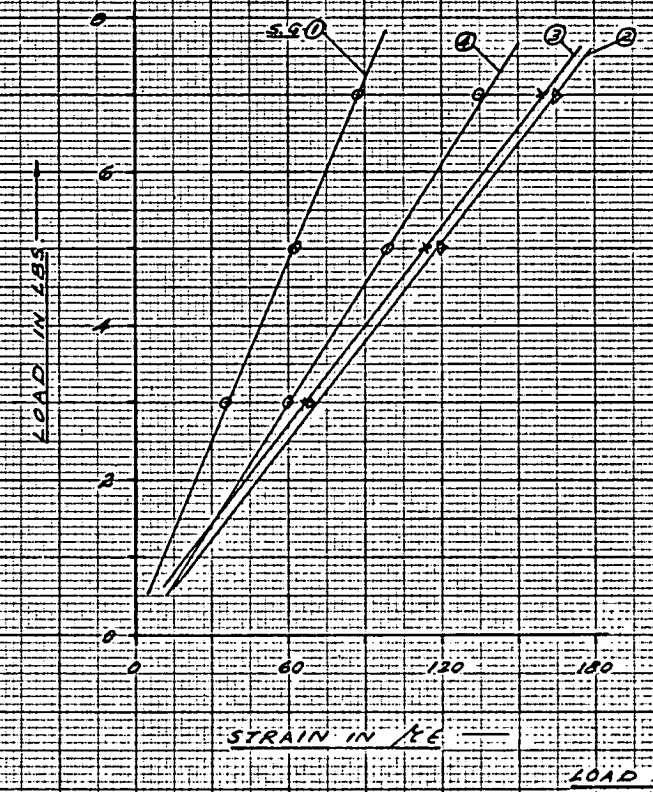

FIGURE : 5-6

CYLINDRICAL SHELL OF PERSPEX: FIXED AT EDGES AND FREE AT END-ARCHES

COMPARISON OF EXPERIMENTAL AND THEORETICAL RESULTS

T A B L E: 5-1 DEFLECTIONS (W)

Dial Gauge No.	Location of Dial Gauge (Mesh Point)	Deflections in 10^{-4} in.		Remarks
		Experimental (From Graph*)	Theoretical	Deviation from Theor. results
1	1	19.0	16.0	+18.7%
2	4	12.0	9.5	+26.3%
3	22	17.0	16.5	+ 3%

* Load Intensity (Uniformly Distributed) = (4/45) lb/in^2

T A B L E: 5-2 STRAINS

Strain Gauge No.	Location of Strain Gauge (Mesh Point)	Strains in $\mu\epsilon$		Remarks
		Experimental (From Graph)*	Theoretical	Deviation from Theor. results
1	1	N.R.	44.0	-
2	2	N.R.	46.5	-
3	4	43.5	53.2	-18.2%
4	7	54.0	66.0	-18.2%
5	14	N.R.	45.5	-
6	17	N.R.	47.5	-
7	20	47.0	54.2	-13.3%
8	23	54.0	66.0	-18.2%
9	41 ($\frac{1}{2}$" from edge)	60.0	80.0	-25.0%

N.R. - No reliable readings

COMPARISON OF DEFLECTIONS

PERSPEX SHELL

FIGURE: 5-7

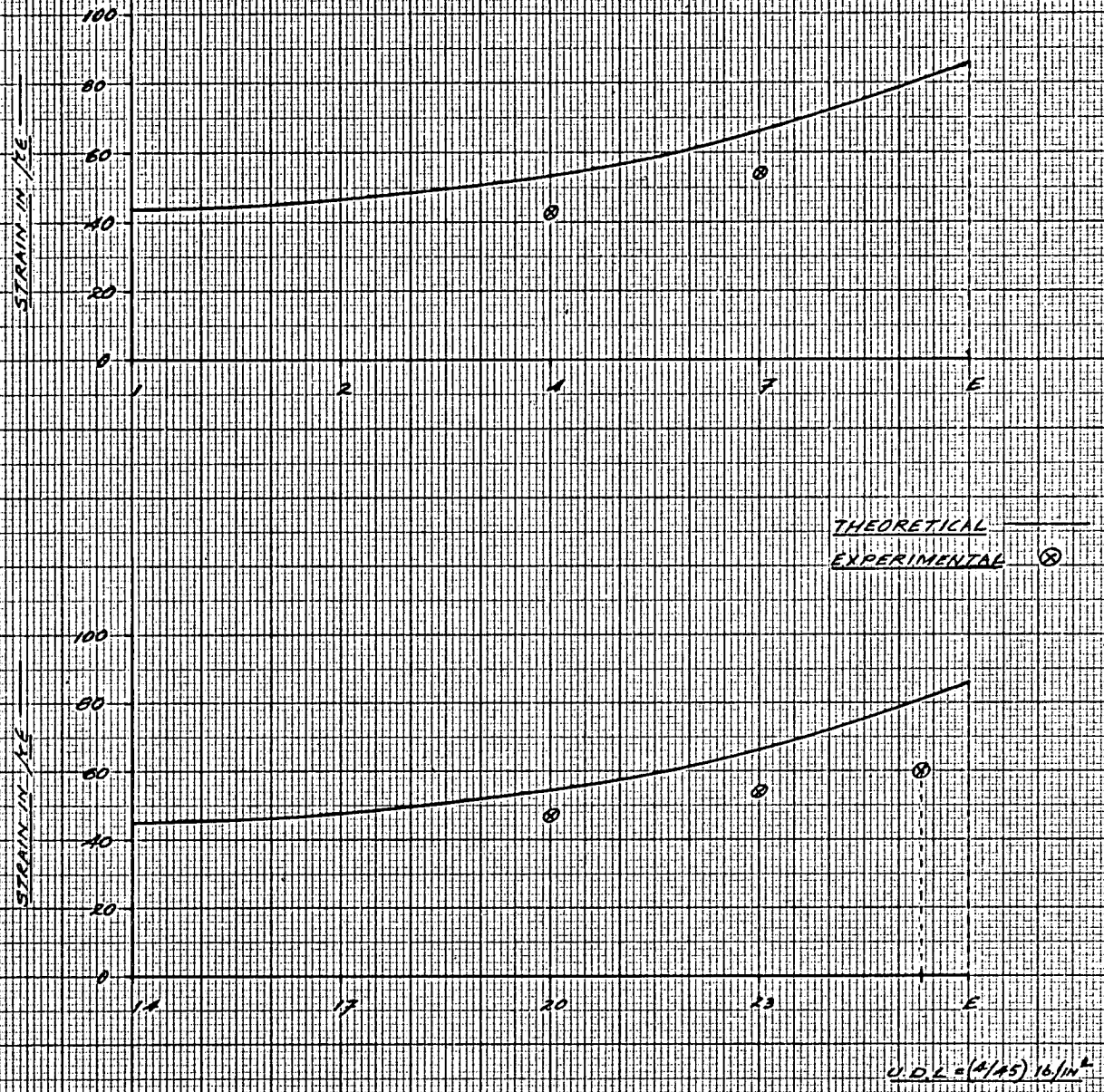

COMPARISON OF STRAINS

PERSPEX SHELL

FIGURE: 5-8:

CYLINDRICAL SHELL OF PERSPEX: FIXED AT EDGES AND FREE AT END-ARCHES

COMPARISON OF EXPERIMENTAL AND THEORETICAL RESULTS

T A B L E: 5-3 DEFLECTIONS (W)

Dial Gauge No.	Location of Dial Gauge (Mesh Point)	Deflections in 10^{-4} in.		Remarks
		Experimental (From Graphs)	Theoretical	Deviation from Theor. results
1	1	9.25	9.85	- 6%
2	4	1.25	0.855	+46%
3	N.R.	-	-	-

T A B L E: 5-4 STRAINS

Strain Gauge No.	Location of Strain Gauge (Mesh Point)	Strains in $\mu\epsilon$		Remarks
		Experimental (from graph *)	Theoretical	Deviation from Theor. results
1	1	(+)12.75	(+)13.75	- 7.27%
2	2	(-)23.25	(-)21.9	+ 6.16%
3	4	(-)23.25	(-)25.8	- 9.9 %
4	7	(-)19.5	(-)21.8	-10.55%

* Load : Conc. 1 lb at M.P. (1).

y								
F	11	15	19	23	27	31	34	36
A	8	12	16	20	24	28	32	35
B	5	9	13	17	21	25	29	33
I	3	6	10	14	18	22	26	30 x

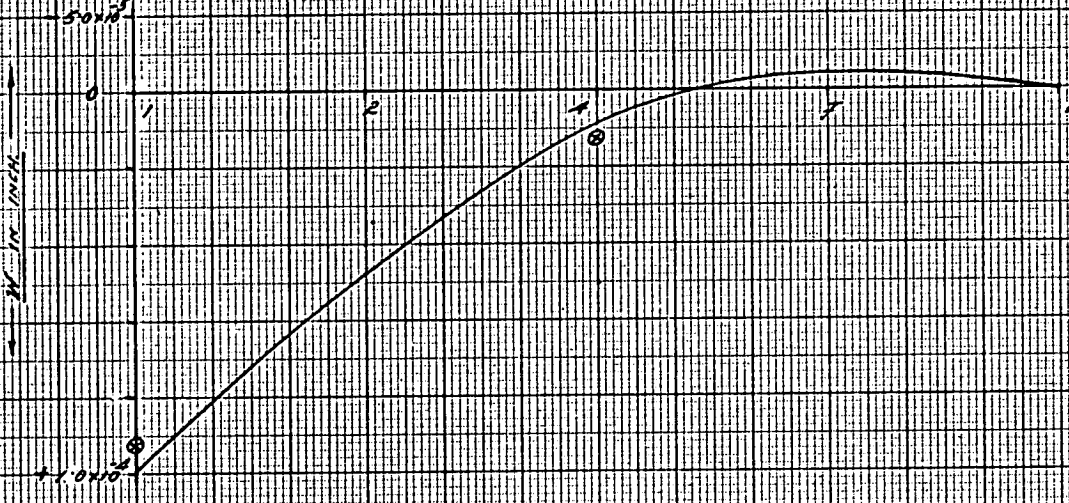

COMPARISON OF DEFLECTIONS

THEORETICAL ——

EXPERIMENTAL ⊗

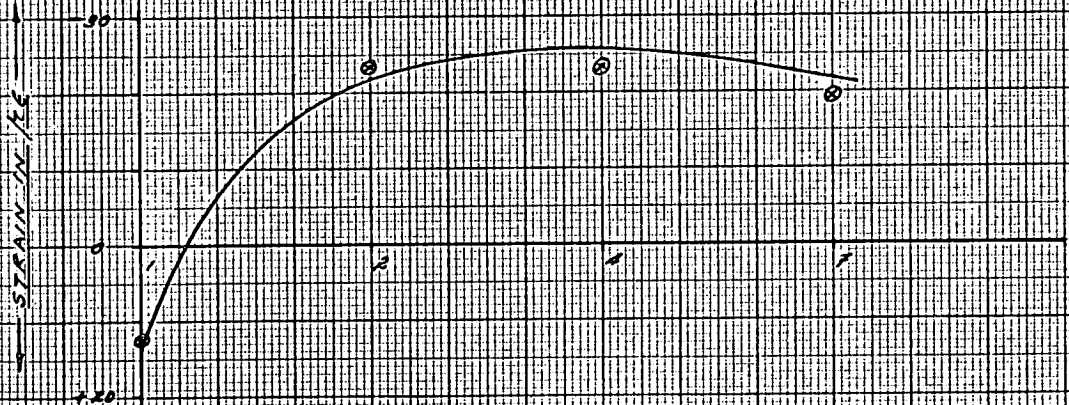

COMPARISON OF STRAINS

LOAD = 1 LB. AT MIDSPAN ⊙

PERSPEX SHELL: CONCLD

FIGURE: 5-9

adjustable sliding clamps were used. The arrangement is shown in Plate (5-10.) The vertical deflections of the shell were measured by dial gauges at eight different points the location of which is shown in Figure (5-10) and Plates (5-11 & 12.) Eight dial gauges were used to measure the vertical and horizontal deflections of the edge beams and gable ends (Plate 5-10). Strains at eighteen different points were measured, ten by the Data Logger and the remaining eight by the Savage & Parsons Strain Recorder. Plate (5-13) shows the general arrangement of the test where the Savage & Parsons Strain Recorder is not included. The rest of the experimental procedure is similar to the previous one.

The deflections and the strains at different load intervals are plotted in Figures (5-12 & 13).

The Tables (5-5 & 6) and Figures (5-14 & 15) show the comparison between the theoretical and experimental results.

5.3 SHELL BUILT OF HOLLOW CLAY BLOCKS:

Fixed at the edges and free at end-arches:

5.3a Construction of Model

In practice most of the cylindrical shells of hollow blocks in Italy are built with boundary conditions fixed at the edges and free at end-arches, so it was decided to test a cylindrical shell built of 1/6th model hollow clay blocks with the above boundary conditions.

As it is very difficult to obtain a perfect fixed condition, it was decided to build the shell on a shuttering and then to cast the edge beams on walls. Two $4\frac{1}{2}$in thick and 2ft 8in long brick walls with corner pillars were built to a height of 3ft 6in spanning 2ft 6in inside to inside. Perforated bricks were used as the top course of the walls for fixing the

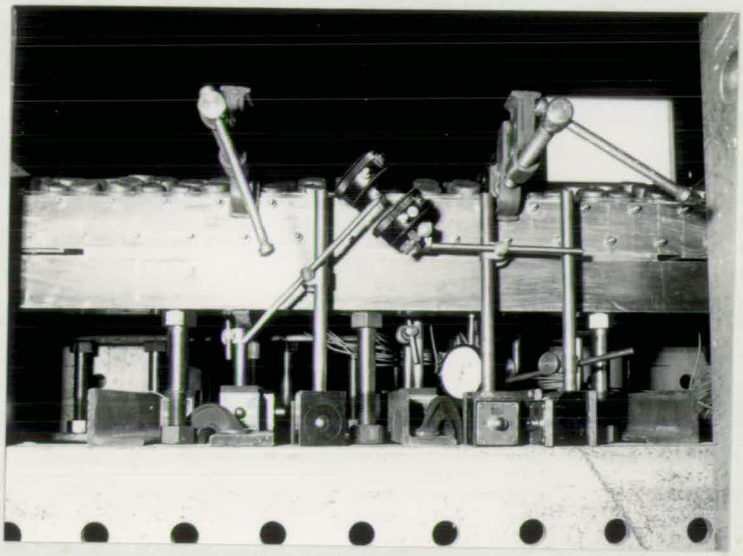

Plate: 5-10

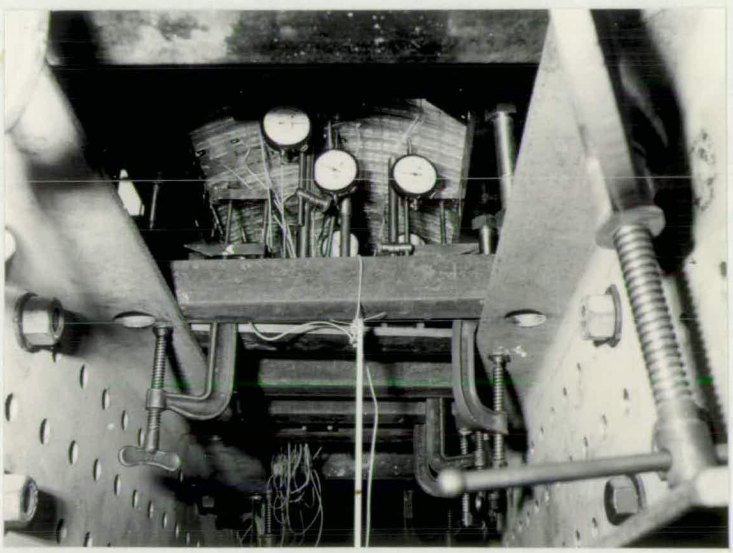

Plate: 5-11

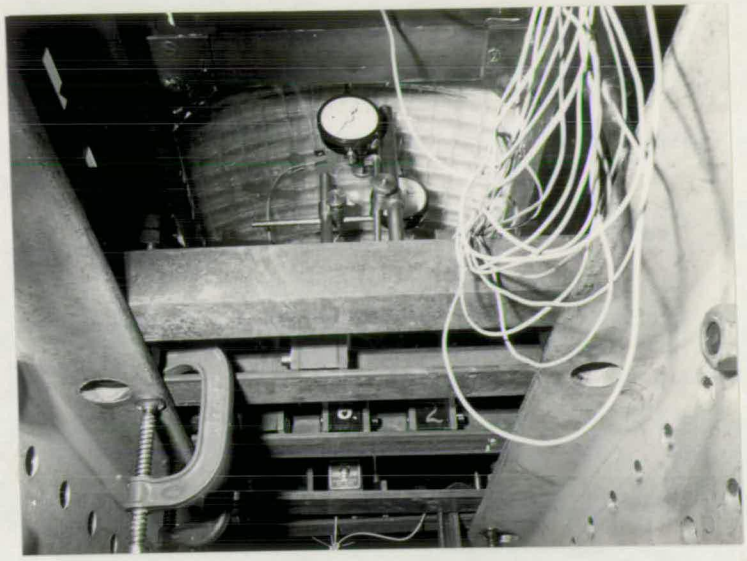

Plate: 5-12

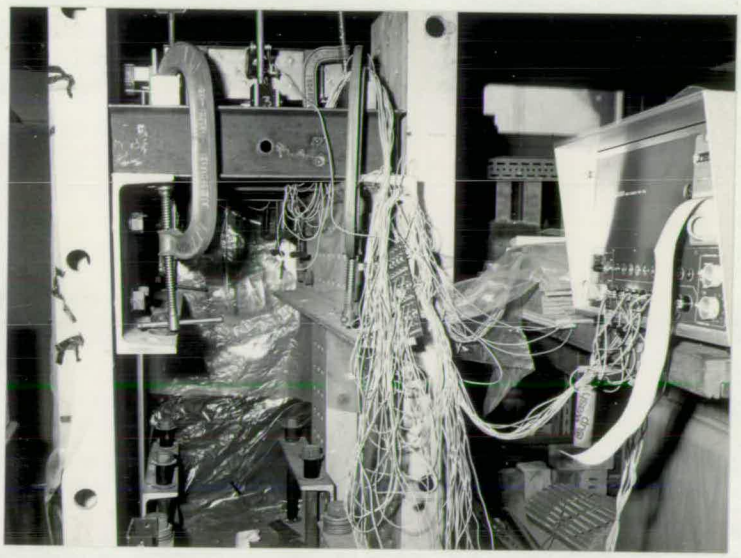

Plate: 5-13

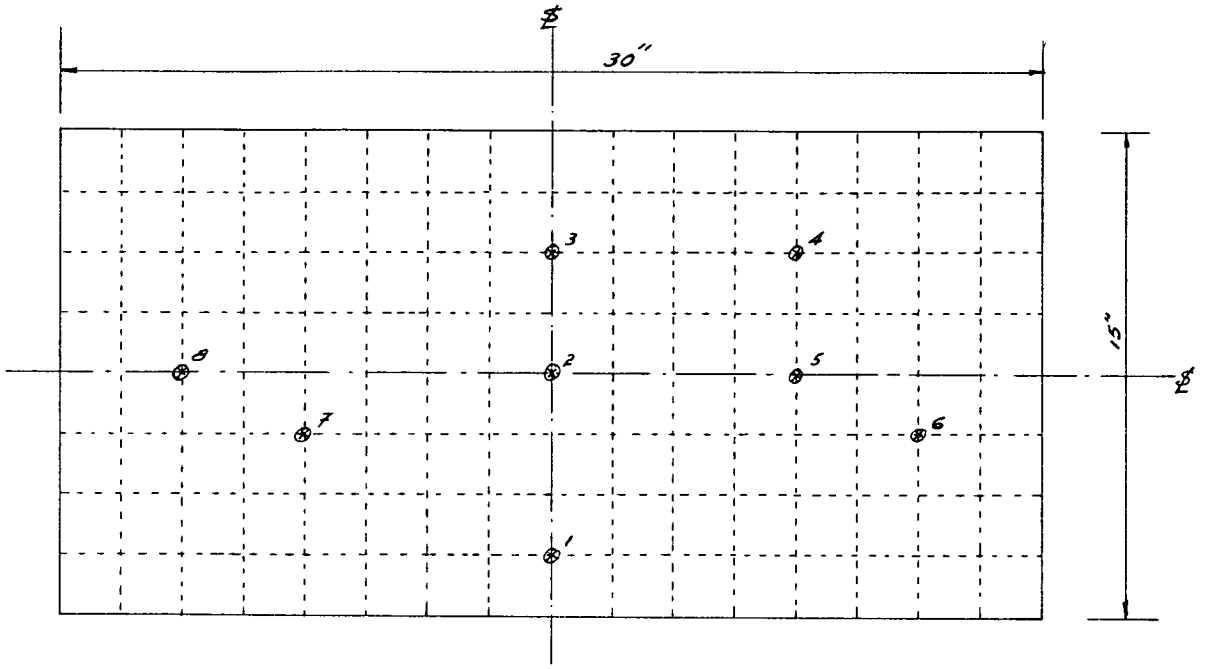

LOCATION OF DIAL GAUGES.

FIGURE: 5-10

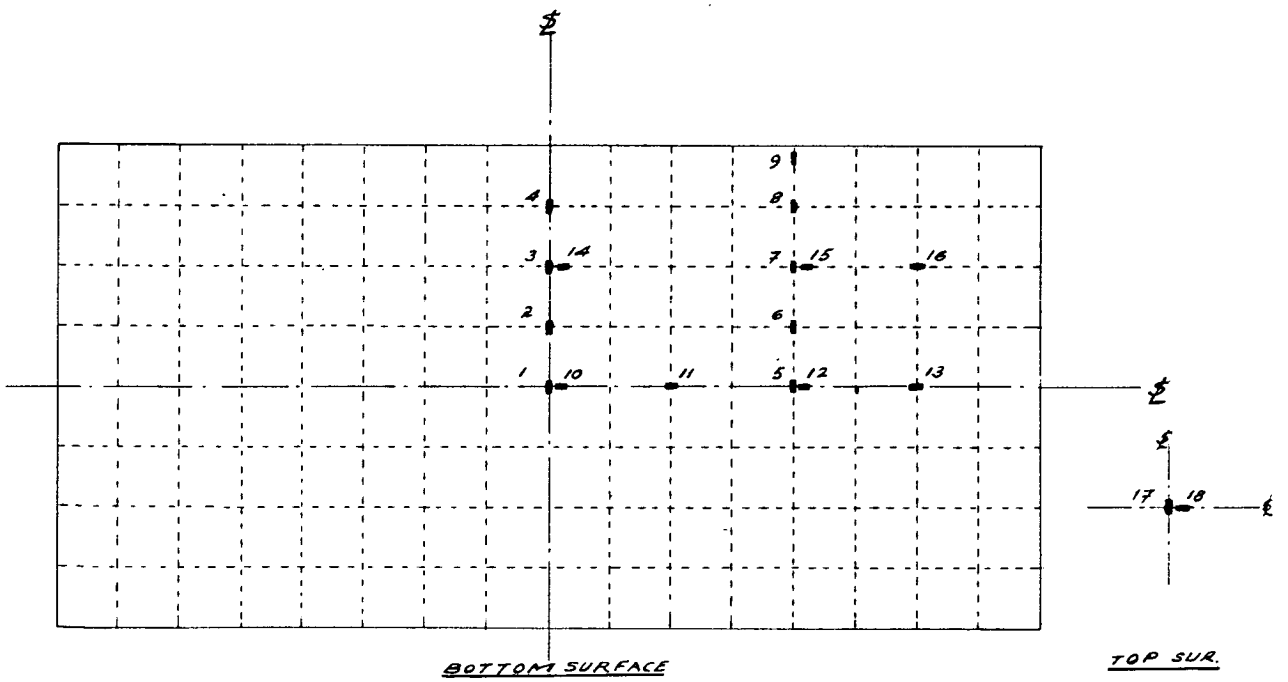

LOCATION OF STRAIN GAUGES.

FIGURE: 5-11.

PERSPEX SHELL: FIXED AT ENDS AND END-ARCHES. U.D.L.

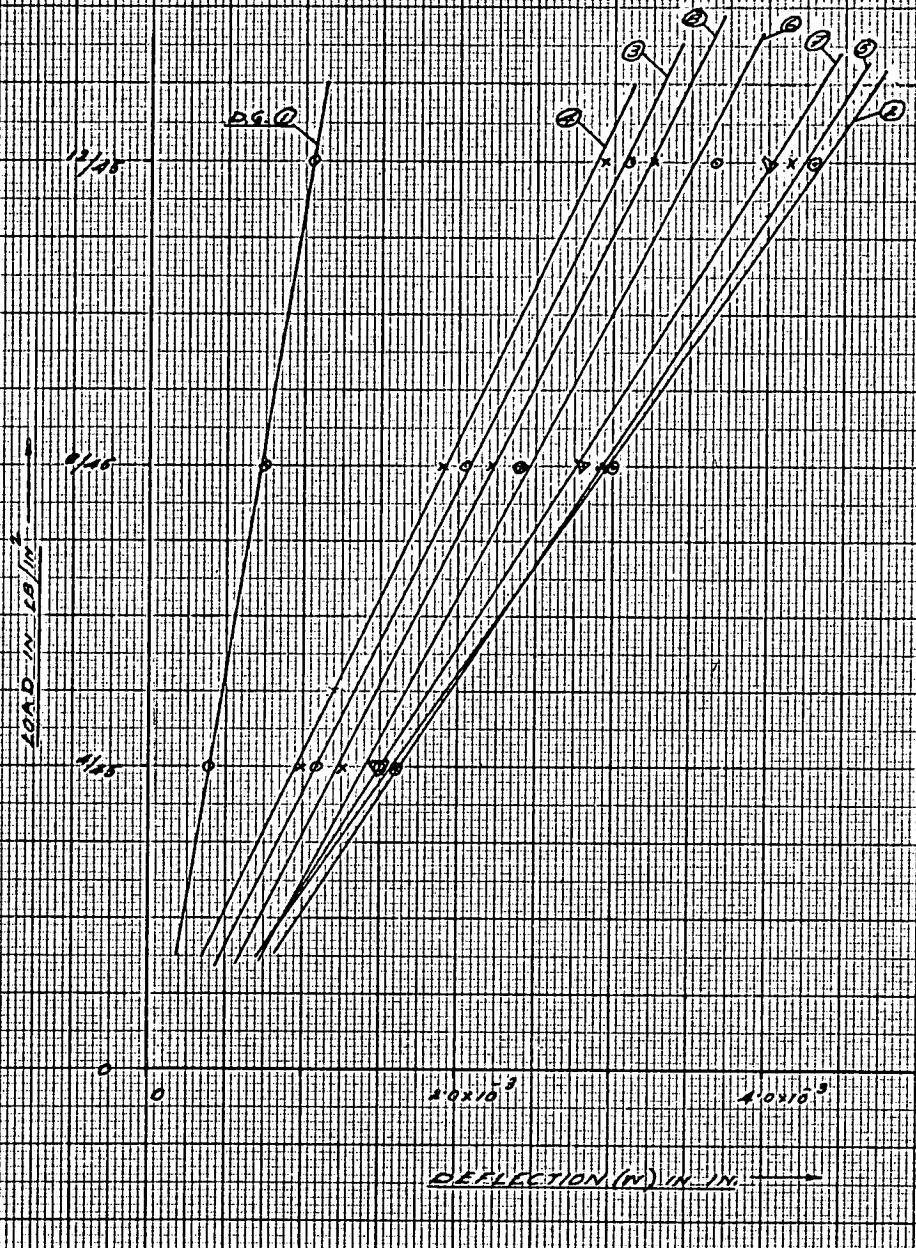
DEG.
12/16
8/16
4/16
LOAD - IN - LBS/IN
0
0
2.0x10⁻³
4.0x10⁻³
DEFLECTION (N) IN IN.
U.D.L.

FIGURE 5-12

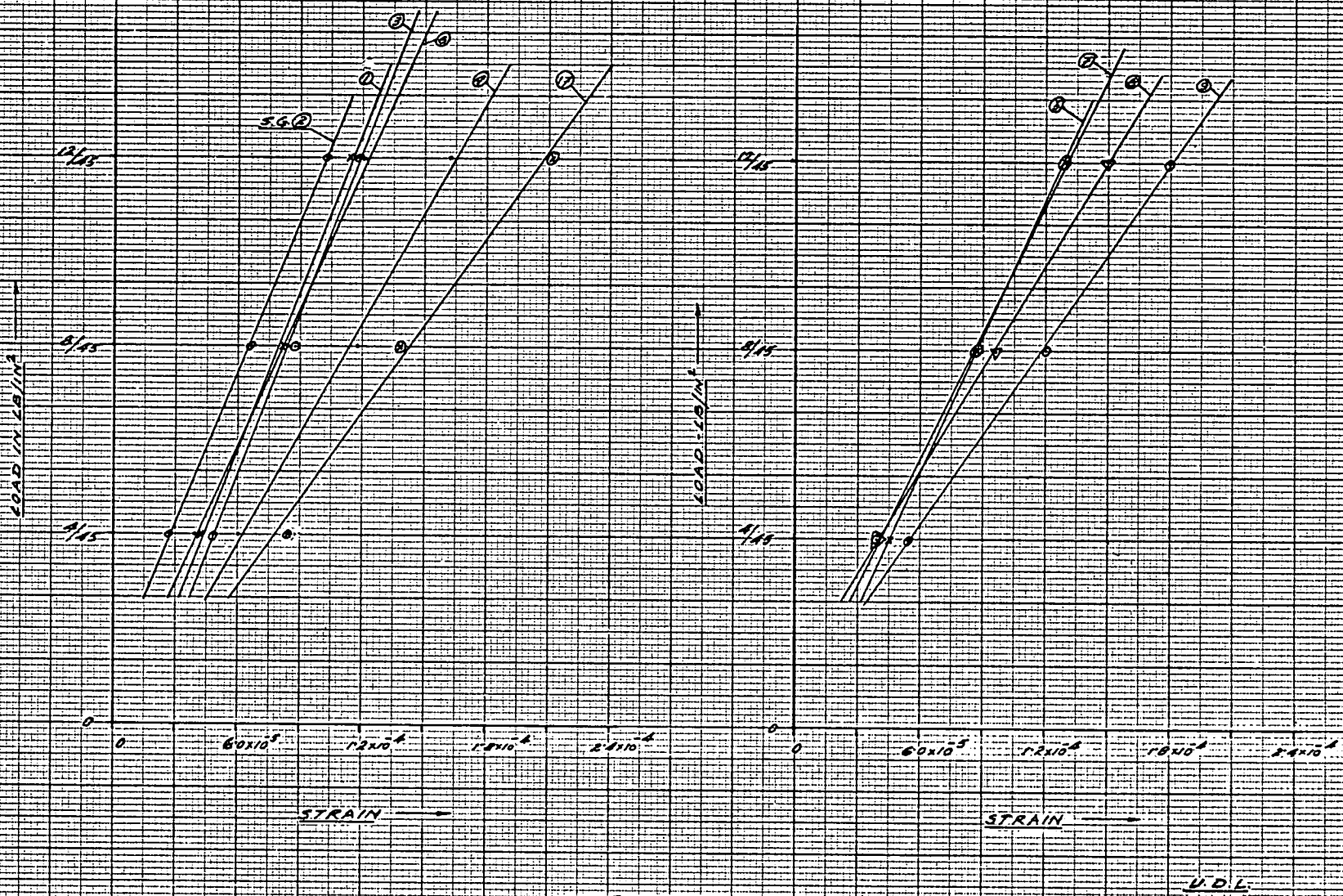
12/15
9/15
6/15
0
LOAD IN LB/IN²
S.G ②
③
④
①
⑥
⑦
⑤
0
6.0x10⁻⁵
1.2x10⁻⁴
1.8x10⁻⁴
2.4x10⁻⁴
STRAIN
12/15
9/15
6/15
0
LOAD LB/IN²
⑦
⑧
⑥
⑨
⑤
0
6.0x10⁻⁵
1.2x10⁻⁴
1.8x10⁻⁴
2.4x10⁻⁴
STRAIN
U.D.L.

FIGURE: 5-13.

CYLINDRICAL SHELL OF PERSPEX: FIXED AT EDGES

AND END-ARCHES

COMPARISON OF EXPERIMENTAL AND THEORETICAL RESULTS

T A B L E 5-5 DEFLECTIONS (W)

Dial Gauge No.	Location of Dial Gauge (Mesh Point)	Deflections in 10^{-4} in.		Remarks
		Experimental (From Graph*)	Theoretical	Deviation from Theor. results
1	7	3.0	3.5	-14.3%
2	1	13.5	15.7	-14.0%
3	4	10.0	9.25	+ 8.1%
4	20	9.75	9.5	+ 2.6%
5	14	13.5	15.7	-14.0%
6	25	10.75	11.4	- 5.7%
7	17	12.75	14.0	- 8.9%
8	22	10.25	12.6	-18.6%

T A B L E 5-6 STRAINS

Strain Gauge No.	Location of Strain Gauge (Mesh Point)	Strains in $\mu\epsilon$		Remarks
		Experimental (From Graph *)	Theoretical	Deviation from Theor. results
1	1	36.0	41.0	-12.2%
2	2	36.0	43.5	-17.2%
3	4	40.5	52.0	-22.1%
4	7	51.0	66.0	-22.7%
5	14	42.0	43.5	- 3.4%
6	17	42.0	45.5	- 7.7%
7	20	45.0	52.5	-14.3%
8	23	55.5	66.7	-16.8%
9	41 ($\frac{1}{2}$" from edge)	63.0	81.0	-22.2%
17	1 (Top)	66.0	78.2	-15.6%

Note: The Strain gauges along x-axis did not give consistant readings.

* Load Intensity (Uniformly Distributed) = (4/45) lb/in^2.

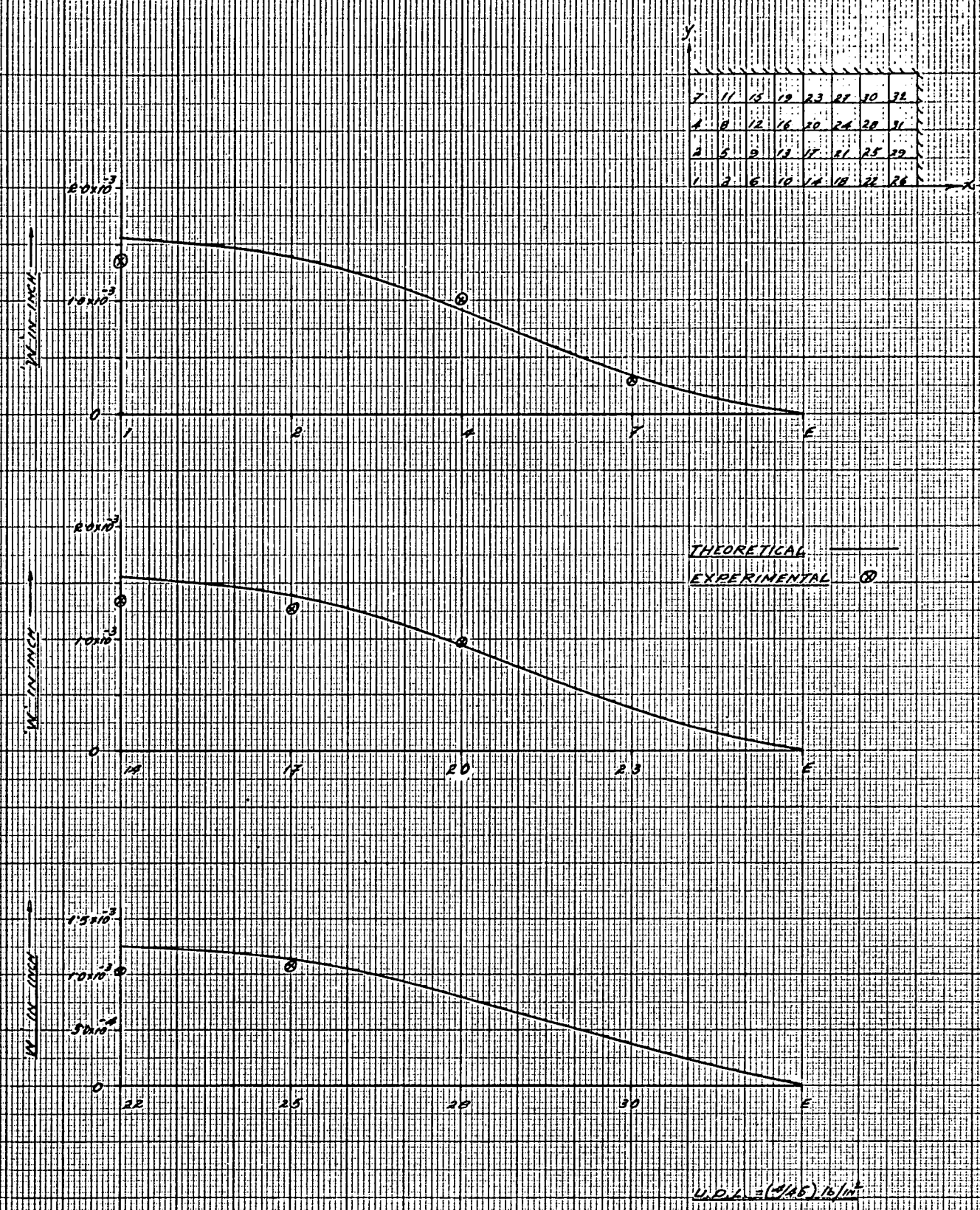

COMPARISON OF DEFLECTIONS : W

PERSPEX SHELL

FIGURE: 5-14

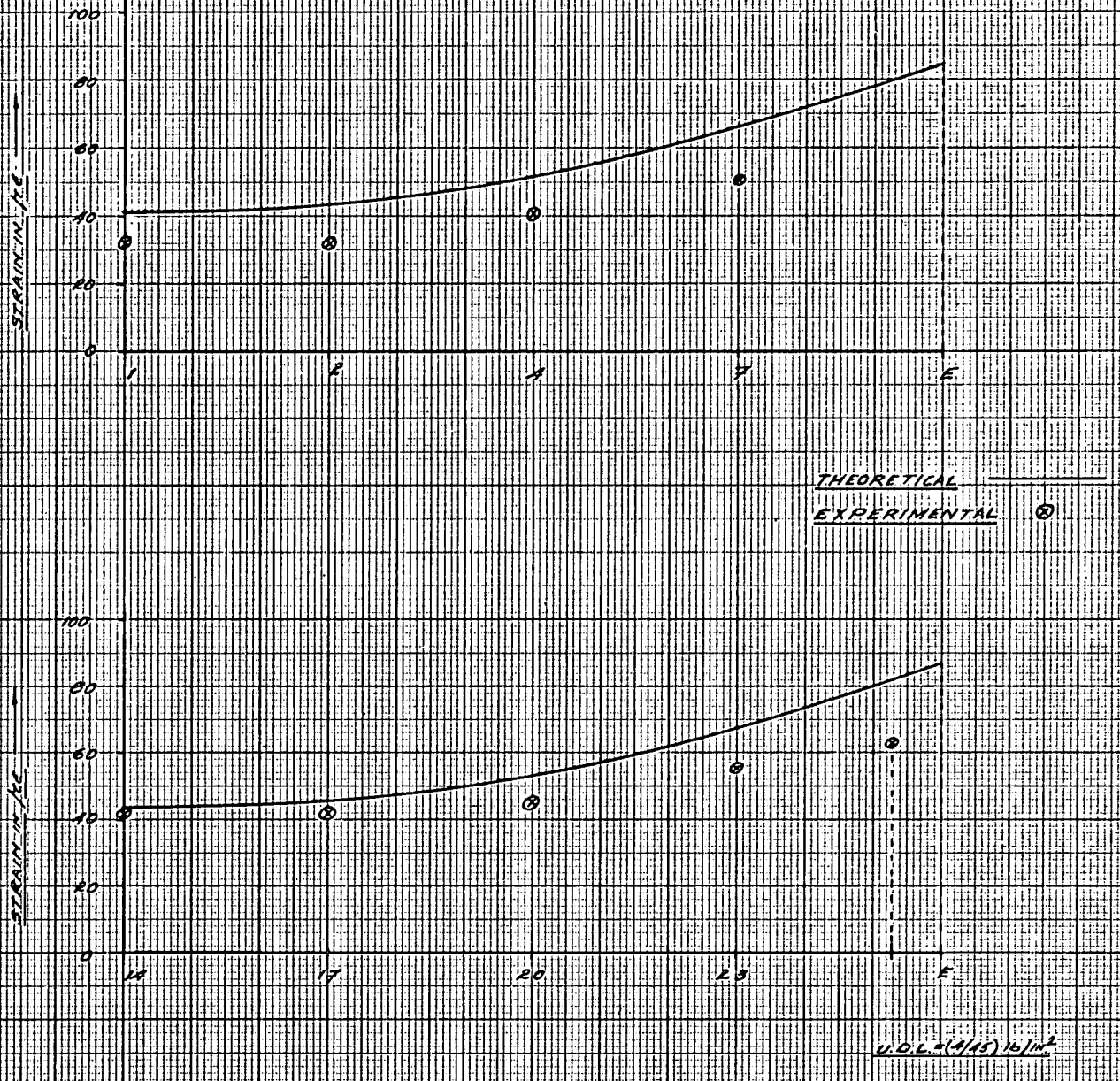

COMPARISON OF STRAINS

PERSPEX SHELL

FIGURE: 5-15.

shear connectors between the walls and the edge beams. A shuttering to give the required profile of the shell was built using plywood which can be seen in Plate (5-14.) In order to facilitate the easy removal of the shuttering gaps between edges of the shuttering and the walls were kept. The edges of the shuttering were curved down to avoid sharp joints. The shuttering was supported on temporary brick pillars. Wooden wedges were used between the brick pillars and the shuttering to maintain the required level of the shuttering (Plate 5-15).

Rectangular grids were marked on the shuttering for alignment and also to guide the location of the plain hollow clay blocks to which the strain gauges were to be attached. Before starting the construction mould oil was applied to the shuttering and its level checked.

Bottom reinforcement was placed during the construction of the slab. The method of cementing the clay blocks together, is shown in Plate (5-14) where the bottom reinforcement along the transverse joints can also be seen. Half size blocks were used for staggering the longitudinal joints. After two days the top of the slab was brushed with a wire brush, and the joints were cleaned to prepare for top reinforcement. Plate (5-16) shows the shell before placing the top reinforcement and the longitudinal section of the shell at the edge. Top reinforcement was then placed and joints were filled with mortar.

Reinforced concrete edge beams 4½in x 6in deep were cast embedding 2in of the shell inside them. Vertical reinforcement bars were used as shear connectors between the edge beams and the walls. Proper care was taken for curing of shell and beams.

The mortar used was in the following proportions:

Cement - 300 gms.

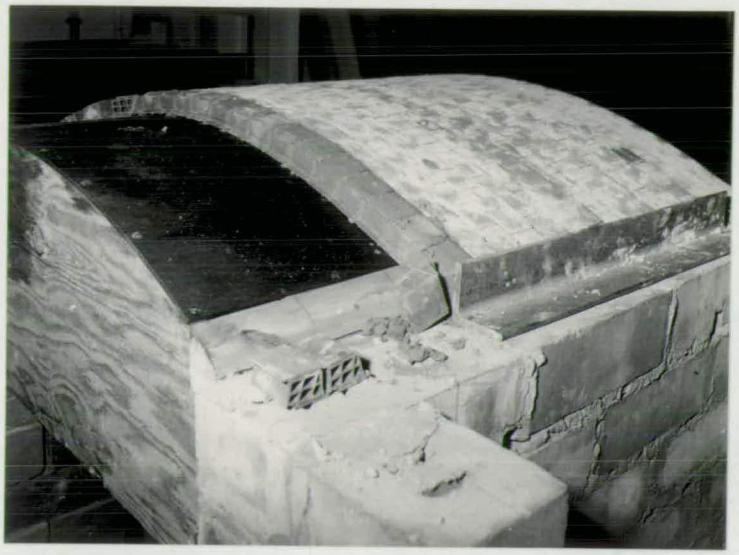

Plate: 5-14

Plate: 5-15

Plate: 5-16

Sand - 900 gms.

Water - 175 c.c.

Cement used was ferro-cement and sand was Leighton Buzzard No. 21.

Two ½in diam steel bars were used as tie bars between the walls. In order to avoid development of any initial stress in the shell due to tightening of the nuts of the tie bars the end plates were embedded in mortar beds, so that stresses were taken by the mortar beds, and thus leaving also no gap between the walls and the end plates. Plates (5-17 & 18)show general views of the finished shell with edge beams and tie bars.

5.3b Strain and Deflection Measurements

Electric resistance strain gauges of PL 10 and PC 10 types of 120 Ω having 10 mm gauge length were used for measuring strains. The surface of the plain blocks in the shell were rubbed with sand paper and cleaned with Acetone. The strain gauges were fixed with PS Cement as recommended by the manufacturer. The location of the gauges is shown in Figure (5-16). Nine PL 10 strain gauges were fixed on plain clay blocks with PS Cement to act as compensating gauges. The strain gauges were covered with polythene sheets to prevent the gauges from drift. For recording the strains a 10 Channel Westland Data Logger was used. A voltage of 5 volts was applied across the bridge.

The shell was built of clay blocks cemented together with mortar and thus due to the high strength of the blocks the strain on a block might not be the strain of the structure as a whole at that location. Strains recorded would be the local strains on the clay blocks. Therefore, it was decided to measure the deflection also. The deflection at any point would be the deflection of the structure as a whole at that point. Figure (5-17)

Plate: 5-17

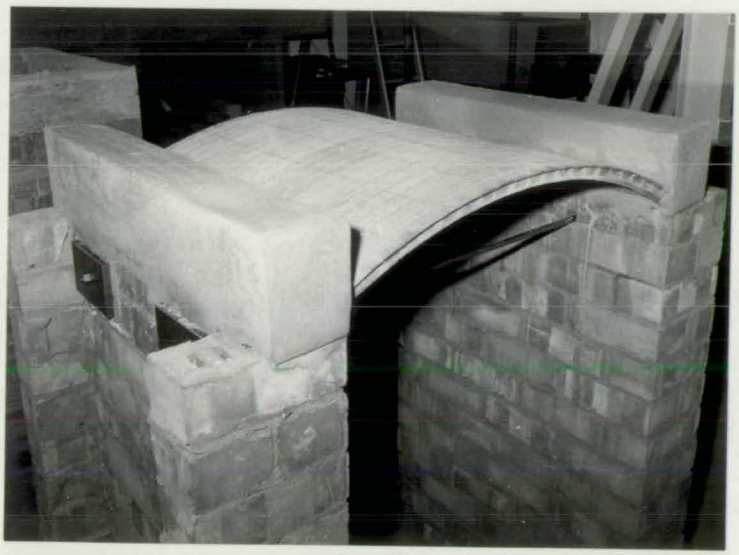

Plate: 5-18

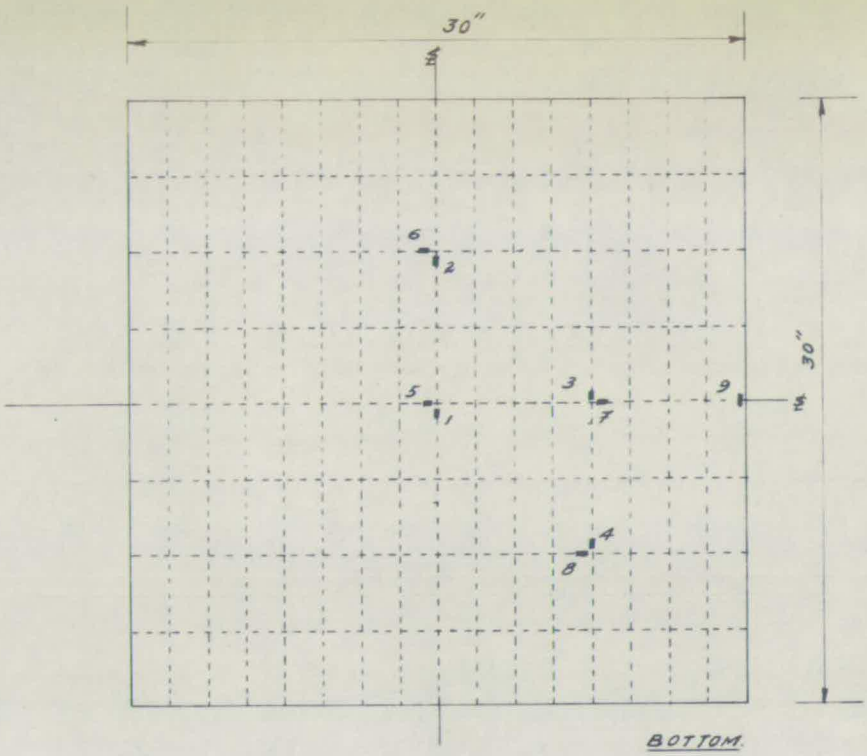

LOCATION OF STRAIN GAUGES.

FIGURE: 5-16.

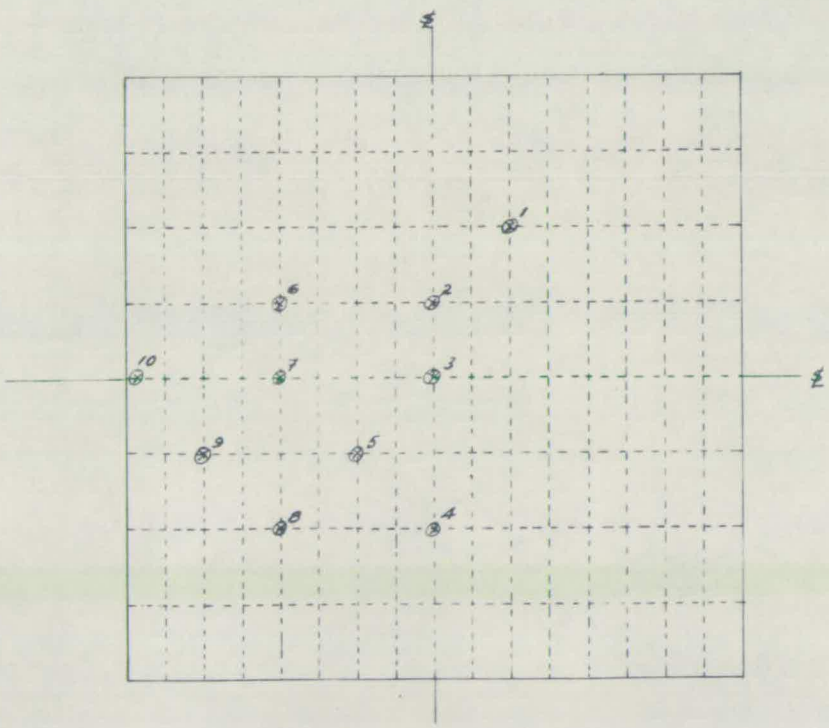

LOCATION OF DIAL GAUGES.

FIGURE: 5-17.

shows the location of the dial gauges and Plate (5-19) shows the arrangement of the dial gauges. During the test it was suspected that there were some horizontal movements of the edge beams along with the walls at the ends. Dial gauges were fixed to measure the horizontal movement (Plate 5-20). Indications of some movements were observed. To prevent horizontal movement of the edge-beams two adjustable sliding clamps were used across the ends of the shell clamping two edge-beams (not shown in Plates 5-20 & 21). Plate (5-21) shows the general arrangement of the test.

5.3c Testing Procedure:

Loads of 60 lbs at each stage and up to a maximum of 360 lbs distributed over the surface of the shell were applied. For the first two load stages lead weights and for remaining load stages bags filled with stone chips were used.

Before starting the experiment all the strain gauges were balanced. Initial readings of the dial gauges were recorded. Readings were taken twice at every load stage, once just after applying the loads and next one 20 minutes after applying the loads, to allow for creep. The test was repeated several times on subsequent days until all the readings were steady for most of the tests.

Unfortunately no reliable strain readings were obtained during the tests.

Deflections at different load intervals are plotted in Figure (5-18).

Table (5-7) and Figures (5-19 & 20) show the comparison between the theoretical and experimental results.

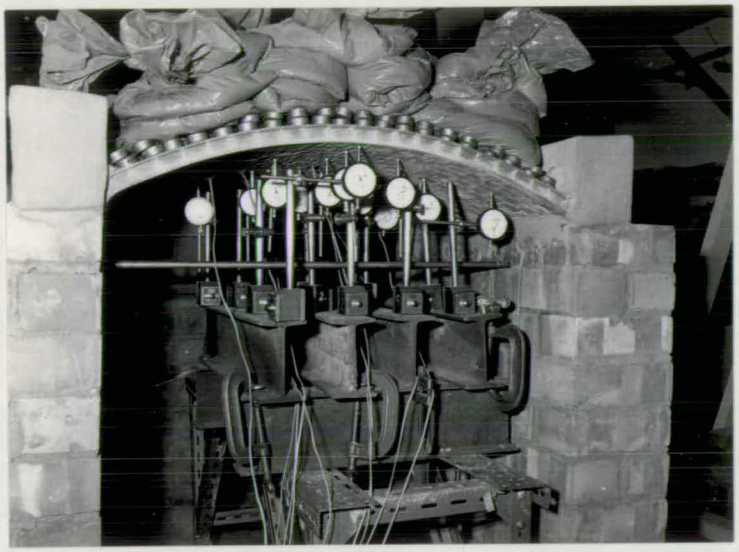

Plate: 5-19

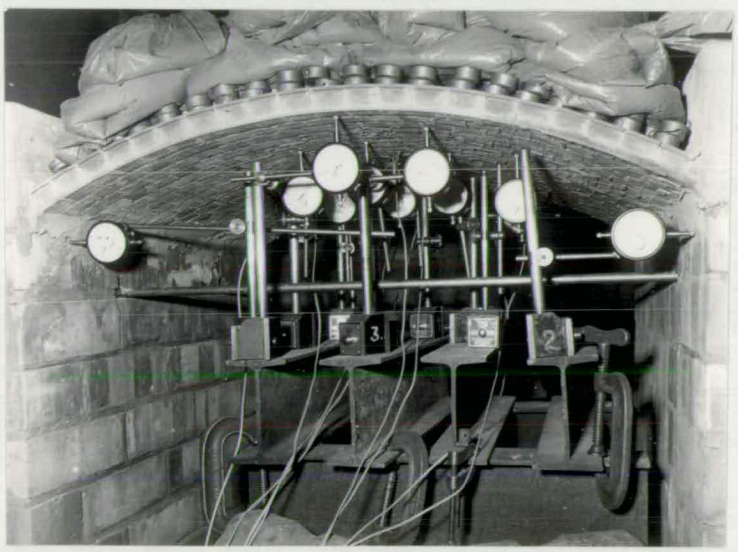

Plate: 5-20

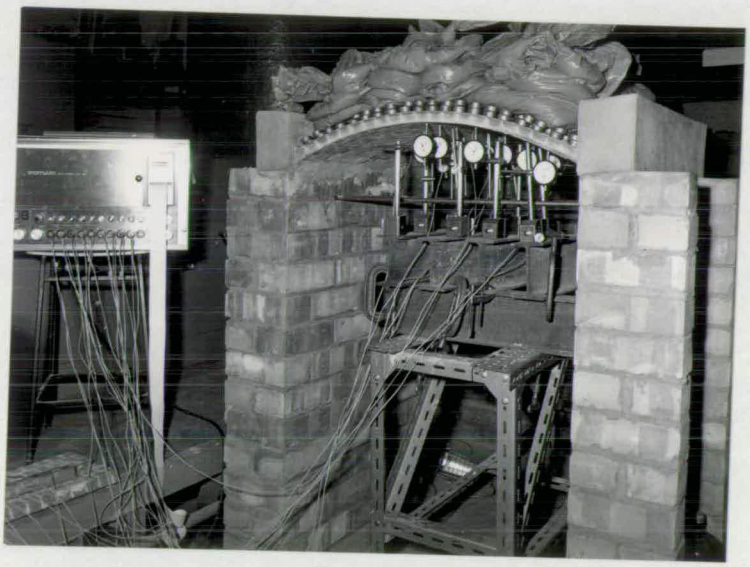

Plate: 5-21

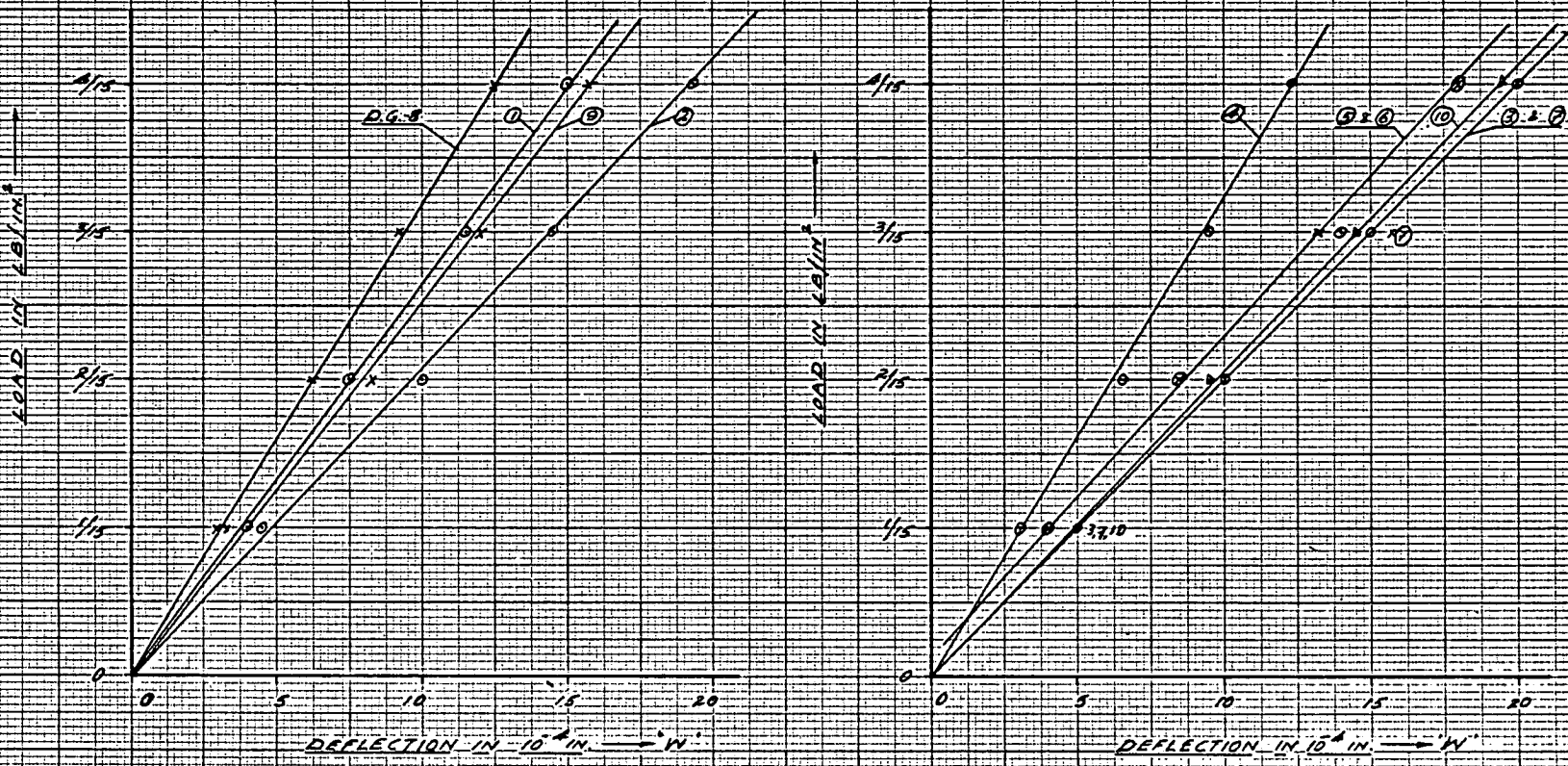
4/15
3/15
2/15
1/15
0
LOAD IN kg/mm²
D.G.-8
0
5
10
15
20
DEFLECTION IN 10⁻⁴ IN. → 'W'
LOAD IN kg/mm²
37.10
U.D.L.

FIGURE : 5-18.

CYLINDRICAL SHELL BUILT OF HOLLOW CLAY BLOCKS:

FIXED AT EDGES AND FREE AT END-ARCHES

COMPARISON OF EXPERIMENTAL AND THEORETICAL RESULTS

T A B L E: 5-7 DEFLECTIONS (W)

Dial Gauge No.	Location of Dial Gauge (Mesh Point)	Deflections in 10^{-4} in.		Remarks
		Experimental (From Graph *)	Theoretical	Deviation from Theor. results
1	12	3.75	2.8	+34.0%
2	2	4.5	4.24	+ 5.8%
3	1	5.0	4.8	+ 4.2%
4	4	3.0	2.8	+ 7.1%
5	9	4.0	4.24	- 5.7%
6	17	4.0	4.24	- 5.7%
7	14	5.0	4.8	+ 4.2%
8	20	3.1	2.8	+10.7%
9	25	4.0	4.24	- 5.7%
10	30	4.9	4.8	+ 2.1%

* Load Intensity (Uniformly Distributed) = (1/15) lb/in.^{2}

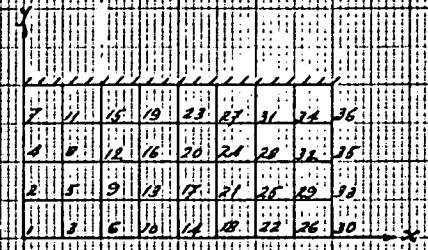

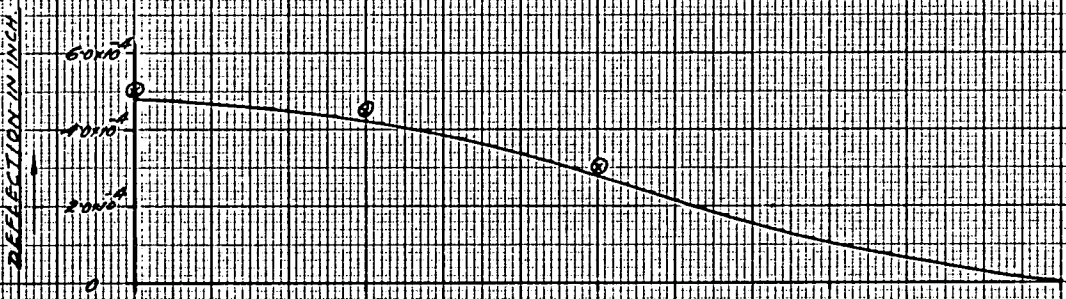

THEORETICAL ——

EXPERIMENTAL ⊗

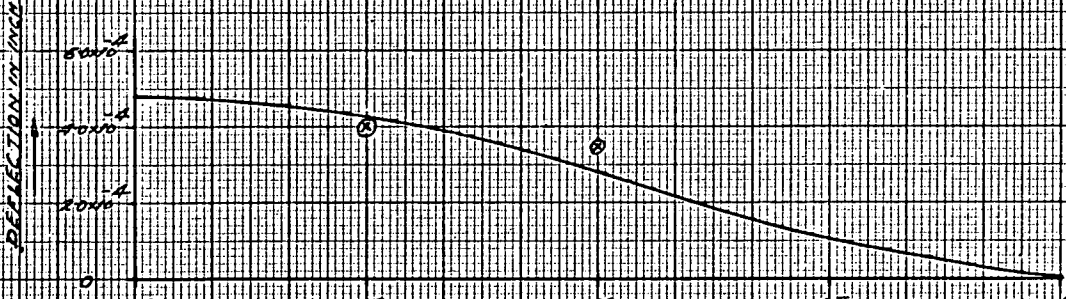

LOAD = 1/15 lb/sq.in.

COMPARISON OF DEFLECTIONS: W

SHELL BUILT OF HOLLOW CLAY BLOCKS

FIGURE : 5-19

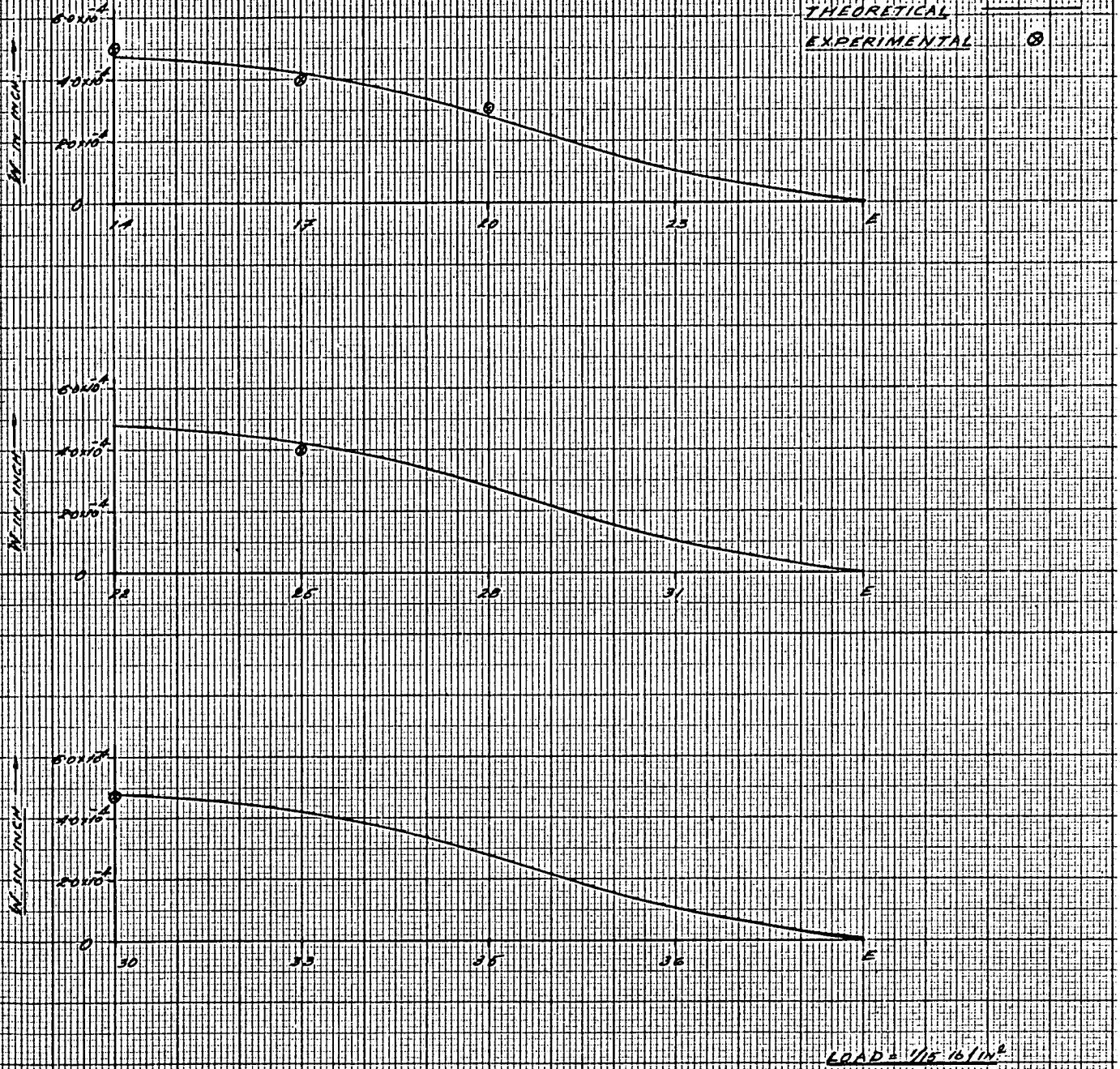

COMPARISON OF DEFLECTIONS

SHELL BUILT OF HOLLOW CLAY BLOCKS

FIGURE : 5-20

5.4 EI VALUE OF CURVED BEAM OF PERSPEX

While calculating the deflections, moments and stresses for a cylindrical shell of perspex in Chapter 4 a value of Young's Modulus was taken as 4.2×10^5 lb/in^2 as specified by the manufacturer. But the test results showed higher values of deflections, moments and stresses. It was therefore suspected that EI value of the model shell might not be the same as specified. So in order to find out the practical EI value two transverse strips each 3 inches wide were cut from the model shell. These were tested as simply supported beams and deflections were measured (Plate 5-22 and Figure 5-21). EI value was calculated from the expression:

$$EI = (WR^2/\delta)(R((\theta_A/2)(1 + 2\sin^2\theta_A) + \tfrac{1}{2}\sin\theta_A\ (3\cos\theta - 4)) - x\ (\theta_A\sin\theta_A + \cos\theta_A - 1))$$

Derivation of the expression together with notation is included in Appendix 5-1.

The practical EI value was found as 4.7×10^2 lb.in^2 against a theoretical value of 1.68×10^3 lb.in^2.

Therefore to compare the theoretical and experimental results it was necessary to use a correction factor to allow for the difference in the EI values.

5.5 EI VALUE OF CURVED BEAM OF HOLLOW BLOCKS

Similarly in the case of a cylindrical shell of clay blocks the experimental results showed higher values of deflections compared to the theoretical values which were calculated on the basis of the value of EI obtained in Part 2 of Chapter 2. In order to determine the practical EI value two curved

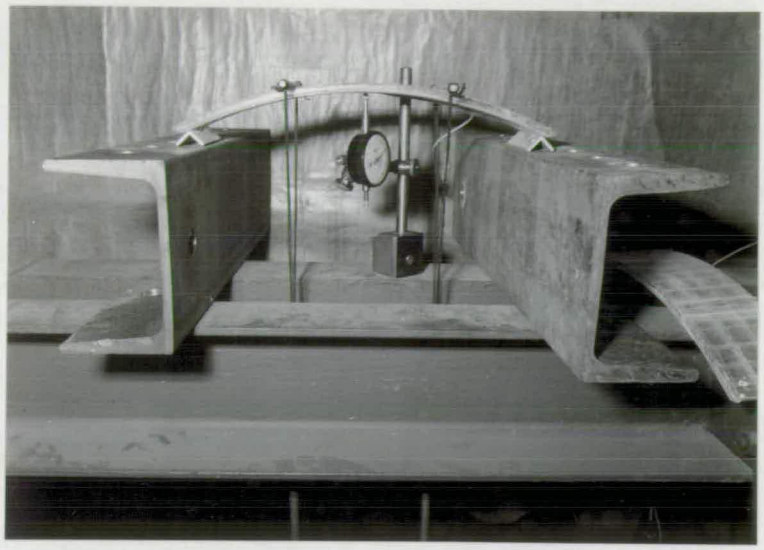

Plate: 5-22

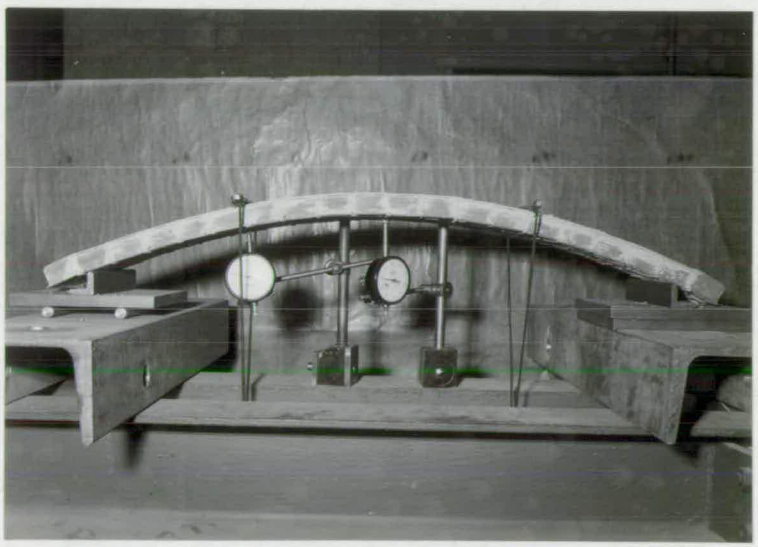

Plate: 5-23

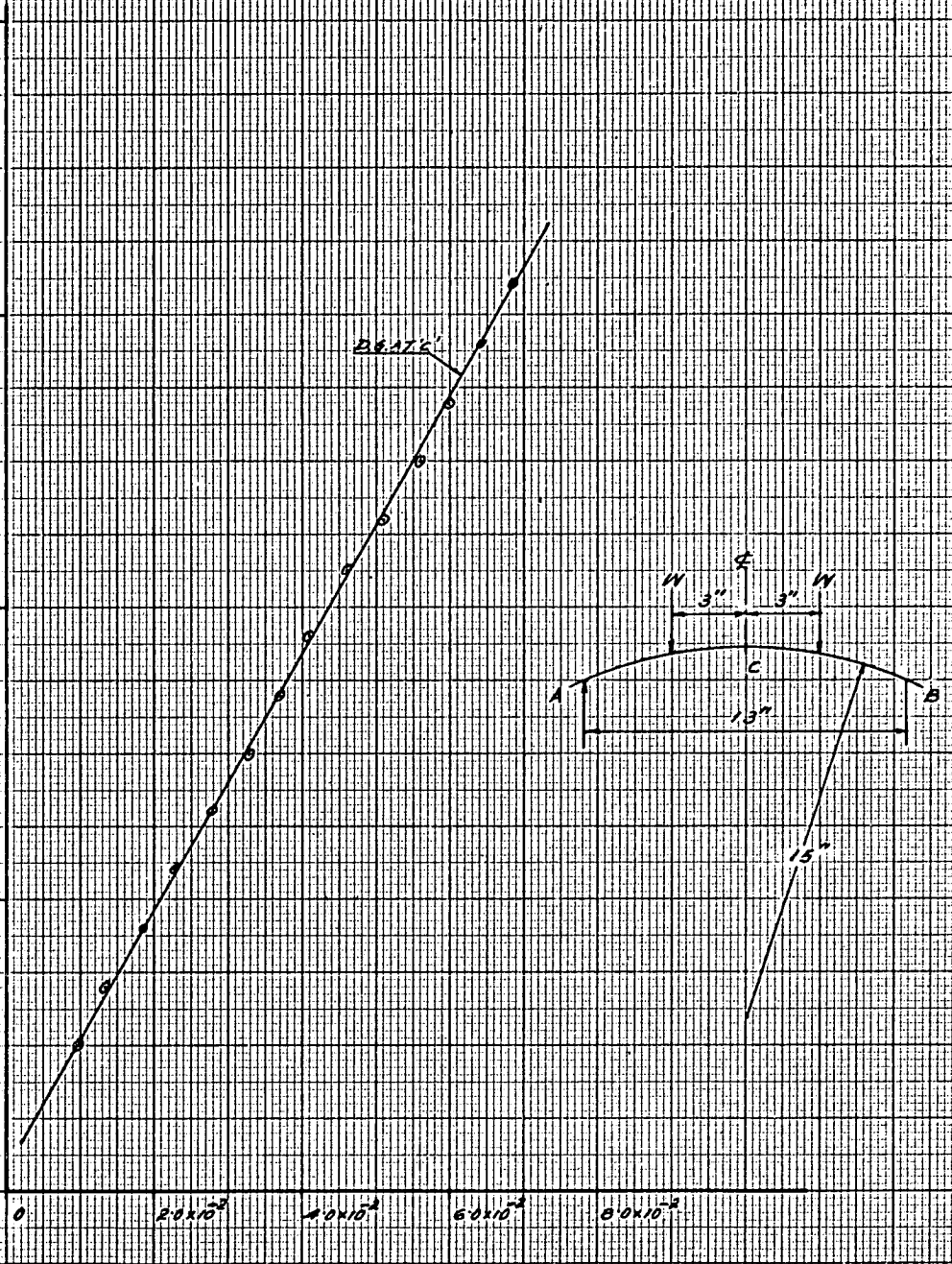

CURVED BEAM OF PERSPEX

FIGURE: 5-21.

beams of clay blocks each 4 inches wide and with a radius of 30 inches similar to the shell, were built. These were also tested as simply supported beams subject to two concentrated loads and the deflections were measured (Plate 5-23 and Figure 5-22).

The Practical EI value was found as 7.1×10^4 lb.in^2

5.6 CONCLUSIONS

5.6 A. PERSPEX SHELL

The comparison of the values of deflections and strains obtained by the theoretical calculations and by experiments are in close agreement. The discrepancies are higher near the boundaries which may be due to the introduction of the fictitious values in the theoretical calculation and due to the possible faults in the supports used during the experiments.

The variation of rigidities at different sections of the shell due to cementing of the strips, workmanship and method of loading may also be the the sources of errors in the experimental results. The discrepancies between the results obtained by the dial gauges and the strain gauges may be due to the fact that a strain gauge indicates the local strain of the perspex strip to which it is fixed whereas a dial gauge shows the deflection of the structure as a whole at that point taking the effect of cementing into account.

During the tests due to the change of room temperature considerable variation in deflections and strains were observed. Although precautions were taken to reduce these variations it would be impossible to avoid all the effects.

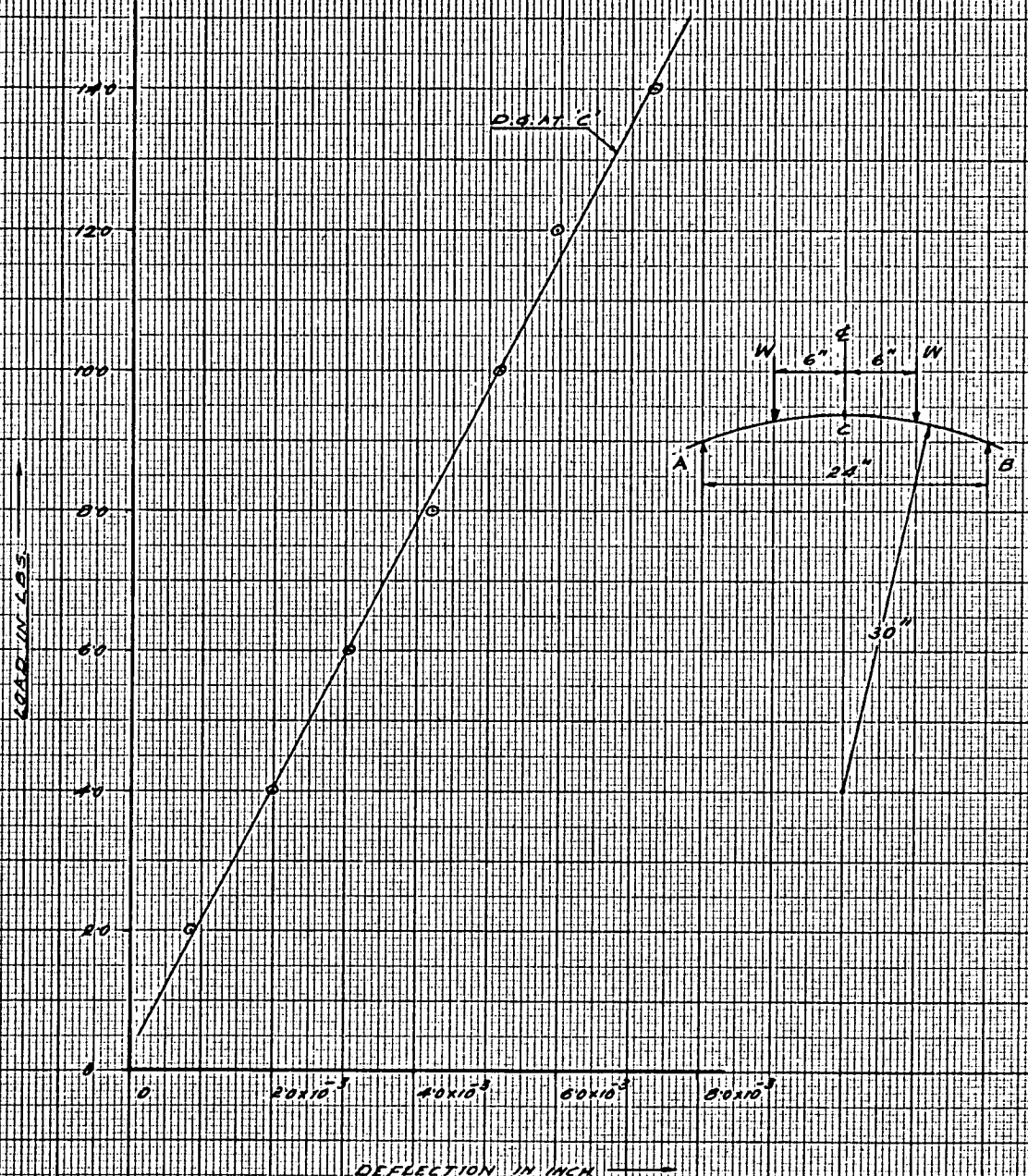

CURVED BEAM OF CLAY BLOCKS

FIGURE: 5-22

5.6 B. SHELL BUILT OF HOLLOW CLAY BLOCKS

The comparison of the values of deflections obtained by the theoretical calculations and by experiments show close agreement. As in the previous cases, here also, discrepancies are higher near the boundaries which are due to the reasons mentioned before.

In addition, the discrepancies might be due to (1) Workmanship, (2) Support conditions (3) Method of loading and (4) Possible change in temperature.

5.6 C. It has been shown that the theoretical results for the shells of hollow cross section are in good agreement with the experimental results for the models tested. It would have been interesting to compare the results obtained from full scale tests but the author was unable to find any published results for comparison.

A P P E N D I X 5-1

EXPRESSION FOR EI VALUE OF A CURVED BEAM

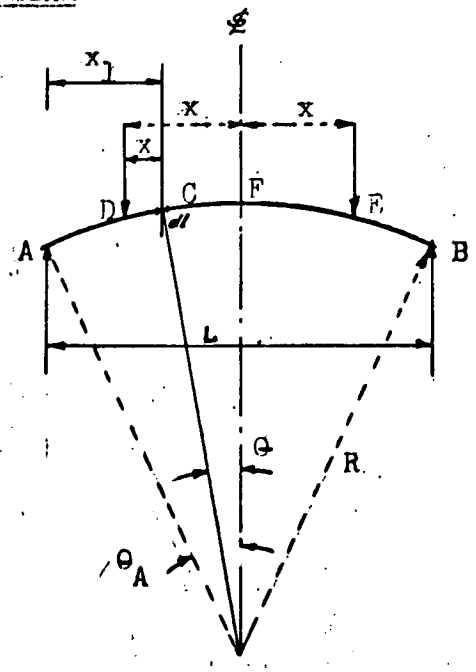

$$M_F = W(x_1 - x)$$

$$d\ell = Rd\theta$$

$$x_1 = R(\sin\theta_A - \sin\theta)$$

$$\text{Deflection } \delta = \int_A^F W(x_1 - x)x_1 Rd\theta/EI$$

at F

$$= (W/EI)\int_A^{\theta_A} (x_1^2 - xx_1)Rd\theta$$

$$= (WR/EI)\int_A^{\theta_A} (R^2(\sin\theta_A - \sin\theta^2) - xR(\sin\theta_A - \sin\theta))d\theta$$

$$= (WR^2/EI)\int_A^{\theta_A} (R^2(\sin\theta_A - \sin\theta)^2 - x(\sin\theta_A - \sin\theta))d\theta$$

$$= (WR^2/EI)(R(\theta_A\sin^2\theta_A + 2\sin\theta_A(\cos\theta_A - 1) + \theta_A/2 - \sin2\theta_A/4) - x(\theta_A\sin\theta_A + \cos\theta_A - 1))$$

$$= (WR^2/EI)(R(\theta_A/2(1 + 2\sin^2\theta_A) + \tfrac{1}{2}\sin\theta_A(3\cos\theta - 4)) - x(\theta_A\sin\theta_A + \cos\theta_A - 1))$$

$$\therefore \quad EI = (WR^2/\delta)(R(\theta_A/2(1 + 2\sin^2\theta_A) + \tfrac{1}{2}\sin\theta_A(3\cos\theta - 4)) - x(\theta_A\sin\theta_A + \cos\theta_A - 1))$$

CHAPTER 6

THEORY FOR DOUBLY CURVED SHELLS OF HOLLOW CROSS SECTION

6.1 INTRODUCTION

Initially the analysis of doubly curved shells were based on membrane theories where bending effects were neglected, but recently more attention has been given to consider the bending effects. Such theories, allowing for the effects of bending, are usually termed general or bending theories.

As for cylindrical shells in the case of doubly curved shells during the derivation of the theories different authors make different assumptions. However, most of the authors assume the shell as a shallow one.

Munro (33) has developed a general heterogeneous equation for doubly curved thin shallow shell. He discusses the equations derived by Vlasov, Goldenviezer and Lurye, Nazarov, Ambartsumyan, Flügge and Conrad, Katchaturyan, Mishonov, Bouma, Bleich and Salvadori. He also co-relates some of the above equations with the equation developed by him.

In this chapter a general approach is made and three equations of equilibrium in terms of the three displacements U, V and W are developed. From these equations expressions for some important particular cases viz. Plate, Cylindrical and Hyperbolic - Paraboloid shells are derived.

6.2 DEVELOPMENT OF THEORY OF DOUBLY CURVED SHELLS OF HOLLOW CROSS SECTION

The following are the assumptions made to develop the theory for a thin doubly curved shell of hollow cross section:

1. The shell is shallow and $\partial z/\partial x$, $\partial z/\partial y$ are negligible compared to unity.
2. Plane sections normal to the middle surface remain plane during the process of deformation and remain normal to it.
3. Normal stresses on planes parallel to the middle surface are neglected in comparison with other stresses.

In order to develop the theory a similar procedure (viz. obtaining relationships connecting strains, stresses, forces and moments and use of the equilibrium equations) as for the case of a cylindrical shell is used and three partial differential equations connecting the three displacements of the middle surface and external forces are obtained.

Strain-Displacement Equations

Figures (6-1 & 2.) show a typical element of a doubly curved shell and longitudinal and transverse sections of such an element.

From Figure (6-2):

$$U_p = (1 - z/R_x)U - z(\partial W/\partial x) \qquad (6.1.1)$$

$$V_p = (1 - z/R_y)V - z(\partial W/\partial y) \qquad (6.1.2)$$

$$W_p = W \qquad (6.1.3)$$

where U_p, V_p and W_p are the displacements of a surface parallel to the middle surface.

Again,

$$\epsilon_x = \partial U_p/\partial x - W_p/R_x \qquad (6.2.1)$$

$$\epsilon_y = \partial V_p/\partial y - W_p/R_y \qquad (6.2.2)$$

$$\gamma_{xy} = \partial V_p/\partial x + \partial U_p/\partial y - 2W_p/R_{xy} \qquad (6.2.3)$$

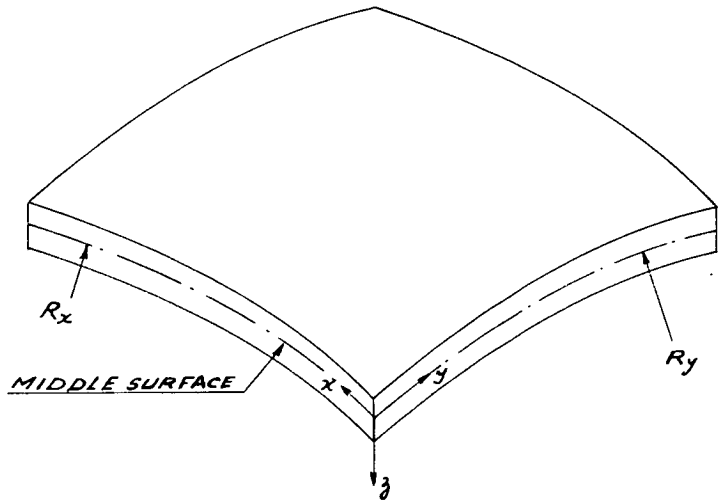

FIGURE: 6-1

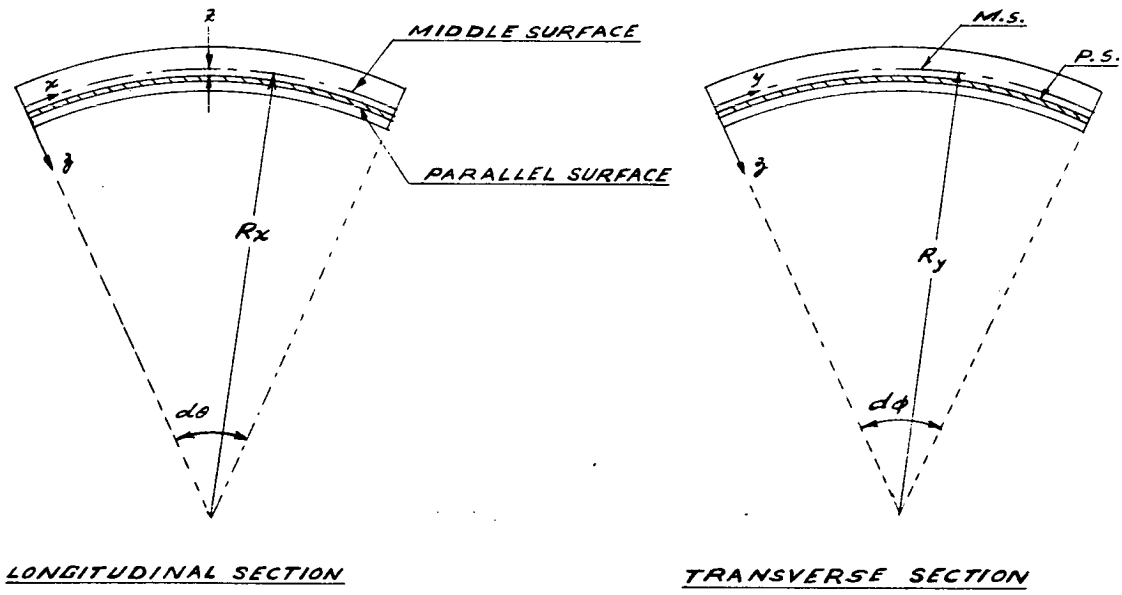

FIGURE: 6-2

From the equations (6.1.1 to 6.1.3) and (6.2.1 to 6.2.3) and neglecting the second order terms, the strain expressions:

$$\epsilon_x = \partial U/\partial x - z(\partial^2 W/\partial x^2) - W/R_x \qquad (6.3.1)$$

$$\epsilon_y = \partial V/\partial y - z(\partial^2 W/\partial y^2) - W/R_y \qquad (6.3.2)$$

$$\gamma_{xy} = \partial U/\partial y + \partial V/\partial x - 2z(\partial^2 W/\partial x \partial y) - 2W/R_{xy} \qquad (6.3.3)$$

Using Hooke's Law and assumption (3) i.e. $\sigma_z = 0$:

For Slabs,

$$\sigma_x = (E/(1-\mu^2))(\epsilon_x + \mu\epsilon_y) \qquad (6.4.1)$$

$$\sigma_y = (E/(1-\mu^2))(\epsilon_y + \mu\epsilon_x) \qquad (6.4.2)$$

$$T_{xy} = T_{yx} = G\gamma_{xy} \qquad (6.4.3)$$

where $G = E/2(1+\mu)$

For Ribs,

$$\sigma_x = E\epsilon_x \qquad (6.4.4)$$

$$\sigma_y = E\epsilon_y \qquad (6.4.5)$$

Considering a section y = constant let b_1 be the length of periodic, repetition of the shaded part and b' be the width of the rib and similarly b_2 and b" for the section x = constant (Figures 6-3 & 4). N_x, N_y, N_{xy}, M_x, M_y and M_{xy} are the integrals of the normal stresses over the combined cross sections of the slabs and the rib. In order to distinguish them, notation 's' for slabs and 'r' for rib to the lower end of the integral sign are used. Therefore:

$$N_x = \int_s \sigma_x\, dz + \int_r \sigma_x(b''/b_2)\, dz \qquad (6.5.1)$$

$$N_y = \int_s \sigma_y\, dz + \int_r \sigma_y(b'/b_1)\, dz \qquad (6.5.2)$$

$$N_{xy} = \int_s T_{xy}\, dz \qquad (6.5.3)$$

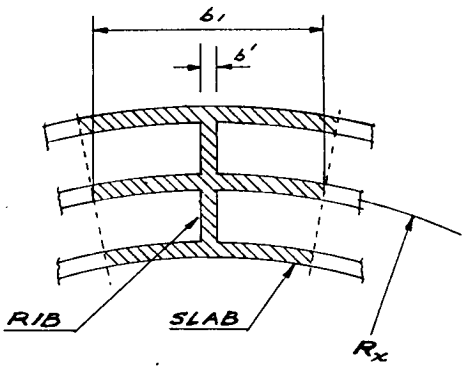

FIGURE: 6-3.

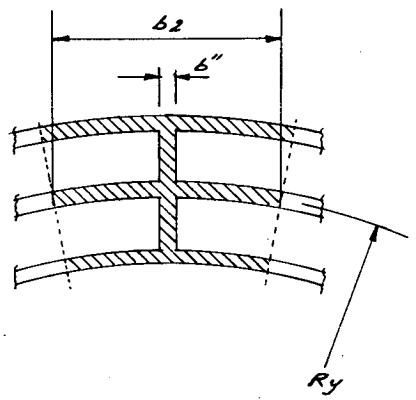

FIGURE: 6-4.

$$M_x = \int_s \sigma_x \, z \, dz + \int_r \sigma_x (b''/b_2) \, z \, dz \qquad (6.5.4)$$

$$M_y = \int_s \sigma_y \, z \, dz + \int_r \sigma_y (b'/b_1) \, z \, dz \qquad (6.5.5)$$

$$M_{xy} = M_{yx} = \int_s T_{xy} \, z \, dz \qquad (6.5.6)$$

It is to be noted that there will be no shear stress T_{xy} or T_{yx} in the cross section of the ribs and all the tangential shear will be carried by the slabs only.

Using the equations (6.3.1 to 6.3.3), (6.4.1 to 6.4.5) and (6.5.1 to 6.5.6) the expressions for forces and moments of the middle surface displacements are as follows:

$$N_x = D_x(\partial U/\partial x - W/R_x) + \mu D(\partial V/\partial y - W/R_y) - S_x(\partial^2 W/\partial x^2) - \mu S(\partial^2 W/\partial y^2) \qquad (6.6.1)$$

$$N_y = D_y(\partial V/\partial y - W/R_y) + \mu D(\partial U/\partial x - W/R_x) - S_y(\partial^2 W/\partial y^2) - \mu S(\partial^2 W/\partial x^2) \qquad (6.6.2)$$

$$N_{xy} = N_{yx} = \frac{D}{2}(1-\mu)(\partial U/\partial y + \partial V/\partial x - 2W/R_{xy}) - S(1-\mu)(\partial^2 W/\partial x \partial y) \qquad (6.6.3)$$

$$M_x = S_x(\partial U/\partial x - W/R_x) + \mu S(\partial V/\partial y - W/R_y) - K_x(\partial^2 W/\partial x^2) - \mu K(\partial^2 W/\partial y^2) \qquad (6.6.4)$$

$$M_y = S_y(\partial V/\partial y - W/R_y) + \mu S(\partial U/\partial x - W/R_x) - K_y(\partial^2 W/\partial y^2) - \mu K(\partial^2 W/\partial x^2) \qquad (6.6.5)$$

$$M_{xy} = M_{yx} = \frac{S}{2}(1-\mu)(\partial U/\partial y + \partial V/\partial x - 2W/R_{xy}) - K(1-\mu)(\partial^2 W/\partial x \partial y) \qquad (6.6.6)$$

where D, D_x and D_y are the extensional rigidities; S, S_x and S_y are the rigidity of moments; and K, K_x and K_y are the bending rigidities. These have already been defined in Chapter 3.

Assuming a symmetrical section of shell element the rigidity moments S, S_x and S_y become zero. Therefore force and moment expression reduce to:

$$N_x = D_x(\partial U/\partial x - W/R_x) + \mu D(\partial V/\partial y - W/R_y) \quad (6.7.1)$$

$$N_y = D_y(\partial V/\partial y - W/R_y) + \mu D(\partial U/\partial x - W/R_x) \quad (6.7.2)$$

$$N_{xy} = N_{yx} = \frac{D}{2}(1-\mu)(\partial U/\partial y + \partial V/\partial x - 2W/R_{xy}) \quad (6.7.3)$$

$$M_x = -(K_x(\partial^2 W/\partial x^2) + \mu K(\partial^2 W/\partial y^2)) \quad (6.7.4)$$

$$M_y = -(K_y(\partial^2 W/\partial y^2) + \mu K(\partial^2 W/\partial x^2)) \quad (6.7.5)$$

$$M_{xy} = M_{yx} = -K(1-\mu)(\partial^2 W/\partial x \partial y) \quad (6.7.6)$$

Equations of Equilibrium can be written down by inspection from Figures (6-5 & 6) as follows:

Equilibrium of Forces

In the x-direction, $\partial/\partial x(N_x) + \partial/\partial y(N_{yx}) + P_x = 0$ (6.8.1)

In the y-direction, $\partial/\partial y(N_y) + \partial/\partial x(N_{xy}) + P_y = 0$ (6.8.2)

In the z-direction, $\partial/\partial x(Q_x) + \partial/\partial y(Q_y) + N_x/R_x + N_y/R_y + 2N_{xy}/R_{xy} + P_z = 0$ (6.8.3)

Equilibrium of Moments

About the x-axis, $\partial/\partial y(M_y) + \partial/\partial x(M_{xy}) - Q_y = 0$ (6.9.1)

About the y-axis, $\partial/\partial x(M_x) + \partial/\partial y(M_{yx}) - Q_x = 0$ (6.9.2)

From the equations (6.9.1 and 6.9.2) values of Q_x and Q_y can be obtained in terms of M_x, M_y and M_{xy} and substituted in the equation (6.8.3). Replacing N_x, N_y, N_{xy}, M_x, M_y and M_{xy} in the equations (6.8.1 to 6.8.3) by the displacement expressions from the equations (6.7.1 to 6.7.6), the equations of equilibrium take the following form:

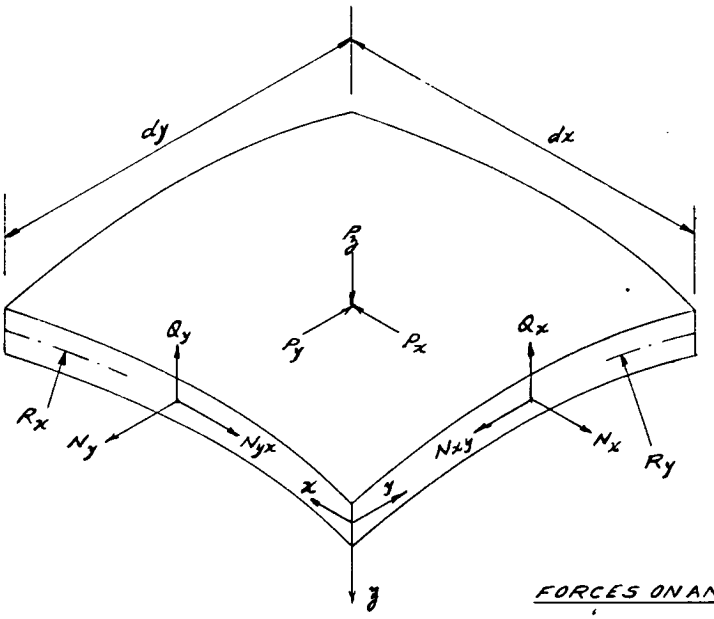

FORCES ON AN ELEMENT.

FIGURE : 6-5.

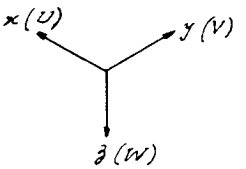

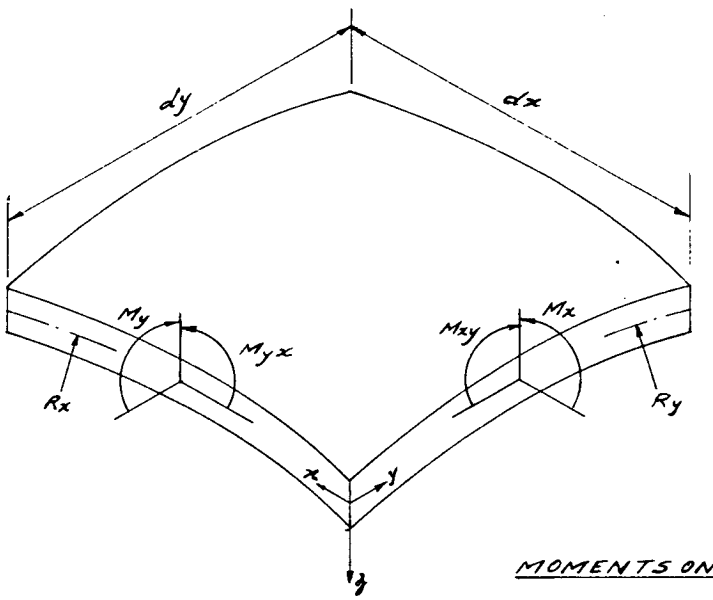

MOMENTS ON AN ELEMENT.

FIGURE : 6-6

$$D_x(\partial^2U/\partial x^2) - (D_x/R_x + \mu D/R_y)(\partial W/\partial x) + \frac{D}{2}(1+\mu)(\partial^2V/\partial x\partial y)$$
$$-(D/R_{xy})(1-\mu)(\partial W/\partial y) + \frac{D}{2}(1-\mu)(\partial^2U/\partial y^2)$$
$$+ P_x = 0 \qquad (6.10.1)$$

$$\frac{D}{2}(1-\mu)(\partial^2V/\partial x^2) - (D/R_{xy})(1-\mu)(\partial W/\partial x) + \frac{D}{2}(1+\mu)(\partial^2U/\partial x\partial y)$$
$$- (D_y/R_y + \mu D/R_x)(\partial W/\partial y) + D_y(\partial^2V/\partial y^2)$$
$$+ P_y = 0 \qquad (6.10.2)$$

$$(D_x/R_x + \mu D/R_y)(\partial U/\partial x) + (D/R_{xy})(1+\mu)(\partial V/\partial x)$$
$$+ (D_y/R_y + \mu D/R_x)(\partial V/\partial y) + (D/R_{xy})(1-\mu)(\partial U/\partial y)$$
$$- (D_x/R_x^2 + 2\mu D/R_xR_y + (2D/R_{xy}^2)(1-\mu) + D_y/R_y^2)W$$
$$- K_x(\partial^4W/\partial x^4) - 2K(\partial^4W/\partial x^2\partial y^2) - K_y(\partial^4W/\partial y^4)$$
$$+ P_z = 0 \qquad (6.10.3)$$

These are the three basic equations of equilibrium in terms of the three displacements U, V and W for a thin shallow doubly curved shell of hollow cross section.

6.3 SOME PARTICULAR CASES

From the above basic displacement equations expressions for some important particular cases can be derived.

6.4 Flat Plate Under Pure Bending

In such case,

$$1/R_x = 1/R_y = 1/R_{xy} = 0$$

Therefore the equations (6.10.1 and 6.10.2) vanish and only the equation (6.10.3) exists in the form:

$$-(K_x(\partial^4W/\partial x^4) + 2K(\partial^4W/\partial x^2\partial y^2) + K_y(\partial^4W/\partial y^4)) + P_z = 0 \qquad (6.11.1)$$

6.5 Cylindrical Shell

In this case, (Figure 6- 7 .),

$$1/R_x = 1/R_{xy} = 0$$

and $$1/R_y = 1/R$$

The equations (6.10.1 to 6.10.3) reduce to:

$$D_x(\partial^2 U/\partial x^2) - (\mu D/R)(\partial W/\partial x) + \frac{D}{2}(1+\mu)(\partial^2 V/\partial x \partial y) + \frac{D}{2}(1-\mu)(\partial^2 U/\partial y^2) + P_x = 0 \qquad (6.12.1)$$

$$\frac{D}{2}(1-\mu)(\partial^2 V/\partial x^2) + \frac{D}{2}(1+\mu)(\partial^2 U/\partial x \partial y) - (D_y/R)(\partial W/\partial y) + D_y(\partial^2 V/\partial y^2) + P_y = 0 \qquad (6.12.2)$$

$$(\mu D/R)(\partial U/\partial x) + (D_y/R)(\partial V/\partial y) - (D_y/R^2)W - K_x(\partial^4 W/\partial x^4) - 2K(\partial^4 W/\partial x^2 \partial y^2) - K_y(\partial^4 W/\partial y^4) + P_z = 0 \qquad (6.12.3)$$

6.6 Hyperbolic Paraboloid Shell

For the hyperbolic paraboloid shell (Figure 6- 8), the equation to the middle surface is of the form:

$$z = C_{xy}$$

and $$1/R_x = 1/R_y = 0$$

$$1/R_{xy} = C = 1/k \qquad \text{where } C = c/(l.m)$$

The displacement equations take the form:

$$D_x(\partial^2 U/\partial x^2) + \frac{D}{2}(1+\mu)(\partial^2 V/\partial x \partial y) - \frac{D}{k}(1-\mu)(\partial W/\partial y) + \frac{D}{2}(1-\mu)(\partial^2 U/\partial y^2) + P_x = 0 \qquad (6.13.1)$$

$$\frac{D}{2}(1-\mu)(\partial^2 V/\partial x^2) - \frac{D}{k}(1-\mu)(\partial W/\partial x) + \frac{D}{2}(1+\mu)(\partial^2 U/\partial x \partial y) + D_y(\partial^2 V/\partial y^2) + P_y = 0 \qquad (6.13.2)$$

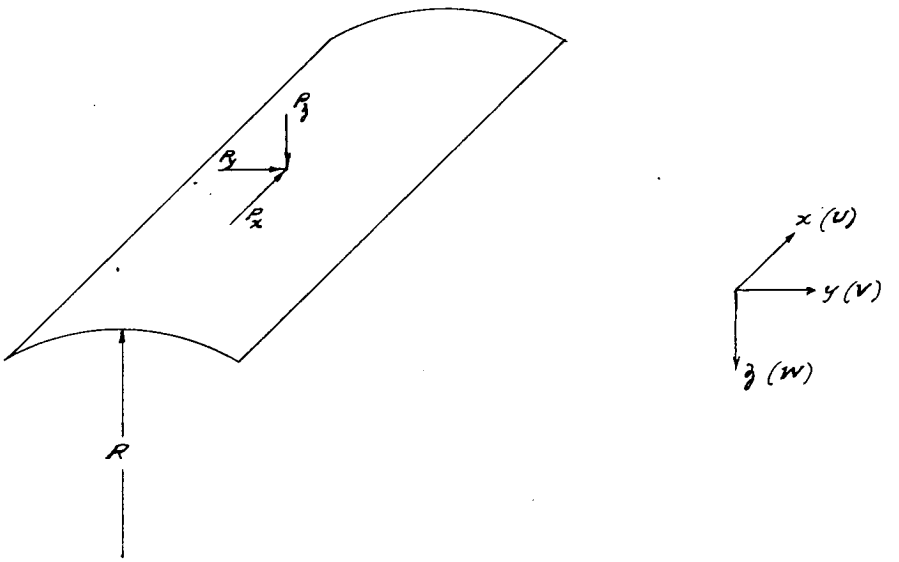

FIGURE : 6-7.

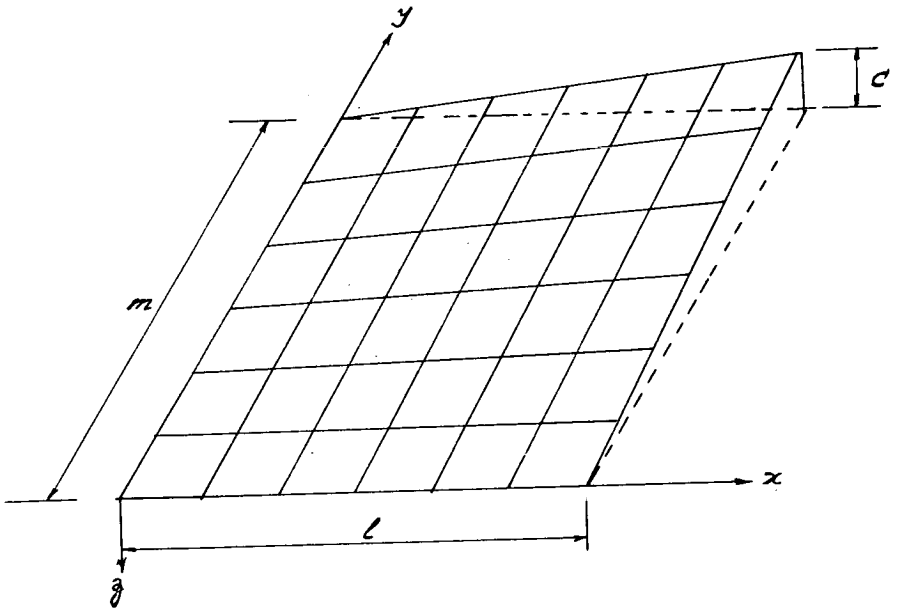

FIGURE : 6-8.

$$\frac{D}{k}(1-\mu)(\partial V/\partial x + \partial U/\partial y - 2W/k) - (K_x(\partial^4 W/\partial x^4) + 2K(\partial^4 W/\partial x^2 \partial y^2) + K_y(\partial^4 W/\partial y^4)) + P_z = 0 \quad (6.13.3)$$

CHAPTER 7

CONCLUSIONS

7.1 CONCLUSIONS

The main object of this project was to investigate the possibilities of the application of elastic theories to the plates and shells of hollow cross sections with special reference to the structures built of hollow clay blocks. With this in view the existing elastic equations have been modified so as to apply to structures of hollow cross section.

The structures considered are:

(a) Plates - modified equation (2.10.1) Page 11.

(b) Cylindrical shells - modified equations (3.12.1 to 3.12.3) Page 50.

(c) Doubly curved shells - modified equations (6.10.1 to 6.10.3) Page 110.

These equations are general and can be used for any cross section, including solid sections. In fact solid sections have been used to check the application of the equations.

1) The modified equation obtained for plates of hollow cross section was solved for various boundary conditions by the Finite Difference/Computer method. As a check, a simply supported plate was also solved by Navier's method and the results, compared with those obtained by the Finite Difference method, were in close agreement.

2) The experimental results obtained for plates under all the three boundary conditions were in close agreement with those obtained by the theoretical calculations. This justifies the validity of the modified equations for plates of hollow cross section.

3) The single eighth order differential equation (3.28.1), in terms of displacement W, developed in Chapter 3 was compared with the existing equation for a solid section by introducing appropriate data for a solid section (equations3.29.1 & 3.29.2). The modified equation was found to reduce to the standard shell equation.

4) The three partial differential equations in terms of displacements U, V and W (equations 3.12.1 to 3.12.3) developed in Chapter 3 were also checked by solving a particular shell of solid section and comparing with published results. Agreement was found to be close.

5) From the study of the influence of Poisson's ratio on the displacement values for a cylindrical shell, fixed at edges and at end-arches, it was observed that the increase in the value of Poisson's ratio decreases the values of V and W but on the other hand increases the U-values.

6) The comparison of the values of the displacements and the moments for shells of six different cross sections showed that these values decrease steadily with the increase in the distance between the slabs up to a certain limit beyond which the rate is lower.

7) The comparison of the values of deflections and strains obtained by the theoretical calculations and by the experiments for perspex cylindrical shell of hollow cross sections under various boundary conditions were in close agreements. The discrepancies were higher near the boundaries which might be due to the introduction of fictitious values in the theoretical calculations and also due to possible faults in the supports used in the tests.

The variation of rigidities at different cross sections of the shell due to cementing of the perspex strips, workmanship, method of loading and possible change of room temperature might be additional reasons for the discrepancies.

8) In the case of a shell built of hollow clay blocks the experimental results were in close agreement with the theoretical results. As for the perspex shell, here also, discrepancies are higher near the boundaries. The discrepancies might be due to the reasons as mentioned in (7).

9) Though the theoretical results for both the plates and the shells of hollow cross sections were in good agreement with the experimental results for the models tested it would have been interesting to compare the results obtained from full scale tests but the author was unable to find any published results for comparison.

7.2 FUTURE RESEARCH

1) In this thesis only a few special cases were considered both for theoretical and experimental works. Further research should be undertaken to examine the validity of the equations developed in this thesis for other boundary conditions.

2) In Chapter 6 three partial differential equations in terms of displacements U, V and W for a doubly curved shell have been developed. It would have been interesting to examine the validity, both theoretically and experimentally, of these equations for such a structure.

3) During the tests, due to the change of room temperature changes in the values of deflections and strains were observed. The effect of temperature

on such structures might form subjects of future research.

4) Not much information regarding the basic properties (e.g. Poisson's ratio, Young's Modulus etc.) of clay block structures are available. As these are the important factors on which the behaviour of a structure depends, the author feels that further research work is needed to determine the basic properties of such materials.

REFERENCES

1. Allen, D.N. de G. "Relaxation methods in engineering and science." McGraw-Hill. 1954.

2. Allen, D.N. de G. & Holman, J.M.L. "A mathematical analysis of the stress distribution in cylindrical concrete shell roofs." Proc. Inst. Civil Engineers, London, August 1962.

3. American Society of Civil Engineers. "Design of cylindrical concrete shell roofs." Manual of Engineering Practice No.31 1952.

4. Bennett, J.D. "The structural possibilities of hyperbolic paraboloids". Civil Engineering, Dec. 1961.

5. Bleich, H.H. & Salvadori, M.G. "Bending moments on shell boundaries". J. Structural Division. American Society of Civil Engineers. Oct.1959.

6. Bouma, A.L. "Some applications of the bending theory regarding doubly curved shells" - Int. Union of Theoretical & Applied Mechanics. Proc. Symp. on the Theory of thin elastic shells. Delft 1959.

7. Bouma, A.L. "On approximate methods of shell analysis : A general survey". Proc. of World.Conf. on Shell structures. San Francisco Oct. 1962.

8. **Bradshaw**, R.R. "A large span cellular shell". Proc. World Conf. on shell structures. San Francisco, Oct. 1962.

9. Candela, F. "Structural applications of hyperbolic paraboloidical shells". J. of the American Concrete Inst. Jan. 1955.

10. Chetty, S.M.K. & Tottenham, H. "An investigation into the bending analysis of hypar shell". Indian Conrete J. vol.38. 1964.

11. Dasgupta, N.C. "Edge problems in hyperbolic paraboloids". Ph.D. Thesis Dec. 1962. Univ. of Leeds.

12. Davies, S.R. "A study of arch dam analysis on the basis of thin shell theory. Ph.D. Thesis 1960. Univ. of Edinburgh.

13. Dieste, E. & Montanez, E.R. "Double-curvature shell of reinforced ceramic". Proc. of World Conf. on shell structures. San Francisco, Oct. 1962

14. Donnel, L. "Stability of thin-walled tubes under torsion". N.C.C.A. Rep. No. 479. 1933.

15. Erredibi "Il laterizio - Bollettino Tecnico Erredibi." Vol 1. to 5. R.D.B., Piacenza.

16. Erredibi "Manualetto Erredibi", Murature, Solai, Coperture Architravi Precompressi, Erredibi, Piacenza, 1962.

17. Esquillan, N. "Conception and construction of two recent shell structures". Proc. of World Conf. San Francisco, Oct. 1962.

18. Finsterwalder, U. "Die theorie der zylindrischen schalengeweble". (Theory of cylindrical shell roofs.) Proc. of the Int. Assoc. for Bridge & Structural Engineering 1932.

19. Flügge, W. "Stress in shells" Springer-Verlag, Berlin. 1960

20. Fulton, R.E. "Stresses in shallow roof shells of sandwich construction". Proc. of World Conf. San Francisco, Oct. 1962.

21. Gibson, J.E. "The design of cylindrical shell roof" 1961. E. &. F.N. Spon, Ltd., London.

22. Goldenveizer, A.L. "Theory of elastic thin shells" Pergamon Press, Oxford, 1961

23. Haas, A.M. "Theory and research in concrete shell design". J. of the Structural division. Proc. of the American Soc. of Civil Engineers.

24. Holand, I. "An application of Donnell's theory of circular cylindrical shells to the analysis of curved edge disturbances". Int. Assoc. of Bridge and struct. Engg. Publ. Vol. 19. Zürich 1959.

25. Holman, J.M.L. "The application of relaxation methods to the determination of stresses in concrete shell roofs." Ph.D. Thesis, June, 1956, Univ. of London.

26. Jenkins, R.S. "Theory and design of cylindrical shell structures," 1947, Ove Arup & Partners, London.

27. Jones, L.L. & Base, G.D. "Test on a one-twelfth scale model of the dome shell roof for Smithfield poultry market". Proc. Inst. Civ. Engrs. Vol. 30. Jan. 1965.

28. Klein, D. "Italiaanse en franse gewapende holle baksteen constructies door". 1955. Eng. Trans. by Butterworth, B.

29. Love, A.E.H. "Mathematical theory of elasticity". Dover, 1927.

30. Lundgren, H. "Cylindrical Shells" Vol.1. Danish Technical Press, Inst. of Danish Civ. Engineers. 1951.

31. McNamee, J.J. "Existing methods for the analysis of concrete shell roofs". Proc. Symp. on conrete shell roof construction 1953.

32. Mitchel, G.R. "Notes on the testing of reinforced concrete model shells". C.B.R.I. Symp. on shell structures. Indian Concrete J. Sp. shell No. Dec. 1959.

33. Munro, J. "The linear analysis of shallow shells". Proc. of Inst. Civil Engineers (London) July, 1961.

34. Munro, J. "Some tests on thin shells of reinforced mortar". Proc. World Conf. San Francisco, Oct. 1962.

35. Novozhilov, V. "The Theory of thin shells". P. Noordhoff, 1959.

36. Nag, K. & Davies, S.R. "A study of the behaviour of a fixed arch built of hollow clay blocks". Research Report, Jan. 1966 S.C.R.U. Dept. of Civil Engineering, Univ. of Edinburgh.

37. Parikh, K.S. & Norris, C.H. "Analysis of shells using framework analogy". Proc. of World Conf. San Francisco, Oct. 1962.

38. Parme, A.L. "Hyperbolic paraboloids and other shells of double curvatures". J. of the Structural division Proc. of American Soc. of Civil Engineers. Sept. 1956.

39. Ramaswamy, G.S. "Funicular brick shell roofs for industrial buildings". Int. Conf. on masonry structural systems, Texas, 1967.

40. Rowe, R.E. "Experimental methods in the study of the behaviour of shell roofs". Proc. World Conf. San Francisco, Oct. 1962.

41. Kühle, H. "Some fundamental observations on the present and future development of precast concrete shells". Proc. World Conf. San.Francisco, 1962.

42. Salmon, E.H. "Materials and structures - Vol. 1.". Longmans.

43. Salvadori, M.G. "Analysis and testing of translation shells". J. of American Concrete Inst. June, 1956.

44. Sánchez Del Rio, I. "Corrugated reinforced ceramic shells for large spans". Proc. of World Cof. San Francisco, Oct. 1962.

45. Schorer, H. "Line load action on thin cylindrical shells". J. American Soc. of Civ. Engineers, March, 1935.

46. Soare, M. "The application of finite difference equations to thin shells". Pergamon Press, Oxford, 1964.

47. Timoshenko, S. "Theory of plates and shells". McGraw-Hill. 1940.

48. Tottenham, H. "Approximate solution to shell problems" Second Symp. on shell roof construction. Oslo, 1957.

49. Tottenham, H. "A simplified method of design for cylindrical shell roofs". The structural engineer . June, 1954.

50. Varghese, P.C. "Testing model concrete barrel shells". The Indian Concrete Journal, Sp. Shell No. Dec. 1959. Central building research Inst. Symp. on shell structures.

51. Vlasov, V.Z. "Cylindrical shells and new ways of developing thin walled spatial system in structural mechanics". Second Symp. on shell roof construction. Oslo, 1957.

52. Wood, R.H. "Plastic and elastic design of slabs and plates". Thames & Hudson, London , 1961.

53. Young, R. W.J. "Investigation of stresses in thin shells of various surface forms". Ph.D. Thesis, 1967, Univ. of Edinburgh.

54. Yu, C.W. & Kriz, L.B. "Tests of a hyperbolic paraboloid reinforced concrete shell". Proc. World Conf. San Francisco, Oct. 1962.

55. Zienkiewicz, O.C. "Notes on the derivation and approximation to thin shell equations". Report, The Technological Inst. North Western Univ. Illinois.

56. Zienkiewicz, O.C. & Holister, G.S. "Stress analysis - recent development in numerical and experimental methods". John Wiley & Sons, 1965.